

Phosphorescent iridium(III) complexes, copolymers and their applications

Dissertation

zur Erlangung des akademischen Grades

Doktor der Naturwissenschaften
(Doktor rerum naturalium)

Eingereicht im Fachbereich C - Mathematik und Naturwissenschaften
der Bergischen Universität Wuppertal

von

Nan Tian

aus Tianjin, China

Wuppertal, 2011

Die Dissertation kann wie folgt zitiert werden:

urn:nbn:de:hbz:468-20120726-104854-7

[<http://nbn-resolving.de/urn/resolver.pl?urn=urn%3Anbn%3Ade%3A468-20120726-104854-7>]

Die vorliegende Arbeit wurde in der Zeit von Februar 2007 bis Januar 2011 in der Arbeitsgruppe für Funktionspolymere des Fachbereiches C - Mathematik und Naturwissenschaften der Bergischen Universität Wuppertal unter Anleitung von Frau Prof. Dr. Elisabeth Holder durchgeführt.

Ich danke Frau Prof. Dr. Elisabeth Holder für ihre wissenschaftliche und persönliche Unterstützung sowie für ihre ständige Diskussionsbereitschaft.

1. Gutachter: Prof. Dr. Elisabeth Holder (Bergische Universität Wuppertal)
2. Gutachter: Prof. Dr. Ullrich Scherf (Bergische Universität Wuppertal)

Eingereicht am:

„Will, work and wait are the pyramidal cornerstones for success. “

Louis Pasteur (1822-1895), French chemist and microbiologist

Für meine Mutter FengHua Xu
und meine Frau Xizhao

Abstract

This work is firstly focused on the synthesis of green, orange-red and red emitting heteroleptic iridium(III) complexes and their application as emitting materials in the area of OLEDs and oxygen sensors. Furthermore, in order to obtain energy transfer from the polymer backbone (host material) to the polymer-incorporated iridium(III) complexes (guest material), a series of metallo-copolymers were designed and synthesised.

Three phenylpyridine-based C^N ligands, namely 1-phenylisoquinoline (**1**, *piq*), 2-(naphthalen-1-yl)pyridine (**2**, *npy*) and 2-phenylpyridine (**3**, *ppy*) and a series of different ancillary acetylacetonate (acac) ligands (**4-8**) containing dibromo-, hexylthiophene- and hexylphenyl-functionalised carbazoles were synthesised by C-C cross-coupling reactions, nucleophilic substitutions and Claisen condensations, and were ongoing characterised by ¹H NMR, ¹³C NMR, elemental analysis, mass- and IR-spectra. Thus, five sets of heteroleptic iridium(III) complexes (**12-16a-c**) emitting green, orange-red and red light were further obtained and a series of 1-D (¹H) and 2-D (¹H-¹H) NMR experiments were used to confirm the structure of the complexes. Owing to these complexes introduced ancillary acetylacetonate ligands furnished with a carbazole unit or its derivatives, their solubility, thermal stability and photo(electro)-luminescence properties were obviously improved. For example, these iridium(III) complexes reveal high quantum yields (44% for **16c**), luminous efficiency (10.3 Cd/A for **13b**), short phosphorescence lifetimes (1.1 μs for **12a** and **16c**) and good thermal stabilities (353 °C for **14c**). In addition, utilising these iridium(III) complexes as temperature sensors, the variations in the luminescence lifetimes of these complexes with the varied temperature revealed a non-linear curve and are described by an Arrhenius-type equation.

Additionally, two types of fluorene-based copolymers with iridium(III) complex (**25**) or iridium(III) complex and fluorenone incorporated into the polyfluorene main chains (**26** and **27**) were synthesised *via* a Yamamoto protocol. The OLED devices of the copolymer **25** with the configuration ITO/PEDOT/QUPD/copolymer**25**/TPBI/CsF/Al generate electroluminescence with the maximum peak at 604 nm, while emission maximum at 535 nm for **26** and 566 nm for **27** was observed. The examination of the electroluminescence emission maximum of copolymer **25** is the most possible evidence for energy-transfer from the fluorene backbone to the iridium-containing carbazole segments or for charge trapping.

Table of Contents

Chapter 1 Introduction	1
1.1 Application of iridium(III) complexes as emitters in OLEDs.....	2
1.1.1 Advantages of iridium(III) complexes applied as emitter in OLEDs.....	2
1.1.2 <i>Triscyclometalated</i> iridium(III) complexes.....	3
1.1.3 <i>Biscyclometalated</i> iridium(III) complexes.....	6
1.1.4 Photophysical properties of iridium(III) complexes.....	7
1.1.4.1 The types of <i>triscyclometalated</i> iridium complexes.....	8
1.1.4.2 The types of <i>biscyclometalated</i> iridium(III) complexes.....	9
1.1.5 Matrix materials suitable for iridium(III) complexes.....	12
1.1.5.1 Small molecules as matrix materials.....	12
1.1.5.2 Polymers as matrix materials.....	13
1.1.5.3 Iridium(III) complexes doped into polymers.....	14
1.1.5.4 Polymer-embedded iridium(III) complexes.....	17
1.1.5.5 Förster and Dexter energy-transfer in host-guest systems.....	26
1.2 Iridium(III) complexes in oxygen and temperature sensor applications.....	29
1.2.1 Applying iridium(III) complexes as oxygen sensors.....	29
1.2.2 Applying iridium(III) complexes as temperature sensors.....	30
1.3 Metal-catalysed C-C couplings.....	31
1.3.1 Suzuki-Miyaura cross-coupling reaction.....	31
1.3.2 Stille cross-coupling reaction.....	32
1.3.3 Yamamoto cross-coupling reaction.....	35
1.4 Motivation.....	37
1.5 References.....	39

Chapter 3 Iridium(III) Complexes	84
3.1 Introduction.....	84
3.2 Synthesis of Ir(III)- μ -chloro-bridged precursor complexes.....	86
3.3 Synthesis of heteroleptic iridium(III) complexes.....	89
3.3.1 Synthesis of iridium(III) complexes 12a-c	91
3.3.2 Synthesis of iridium(III) complexes 13a-c	95
3.3.3 Synthesis of iridium(III) complexes 14a-c	100
3.3.4 Synthesis of iridium(III) complexes 15a-b	104
3.3.5 Synthesis of iridium(III) complexes 16a-c	108
3.4 Electrophosphorescence.....	114
3.5 Pressure and temperature sensitivity.....	123
3.6 Summary.....	129
3.7 Experimental Section.....	130
3.7.1 General procedure of Ir(III)- μ -chloro-bridged precursor complexes $[(C^{\wedge}N)_4Ir^{III}_2Cl_2]$	131
3.7.2 Ir(III)- μ -chloro-bridged precursor complex $[(piq)_4Ir^{III}_2Cl_2]$ (9).....	132
3.7.3 Ir(III)- μ -chloro-bridged precursor complex $[(npq)_4Ir^{III}_2Cl_2]$ (10).....	132
3.7.4 Ir(III)- μ -chloro-bridged precursor complex $[(ppy)_4Ir^{III}_2Cl_2]$ (11).....	133
3.7.5 General procedure of heteroleptic iridium(III) complexes $[Ir^{III}(C^{\wedge}N)_2\{acac\}]$	134
3.7.6 $[Ir^{III}(piq)_2\{2,2,6,6\text{-tetramethylheptane-3,5-dione}\}]$ (12a).....	134
3.7.7 $[Ir^{III}(npq)_2\{2,2,6,6\text{-tetramethylheptane-3,5-dione}\}]$ (12b).....	135
3.7.8 $[Ir^{III}(ppy)_2\{2,2,6,6\text{-tetramethylheptane-3,5-dione}\}]$ (12c).....	136
3.7.9 $[Ir^{III}(piq)_2\{1\text{-carbazol-9-yl-5,5-dimethyl-hexane-2,4-dione}\}]$ (13a)	137
3.7.10 $[Ir^{III}(npq)_2\{1\text{-carbazol-9-yl-5,5-dimethyl-hexane-2,4-dione}\}]$ (13b)	138
3.7.11 $[Ir^{III}(ppy)_2\{1\text{-carbazol-9-yl-5,5-dimethyl-hexane-2,4-dione}\}]$ (13c)	139
3.7.12 $[Ir^{III}(piq)_2\{1\text{-(3,6-dibromocarbazol-9-yl)-5,5-dimethyl-hexane-2,4-dione}\}]$ (14a).....	140
3.7.13 $[Ir^{III}(npq)_2\{1\text{-(3,6-dibromocarbazol-9-yl)-5,5-dimethyl-hexane-2,4-}$	

dione}] (14b).....	141
3.7.14 [Ir ^{III} (ppy) ₂ {1-(3,6-dibromocarbazol-9-yl)-5,5-dimethyl-hexane-2,4-dione}] (14c).....	142
3.7.15 [Ir ^{III} (npy) ₂ {1-[3,6- <i>bis</i> (5-hexyl-2-thienyl)carbazol-9-yl]-5,5-dimethyl-hexane-2,4-dione}] (15a).....	143
3.7.16 [Ir ^{III} (ppy) ₂ {1-[3,6- <i>bis</i> (5-hexyl-2-thienyl)-2-yl)carbazol-9-yl]-5,5-dimethyl-hexane-2,4-dione}] (15b).....	144
3.7.17 [Ir ^{III} (piq) ₂ {1-[3,6- <i>bis</i> (4-hexylphenyl)carbazol-9-yl]-5,5-dimethyl-hexane-2,4-dione}] (16a).....	145
3.7.18 [Ir ^{III} (npy) ₂ {1-[3,6- <i>bis</i> (4-hexylphenyl)carbazol-9-yl]-5,5-dimethyl-hexane-2,4-dione}] (16b).....	146
3.7.19 [Ir ^{III} (ppy) ₂ {1-[3,6- <i>bis</i> (4-hexylphenyl)carbazol-9-yl]-5,5-dimethyl-hexane-2,4-dione}].....	147
3.8 References.....	149
Chapter 4 Copolymers containing iridium(III) complexes.....	151
4.1 Introduction.....	151
4.2 Results and discussions.....	152
4.2.1 Synthesis of iridium(III)-based copolymers 25-27	153
4.2.2 Optical properties.....	157
4.2.3 Electroluminescence properties.....	161
4.3 Summary.....	165
4.4 Experimental Section.....	166
4.4.1 2,7-Dibromo-9,9-di- <i>n</i> -octyl-9 <i>H</i> -fluorene (23).....	168
4.4.2 2,7-Dibromo-9 <i>H</i> -fluoren-9-one (24).....	168
4.4.3 Copolymer Ir5PF95 (25).....	168
4.4.4 General procedure of copolymers 26 and 27	169
4.4.5 Copolymer Ir5PF90PO5 (26).....	169
4.4.6 Copolymer Ir10PF89PO1 (27).....	170
4.5 References.....	171

List of Symbols and Abbreviations.....	173
List of Publications out of this work.....	175
Acknowledgement.....	178

Chapter 1 Introduction

Owing to their property of controlling the energies of singlet and triplet excitons after charge recombination, transition metal-based phosphorescent materials have received significant attention in the fabrication of organic light-emitting diodes (OLEDs). In addition, their strong spin-orbit coupling can lead to relatively short triplet lifetimes, which allows full exploitation of both singlet and triplet excitons in order to achieve 100% internal quantum efficiency in an electroluminescent device [1]. During the last twenty years, research has concentrated on various kinds of metal complexes such as Ru(II) [2], Re(I) [3], Os(II) [5], Ir(III) [2,4-10], Pt(II) [2,7,11-13], Au(I) [2,9], and Cu(I) [14], which were utilised as phosphorescent emitters in electro-optical devices such as light-emitting devices [15,16], solar cells [17,18], or sensors [19,20].

Platinum octaethylporphyrin (PtOEP) was the first triplet emitter fulfilling the essential criteria (strong spin-orbit leading to fast intersystem crossing and efficient phosphorescence at room temperature) in order to be incorporated into an OLED [21]. PtOEP has a photoluminescent (PL) quantum yield of 0.5 at RT both in solution and in a rigid polystyrene matrix, while in a frozen glass (at 77 K), the quantum yield is above 0.9. The emission lifetimes at room temperature and 77 K have been measured to be 90 μs and 131 μs , respectively. In the first OLEDs prepared using PtOEP, a two-component emissive layer was utilised, composed of PtOEP doped into Alq₃ (*tris*(8-hydroxyquinolato)aluminium). The optimal doping

level was found to be 6% with a maximal external quantum efficiency of 4% and quenching of 1.3% at low current density [21].

1.1 Application of iridium(III) complexes as emitters in OLEDs

In 1999, Baldo *et al.* succeeded in developing an efficient green phosphorescent OLED with a η_{ex} of 8%, using the iridium complex [*fac*-Ir(ppy)₃] [22]. The latter was at first reported by King *et al.* in 1985 [5,23] as an emissive dopant directing the attention and work of many research groups on the use of these complexes as emitters. Given the fact that iridium(III) complexes display shorter triplet lifetimes, well-defined oxidation potentials, relatively good stability, and environmental inertness when compared to other metal-ligand complexes, OLED devices based on iridium(III) complexes as emitters exhibit superior properties as well, like higher quantum efficiencies [24-26]. Varying the respective set of ligands on the iridium(III) centre permits a variety of efficient emission wavelengths, such as blue, green, yellow or red, which can be used in colour tuning and full-colour applications [27-35].

1.1.1 Advantages of iridium(III) complexes applied as emitters in OLEDs

As mentioned before, complexes comprising heavy metals like the square planar d^8 Pt(II), Pd(II), and Au(II) complexes or the octahedral $4d^6$ or $5d^6$ Ru(II), Rh(III), Re(I), Ir(III), and Pt(IV) complexes, are suitable candidates for applications as emitters in OLED devices due to their long-lived excited states and their high luminescence quantum yields. Previous research focused on using Ru(II) or Os(II) complexes containing bipyridine and phenanthroline ligands. However, there is a

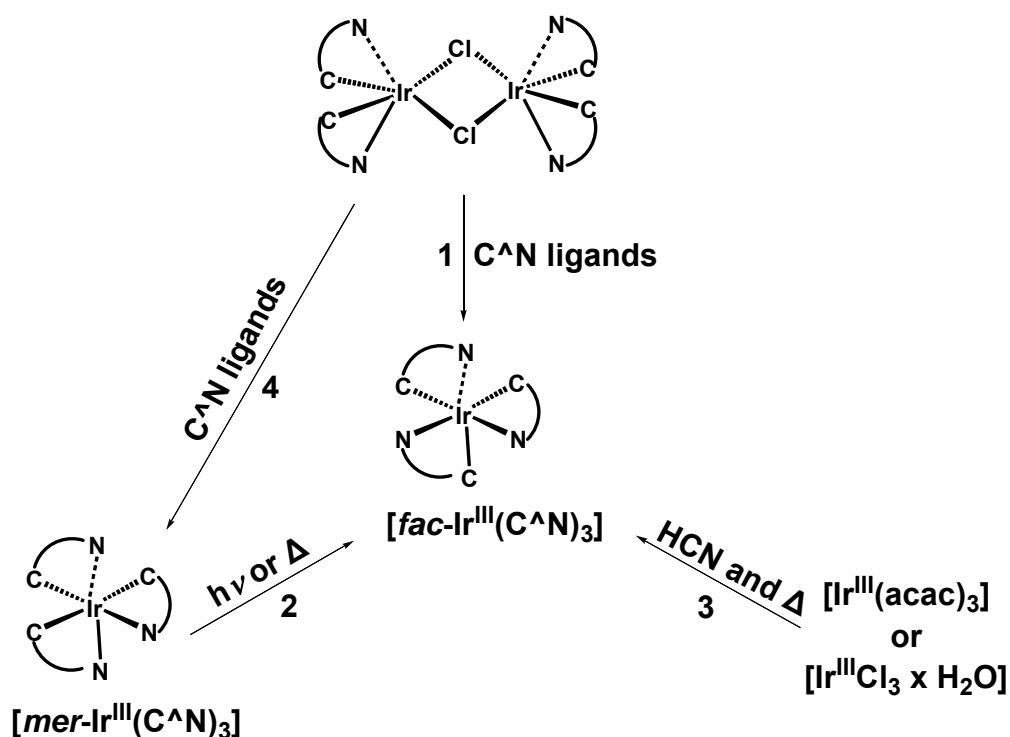
limitation regarding the variation of the emission colour of these complexes because of their thermal population of a non-emissive metal-centred (MC^3) state [36]. In contrast, iridium(III) complexes are able to acquire a broader range of colours favoured by an increase in the ligand-field stabilisation energy (LFSE), which results in a less thermally accessible MC^3 state [37]. On the other hand, iridium(III) or Rh(III) complexes are commonly electro-neutral as they form *tris*- and *biscyclometalated* complexes, which are isoelectronic with cationic Ru(II) and Os(II) complexes. Regarding the same neutral Ir(III) and Rh(III) complexes, the charged iridium(III)-based complexes exhibit stronger phosphorescence at room temperature, while the emission spectra of Ru(II) complexes can only be observed only at a low temperature [38]. The iridium atom is a heavy metal with a large atomic number that can offer strong spin-orbital coupling in an iridium(III) complex. The strong spin-orbital coupling results in efficient intersystem crossing from the singlet to the triplet excited state and provides a relatively short lifetime of the triplet metal-to-ligand charge transfer (MLCT) state, which allows efficient utilisation of triplet excitons in addition to singlet excitons in order to achieve nearly 100% internal quantum efficiency of the electroluminescent device at room temperature [30,33,39,40]. Additionally, the stable oxidation state of Ir(III) facilitates the formation of neutral complexes, allowing sublimation under vacuum. Regarding the thermal stability of phosphorescent emitters, designing homoleptic complexes is one of the strategies applied [34,38]. Therefore, the advantages of iridium(III) complexes make them good candidates as emitting sources in OLED devices.

1.1.2 *Triscyclometalated* iridium(III) complexes

Since 1984 when Watts isolated the *tris*(2-phenylpyridine)iridium(III) complex as a side product and reported a general protocol for the synthesis of *tris*(2-phenylpyridine)iridium(III) complexes in higher yields, a number of scientific

Chapter 1. Introduction

researchers have dedicated their work to synthesising *triscyclometalated* iridium(III) complexes. Thus, Guedel and co-workers [5,24, 41] utilised silver triflate (AgCF_3SO_3) as a catalyst to improve the yield, while Grushin, Petrov, Wang, and co-workers synthesised complexes under solvent-free conditions [42]. Thompson and co-workers summarised and discussed different synthetic routes for the acquisition of *triscyclometalated* iridium(III) complexes, embracing either homoleptic or heteroleptic phenylpyridine derivatives. The typical synthetic approaches of *triscyclometalated* iridium(III) complexes are presented in Scheme 1.1. The forerunners, namely cyclometalated Ir(III) chloro-bridged dimers of the general formula $[\text{Ir}^{\text{III}}(\text{C}^{\wedge}\text{N})_2\text{-}\mu\text{-Cl}_2]_2$, were synthesised according to the Nonoyama route [43] by refluxing $[\text{Ir}^{\text{III}}\text{Cl}_3 \times \text{H}_2\text{O}]$ with 2.5 equivalents of the cyclometalating ligand in a 3:1 mixture of 2-ethoxyethanol and water [5,24,44-50].



Scheme 1.1. Schematic representation of the synthetic routes of homo- and heteroleptic *triscyclometalated* iridium(III) complexes [24,38].

The *triscyclometalated* iridium(III) complexes are available in two configurationally disparate isomers, namely facial (*fac*) and meridional (*mer*) complexes (Figure 1.1).

Chapter 1. Introduction

The facial isomers usually exhibit longer lifetimes and higher quantum efficiencies compared to the meridional isomer [51]. Nevertheless, a *mer*-Ir(mppy)₃ (mppy = 2-phenyl-4-methyl-pyridine) complex was synthesised by Sun and *et al.*, exhibiting a high quantum efficiency [52]. In general, meridional isomers display a red-shifted emission compared to the facial species. Facial isomers are favoured under high reaction temperatures due to their thermodynamic stability. Thus, the reaction parameters for facial isomers require more rigorous conditions than for meridional complexes. The kinetically favoured *mer*-isomers can be isolated by performing the reactions at lower temperatures. Therefore, synthetic methods **2** and **3** performed at higher reaction temperatures lead to the thermodynamically stable facial isomers of the *triscyclometalated* iridium(III) complexes [38].

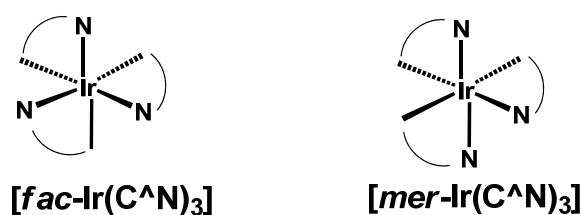
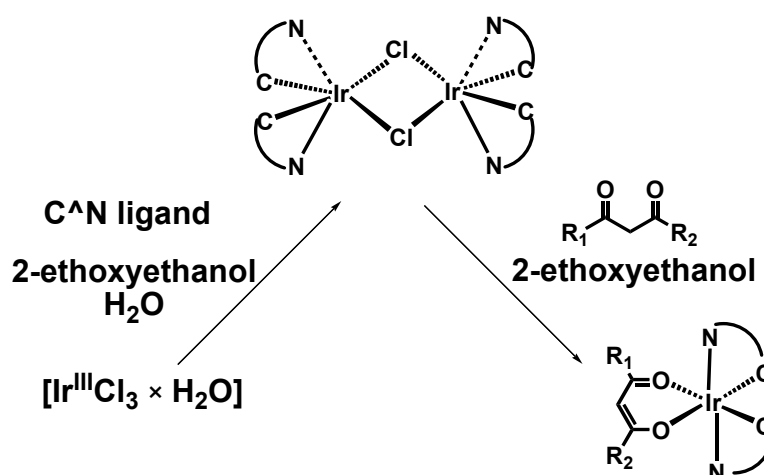


Figure 1.1. Facial and meridional isomers of the *triscyclometalated* iridium complexes [38].

Besides these conventional methods, microwave-assisted synthetic approaches have been extensively utilised as well. Using microwave irradiation, the reaction times can be remarkably shortened. Nevertheless, the necessity of an excess of ligands and the still low yields obtained after microwave reactions restrict further applications [53,54]. To achieve full-colour OLED devices, three primary colours, namely blue, green, and red are necessary. Homoleptic iridium(III) complexes as red, blue, or white light emitters at room temperature and exhibiting facial geometry are rare compared to the green emitters [55,56] of the same geometry. Thus, the development of stable and efficient light-emitting iridium(III) complexes is still a major goal.

1.1.3 *Biscyclometalated iridium(III) complexes*

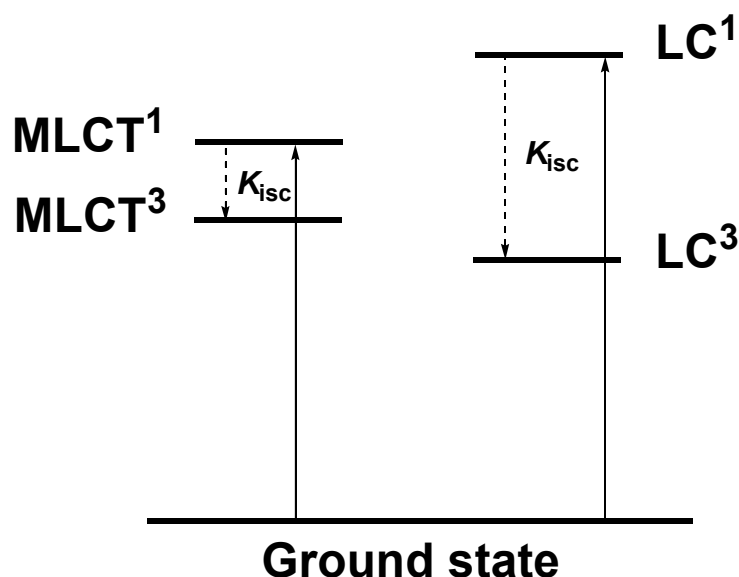
Biscyclometalated iridium(III) complexes can be easily obtained from the corresponding chloro-bridged dimer complexes *via* the so called bridge-splitting method using cyclometalated Ir(III) chloro-bridged dimers as precursors. Since iridium(III) intermediates are sensitive to oxygen, the complexation reactions must be performed under inert conditions. Nonoyama first introduced an efficient synthetic procedure in 1974 [57]. Ten years later, Watts and co-workers improved the reaction conditions, obtaining higher yields [58,59]. The synthesis of neutral *biscyclometalated acetoacetonate* and *picolinate* Ir(III) complexes is carried out in a two-step reaction (Scheme 1.2). Cyclometalated Ir(III) chloro-bridged dimers precursors are obtained by refluxing iridium trichloride hydrate in the presence of C^N ligands in a mixture of high boiling point alcohols (2-ethoxyethanol) and water under an inert atmosphere. Subsequently, the resulting dimeric Ir(III) complex, the specified ancillary acetylacetonate ligand and a weak base (K₂CO₃ or Na₂CO₃) are stirred in 2-ethoxyethanol under reflux for several hours, usually giving the target complex in good yields after purification by means of flash chromatography [5,24,60,61].



Scheme 1.2. Schematic representation of the synthetic routes of neutral *biscyclometalated acetoacetonate* iridium(III) complexes [5,24,60,61].

1.1.4 Photophysical properties of iridium(III) complexes

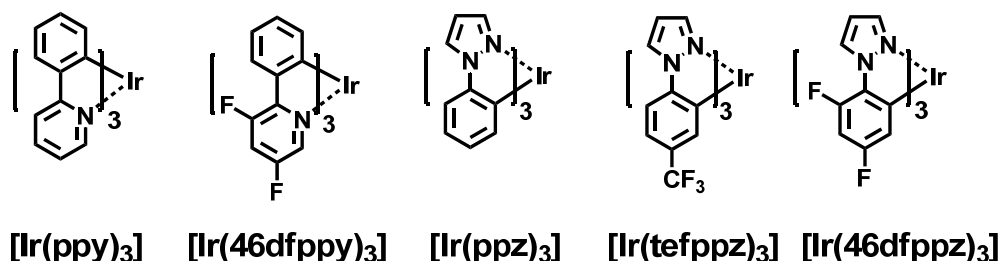
The iridium(III) complexes are known to exhibit high triplet quantum yields due to the mixing of their singlet and triplet excited states *via* spin-orbit coupling, leading to high phosphorescence efficiencies. Theoretically, there are four types of electronic states (Scheme 1.3) in these complexes that compete for the lowest unoccupied molecular orbital. Two of them are singlet and triplet metal-to-ligand charge transfer states, so called MLCT^1 and MLCT^3 , in which the electron migrates from the d-orbital of the metal to a vacant π^* -orbital of the ligand. The remaining two are the singlet (LC^1) and triplet ligand-centred (LC^3) states where the electron migrates between the π -orbitals of the coordinated ligands. The involvement of the d-orbital in the bonding is expected to be higher for MLCT states and this is reflected in the lower intensities of the corresponding absorption bands relative to those involving ligand-centred states [62-66].



Scheme 1.3. Schematic representation of four types of electronic states of a homoleptic iridium(III) complex [63,64].

1.1.4.1 The types of *triscyclometalated iridium(III)* complexes

With the above-described four electronic states in mind, two basic transitions can be observed for the *triscyclometalated iridium(III)* complexes, namely metal-to-ligand charge transfer (MLCT) and ligand-centred transitions (LC). Phosphorescence in this type of complex, promoted by strong spin-orbit coupling, mainly arises from a mixture of the MLCT³ and LC³ excited states, whereas the emissive excited state is predominantly the excited state with the lowest energy. Either changing the electron-donating and electron-withdrawing substituents of the C^N ligands or varying the configuration of the C^N ligands can result in tuning of the lowest excited state of *triscyclometalated iridium(III)* complexes (Scheme 1.4, Table 1.1) [5,24,67,68].



Scheme 1.4. Schematic representation of the selected *triscyclometalated iridium(III)* complexes [69,70].

In addition, the photophysical properties between the facial and meridional *triscyclometalated iridium(III)* complexes are obviously different. The emission maximum of the meridional configuration reveals a distinct red-shifted emission compared to the facial complexes, which can be attributed to the fact that the meridional arrangement usually arises from phenyl groups being opposite to each other [69].

Chapter 1. Introduction

Table 1.1. Photophysical properties of the selected *triscyclometalated* iridium(III) complexes [69,70].

Ir(III) complex	Emission at 77 K	Emission at 298 K
[<i>fac</i> -Ir(ppy) ₃] (Ir-1)	492	510
[<i>mer</i> -Ir(ppy) ₃] (Ir-2)	493	512
[<i>fac</i> -Ir(46dfppy) ₃] (Ir-2)	450	468
[<i>fac</i> -Ir(46dfppy) ₃] (Ir-4)	460	482
[<i>fac</i> -Ir(ppz) ₃] (Ir-5)	414	--
[<i>mer</i> -Ir(ppz) ₃] (Ir-6)	427	--
[<i>fac</i> -Ir(tefppz) ₃] (Ir-7)	422	428
[<i>mer</i> -Ir(tefppz) ₃] (Ir-8)	430	--
[<i>fac</i> -Ir(46dfppz) ₃] (Ir-9)	390	--
[<i>mer</i> -Ir(46dfppz) ₃] (Ir-10)	402	--

1.1.4.2 The types of *biscyclometalated* iridium(III) complexes

The control over heteroleptic iridium(III) complex emission colours can be achieved by varying the ancillary ligands or by introducing various substituents at suitable positions of the cyclometalated ligands [2,8,24,62-65]. Due to the fact that the lowest triplet energy level of the ancillary ligand is always higher than the energies of the LC³ and MLCT³ excited states, the emission maximum of *biscyclometalated* iridium(III) type complexes is dominated by LC³ and MLCT³ transitions. Calculations using density functional theory (DFT) proved that the HOMOs (highest occupied molecular orbitals) are mostly metal-centred, whereas the LUMOs (lowest unoccupied molecular orbitals) are primarily located on the heterocyclic rings of the cyclometalated C^N ligands. In other words, the ancillary

Chapter 1. Introduction

ligand is not directly involved in the lowest excited state [60,61]. Nevertheless, if the ancillary ligand has a higher triplet energy level, it can indeed alter the excited energy state by modifying the electron density at the metal centre. Additionally, interligand electron transfer from the cyclometalated C^N ligand to the ancillary ligand can occur, especially if the triplet energy of the ancillary ligand is much lower. For instance, Park and co-workers observed emission across the visible spectrum by varying the ancillary ligand structures in a series of iridium(III) complexes [71]. However, in principle, the configuration of cyclometalated C^N ligand is dominant in the case of tuning of the emission maxima of *biscyclometalated* iridium(III) complexes. For example, increasing the π -conjugation length or introducing fused heteroaromatic rings into the cyclometalated C^N ligand causes a red-shift in the emission [72-76]. On the other hand, lowering the highest occupied molecular orbital by adding an electron-withdrawing group or raising the triplet energy state by use of a C^N ligand with a strong ligand strength results in a blue-shifted emission [77-79].

Some examples of heteroleptic iridium(III) complexes with cyclometalated ligands, which emit green or red colours, are illustrated in Figure 1.2. These complexes possess the same molecular formula [(C^N)₂Ir(III)(acac)] and similar ancillary acac-ligands. Thus, their emission colour is determined by the respective cyclometalated ligands such pyridine or quinoline-arene ligands.

Chapter 1. Introduction

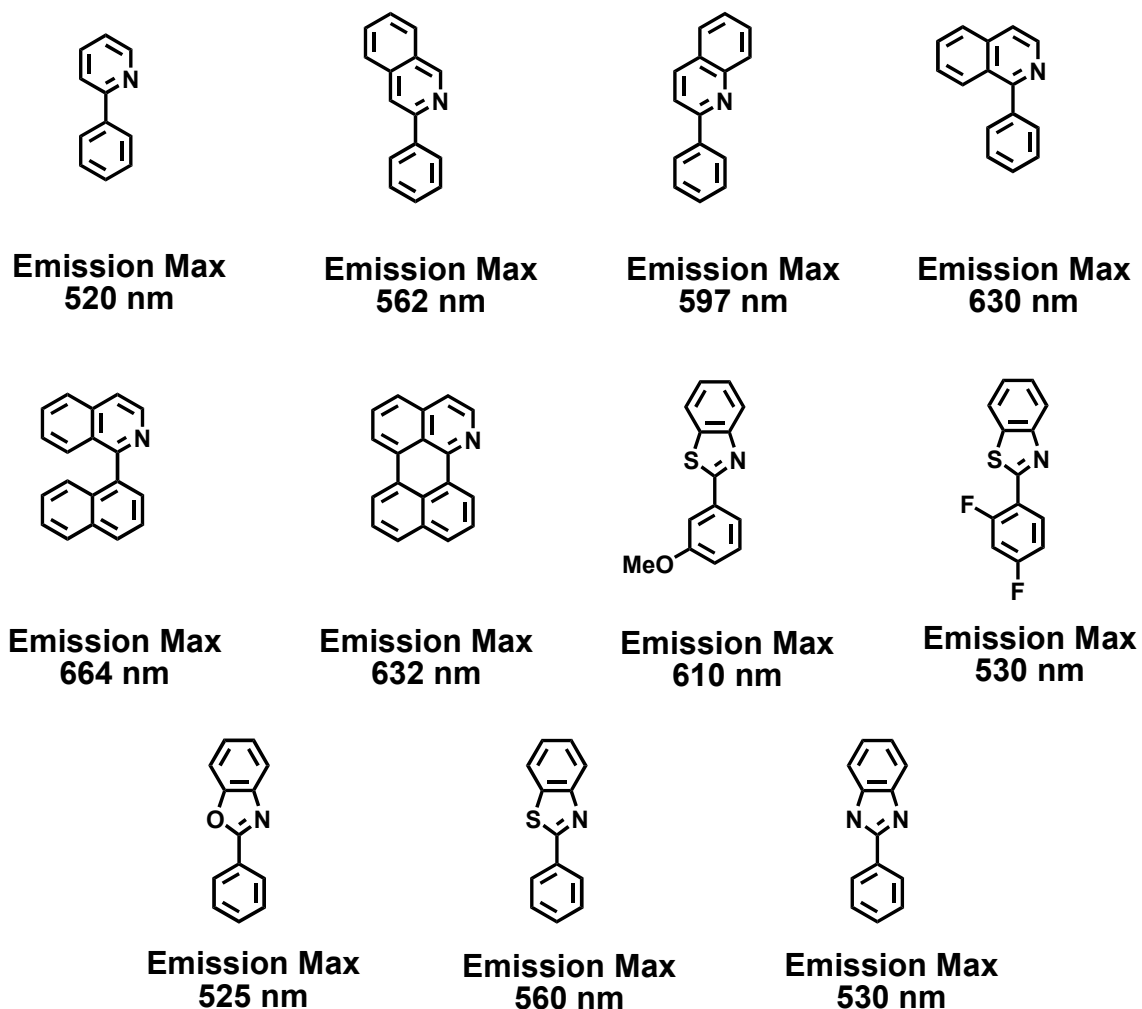


Figure 1.2. Selected cyclometalated C^N ligands and emission maxima of these Ir(III) complexes [80].

The emission tuning of the above-mentioned Ir(III) complexes can be achieved either through varying the position of the phenyl ring at the phenylpyridine segment, involving expansion of the size of the π -system, or by adding electron-donating (-OMe) and -accepting functional (-F) groups. Additionally, a change in the heteroatom (O, S or N) in molecules of the same configuration can also cause a small shift of the emission maximum due to the different electronegativities of the heteroatoms.

1.1.5 Matrix materials suitable for iridium(III) complexes

1.1.5.1 Small molecules as matrix materials

The phosphorescent iridium(III) complexes are always employed as emitting guests in small molecule hosts to avoid triplet-triplet annihilation or quenching effects associated with the relatively long excited state lifetimes, while an efficient phosphorescent OLED device is fabricated. In general, a prerequisite for suitable small molecule host materials is that the triplet level of the host is larger than the triplet level of the phosphorescent guest for preventing undesired energy back-transfer processes [81,82]. Padmaperuma *et al.* [83] reported organic light-emitting devices incorporating 2,7-*bis*(diphenylphosphineoxide)-9,9-dimethylfluorene (PO6, Figure 1.3), in which the phosphine oxide group (P=O) act as a point of saturation between the “active” chromophore bridge and the outer phenyl groups and results in higher triplet energy of 2.72 eV. Using PO6 as the host material doped with Ir(III)*bis*(4,6-(difluorophenyl)pyridinato-*N,C*²), picolinate (FIrpic) exhibited blue emission with a peak external quantum efficiency of 8.1% and luminous power efficiency of 25.1 lm/W. Burrows *et al.* achieved a blue electrophosphorescent organic LED device with FIrpic as the dopant and 2,8-*bis*(diphenylphosphine oxide)dibenzofuran (PODBF, Figure 1.3) as the host and obtained an external quantum efficiency of 10.1%. This result can be attributed to the fact that PODBF has a higher triplet energy (3.14 eV) than PO6. Tsai *et al.* [84] synthesised (9-(4-*tert*butylphenyl)-3,6-*bis*(triphenylsilyl)-9*H*-carbazole (CzSi, Figure 1.3) and built an organic OLED device using CzSi as the small host material doped with 8 wt% of the typical blue phosphorescent dopant iridium(III)*bis*((4,6-difluorophenyl)-pyridinato-*N,C*²)picolinate, which showed a high external quantum efficiency of 16% (30.6 Cd/A_{maximum}), a maximum brightness as high as 59000 Cd/m² (at 14.5 V), and a luminous power efficiency of 26.7 lm/W.

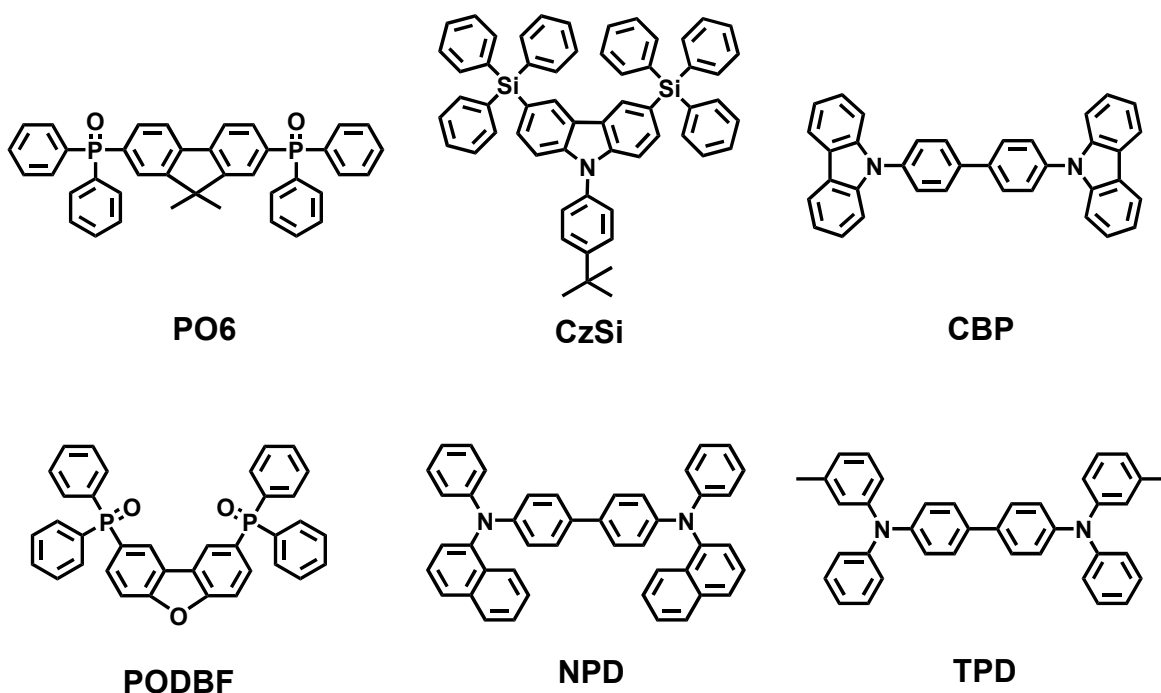


Figure 1.3. Selected examples of small molecule host materials for phosphorescent iridium(III) complexes [83-85].

1.1.5.2 Polymers as matrix materials

Although doping small molecules with iridium(III) complexes is extensively used in fabricating the organic LED devices, vacuum deposition of small molecules in organic light-emitting diodes is not effective, especially for processing large area displays. Polymers as host materials have an advantage compared to small molecules as hosts, because phosphorescent organic LED devices can be easily fabricated at room temperature by processing the polymer from solution by spin casting, screen printing, or inkjet printing [86,87].

Polymeric phosphorescent materials comprising heavy metal complexes have attracted the scientific interest due to their high quantum efficiency and their remarkable photo- and electro-physical performance [88-90]. Iridium(III) complexes, with their relatively short phosphorescent lifetimes and their intensive phosphorescent emission at room temperature, are considered suitable comonomers for the polymeric backbones. Generally, there are two combination

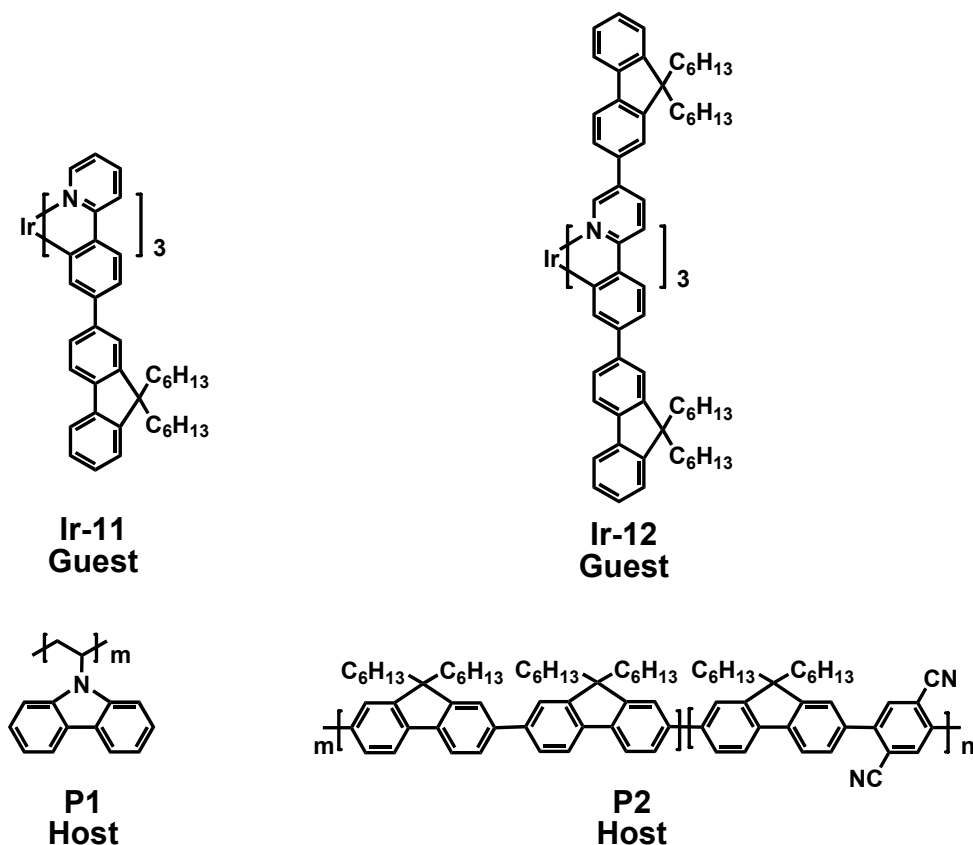
modes for iridium(III) polymer systems. In one of them, the phosphorescent iridium(III) complex is doped in the host polymer matrix (blending system), whereby polymer light-emitting diode (PLED) devices are easily fabricated by processing the materials from solution, such as by spin coating or printing techniques [91,92]. In the other, iridium(III) complexes can be introduced to non-conjugated or conjugated polymer chains. In these conjugated metallo-polymers, the energy-transfer from the conjugated main chain (host) to the iridium(III) complex (guest) can be monitored and the luminescence efficiency can be increased by harvesting a large percentage of triplet excitons generated upon electron-hole recombination [93-95].

1.1.5.3 Iridium(III) complexes doped into polymers

By virtue of the strong spin-orbit coupling of the heavy metal centre, iridium(III) complexes usually have efficient phosphorescence and short lifetimes, which typically range from 1 to 14 ms [96]. The shorter exciton lifetime makes iridium(III) complexes more attractive candidates as phosphorescent guest materials with polymer hosts in blended systems [97]. To maximise the performance of electro-phosphorescent devices in a blended system comprised of a phosphorescent iridium(III) complex as guest and a polymer host, it is necessary to disperse the iridium(III) guest in a suitable host material in order to reduce triplet-triplet annihilation and concentration quenching. Generally, a suitable combination of a metal complex as the guest and a polymer host requires that the triplet energy level of the polymer host should be higher, or close to, that of the metal complex so as to minimise energy back-transfer to the polymer [98]. Polyvinylcarbazole (PVK) and polyfluorene (PF) are the most commonly used polymer host materials because of their excellent film-forming properties, high glass transition temperature, rather wide energy-gap emission observed in the blue spectral region,

Chapter 1. Introduction

and good hole mobility [99]. An external quantum efficiency of 1.9% photons per electron and a luminance of 2500 Cdm^{-2} for *tris*(2-phenylpyridine)iridium (**Ir-1**) doped into PVK was reported by Kim *et al.* [100]. Gong *et al.* introduced a blending system where iridium(III) complexes with different triplet energies are blended into PVK and polyfluorene hosts. A quantum efficiency of 10% photons per electron and a luminous efficiency of 36 Cd/A at 2500 Cdm^{-2} have been found, which were achieved by doping *tris*[9,9'-dihexyl-2-(pyridyl-2')fluorene]iridium(III) (**Ir-11**) into a blend of PVK [101]. In contrast, a quantum efficiency of 1.5% photons per electron and a luminous efficiency of 3 Cd/A at 142 Cdm^{-2} were observed by doping *tris*(2,5-bis-2'-(9,9-dihexylfluorene)-pyridine)iridium (**Ir-12**) in polyfluorene as the host material (Figure 1.4) [102].



By Gong et al.

Figure 1.4. Selected examples of PVK and polyfluorene as host (polymer) materials [101,102].

Chapter 1. Introduction

Polyfluorenes and derivatives have been commonly employed as host polymers in blend systems and are especially suitable for red phosphorescent Ir(III) complex guests that emit at energies lower than 2.09 eV, although an unwanted green polyfluorene emission is observed because of irreversible oxidation attributed to the presence of monoalkylated fluorene [103-105]. In contrast, silicon-based polymers have emerged as more colour-stable polymers than polyfluorene [106,107]. In addition, the triplet energy level of silicon-based polymers (e.g. poly[9,9-dihexyl-2,7-dibenzosilole]: 2.14 eV) qualifies them an appropriate host materials for red emitters (Figure 1.5).

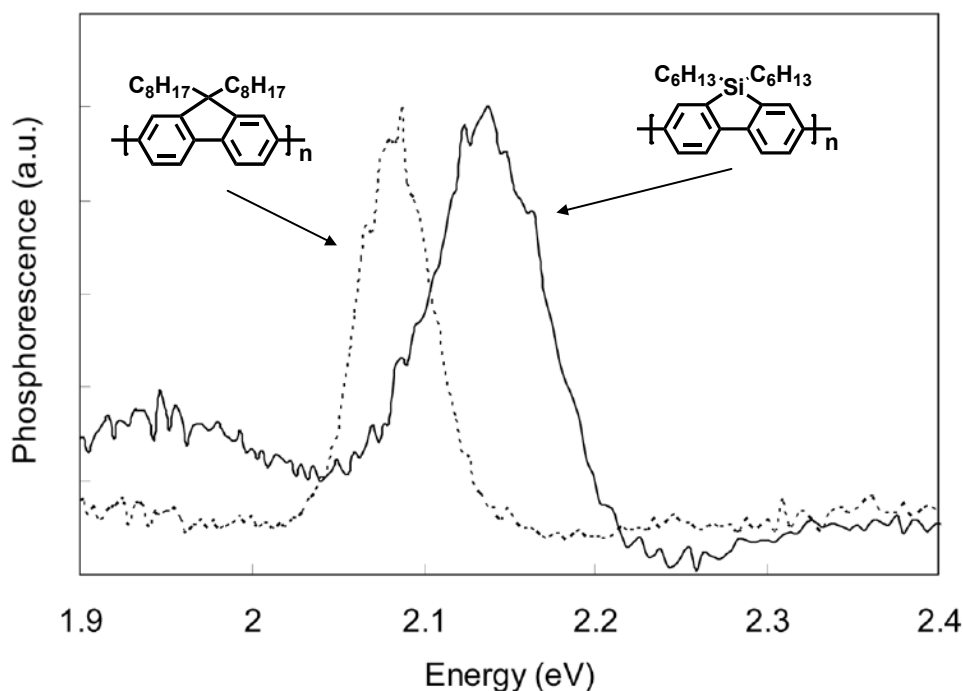
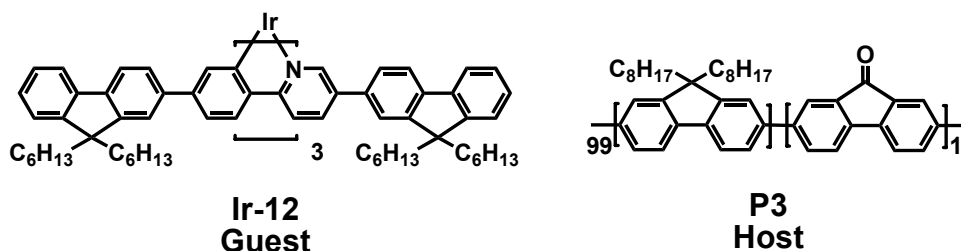


Figure 1.5. Phosphorescence spectra of poly(9,9-di-*n*-octylfluorenyl-2,7-diyl) and poly(9,9-dihexyl-2,7-dibenzosilole) [108].

As mentioned above, a low-energy green emission band from polyfluorene appears over time. It was found that the green emission band originates from *keto* defects introduced either during synthesis or by photooxidation [109-112]. In fact, the existence of *keto* defects in a polyfluorene chain can be utilised in the fabrication of PLED devices as a stable green emitting source, if used properly

Chapter 1. Introduction

[112]. Gong and co-workers doped red-emitting iridium(III) complex *tris*[9,9'-dihexyl-2-(pyridinyl-2')fluorene]iridium(III) (**Ir-12**, Figure 1.6) into poly(9,9-di-*n*-octylfluorene-co-fluorenone) with 1% fluorenone as the host material to achieve a white electrophosphorescent light-emitting diode with a luminance efficiency of 6100 Cd/m² at 17 V and CIE coordinates of 0.352 and 0.388, which are very close to the CIE coordinates of pure white light (0.333, 0.333) [113]. In this electrophosphorescent system, injected holes and electrons recombine by two processes: a direct recombination process on the polymer main chain to produce blue emission in conjunction with electron and hole trapping on the fluorenone units and on the **Ir-12** and a radiative recombination process with green light from 1% fluorenone defects and red light from the triplet excited state of **Ir-12**.



By Gong et al.

Figure 1.6 Selected example of polyfluorene containing 1% fluorenone defects as a host (polymer) material [113].

1.1.5.4 Polymer-embedded iridium(III) complexes

Although high quantum efficiency and luminous efficiency in blend systems can be achieved by doping phosphorescent iridium(III) complexes in polymer matrixes, the blend systems may intrinsically suffer from limitations in efficiency and stability because of possible energy loss due to energy-transfer from the host to low-lying triplet states, aggregation of dopants even at low doping concentrations, and potential phase separation [114,115]. In addition, the processing of blend systems usually requires deposition under high vacuum, controlled temperature, and the

Chapter 1. Introduction

use of multiple layers. These requirements are limiting the application of iridium(III) complexes as blends in polymer hosts for organic LED devices [116,117]. More recently, electrophosphorescent polymers, in which phosphorescent iridium(III) complexes can be attached as pendant- or end-capping groups to the conjugated main chain, have been developed to address these issues. Additionally, phosphorescent iridium(III) complexes can also be incorporated into a conjugated backbone through cyclometalating ligand units. Conjugated polymers such as polyfluorenes [118-121] poly(*p*-phenylene vinylene)s (PPV)s [122,123], and polycarbazoles (PC)s [124,125] are currently applied as host materials in combination with iridium(III) complexes. The photooxidative degradation of poly(*p*-phenylene vinylene) and its derivatives leads to the quenching of fluorescence and reduced carrier mobility, limiting their applications as host materials. On the other hand, polycarbazole and its derivatives may be more stable compared to PPV, but their photo- and electroluminescence is rather low, thus reducing their usefulness as hosts. In contrast, poly(9,9-dialkylfluorene)s with their high efficiency, good charge transport properties, as well as their chemical and thermal stability [126-131] are suitable as host materials for phosphorescent iridium(III) complexes in the red emission range. Efficient energy-transfer between the host and the guest occurs when the triplet energy level of the phosphorescent guest is below the energy level of the conjugated polymer host [132,133]. This prerequisite inhibits the migration of excitons from the guest to the non-phosphorescent host. The triplet energy level of blue fluorescent polyfluorene and polyfluorene derivatives appears at around 2.15 eV [134,135]. Thus, by choosing fluorescent polyfluorenes as hosts, a theoretically efficient red light emission of the iridium(III) complex (guest) is feasible, which is not the case for green and yellow light-emitting iridium complexes [136,137]. The first red light-emitting maximum of polyfluorene **P4** containing iridium(III) complexes as pendant groups (Figure 1.7) was introduced by Chen *et al.* The polymer shows a high efficiency of 2.8 Cd/A. The addition of carbazole groups increases efficiency and reduces the turn-on voltage. Device

Chapter 1. Introduction

performance can be obviously improved by energy-transfer from the PF main chain and the carbazole side chains to the red iridium complex [138]. Evans *et al.* have investigated the influence-relation between the length of the pendant chain and the photo- and electroluminescence efficiencies of the polymer, resulting in a larger distance between the Ir(III)-pendant guest and the polymer host due to higher photo- and electroluminescence efficiencies (see Table 1.2) [139]. This result can be attributed to the incorporation of a $-(\text{CH}_2)_8-$ chain between the polymer host and the phosphorescent guest, thus inhibiting or weakening the back transfer of triplets from the red phosphorescent iridium(III) complex to the polyfluorene backbone in **P5** (Figure 1.7) [139].

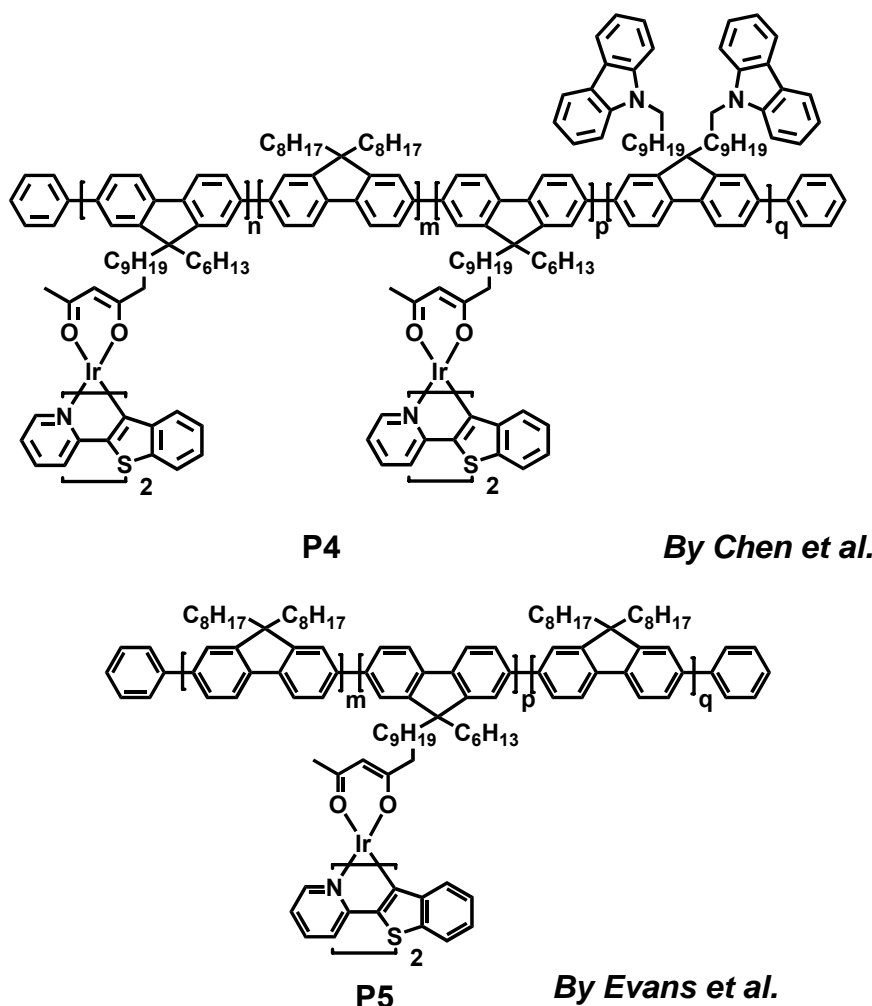


Figure 1.7. Selected examples of polymers with red iridium(III) complexes as side chains [138,139].

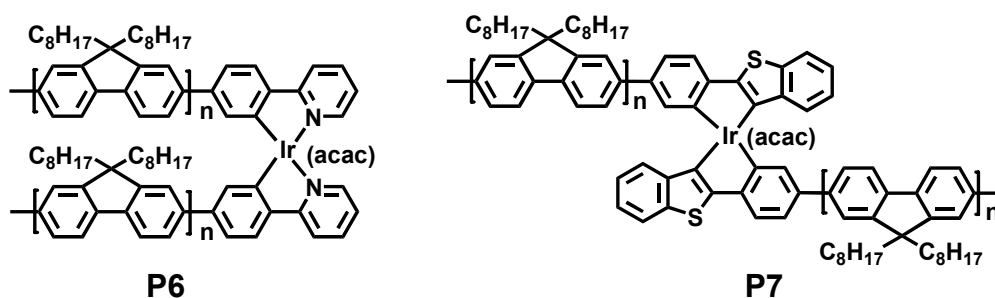
Chapter 1. Introduction

Table 1.2. The photoluminescence and electroluminescence quantum yields of copolymers **P4** and **P5** [138,139].

Ir(III) copolymer	Estimated Ir(III)		Phosphorescence	Electroluminescence
	complex	loading	quantum yield	quantum yield
	(wt%)		(%)	(%) ^a
P4	0.6		12	1.1
P5	0.7		22	2.0
P4	1.8		19	1.7
P5	2.8		40	1.9

^a Electroluminescence quantum yield at 100 Cdm⁻².

Using Suzuki as coupling reaction, a series of well-defined oligomers and polymers (**P6** and **P7**) (Figure 1.8) consisting of 9,9-dialkylfluorene segments and iridium(III) complexes were discussed by Sandee *et al.* [140]. All the copolymers exhibit emission from a mixed triplet state in both photoluminescence and electroluminescence, with efficient quenching of the fluorene singlet emission. Short-chain copolymers, which contain just zero to two fluorene units, show green light emission, while quenching occurs in longer chain copolymers because of the lower energy triplet state associated with polyfluorene. Maximum external quantum efficiencies of 1.5% and 0.12% ph/el were achieved when the complexes [(btp)₂Ir^{III}(acac)] (btp: 2-(benzo[*b*]thiophen-2-yl)pyridine) and [(ppy)₂Ir^{III}(acac)] (ppy: 2-phenylpyridine) were covalently attached to a poly(9,9-dioctylfluorene) backbone, respectively [140].



by Sandee et al.

Figure 1.8. Selected examples of copolymers with red iridium(III) complex in main chain [140].

Schulz *et al.* [141] synthesised conjugated fluorene-*alt*-pyridine (**P8**) and fluorene-*alt*-thiophene (**P9**) copolymers containing green phosphorescent iridium(III) complexes. As shown in Figure 1.9, the singlet energy-transfer (**a**) from the polymer host to the phosphorescent guest always exists because the singlet energy of the guest is lower compared to the singlet energy of polymer host. However, a triplet energy of the polymer backbone below the triplet energy of the phosphorescent guest leads to back-transfer (**b**) of triplets from the phosphorescent guest to the polymer host and to emission quenching of the phosphor, namely by a non-radiative decaying process [119, 141]. The triplet energy of **P9** at 2.88 eV is greater than 2.4 eV, the triplet energy of the green phosphorescent guest. The increased triplet energy of **P9** by incorporation of a 3,4-linked thienyl group decreases triplet energy-transfer from the phosphorescent iridium(III) complex emitter to the non-emitting polymer backbone.

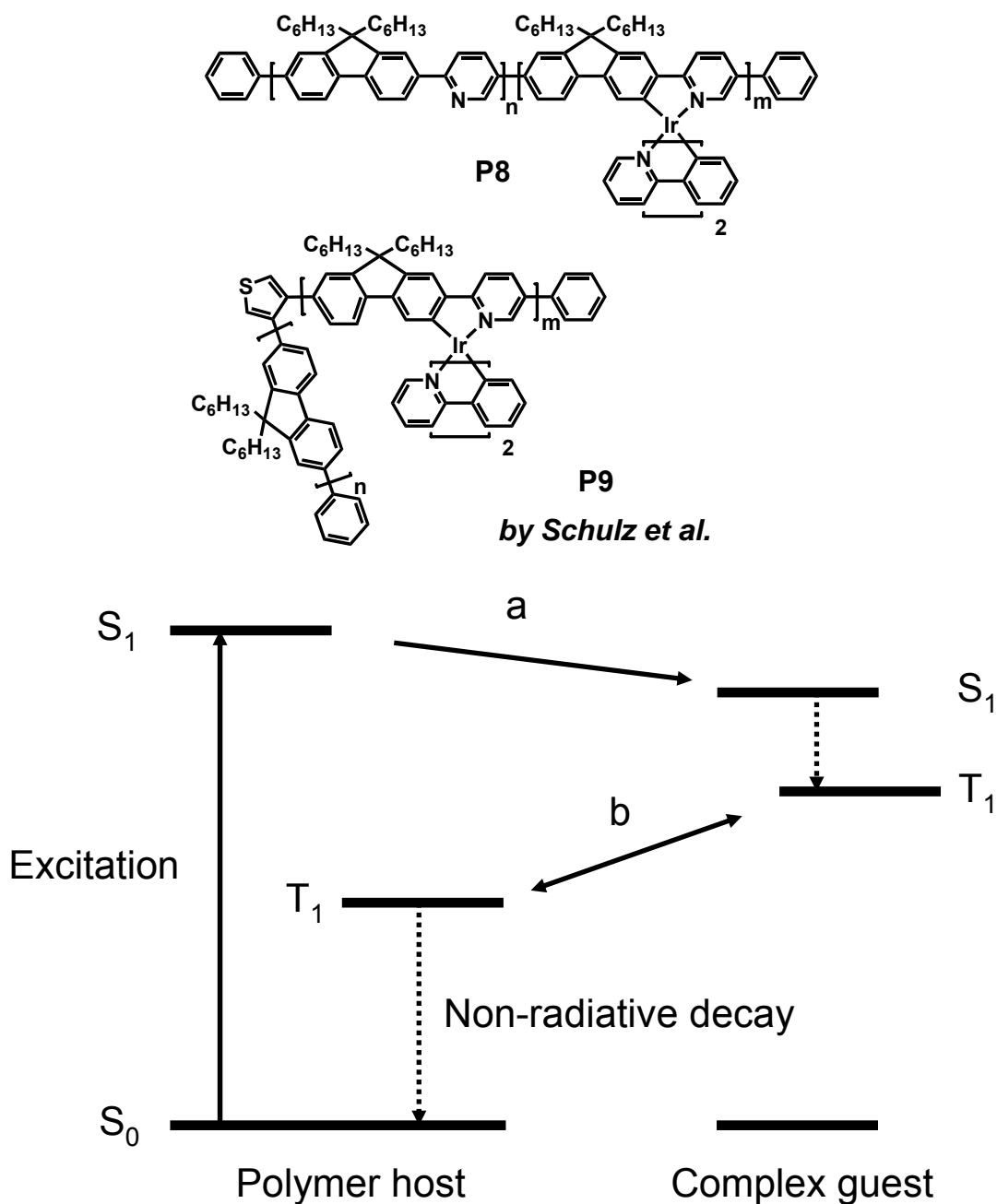


Figure 1.9. Selected examples of copolymers with iridium(III) complexes in the main chain and a depiction of energy-transfer in electrophosphorescent copolymers [141].

Zhang *et al.* reported the first copolymer **P10** (Figure 1.10) with a phosphorescent red iridium(III) complex as an end-capping group and compared its photophysical and electroluminescent properties to copolymer embedded iridium(III) complexes (polyfluorene main chain) [142]. Their electroluminescent spectra show

Chapter 1. Introduction

phosphorescent emission at 626–633 nm, dominated by the charge-trapping mechanism. A device using **P10** as the emitting layer displays a significantly higher efficiency (maximum external quantum efficiency of 1.70% at a current density (J) of 3.58 mAcm^{-2} and a maximum luminance of 706 Cdm^{-2} at 18 V) compared to those based on **P11** and **P12**, which is mainly attributed to the fact that **P10** suffers much less from triplet exciton back-transfer from the iridium(III) complex to the polyfluorene backbone compared to **P11** and **P12**.

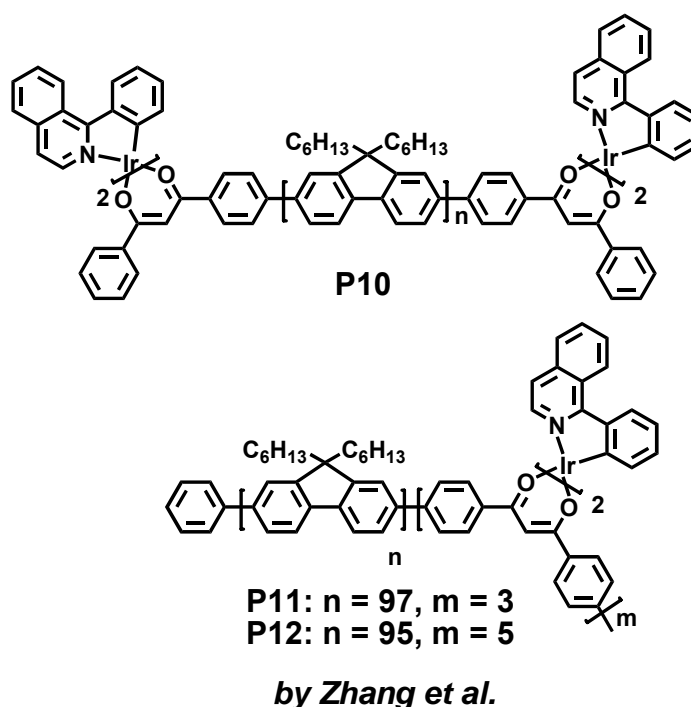


Figure 1.10. Selected examples of copolymers with red iridium(III) complexes as the end-capping group and in the main chain [142].

Using Suzuki as coupling reaction, a series of fluorene-based copolymers comprising a red light-emitting iridium(III) complex and fluorenone on the main chain were introduced by Zhang *et al.* (Figure 1.11) [143]. The added iridium(III) complexes and fluorenone units can function as traps for both electrons and holes. Due to the incorporation of the red-emitting iridium(III) complex and green emitting fluorenone into the polyfluorene backbone, efficient and electrophosphorescent white light-emitting PLED devices have been achieved by utilising these

Chapter 1. Introduction

copolymers as emitting dyes. The device with **P13** exhibits the best maximum luminance efficiency of 5.50 Cd/A with CIE coordinates of 0.32 and 0.45, while **P14**, **P15** and **P16** show a maximum luminance efficiency of 2.22 Cd/A (CIE coordinates: 0.30, 0.35), 3.25 Cd/A (CIE coordinates: 0.28, 0.32), and 2.53 Cd/A (CIE coordinates: 0.28, 0.32), respectively [143].

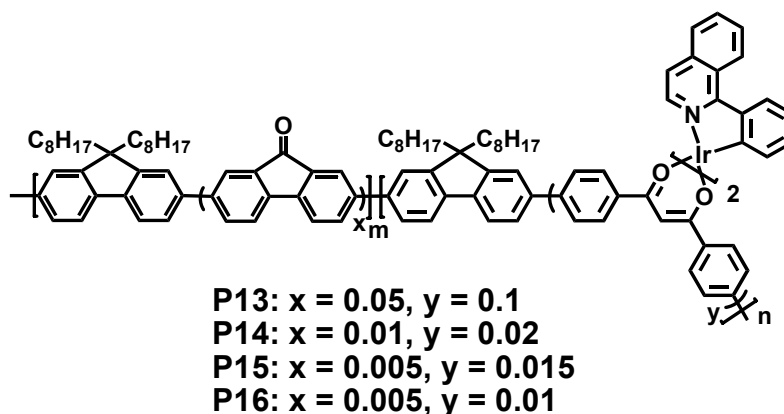


Figure 1.11. Selected examples of polyfluorene-containing red iridium(III) complexes and fluorenone units.

More recently, Guan and co-workers successfully synthesised a green light-emitting branched polymer **P17** with a *tris*(2-phenylpyridine) iridium(III) complex as the core and 3,6-carbazole-*co*-2,6-pyridine as the branch (Figure 1.12) [144]. Because the *interchain* interaction between the facial iridium complex and the self-quenching of the iridium(III) complex due to aggregation can be significantly suppressed in more branched structures, the efficiency-loss upon the increase of current density was considerably reduced. An external quantum efficiency, luminous efficiency, and power efficiency of 13.3%, 30.1 Cd/A, and 16.6 lm/W were observed at 5.6 V, respectively.

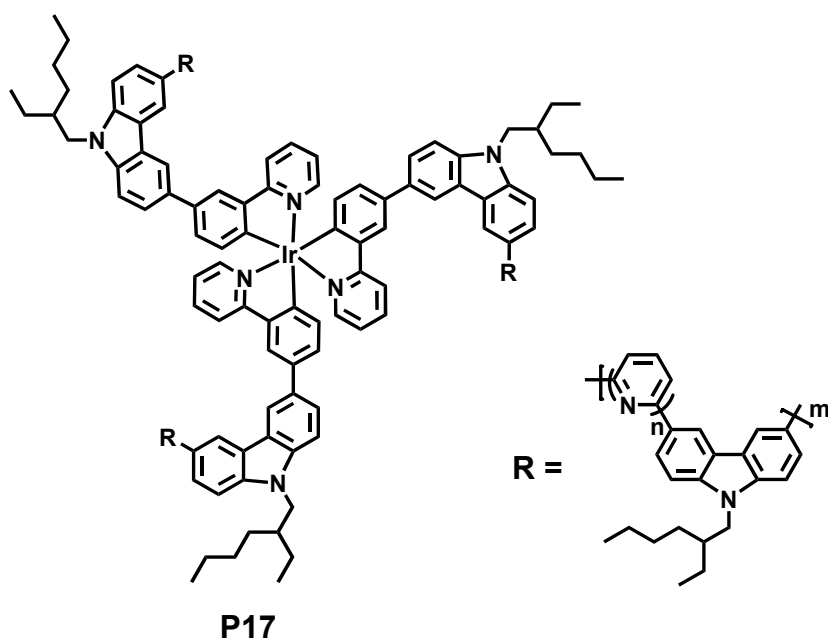
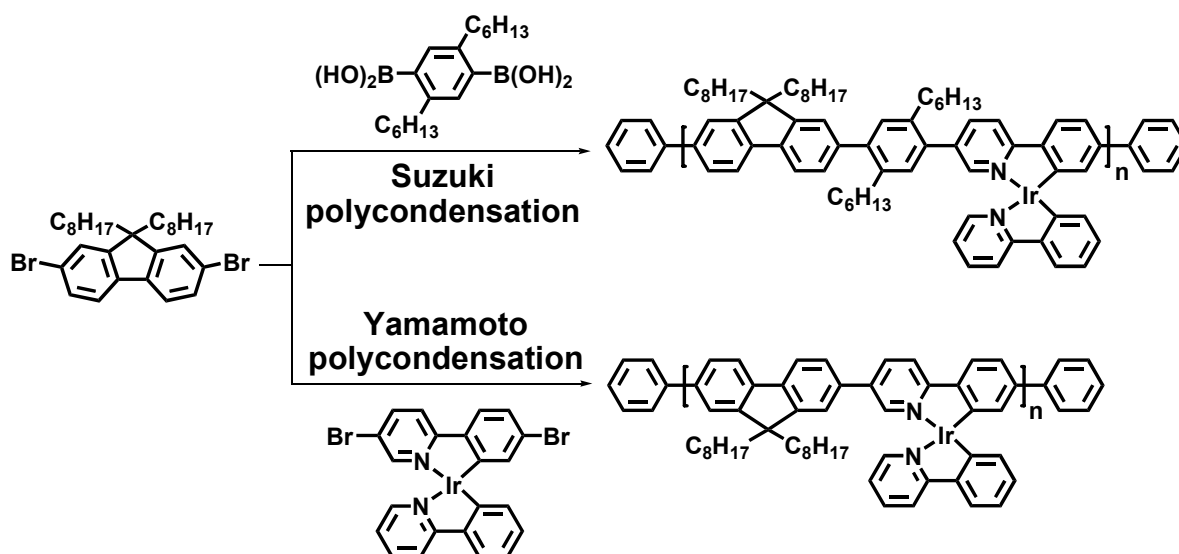


Figure 1.12. Selected example of a branched polymer with an iridium(III) complex as the core and 3,6-carbazole-co-2,6-pyridine as the branch [144].

Yamamoto and Suzuki cross-couplings as synthetic methods are popular when preparing conjugated polymers containing phosphorescent Ir(III) complexes. In the Suzuki reaction, aryl boronic acids or esters are coupled to brominated aryl derivatives in the presence of a Pd catalyst, leading to the formation of aryl carbon-carbon bonds. Using the Yamamoto methodology, aryl bromides were reacted with each other under an excess of a *bis*(1,5-cyclooctadiene)nickel(0) catalyst [Ni(0)(COD)₂] and in the presence of 2,2'-bipyridyl in order to gain coupled aromatic systems. Langecker and Rehahn [145] presented iridium(III)-functionalised polyfluorenes, prepared *via* the Suzuki and Yamamoto coupling reactions and discussed the advantages and disadvantages of each polymerisation (Scheme 1.5).



By Langecker and Rehahn et al.

Scheme 1.5. Selected examples of polymers containing iridium(III) complexes *via* Suzuki or Yamamoto coupling reactions [145].

The comparison of the two synthetic approaches shows that the Suzuki polymerisation is superior since this method delivers products of higher purity compared to the Yamamoto polymerisation. However, the Suzuki reaction provides polymers of lower average molecular weights and moderate yields, while Yamamoto produces homogeneous polymers with a high degree of polymerisation and a satisfying yield. Nevertheless, nickel-contaminated products are obtained and Ni cannot always be fully removed [145].

1.1.5.5 Förster and Dexter energy-transfer in host-guest systems

In organic LED devices, the electrons and holes are initially injected into the organic small-molecules/polymer host transport materials, and then the excitation is transferred to the organometallic emitters, producing phosphorescent excited

Chapter 1. Introduction

states. As usual, the efficient excitation transfer consists of Förster (Figure 1.13) and Dexter (Figure 1.14) energy-transfer from the host transport to the metal-organic centre [146]. In an efficient Förster energy-transfer, the singlet excited-state energy is transferred from the host to the phosphorescent guest because of the dipole-dipole interaction, leading to lower self-absorption losses owing to the red-shift of the emission relative to the absorption in the blends [147]. Besides this, the efficiency of the Förster energy-transfer is also dependent on the overlap between the host emission spectrum and the guest absorption spectrum [146].

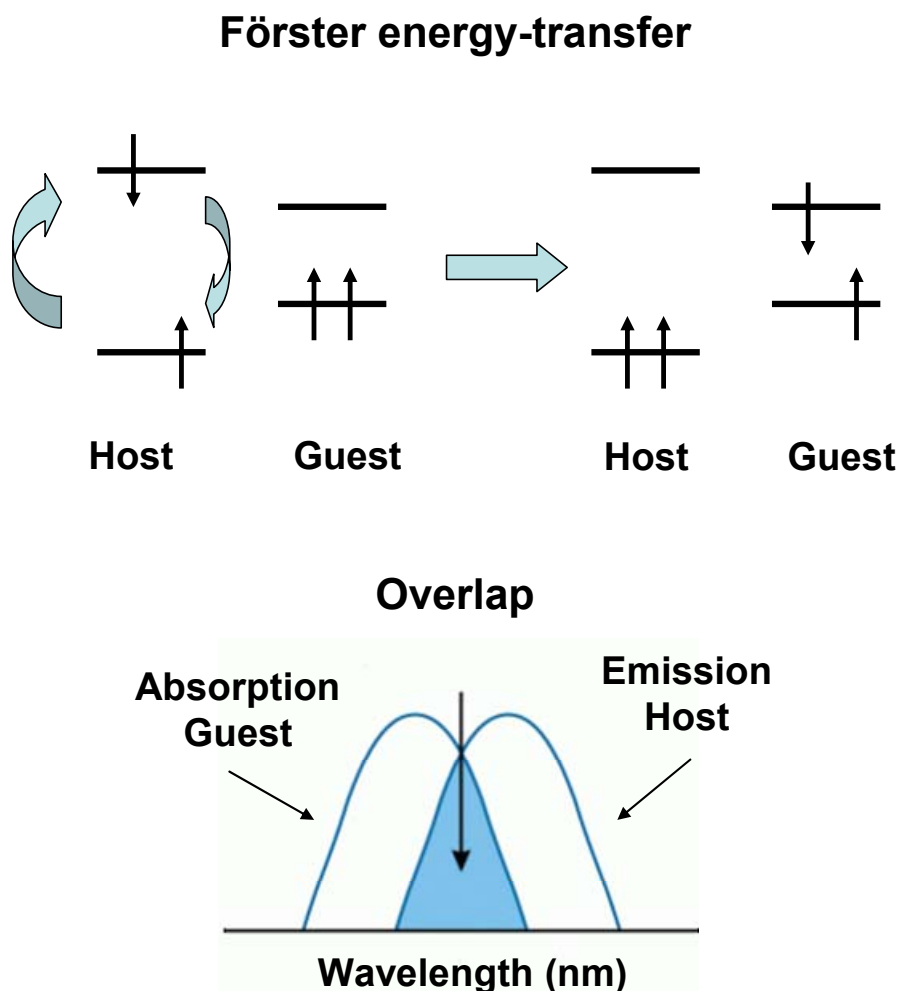
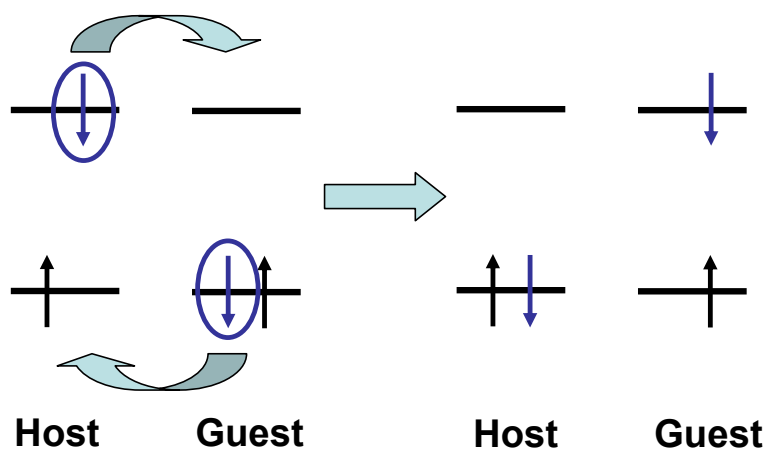


Figure 1.13. Förster energy-transfer and overlap integral between the host emission and the guest absorption [146,147].

Dexter energy-transfer is a process where two molecules (*intermolecular*) or two parts of a molecule (*intramolecular*) bilaterally exchange their electrons. In host-guest systems, the direct quantum mechanical tunnelling of electrons between the host and guest is warranted during the Dexter energy-transfer of a neutral exciton from the host to a neutral exciton on the guest. In addition, a Dexter energy-transfer allows singlet-singlet and triplet-triplet energy-transfer [148].

Singlet-Singlet Dexter energy-transfer



Triplet-Triplet Dexter energy-transfer

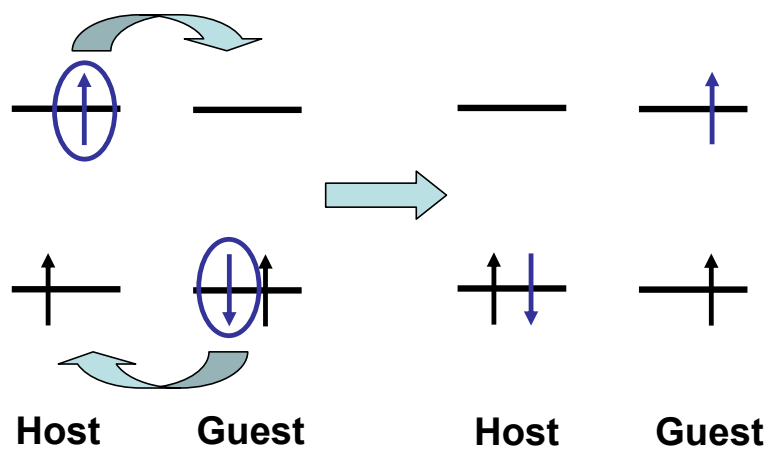


Figure 1.14. The schematic process of Dexter energy-transfer [148].

1.2 Iridium(III) complexes in oxygen and temperature sensor applications

Chemical sensors based on luminescence have been widely investigated in order to be used as molecular reporters [149-152]. As luminescence is non-destructive and easy to use, it represents one of the most sensitive analytical techniques. The implementation of phosphorescent heavy metal complexes as chemosensors [153-159] and biological labels [160-166] has recently attracted considerable attention due to their advantageous photophysical properties like long lifetimes and increased photostability compared to pure organic luminescent compounds.

1.2.1 Applying iridium(III) complexes as oxygen sensors

Iridium(III) complexes are effectively quenched by molecules with a triplet ground state, such as oxygen. Therefore, iridium(III) complexes used as oxygen sensors is a useful application. The criteria for an ideal oxygen sensor include high emission quantum yields, long emission lifetimes, high sensitivity, high reversibility, and a fast response time [154]. The applications of iridium(III) complexes as oxygen sensors are related to static quenching. In this case, the excited iridium(III) complexes are combined with added oxygen molecules (the quencher) to build a new excited state iridium(III)-oxygen complex. Compared to the original ground state iridium(III) complexes, the newly-formed iridium(III)-oxygen complexes have commonly shorter luminescence lifetimes and decreased emission intensity, since the long-living triplet excited state of iridium(III) complexes makes efficient energy-transfer to the triplet ground state of molecular oxygen feasible, resulting in luminescence quenching and the formation of singlet oxygen [167 - 169]. Theoretically, the variations in luminescence emission intensity and lifetime show a linear Stern-Volmer relationship with different concentrations of oxygen and can

be mathematically described by the static Stern-Volmer equation (1) [170]:

$$\frac{I_0}{I} = \frac{\tau_0}{\tau} = 1 + K_{sv}(PO_2) \quad (1)$$

where I_0 and I are the luminescence emission intensities in the absence/presence of oxygen, τ_0 and τ are the luminescence lifetimes in the absence/presence of oxygen, K_{sv} is the static Stern-Volmer constant and PO_2 is the concentration of oxygen.

1.2.2 Applying iridium(III) complexes as temperature sensors

In contrast to static quenching in the presence of oxygen, the deactivation of excited iridium(III) complexes at high temperature is related to dynamic quenching. In other words, the variation in luminescence lifetime and the emission intensity of iridium(III) complexes are mainly caused by collision reactions [160]. The collision probability of these complexes is directly proportional to increased temperature. The luminescence lifetime and emission intensity of the complexes are reduced by colliding incidents at higher temperatures. Compared to static quenching, the variations in luminescence lifetime and emission intensity with changes in temperature display a non-linear relationship and are described by an Arrhenius-type equation [171,172]:

$$\frac{1}{\tau} = k_0 + k_1 \cdot \exp\left(-\frac{\Delta E}{RT}\right) \quad (2)$$

where τ is the luminescence lifetime, k_0 is the temperature-independent decay rate

Chapter 1. Introduction

for the deactivation of the excited state, k_1 is the pre-exponential factor, ΔE is the energy gap between the emitting level and an upper deactivating excited state, R is the gas constant, and T is the temperature in Kelvin.

According to the description of the Stern-Volmer and Arrhenius-type equations, iridium(III) complexes with longer luminescence lifetimes τ_0 and greater emission intensities I_0 are more sensitive and suitable to be used as oxygen and temperature sensors. In the ideal case, a linear Stern-Volmer relationship where the luminescence emission intensity and lifetime values vary, should be observed by increasing or decreasing the concentration of oxygen, and the variation tendency of the luminescence emission intensity and lifetime should show a non-linear Arrhenius-type curve by varying the temperature [169,171,172].

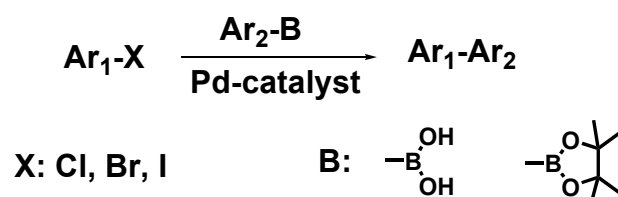
1.3 Metal-catalysed C-C coupling

1.3.1 The Suzuki-Miyaura cross-coupling reaction

Pd-catalysed Suzuki-Miyaura coupling (Scheme 1.6) includes biaryls with aryl boronates and aryl halides as coupling partners in the presence of a weak base and is currently one of the most efficient methods for the building of C-C bonds [173,174]. The Nobel Prize in Chemistry 2010 was awarded jointly to Richard F. Heck, Ei-ichi Negishi and Akira Suzuki for “Palladium-Catalysed Cross-Couplings in Organic Synthesis”. Aryl bromides and iodides are used as starting aryl halides in contrast to aryl chlorides [175-177]. The different coupling rates of these aryl halides are related to the strength of the Ar-X bond, which increases: $I < Br < Cl$ and makes the oxidative addition step increasingly difficult. This means that the relative reactivity for this reaction follows the order: $Ar-I > Ar-Br > Ar-Cl$ at same reaction conditions [178-180]. Nevertheless, aryl chlorides are often used as starting materials because of their lower costs [181-185]. Arylboronic acids and

Chapter 1. Introduction

alkoxyboranes play the role of nucleophiles, which are essential for the cross-coupling reaction with aryl halides owing to their thermal stability and simplicity. Tetrahydrofuran (THF) or toluene are generally utilised as organic solvents. The addition of a small amount of an alcoholic solvent makes the mixing of the organic and inorganic components easier. The most commonly used base in the Suzuki-Miyaura cross-coupling reaction is Na_2CO_3 , but it is often ineffective when dealing with sterically demanding substrates. In our synthetic approach, K_2CO_3 was utilised as the base, resulting in good yields. The different C^N ligands used in this work, 1-phenylisoquinoline (**1**) and 2-(naphthalen-1-yl)pyridine (**2**), were obtained successfully *via* the Suzuki-Miyaura cross-coupling reaction.



Scheme 1.6. Schematic representation of the Suzuki-Miyaura cross-coupling reaction [173].

1.3.2 Stille cross-coupling reaction

In 1978, Stille *et al.* introduced an effective synthetic route for ketones, obtained from acid chlorides and organotin compounds in the presence of a Pd catalyst [186]. The Stille reaction (Scheme 1.7) replaces the organoboron reagents of the Suzuki reaction with organostannanes and is therefore a versatile option. It is important in this type of reaction to understand transmetalation rates of the four organic groups anchored on the tin atom. The Stille mechanism is almost identical to the Suzuki-Miyaura mechanism, consisting of the processes of oxidative addition, transmetalation, and reductive elimination (Scheme 1.8). Furthermore, this reaction can operate without the use of a base in an organic

Chapter 1. Introduction

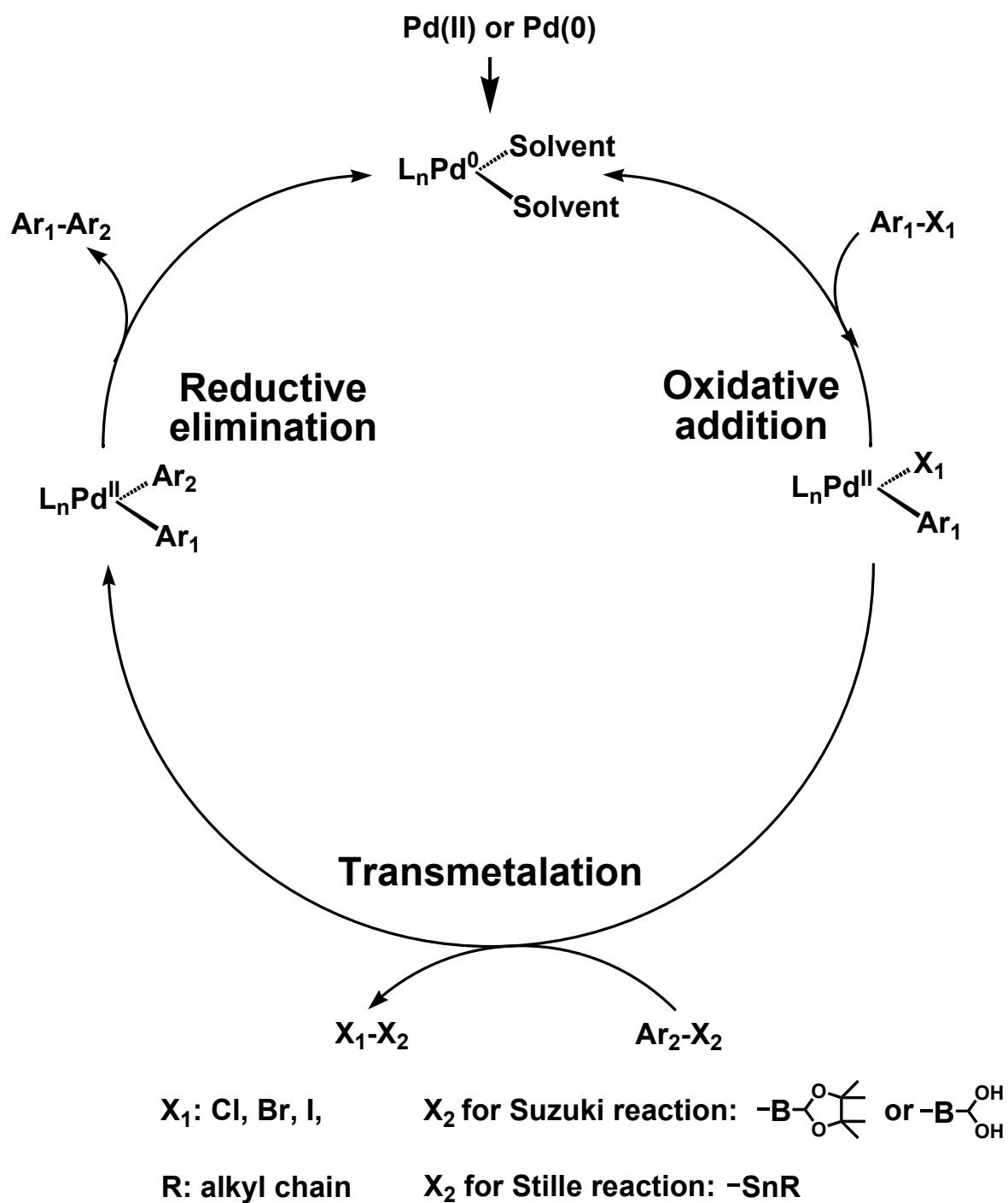
solvent [187,188].



Scheme 1.7. Schematic representation of the Stille cross-coupling reaction [186].

Stille coupling is popular due to the simple preparation, purification, and storage of the organostannanes. A further advantage is the neutral reaction conditions, which can be applied, making the Stille reaction tolerant to more functional groups than the Suzuki reaction. The main drawback is, however, the toxicity of the tin compounds and their low polarity, which makes them poorly soluble in water [189]. This drawback has a considerable impact in the case of polymerisation reactions.

Generally, Suzuki and Stille cross-coupling reactions start with the oxidative addition of aryl-halides (halides: I, Br or Cl) to Pd(0) to give an organopalladium compound. In a second step, the organic groups (arylboronic acids, alkoxyboranes, or arylstannane) are transferred to the palladium atom, a process called transmetalation. The result is the formation of palladium-carbon bonds, through the binding of the two organic groups on the same palladium atom. In the final step, the Ar₁ and Ar₂ segments couple with each other to give a new single carbon-carbon bond and Ar₁-Ar₂ is released from the palladium centre. During this process, Pd(II) is reduced to Pd(0) and therefore the final step is called a reductive elimination [190].

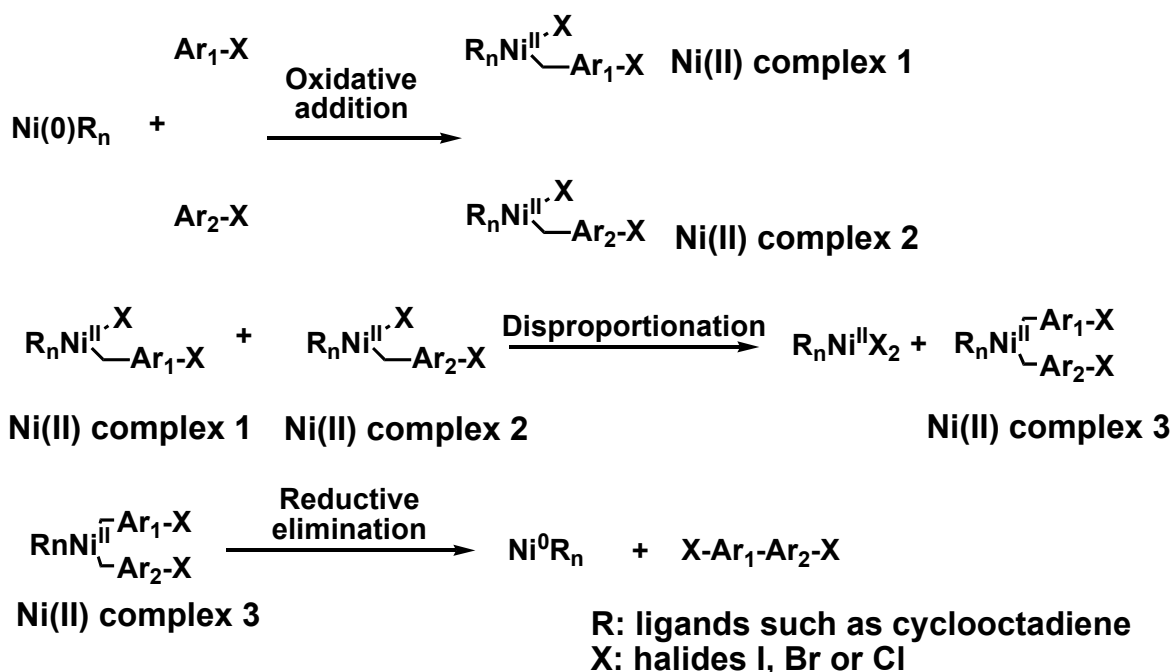


Scheme 1.8. Schematic representation of the mechanisms of the Suzuki and Stille cross-coupling reactions [191-193].

1.3.3 Yamamoto cross-coupling reaction

The Yamamoto C-C coupling reaction (Scheme 1.9, 1.10) is widely utilised to yield π -conjugated polymers such as poly(9,9-dialkylfluorene)s and poly(alkylcarbazole)s and is thus one of the most important synthetic approaches in this particular research field [194-220].

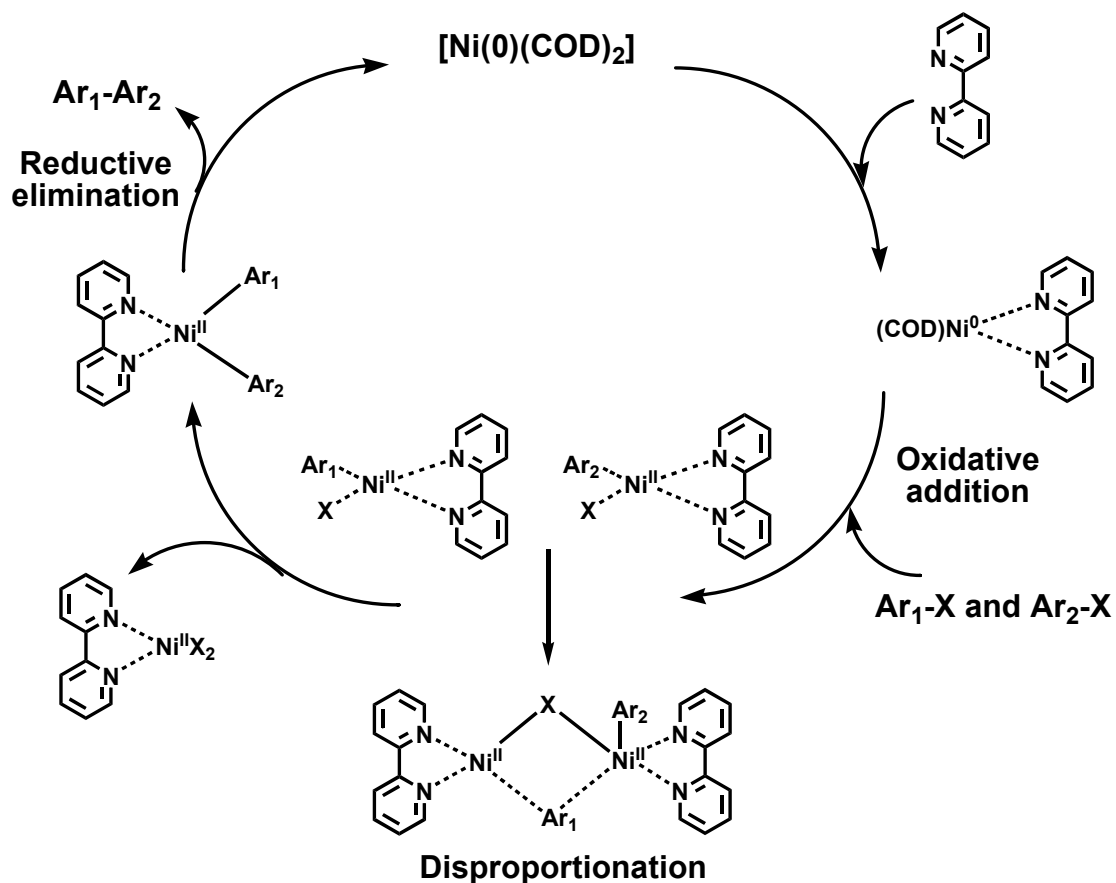
Yamamoto couplings usually use dibromo- or diiodo-monomers as the starting materials, which are interconnected *via* a reductive coupling reaction. Research has also been performed in terms of dichloro-monomers as starting materials for the polymerisation, giving satisfying results. Compared to the previously mentioned Suzuki and Stille reactions, polymerisations *via* the Yamamoto reaction are normally carried out using *bis*(cyclooctadiene)nickel(0) and 2,2'-bipyridyl as the catalyst system. The catalytic cycle of Yamamoto polymerisation consists of the following fundamental reactions [219,220]:



Scheme 1.9. Schematic representation of the Yamamoto cross-coupling reaction [219].

Chapter 1. Introduction

When $[\text{Ni}(0)(\text{COD})_2]$ and 2,2'-bipyridyl are used as the catalyst duo, the synthetic procedure can be described in the following catalytic cycle (Scheme 1.10). The entire catalytic process consists of an oxidative addition, a disproportionation, and a reductive elimination.



Scheme 1.10. Schematic representation of the mechanism of the Yamamoto cross-coupling reaction [191-193,221].

1.4 Motivation

The fabrication of an organic light-emitting diode, in which iridium(III) complexes are used as the emitting layer, requires that these complexes emit various colours excited at low voltages (electroluminescence). While OLEDs with green emitting *fac*-Ir(ppy)₃ have achieved the highest EQE (the maximum external quantum efficiency) of 24% that is equivalent to an IQE (internal quantum efficiency) of 100%, fabricating a highly efficient red organic light-emitting diode applying a truly red phosphorescent iridium(III) complex with a large luminescence quantum yield is still a challenge for current research. In our strategy, we designed a set of green, orange-red and red heteroleptic iridium(III) complexes with ancillary ligands containing carbazole derivatives and acetylacetonate moieties. Due to the ancillary ligands consisting of hexylthiophene and hexylphenyl functional groups, which were mounted at the 3 and 6 position of the carbazole unit, the solubility in organic solvents had to be improved. With increased solubility, the miscibility of host materials and iridium(III) complexes as guest materials will be enhanced as well and the phase separation of binary emitting layers, which greatly influences luminescence efficiency can also be avoided to some degree. On the other hand, the charge recombination at the emitter site should also be increased, providing high quantum yields, short phosphorescence lifetimes, and favourable thermal stability as well. Simultaneously, it is expected that variations in the luminescence emission intensity and lifetimes of these complexes will show a linear Stern-Volmer relationship with varying concentrations of oxygen and a non-linear Arrhenius-type relationship with changing temperature.

Compared to OLED devices fabricated by vacuum evaporation, polymer light-emitting diodes are of particular interest due to their facile and low-cost fabrication by means of spin coating and printing techniques [222,223]. The efficiency and

Chapter 1. Introduction

stability of PLEDs made from iridium(III) complexes doped or blended with polymers are limited by the possibility of phase separation and emitted colour shifts with applied voltage. Based on these limitations, we have attempted to design and synthesise a set of copolymers, in which iridium(III) complexes are directly inserted as comonomers into the copolymer main chain. In this attempt, three segments are incorporated in the copolymer backbone, with the fluorene segments acting as excitation donors and the iridium(III) complexes and fluorenone moieties acting as excitation acceptors. On the basis of efficient Förster energy-transfer and charge carrier trapping on the emitter sites (iridium(III) complexes and fluorenone moieties), white light-emitting PLED devices based on polyfluorene and a red iridium(III) complex or polyfluorene with a red iridium(III) complex and fluorenone moieties may be basically possible by avoiding phase separation, thereby also increasing the efficiency of PLED devices [224-227].

1.5 References

- [1] C. Adachi, M. A. Baldo, S. R. Forrest, M. E. Thompson, *Appl. Phys. Lett.* **2000**, *77*, 904.
- [2] P. Reveco, R. H. Schmehl, W. R. Cherry, F. R. Fronczek, J. Selbin, *Inorg. Chem.* **1985**, *24*, 4078.
- [3] P. Spellane, R. J. Watts, A. Vogler, *Inorg. Chem.* **1993**, *32*, 5633.
- [4] S. Tokito, T. Lijima, Y. Suzuri, H. Kita, Y. Tsuzuki, F. Sato, *Appl. Phys. Lett.* **2003**, *83*, 569.
- [5] C. Ulbricht, B. Beyer, C. Friebe, A. Winter, U. S. Schubert, *Adv. Mater.* **2009**, *21*, 4418.
- [6] T. Motoyama, H. Sasabe, Y. Seino, J. Takamatsu, Junji Kido, *Chem. Lett.* **2011**, *40*, 306.
- [7] T. D. Anthopoulos, M. J. Frampton, E. B. Namdas, P. L. Burn, I. D. W. Samuel, *Adv. Mater.* **2004**, *16*, 557.
- [8] N. Stylianides, A. A. Danopoulos, N. Tsoureas, *J. Organomet. Chem.* **2005**, *690*, 5948.
- [9] S. C. Lo, T. D. Anthopoulos, E. B. Namdas, P. L. Burn, I. D. W. Samuel, *Adv. Mater.* **2005**, *17*, 1945.
- [10] J. P. Markham, S. C. Lo, S. W. Magennis, P. L. Burn, I. D. W. Samuel, *Appl. Phys. Lett.* **2002**, *80*, 2645.
- [11] L. Chassot, A. von Zelewsky, D. Sandrini, M. Maestri, V. Balzani, *J. Am. Chem. Soc.* **1986**, *108*, 6084.
- [12] L. Chassot, A. von Zelewsky, *Inorg. Chem.* **1987**, *26*, 2814.
- [13] M. Maestri, D. Sandrini, V. Balzani, L. Chassot, P. Jolliet, *Chem. Phys. Lett.* **1985**, *122*, 375.
- [14] A. Barbieri, G. Accorsi, N. Armaroli, *Chem. Commun.* **2008**, *19*, 2185.
- [15] J. Kido, M. Kimura, K. Nagai, *Science* **1995**, *267*, 1332.
- [16] H. Rudmann, S. Shimada, M. F. Rubner, *J. Am. Chem. Soc.* **2002**, *124*, 4918.
- [17] O. Kohle, M. Graetzel, A. F. Meyer, T. B. Meyer, *Adv. Mater.* **1997**, *9*, 904.

Chapter 1. Introduction

- [18] S. H. Wadman, J. M. Kroon, K. Bakker, M. Lutz, A. L. Spek, G. P. M. van Klink, G. van Koten, *Chem. Commun.* **2007**, 19, 1907.
- [19] S. W. Thomas III, K. Venkatesan, P. Mueller, T. M. Swager, *J. Am. Chem. Soc.* **2006**, 128, 16641.
- [20] M. I. J. Stich, S. Nagl, O. S. Wolfbeis, U. Henne, M. Schaeferling, *Adv. Funct. Mater.* **2008**, 18, 1399.
- [21] P. E. Burrows, M. E. Thompson, S. R. Forrest, *Curr. Opin. Solid State Mater. Sci.* **1999**, 4, 369.
- [22] M. A. Baldo, S. Lamansky, P. E. Burrows, M. E. Thompson, S. R. Forrest, *Appl. Phys. Lett.* **1999**, 75, 4.
- [23] K. A. King, P. J. Spellane, R. J. Watts, *J. Am. Chem. Soc.* **1985**, 107, 1431.
- [24] C. Ulbricht, doctoral dissertation “*Phosphorescent systems based on iridium(III) complexes*”, **2009**, Eindhoven University of Technology.
- [25] Y. Cao, I. D. Parker, G. Yu, C. Zhang, A. J. Heeger, *Nature* **1999**, 397, 414.
- [26] M. Wohlgenannt, K. Tandon, S. Mazumdar, S. Ramasesha, Z. V. Vardeny, *Nature* **2001**, 409, 494.
- [27] H. J. Bolink, L. Cappelli, E. Coronado, A. Parham, P. Stössel, *Chem. Mater.* **2006**, 18, 2778.
- [28] S. Tokito, T. Lijima, T. Tsuzuki, F. Sato, *Appl. Phys. Lett.* **2003**, 83, 2459.
- [29] M. K. Nazeeruddin, R. Humphry-Baker, D. Berner, S. Rivier, L. Zuppiroli, M. Graetzel, *J. Am. Chem. Soc.* **2003**, 125, 8790.
- [30] W. Zhu, Y. Mo, M. Yuan, W. Yang, Y. Cao, *Appl. Phys. Lett.* **2002**, 80, 2045.
- [31] R. Ragni, E. A. Plummer, K. Brunner, J. W. Hofstraat, F. Babudri, G. M. Farinola, F. Naso, L. De Cola, *J. Mater. Chem.* **2006**, 16, 1161.
- [32] T. Sajoto, P. I. Djurovich, A. Tamayo, M. Yousufuddin, R. Bau, M. E. Thompson, *Inorg. Chem.* **2005**, 44, 7992.
- [33] Y. M. You, S. Y. Park, *J. Am. Chem. Soc.* **2005**, 127, 12438.

Chapter 1. Introduction

- [34] C. Adachi, M. A. Baldo, S. R. Forrest, M. E. Thompson, *Appl. Phys. Lett.* **2000**, *77*, 904.
- [35] Y. Kawamura, K. Goushi, J. Brooks, J. J. Brown, H. Sasabe, C. Adachi, *Appl. Phys. Lett.* **2005**, *86*, 071104.
- [36] K. Kalyanasundaram, *Photochemistry of Polypyridine and Porphyrin Complexes*, Academic Press, New York, NY, **1992**.
- [37] M. S. Lowry, S. Bernhard, *Chem. Eur. J.* **2006**, *12*, 7970.
- [38] S. Lamansky, P. Djurovich, D. Murphy, F. Abdel-Razzaq, H. E. Lee, C. Adachi, P. E. Burrows, S. R. Forrest, M. E. Thompson, *J. Am. Chem. Soc.* **2001**, *123*, 4304.
- [39] A. Tsuboyama, H. Iwawaki, M. Furugori, T. Mukaide, J. Kamatani, S. Igawa, T. Moriyama, S. Miura, T. Takiguchi, S. Okada, M. Hoshino, K. Ueno, *J. Am. Chem. Soc.* **2003**, *125*, 12971.
- [40] B. X. Mi, P. F. Wang, Z. Q. Gao, C. S. Lee, S. T. Lee, H. L. Hong, X. M. Chen, M. S. Wong, P. F. Xia, K. W. Cheah, C. H. Chen, W. Huang, *Adv. Mater.* **2009**, *21*, 339.
- [41] H. G. Colombo, T. C. Brunold, T. Riedener, H. W. Guedel, *Inorg. Chem.* **1994**, *33*, 545.
- [42] V. V. Grushin, N. Herron, D. D. LeCloux, W. J. Marshall, V. A. Petrov, Y. Wang, *Chem. Commun.* **2001**, 1494.
- [43] M. Nonoyama, *Bull. Chem. Soc. Jpn.* **1974**, *47*, 767.
- [44] A. J. Wilkinson, H. Puschmann, J. A. K. Howard, C. E. Foster, J. A. G. Williams, *Inorg. Chem.* **2006**, *43*, 8685.
- [45] K. Dedeian, J. Shi, N. Shepherd, E. Forsythe, D. C. Morton, *Inorg. Chem.* **2005**, *44*, 4445.
- [46] G. Zhou, W. Y. Wong, B. Yao, Z. Xie, L. Wang, *Angew. Chem. Int. Ed.* **2007**, *46*, 1149.
- [47] E. Orselli, G. S. Kottas, A. E. Konradsson, P. Coppo, R. Froehlich, L. De Cola, A. van Dijken, M. Buechel, H. Boerner, *Inorg. Chem.* **2007**, *46*, 11082.

Chapter 1. Introduction

- [48] X. H. Yang, D. C. Müller, D. Neher, K. Meerholz, *Adv. Mater.* **2006**, *18*, 948.
- [49] S. H. Kim, J. Jang, J. Y. Lee, *Synthetic Metals.* **2007**, *157*, 228.
- [50] A. Endo, K. Suzuki, T. Yoshihara, S. Tobita, M. Yahiro, C. Adachi, *Chem. Phys. Lett.* **2008**, *460*, 155.
- [51] A. B. Tamayo, B. D. Alleyne, P. I. Djurovice, S. Lamansky, I. Tysba, N. N. Ho, R. Bau, M. E. Thompson, *J. Am Chem. Soc.* **2003**, *125*, 7377.
- [52] F. Neve, A. Crispini, *Eur. J. Inorg. Chem.* **2000**, 1039.
- [53] H. Konno, Y. Sasaki, *Chem. Lett.* **2003**, *32*, 252.
- [54] K. Saito, N. Matsusue, H. Kanno, Y. Hamada, H. Takahashi, T. Matsumura, *Jap. J. App. Phys.* **2004**, *43*, 2733.
- [55] T. Sajoto, P. I. Djurovich, A. Tamayo, M. Yousufuddin, R. Bau, M. E. Thompson, R. J. Holmes, S. R. Forrest, *Inorg. Chem.* **2005**, *44*, 7992.
- [56] Y. S. Yeh, Y. M. Cheng, P. T. Chou, G. H. Lee, C. H. Yang, Y. Chi, C. F. Shu, C. H. Wang, *Chem. Phys. Chem.* **2006**, *7*, 2294.
- [57] M. Nonoyama, *Bull. Jpn. Chem. Soc.* **1974**, *47*, 767.
- [58] I. M. Dixon, J. P. Collin, J. P. Sauvage, L. Flamigni, S. Encinas, F. Barigelletti, *Chem. Soc. Rev.* **2000**, *29*, 385.
- [59] S. Sprouse, K. A. King, P. J. Spellane, R. J. Watts, *J. Am. Chem. Soc.* **1984**, *106*, 6647.
- [60] Y. You, Y. Park, *J. Am. Chem. Soc.* **2005**, *127*, 12438.
- [61] T. H. Kwon, M. K. Kim, J. Kwon, D. Y. Shin, S. J. Park, C. L. Lee, J. J. Kim, J. I. Hong, *Chem. Mater.* **2007**, *19*, 3673.
- [62] C. Adachi, M. A. Baldo, M. E. Thompson, S. R. Forrest, *J. Appl. Phys.* **2001**, *90*, 5048.
- [63] Y. Kawamura, K. Goushi, J. Brooks, J. J. Brown, H. Sasabe, C. Adachi, *Appl. Phys. Lett.* **2005**, *86*, 071104.
- [64] P. Jeffrey Hay, *J. Phys. Chem. A.* **2002**, *106*, 1634.
- [65] C. Jiang, W. Yang, J. Peng, S. Xiao, Y. Cao, *Adv. Mater.* **2004**, *16*, 537.

Chapter 1. Introduction

- [66] F. C. Chen, Y. Yang, M. E. Thompson, J. Kido, *Appl. Phys. Lett.* **2002**, *80*, 2308.
- [67] S. Q. Huo, J. C. Deaton, M. Rajeswaran, W. C. Lenhart, *Inorg. Chem.* **2006**, *45*, 3155.
- [68] T. H. Kwon, H. S. Cho, M. K. Kim, J. W. Kim, Y. K. Chung, J. I. Hong, *Organometallics* **2005**, *24*, 1578.
- [69] A. B. Tamayo, B. D. Alleyne, P. I. Djurovich, S. Lamansky, I. Tsyba, N. N. Ho, R. Bau, M. E. Thompson, *J. Am. Chem. Soc.* **2003**, *125*, 7377.
- [70] T. Hofbeck, H. Yersin, *Inorg. Chem.* **2010**, *49*, 9290.
- [71] Y. You, S. Y. Park, *J. Am. Chem. Soc.* **2005**, *127*, 12438.
- [72] E. Holder, B. M. W. Langeveld, U. S. Schubert, *Adv. Mater.* **2005**, *17*, 1109.
- [73] G. Zhou, W. Y. Wong, B. Yao, Z. Xie, L. Wang, *Angew. Chem. Int. Ed.* **2007**, *46*, 1149.
- [74] M. K. Nazeeruddin, R. Humphry-Baker, D. Berner, S. Rivier, L. Zuppiroli, M. Graetzel, *J. Am. Chem. Soc.* **2003**, *125*, 8790.
- [75] T. D. Anthopoulos, M. J. Frampton, E. B. Namdas, P. L. Burn, I. D. W. Samuel, *Adv. Mater.* **2004**, *16*, 557.
- [76] A. Tsuboyama, H. Iwawaki, M. Furugori, T. Mukaide, J. Kamatani, S. Igawa, T. Moriyama, S. Miura, T. Takiguchi, S. Okada, M. Hoshino, K. Ueno, *J. Am. Chem. Soc.* **2003**, *125*, 12971.
- [77] J. Li, P. I. Djurovich, B. D. Alleyne, I. Tsyba, N. Ho, R. Bau, M. E. Thompson, *Polyhedron* **2004**, *23*, 419.
- [78] S.-J. Yeh, M.-F. Wu, C.-T. Chen, Y.-H. Song, Y. Chi, M.-H. Ho, S.-F. Hsu, C. H. Chen, *Adv. Mater.* **2005**, *17*, 285.
- [79] C. H. Yang, Y. M. Cheng, Y. Chi, C. J. Hsu, F. C. Fang, K. T. Wong, P. T. Chou, C. H. Chang, M. H. Tsai, C. C. Wu, *Angew. Chem. Int. Ed.* **2007**, *46*, 2418.
- [80] H. Yersin, *Highly Efficient OLEDs with Phosphorescent Materials*, Wiley-VCH Verlag GmbH & Co. KGaA, Weinheim, **2008**.
- [81] K. T. Wong, Y. M. Chen, Y. T. Lin, H. C. Su, C. C. Wu, *Org. Lett.* **2005**, *7*, 5361.

Chapter 1. Introduction

- [82] S. Kappaun, C. Slugovc, J. W. List, *Int. J. Mol. Sci.* **2008**, *9*, 1527.
- [83] A. B. Padmaperuma, L. S. Sapochak, P. E. Burrows, *Chem. Mater.* **2006**, *18*, 2389.
- [84] M. H. Tsai, H. W. Lin, H. C. Su, T. H. Ke, C. C. Wu, F. C. Fang, Y. L. Liao, K. T. Wong, C. I. Wu, *Adv. Mater.* **2006**, *18*, 1216.
- [85] Z. Su, W. I. Li, M. I. Xu, T. I. Li, D. Wang, B. Chu, *J. Phys. D: Appl. Phys.* **2007**, *40*, 2783.
- [86] S. Lamansky, R. C. Kwong, M. Nugent, P. I. Djurovich, M. E. Thompson, *Org. Electron.* **2001**, *2*, 53.
- [87] C. L. Lee, K. B. Lee, J. J. Kim, *Appl. Phys. Lett.* **2000**, *77*, 2280.
- [88] M. Ikai, S. Tokito, Y. Sakamoto, T. Suzuki, Y. Taga, *Appl. Phys. Lett.* **2001**, *79*, 156.
- [89] F. I. Wu, H. J. Su, C. F. Shu, L. Luo, W. G. Diao, C. H. Cheng, J. P. Duan, G. H. Lee, *J. Mater. Chem.* **2005**, *15*, 1035.
- [90] J. Kim, I. S. Shin, H. Kim, J. K. Lee, *J. Am. Chem. Soc.* **2005**, *127*, 1614.
- [91] C. Y. Jiang, W. Yang, J. B. Peng, S. Xiao, Y. Cao, *Adv. Mater.* **2004**, *16*, 537.
- [92] X. Gong, J. C. Ostrowski, M. R. Robinson, D. Moses, G. C. Bazan, A. J. Heeger, *Adv. Mater.* **2002**, *14*, 581.
- [93] X. Chen, J. L. Liao, Y. Liang, M. O. Ahmed, H. E. Tseng, S. A. Chen, *J. Am. Chem. Soc.* **2003**, *125*, 636.
- [94] Y. G. Ma, H. Y. Zhang, J. C. Shen, *Synth. Met.* **1998**, *94*, 245.
- [95] A. J. Sandee, C. K. Williams, N. R. Evans, J. E. Davies, C. E. Boothby, A. Kohler, R. H. Friend, A. B. Holmes, *J. Am. Chem. Soc.* **2004**, *126*, 7041.
- [96] S. Lamansky, P. Djurovich, D. Murphy, F. Abdel-Razzaq, H.-E. Lee, C. Adachi, P. E. Burrows, S. R. Rorrest, M. E. Thompson, *J. Am. Chem. Soc.* **2001**, *123*, 4304.
- [97] F. C. Chen, Y. Yang, *Appl. Phys. Lett.* **2002**, *80*, 2308.
- [98] F. Shen, H. Xia, C. Zhang, D. Lin, X. Liu, Y. Ma, *Appl. Phys. Lett.* **2004**, *84*, 55.
- [99] S. Lamansky, P. I. Djurovich, F. A. Razzaq, S. Garon, D. L. Murphy, M. E. Thompson, *J. Appl. Phys.* **2002**, *92*, 1570.

Chapter 1. Introduction

- [100] C. L. Lee, K. B. Lee, J. J. Kim, *Appl. Phys. Lett.* **2000**, *77*, 2280.
- [101] X. Gong, J. C. Ostrowski, M. R. Robinson, D. Moses, G. C. Bazan, A. J. Heeger, *Adv. Mater.* **2002**, *14*, 581.
- [102] X. Gong, J. C. Ostrowski, M. R. Robinson, D. Moses, G. C. Bazan, A. J. Heeger, M. S. Liu, *Adv. Mater.* **2003**, *15*, 45.
- [103] E. J. W. List, R. Guentner, P. Scanducci de Freitas, U. Scherf, *Adv. Mater.* **2002**, *14*, 374.
- [104] U. Scherf, E. J. W. List, *Adv. Mater.* **2002**, *14*, 477.
- [105] M. Leclerc, *J. Polym. Sci. Part A.* **2001**, *39*, 2867.
- [106] J. Chen, Y. Cao, *Macromol. Rapid Commun.* **2007**, *28*, 1714.
- [107] K. L. Chan, M. J. McKiernan, C. R. Towns, A. B. Holmes, *J. Am. Chem. Soc.* **2005**, *127*, 7662.
- [108] S. E. Watkins, K. L. Chan, S. Y. Cho, N. R. Evans, A. C. Grimsdale, A. B. Holmes, C. S. K. Mak, A. J. Sandee, C. K. Williams, *Macromol. Res.* **2007**, *15*, 129.
- [109] E. J. W. List, R. Guentner, P. S. de Freitas, U. Scherf, *Adv. Mater.* **2002**, *14*, 374.
- [110] E. J. W. List, M. Gaal, R. Guentner, P. Scanducci de Freitas, U. Scherf, *Synth. Met.* **2003**, *139*, 759.
- [111] X. Gong, D. Moses, A. J. Heeger, S. Xiao, *J. Phys. Chem. B* **2004**, *108*, 8601.
- [112] X. Gong, P. K. Iyer, D. Moses, G. C. Bazan, A. J. Heeger, *Adv. Funct. Mater.* **2003**, *13*, 325.
- [113] X. Gong, D. M. Moses, A. J. Heeger, *J. Phys. Chem. B* **2004**, *108*, 8601.
- [114] K. Zhang, Z. Chen, Y. Zou, C. Yang, J. G. Qin, Y. Cao, *Organometallics* **2007**, *26*, 3699.
- [115] K. Zhang, Z. Chen, C. L. Yang, Y. Zou, S. L. Gong, J. G. Qin, Y. Cao, *J. Phys. Chem.* **2008**, *112*, 3907.
- [116] R. J. Holmes, S. R. Forrest, Y. J. Tung, R. C. Kwong, J. J. Brown, S. Garon, M. E. Thompson, *Appl. Phys. Lett.* **2003**, *82*, 2422.

Chapter 1. Introduction

- [117] C. Adachi, M. A. Baldo, S. R. Forrest, M. E. Thompson, *Appl. Phys. Lett.* **2000**, *77*, 904.
- [118] X. G. Jacek, C. Ostrowski, G. C. Bazan, D. Moses, A. J. Heeger, *Appl. Phys. Lett.* **2002**, *81*, 3711.
- [119] M. Sudhakar, P. I. Djurovich, T. E. H. Esch, M. E. Thompson, *J. Am. Chem. Soc.* **2003**, *125*, 7796.
- [120] W. G. Zhu, Y. Q. Mo, M. Yuan, W. Yang, Yong Cao, *Appl. Phys. Lett.* **2002**, *80*, 2045.
- [121] N. R. Evans, L. S. Devi, C. S. K. Mak, S. E. Watkins, S. I. Pascu, A. Köhler, R. H. Friend, C. K. Williams, A. B. Holmes, *J. Am. Chem. Soc.* **2006**, *128*, 6647.
- [122] H. Eckhardt, L. W. Shacklette, K. Y. Jen, R. L. Elsenbaumer, *J. Chem. Phys.* **1989**, *91*, 1303.
- [123] Y. Z. Lee, X. W. Chen, S. A. Chen, P. K. Wei, W. S. Fann, *J. Am. Chem. Soc.* **2001**, *123*, 2296.
- [124] R. Guan, Y. Xu, L. Ying, W. Yang, H. Wu, Q. Chen, Y. Cao, *J. Mater. Chem.* **2009**, *19*, 531.
- [125] K. Brunner, A. van Dijken, H. Börner, J. J. A. M. Bastiaansen, N. M. M. Kiggen, B. M. W. Langeveld, *J. Am. Chem. Soc.* **2004**, *126*, 6035.
- [126] X. Zhan, Y. Liu, G. Yu, X. Wu D. B. Zhu, R. Sun, D. Wang, A. J. Epstein, *J. Mater. Chem.* **2001**, *11*, 1606.
- [127] A. C. Grimsdale, K. Müllen, *Adv. Polym. Sci.* **2006**, *199*, 1.
- [128] W. L. Yu, J. Pei, W. Huang, A. J. Heeger, *Adv. Mater.* **2000**, *12*, 828.
- [129] B. Liu, W. L. Yu, Y. H. Lai, W. Huang, *Chem. Mater.* **2001**, *13*, 1984.
- [130] G. Zeng, W. L. Yu, S. J. Chua, W. Huang, *Macromolecules* **2002**, *35*, 6907.
- [131] W. Huang, H. Meng, W. L. Yu, J. Gao, A. J. Heeger, *Adv. Mater.* **1998**, *10*, 593.
- [132] A. Koehler, D. Beljonne, *Adv. Funct. Mater.* **2004**, *14*, 11.
- [133] V. Cleave, G. Yahioglu, P. Le Barny, D. H. Hwang, A. B. Holmes, R. H. Friend, N.

Chapter 1. Introduction

- Tessler, *Adv. Mater.* **2001**, *13*, 44.
- [134] D. Hertel, S. Setayesh, H. G. Nothofer, U. Scherf, K. Muellen, H. Baessler, *Adv. Mater.* **2001**, *13*, 65.
- [135] C. Rothe, A. P. Monkman, *Phys. Rev. B.* **2002**, *65*, 073201.
- [136] F. C. Chen, S. C. Chang, G. He, S. Pyo, Y. Yang, M. Kurotaki, J. Kido, *J. Polym. Sci., Part B: Polym. Phys.* **2003**, *41*, 2681.
- [137] F. C. Chen, G. He, Y. Yang, *Appl. Phys. Lett.* **2003**, *82*, 1006.
- [138] X. Chen, J. L. Liao, Y. Liang, M. O. Ahmed, H. E. Tseng, S. A. Chen, *J. Am. Chem. Soc.* **2003**, *125*, 636.
- [139] N. R. Evans, L. S. Devi, C. S. K. Mak, S. E. Watkins, S. I. Pascu, A. Kohler, R. H. Friend, C. K. Williams, A. B. Holmes, *J. Am. Chem. Soc.* **2006**, *128*, 6647.
- [140] A. J. Sandee, C. K. Williams, N. R. Evans, J. E. Davies, C. Boothby, A. Kohler, R. H. Friend, A. B. Holmes, *J. Am. Chem. Soc.* **2004**, *126*, 7041.
- [141] G. L. Schulz, X. Chen, S. A. Chen, S. Holdcroft, *Macromolecules* **2006**, *39*, 9157.
- [142] K. Zhang, Z. Chen, C. Yang, Y. Zou, S. I. Gong, J. Qin, Y. Cao, *J. Phys. Chem. C* **2008**, *112*, 3907.
- [143] K. Zhang, Z. Chen, C. Yang, Y. Tao, Y. Zou, J. Qin, Y. Cao, *J. Mater. Chem.* **2008**, *18*, 291.
- [144] R. Guan, Y. Xu, L. Ying, W. Yang, H. B. Wu, Q. Chen, Yong Cao, *J. Mater. Chem.* **2009**, *19*, 531.
- [145] J. Langecker, M. Rehahn, *Macromol. Chem. Phys.* **2008**, *209*, 258.
- [146] X. Gong, J. C, Ostrowski, D, Moses, G, C. Bazan, A, J, Heeger, *Adv. Funct. Mater.* **2003**, *13*, 439.
- [147] R. Gupta, M. Stevenson, A. Dogariu, H, Wang, M. D. McGehee, J. Y. Park, A. J. Heeger, *Appl. Phys. Lett.* **1998**, *73*, 3492.
- [148] C. B. Murphy, Y. Zhang, T. Troxler, V. Ferry, J. J. Martin, W. E. Jones, *Phys. Chem. B*, **2004**, *108*, 1537.

Chapter 1. Introduction

- [149] A. P. De Silva, H. Q. N. Gunaratne, T. Gunnlaugsson, A. J. M. Huxley, C. P. McCoy, J. T. Rademacher, T. E. Rice, *Chem. Rev.* **1997**, *97*, 1515.
- [150] L. Fabbrizzi, M. Licchelli, P. Pallavicini, A. Perotti, A. Taglietti, D. Sacchi, *Chem. Eur. J.* **1996**, *2*, 75.
- [151] A. W. Czarnik, *Acc. Chem. Res.* **1994**, *27*, 302.
- [152] O. S. Wolfbeis, *Fiber Optical Chemical Sensors and Biosensors*; CRC Press: Boca Raton, FL, **1991**, Vol. 1.
- [153] M. L. Ho, F. M. Hwang, P. N. Chen, Y. H. Hu, Y. M. Cheng, K. S. Chen, G. H. Lee, Y. Chi, P. T. Chou, *Org. Biomol. Chem.* **2006**, *4*, 98.
- [154] K. K. W. Lo, S. P. Y. Li, K. Y. Zhang, *New J. Chem.* **2011**, *35*, 265.
- [155] Q. Zhao, S. J. Liu, M. Shi, F. Y. Li, H. Jing, T. Yi, C. H. Huang, *Organometallics* **2007**, *26*, 5922.
- [156] Q. Zhao, T. Y. Cao, F. Y. Li, X. H. Li, H. Jing, T. Yi, C. H. Huang, *Organometallics* **2007**, *26*, 2077.
- [157] M. Licini, J. A. G. Williams, *Chem. Commun.* **1999**, 1943.
- [158] R. P. Brinas, T. Troxler, R. M. Hochstrasser, S. A. Vinogradov, *J. Am. Chem. Soc.* **2005**, *127*, 11851.
- [159] R. Gao, D. G. Ho, B. Hernandez, M. Selke, D. Murphy, P. Djurovich, *J. Am. Chem. Soc.* **2002**, *124*, 14828.
- [160] K. K. W. Lo, W. K. Hui, C. K. Chung, K. H. K. Tsang, T.K. Lee, C. K. Li, J. S. Y. Lau, *Coord. Chem. Rev.* **2006**, *250*, 1724.
- [161] K. K.-W. Lo, K. Y. Zhang, C. K. Chung, K. Y. Kwok, *Chem. Eur. J.* **2007**, *13*, 7110.
- [162] K. K.-W. Lo, C. K. Li, J. Lau, *Organometallics* **2005**, *24*, 4594.
- [163] K. K. W. Lo, J. S. Y. Lau, *Inorg. Chem.* **2007**, *46*, 700.
- [164] K. K. W. Lo, C. K. Chung, T. K. Lee, L. H. Lui, K. H. Tsang, N. Zhu, *Inorg. Chem.* **2003**, *42*, 6886.
- [165] K. K. W. Lo, J. S. W. Chan, L. H. Lui, C. K. Chung, *Organometallics* **2004**, *23*, 3108.

Chapter 1. Introduction

- [166] K. K. W. Lo, C. K. Chung, N. Zhu, *Chem. Eur. J.* **2003**, *9*, 475.
- [167] M. C. DeRosa, P. J. Mosher, C. E. B. Evans, R. J. Crutchley, *Macromol. Symp.* **2003**, *196*, 235.
- [168] Y. Amao, Y. Ishikawa, I. Okura, *Anal. Chim. Acta.* **2001**, *445*, 177.
- [169] M. C. DeRosa, D. J. Hodgson, G. D. Enright, B. Dawson, C. E. B. Evans, R. J. Crutchley, *J. Am. Chem. Soc.* **2004**, *126*, 7619.
- [170] E. Baranoff, J. H. Yum, M. Graetzel, M. K. Nazeeruddin, *J. Organomet. Chem.* **2009**, *694*, 2661.
- [171] N. Tian, D. Lenkeit, S. Pelz, L. H. Fischer, D. Escudero, R. Schiewek, D. Klink, O. J. Schmitz, L. González, M. Schäferling, E. Holder, *Eur. J. Inorg. Chem.* **2010**, *30*, 4875.
- [172] J. N. Demas, B. A. DeGraff, *Anal. Chem.* **1991**, *63*, 829.
- [173] N. Miyaoura, K. Yamada, A. Suzuki, *Tetrahedron Lett.* **1979**, *20*, 3437.
- [174] N. Miyaoura and A. Suzuki, *J. Chem. Soc. Chem. Commun.* **1979**, 866.
- [175] (a) A. Suzuki, *A. Pure, Appl. Chem.* **1985**, *57*, 1749. (b) A. Suzuki, *A. Pure, Appl. Chem.* **1991**, *63*, 419.
- [176] A. R. Martin, Y. Yang, *Acta Chem. Scand.* **1993**, *47*, 221.
- [177] A. Suzuki, *A. Pure, Appl. Chem.* **1994**, *66*, 213.
- [178] N. Miyaoura, A. Suzuki, *Chem. Rev.* **1995**, *95*, 2457.
- [179] A. J. Suzuki, *Organomet. Chem.* **1999**, *576*, 147.
- [180] S. P. Stanforth, *Tetrahedron* **1998**, *54*, 263.
- [181] A. F. Indolese, *Tetrahedron Lett.* **1997**, *38*, 3513.
- [182] S. Saito, S. Oh-tani, N. Miyaoura, *J. Org. Chem.* **1997**, *62*, 8024.
- [183] S. Saito, M. Sakai, N. Miyaoura, *Tetrahedron Lett.* **1996**, *37*, 2993.
- [184] M. G. Andreu, A. Zapf, M. Beller, *Chem. Commun.* **2000**, 2475.
- [185] D. W. Old, D. J. P. Wolfe, S. L. Buchwald, *J. Am. Chem. Soc.* **1998**, *120*, 9722.
- [186] D. Milstein, J. K. Stille, *J. Am. Chem. Soc.* **1978**, *100*, 3636.
- [187] J. K. Stille, *Angew. Chem. Int. Ed.* **1986**, *25*, 508.

Chapter 1. Introduction

- [188] A. F. Littke, L. Schwarz, G. C. Fu, *J. Am. Chem. Soc.* **2002**, *124*, 6343.
- [189] N. Belfrekh, C. Dietrich-Buchecker, J. P. Sauvage, *Tetrahedron Lett.* **2001**, *42*, 2779.
- [190] G. T. Crisp, *Chem. Soc. Rev.* **1998**, *27*, 427.
- [191] S. Pelz, Master thesis „*Synthese und Charakterisierung von sternförmigen Donor-Akzeptor-Donor-Strukturen*“, **2011**, University of Wuppertal.
- [192] M. Bötzer, Bachelor thesis „*C-C Kupplungsreaktionen zum Aufbau von neuartigen konjugierten Polymeren*“, **2008**, University of Wuppertal.
- [193] M. Butz, Bachelor thesis „*Modifikation von konjugierten Polymeren mittels lebender Polymerisation*“, **2008**, University of Wuppertal.
- [194] T. Yamamoto, A. Yamamoto, *Chem. Lett.* **1977**, 353.
- [195] T. Yamamoto, A. Morita, Y. Miyazaki, T. Maruyama, H. Wakayama, Z. H. Zhou, Y. Nakamura, T. Kanbara, S. Sasaki, K. Kubota, *Macromolecules* **1992**, *25*, 1214.
- [196] T. Yamamoto, Y. Hayashi, A. Yamamoto, *Bull. Chem. Soc. Jpn.* **1978**, *51*, 2091.
- [197] T. Yamamoto, K. Sanechika, A. Yamamoto, *Jpn. Kokai Pat.* **1983**, 147426.
- [198] T. Yamamoto, K. Sanechika, A. Yamamoto, *J. Polym. Sci.* **1979**, *18*, 9.
- [199] T. Yamamoto, K. Sanechika, A. Yamamoto, *Bull. Chem. Soc. Jpn.* **1983**, *56*, 1497.
- [200] T. Yamamoto, K. Sanechika, *Chem. Ind.* **1982**, 301.
- [201] Y. Miyazaki, T. Yamamoto, *Synth. Met.* **1994**, *64*, 69.
- [202] T. Yamamoto, M. Omote, Y. Miyazaki, A. Kashiwazaki, B. L. Lee, T. Kanbara, K. Osakada, T. Inoue, K. Kubota, *Macromolecules* **1997**, *30*, 7158.
- [203] T. Yamamoto, A. Kashiwazaki, K. Kato, *Makromol. Chem.* **1989**, *190*, 1649.
- [204] T. Yamamoto, Z. H. Zhou, I. Ando, M. Kikuchi, *Makromol. Chem. Rapid Commun.* **1993**, *14*, 833.
- [205] T. Yamamoto, K. Sanechika, H. Sakai, *J. Macromol. Sci. Chem.* **1990**, *A27*, 1147.
- [206] T. Yamamoto, Y. Hayashi, A. Yamamoto, *Bull. Chem. Soc. Jpn.* **1978**, *51*, 2091.
- [207] T. Yamamoto, K. Kubota, *Chem. Lett.* **1988**, 153.
- [208] T. Yamamoto, T. Maruyama, Z. H. Zhou, T. Ito, T. Fukuda, Y. Yoneda, F. Begum, T.

Chapter 1. Introduction

- Ikeda, S. Sasaki, H. Takezoe, A. Fukuda, K. Kubota, *J. Am. Chem. Soc.* **1994**, *116*, 4832.
- [209] T. Yamamoto, T. Ito, K. Sanechika, M. Hishinuma, *Synth. Met.* **1988**, *25*, 103.
- [210] T. Kanbara, T. Kushida, N. Saito, I. Kuwajima, K. Kubota, T. Yamamoto, *Chem. Lett.* **1998**, 583.
- [211] N. Hayashida, T. Yamamoto, *Bull. Chem. Soc. Jpn.* **1999**, *72*, 1153.
- [212] N. Saito, T. Kanbara, T. Sato, T. Yamamoto, *Polym. Bull.* **1993**, *30*, 285.
- [213] T. Yamamoto, H. Suganuma, T. Maruyama, K. Kubota, *J. Chem. Soc. Chem. Commun.* **1995**, 1613.
- [214] T. Yamamoto, D. Komarudin, M. Arai, B. L. Lee, H. Suganuma, N. Asakawa, Y. Inoue, K. Kubota, S. Sasaki, T. Fukuda, H. Matsuda, *J. Am. Chem. Soc.* **1998**, *120*, 2047.
- [215] N. Saito, T. Yamamoto, *Macromolecules* **1995**, *28*, 4260.
- [216] T. Yamamoto, K. Sugiyama, T. Kushida, T. Inoue, T. Kanbara, T. *J. Am. Chem. Soc.* **1996**, *118*, 3930.
- [217] N. Saito, T. Kanbara, T. Kushida, K. Kubota, T. Yamamoto, *Chem. Lett.* **1993**, 1775.
- [218] T. Kanbara, T. Yamamoto, *Chem. Lett.* **1993**, 419.
- [219] T. Yamamoto, T. Maruyama, Z. H. Zhou, T. Ito, T. Fukuda, Y. Yoneda, F. Begum, T. Ikeda, S. Sasaki, H. Takezoe, A. Fukuda, K. Kubota, *J. Am. Chem. Soc.* **1994**, *116*, 4832.
- [220] T. Yamamoto, S. Wakabayashi, K. Osakada, *J. Organomet. Chem.* **1992**, *428*, 223.
- [221] A. Bilge, PhD thesis „Neuartige kreuzförmige Oligomere aus Thienylen und Phenylen-Bausteinen“, **2010**, University of Wuppertal.
- [222] K. Zhang, Z. Chen, C. Yang, Y. Tao, Y. Zou, J. Qin, Y. Cao, *J. Mater. Chem.* **2008**, *18*, 291.
- [223] C. I. Chao, S. A. Chen, *Appl. Phys. Lett.* **1998**, *73*, 426.
- [224] C. H. Lyons, E. D. Abbas, J. K. Lee, M. F. Rubner, *J. Am. Chem. Soc.* **1998**, *120*,

Chapter 1. Introduction

12100.

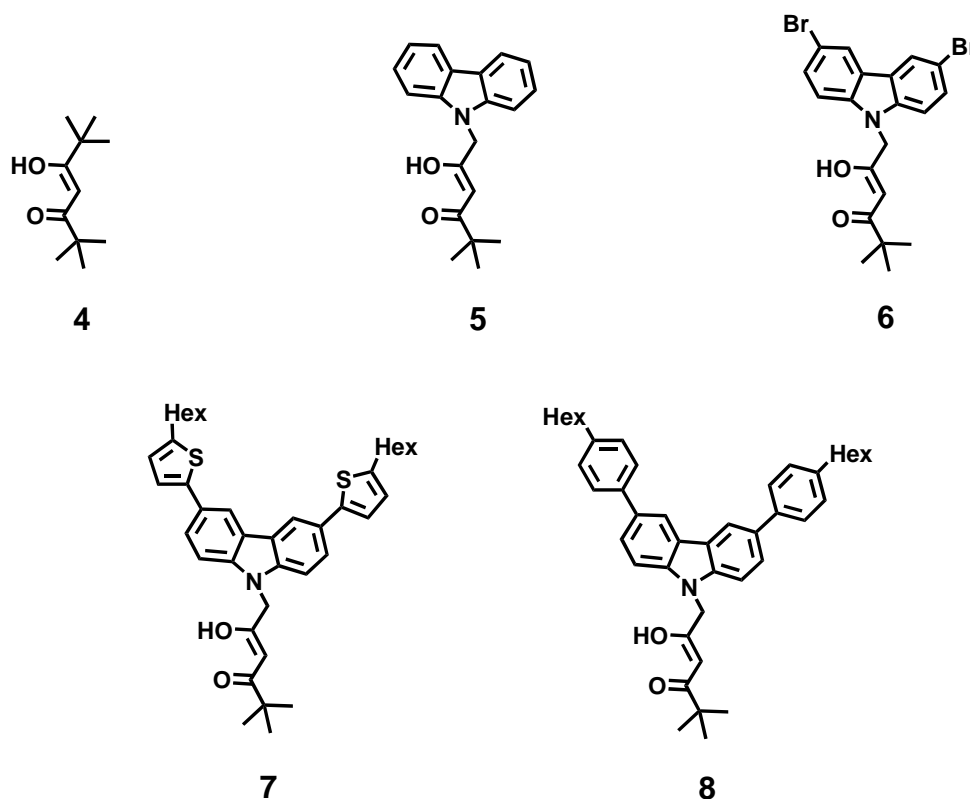
[225] H. Rudmann, S. Shimada, M. F. Rubner, *J. Appl. Phys.* **2003**, *94*, 115.

[226] J. D. Slinker, A. A. Gorodetsky, M. S. Lowry, J. Wang, S. Parker, R. Rohl, S. Bernhard, G. G. Malliaras, *J. Am. Chem. Soc.* **2004**, *126*, 2763.

[227] J. D. Slinker, G. G. Malliaras, S. Flores-Torres, H. D. Abruna, W. Chunwachirasiri, M. J. Winokur, *J. Appl. Phys.* **2004**, *95*, 4381.

Chapter 2. Ligands

In addition, apart from the commercially obtained 5-hydroxy-2,2,6,6-tetramethylhept-4-en-3-one (**4**), a series of different ancillary acetylacetonate (acac) ligands **5-8** [10-15] containing carbazole functional groups (Scheme 2.1) were prepared by a nucleophilic substitution and a subsequent Claisen condensation, respectively. The precursor products of ligands **7** and **8**, namely hexylthiophene- and hexylphenyl-functionalised carbazoles, were prepared by C-C cross-coupling reactions using a Pd-catalyst performing Suzuki or Stille reactions. Due to this, the solubility of ligands **7** and **8** and of the following heteroleptic iridium(III) complexes should be increased through introducing phenyl rings and alkyl chains as moieties into the carbazole units. Moreover, compound **6**, containing a brominated carbazole unit, can be employed as a monomer to further synthesise the copolymer in the presence of a halogenated monomer or compounds embodying arylboronic acids or alkoxyborane groups under metal-catalysed copolymerisation reactions.

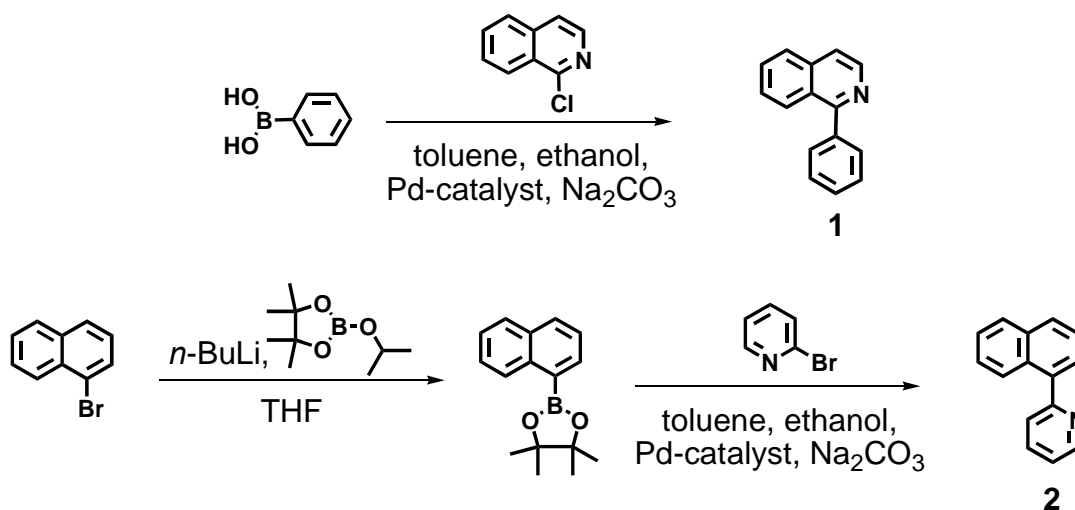


Scheme 2.1. Structures of ancillary acetylacetonate (acac) ligands **4-8**.

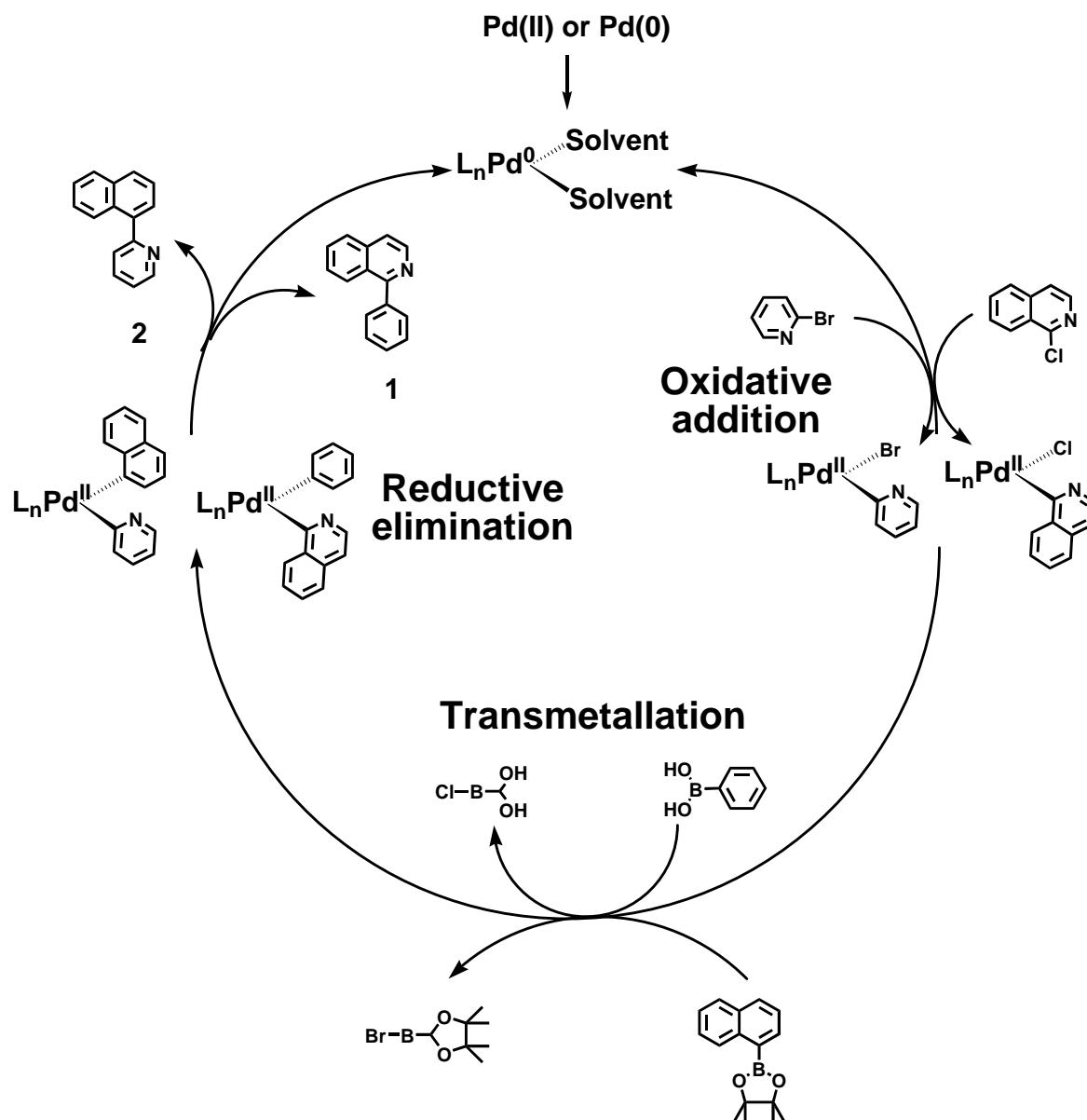
2.2 Results and Discussion

2.2.1 Synthesis of C[^]N ligands

Of the three different C[^]N ligands mentioned above, 2-phenylpyridine (**3**) is commercially available. Contrary, the ligands 1-phenylisoquinoline (**1**, yield: 92%) [24] and 2-(naphthalen-1-yl)pyridine (**2**, yield: 73%) [25,26] were obtained from the *tetrakis*(triphenylphosphine)palladium(0) catalysed Suzuki coupling of 1-chloroisoquinoline with phenylboronic acid as well as 2-bromopyridine with 4,4,5,5-tetramethyl-2(naphthalen-1-yl)-1,3,2-dioxaborolane (Scheme 2.2 and 2.3), respectively.



Scheme 2.2. Efficient synthetic route to compounds **1** and **2**.



Scheme 2.3. Schematic representation of the mechanism of the Suzuki cross-coupling reaction for compounds **1** and **2**.

To synthesise ligand **2**, the compound 4,4,5,5-tetramethyl-2-(naphthalen-1-yl)-1,3,2-dioxaborolane (yield: 81%) was prepared by the lithiation of 1-bromonaphthalene with *n*-butyllithium (*n*-BuLi) (1.6 M in *n*-hexane) and the subsequent addition of 2-*isopropoxy*-4,4,5,5-tetramethyl-1,3,2-dioxaborolane [27]. Although the relative reactivity of the Suzuki-Miyaura cross-coupling reactions follow the order Ar-I>Ar-Br>Ar-Cl under same reaction conditions, the yield of

Chapter 2. Ligands

ligand **1** was satisfactory after a short reaction time (for a description of the Suzuki reaction, see chapter 1.3.1).

The ligands **1** and **2** were fully characterised by IR, mass, ^1H and ^{13}C NMR spectra, as well as elemental analysis. In fact, the ^1H NMR spectra (Figure 2.2) of **1** and **2** are very similar. The doublet at 8.80 ppm and 8.81 ppm can be assigned to protons from the $\text{CH}_2\text{-N}$ group, which have a chemical shift in the low-field region compared to protons at other positions.

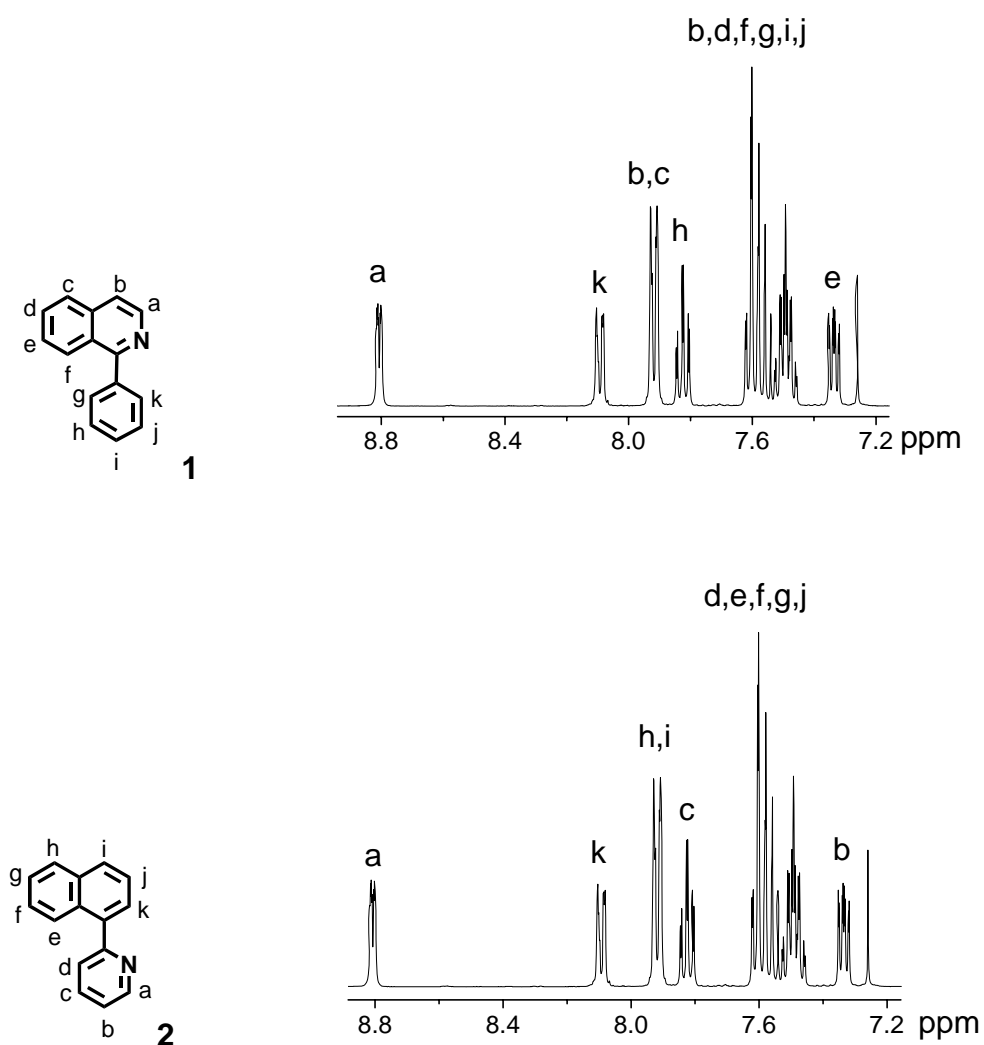
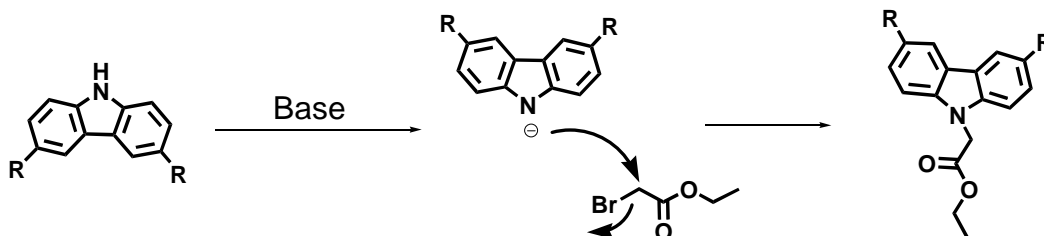


Figure 2.2. ^1H NMR of the aromatic region of **1** and **2** in CDCl_3 .

2.2.2 Synthesis of ancillary acac ligands

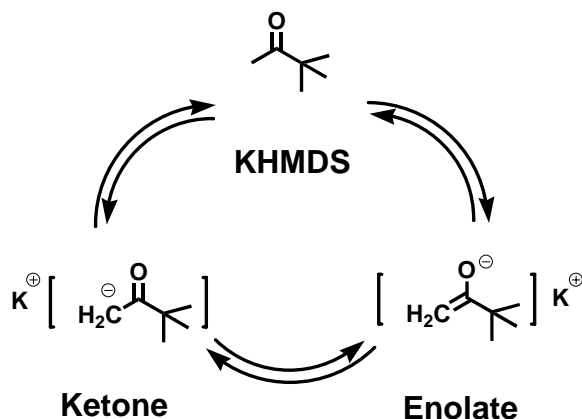
In addition to commercially available 2,2,6,6-tetramethylheptane-3,5-dione (**4**), the synthetic approach to compound 1-carbazol-9-yl-5,5-dimethyl-hexane-2,4-dione (**5**) and its derivatives 1-(3,6-dibromocarbazol-9-yl)-5,5-dimethyl-hexane-2,4-dione (**6**), 1-[3,6-*bis*(5-hexyl-2-thienyl)carbazol-9-yl]-5,5-dimethyl-hexane-2,4-dione (**7**) and 1-[3,6-*bis*(4-hexylphenyl)carbazol-9-yl]-5,5-dimethyl-hexane-2,4-dione (**8**), was generally based on Claisen condensation and C-C cross-coupling reactions.

In the following nucleophilic substitution, the carbazole unit was reduced to its carbazole-anion in a basic medium. The ionised carbazole unit (nucleophile) attacks the C-atom with the attached bromine in the ethyl-2-bromacetate and simultaneously bromine plays the role of the leaving group (Scheme 2.4) [28].



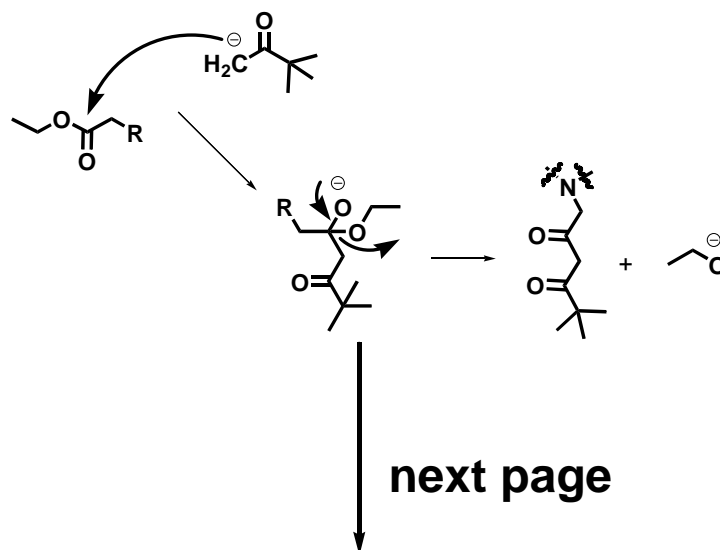
Scheme 2.4. Reaction mechanism of the synthesis of carbazole-ethylacetate [29].

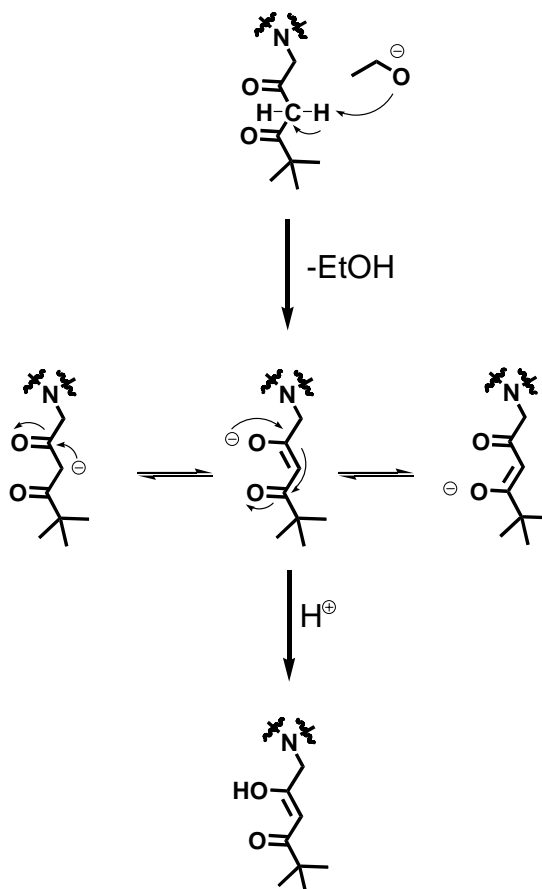
In the next step (Scheme 2.5), a dehydrogenation reaction of 3,3-dimethylbutan-2-one occurs using an excess of potassium *bis*(trimethylsilyl)amide (KHMDs) as a non-sterically hindered base. As a whole, treatment of aldehydes and ketones with a suitable base can lead to the formation of nucleophilic species called enolates. In this case, two kinds of negative compositions, i.e. a ketone and an enolate, are produced and exist in the reaction solvent. In most cases, the equilibrium lies almost completely on the side of the ketone. However, the balance of the dehydrogenation process at low reaction temperatures lies on the side of the enolate [30].



Scheme 2.5. Reaction mechanism 1 of the synthesis of ancillary acac ligands [29].

In the following reaction (Scheme 2.6), the enolate acts as a nucleophile and reacts with the above-obtained acetate compound to produce diketone-structured ligands and ethanolate anions, which can also act as a nucleophile and further attack the CH_2 group between the two carbonyl groups in order to produce the target ancillary ligand.





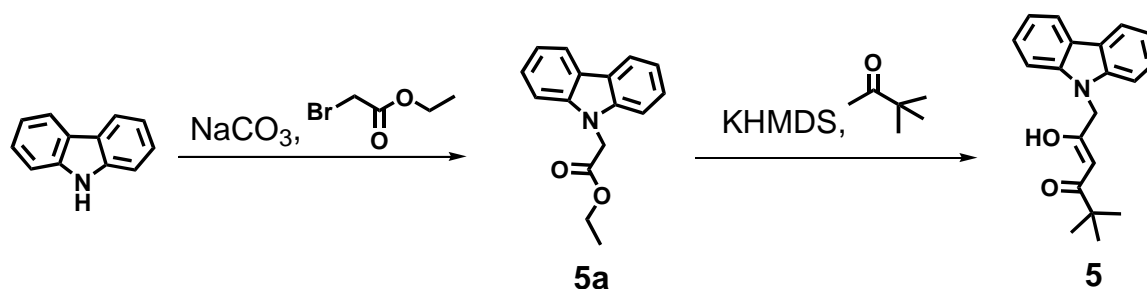
Scheme 2.6. Reaction mechanism 2 of the synthesis of ancillary acac ligands [29].

As the ethanolate molecule offers unshared electrons, it is attracted to acids and can thus, after treatment with H⁺ originating from water or acids, give the final acac ligands (Scheme 2.6).

2.2.2.1 Synthesis of 1-carbazol-9-yl-5,5-dimethyl-hexane-2,4-dione (5)

The compound 1-carbazol-9-yl-5,5-dimethyl-hexane-2,4-dione (**5**) [31] was prepared in a two-step procedure (Scheme 2.7). In the presence of sodium hydride (NaH) and potassium hexamethyldisilazane (KHMDs), a strong but non-nucleophilic base, the selective deprotonation of the amino functional group of the

9*H*-carbazole was achieved, giving ethyl-2-carbazol-9-ylacetate (**5a**, yield: 91%) when utilising ethyl-2-bromoacetate in dimethylformamide (DMF) at 80 °C. The subsequent Claisen-type reaction yielded 1-carbazol-9-yl-5,5-dimethyl-hexane-2,4-dione (**5**, yield: 83%).



Scheme 2.7. Efficient synthetic route to compound **5**.

In the ^1H NMR spectrum of **5**, the signal of the protons of the three methyl groups is located at 2.15 ppm (Figure 2.3). The calculated integrations of the H-protons at position b and c with one proton and two protons confirmed the existence of a $\text{CO-CH}^b=\text{COOH-CH}_2^c\text{-N-structure}$. The ^{13}C NMR spectrum of **5** displays two signals for the two different C=O carbonyl groups at 190.9 ppm and 200.2 ppm.

The C=C-H group gives a strong band at 3056 cm^{-1} in the infrared spectrum. The stretching vibration of the C-C-H group appears between 2996 cm^{-1} and 2860 cm^{-1} . The band belonging to the vibration from the C=O functional group can be observed at about 1771 cm^{-1} . The mass spectra show dominant ions at m/z 253.11 for **5a** and 307.40 for **5**, which are in good agreement with the theoretical molecular mass values of 253.10 g/mol and 307.39 g/mol, respectively.

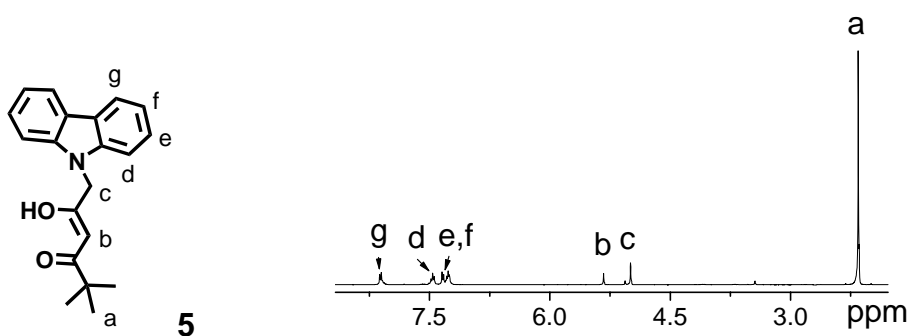
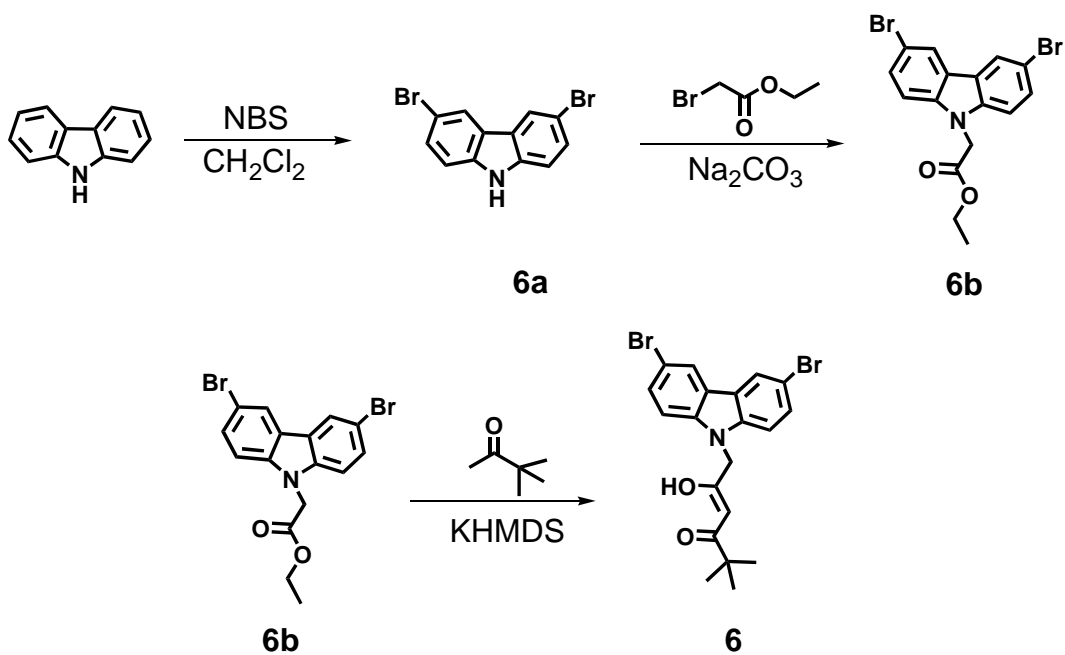


Figure 2.3. ^1H NMR spectrum of acac ligand **5** in CDCl_3 .

2.2.2.2 Synthesis of 1-(3,6-dibromocarbazol-9-yl)-5,5-dimethyl-hexane-2,4-dione (**6**)

Compound **6** was synthesised according to the procedure used for compound **5**, after bromination of 9*H*-carbazole (Scheme 2.8). The compounds 3,6-dibromo-9*H*-carbazole (**6a**, yield: 93%), ethyl-2-(3,6-dibromocarbazol-9-yl)acetate (**6b**, yield: 91%), and 1-(3,6-dibromocarbazol-9-yl)-5,5-dimethyl-hexane-2,4-dione (**6**, yield: 83%) were fully characterised by IR, mass spectrometry, ^1H and ^{13}C NMR spectroscopy, as well as elemental analysis. Compared to the ^1H NMR spectrum of ligand **5**, the proton resonances of ligand **6** in the aliphatic region are similar to the shift of the protons of compound **5** and show three doublet signals at 7.19 ppm, 7.55 ppm, and 8.14 ppm in the aromatic region (Figure 2.4).

The weak signal at 3303 cm^{-1} can be attributed to the vibration of the CO-H group. The C=C-H group of **6** gives a sharp band at 3078 cm^{-1} in the infrared spectrum. The stretching vibrations of the C-H group appear between 2994 cm^{-1} and 2867 cm^{-1} . The band belonging to the vibration of the C=O functional group can be observed at about 1706 cm^{-1} . The *m/z* spectra contain ions at 322.90 for **6a**, 412.08 for **6b**, and 465.10 for **6**, values consistent with the theoretical molecular masses of 322.89 g/mol (**6a**), 412.09 g/mol (**6b**) and 465.18 g/mol (**6**), respectively.



Scheme 2.8. Efficient synthetic route to compound 6.

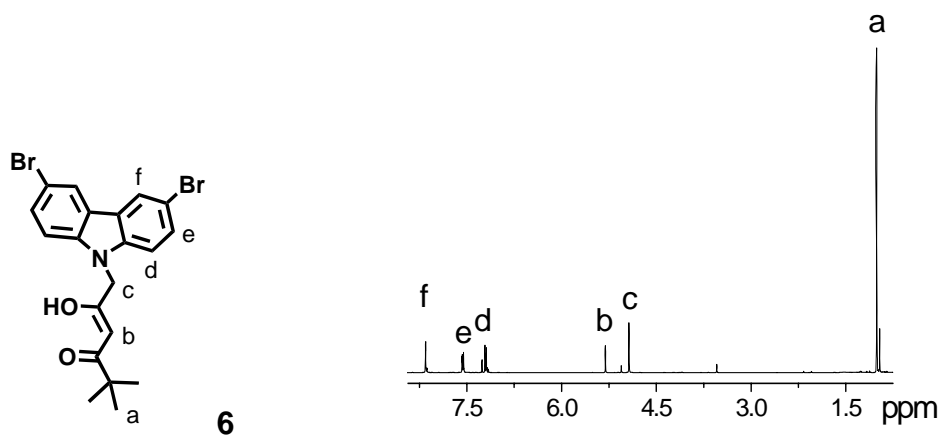
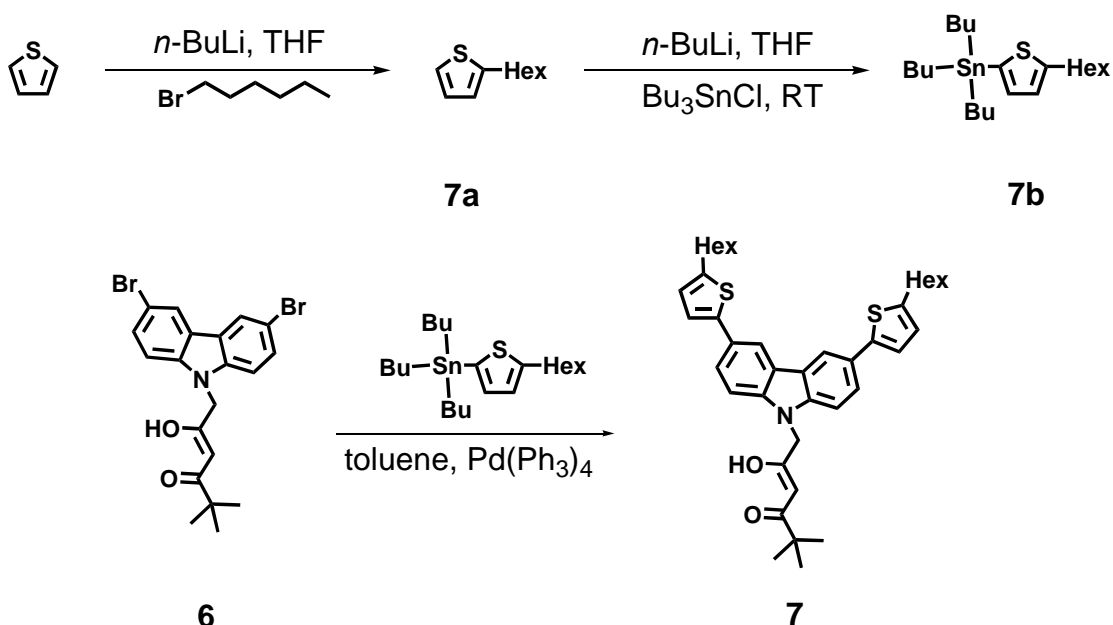


Figure 2.4. ^1H NMR spectrum of acac ligand 6 in CDCl_3

2.2.2.3 Synthesis of 1-[3,6-bis(5-hexyl-2-thienyl)-carbazol-9-yl]-5,5-dimethyl-hexane-2,4-dione (7)

The compound 1-[3,6-bis(5-hexyl-2-thienyl)carbazol-9-yl]-5,5-dimethyl-hexane-2,4-dione (**7**, yield: 56%) could be conventionally synthesised *via* Stille coupling [32,33] (Scheme 2.9). Firstly, 2-hexylthiophene (**7a**, yield: 90%) was obtained by the alkylation of 2-thiophene with 1-bromohexane in THF at room temperature. Then, 2-hexylthiophene was purified by distillation and subsequently lithiated by treatment with *n*-BuLi in THF at -25 °C and afterwards reacted with Bu₃SnCl at 0 °C, yielding thiophen-stannane (**7b**, yield: 95%) as a pale yellow oil. Compounds **6** and **7b** were allowed to react following a Stille reaction in toluene under reflux for 24 h by using *tetrakis*(triphenylphosphine)palladium(0) as a catalyst [32,34]. The product was purified by utilising silica gel column chromatography to yield compound **7**.



Scheme 2.9. Efficient synthetic route to compound **7**.

The ¹H NMR spectrum of **7** exhibits four doublet signals at 6.78 ppm, 7.17 ppm,

7.29 ppm, and 7.69 ppm and a singlet at 8.29 ppm in the aromatic area, while five peaks at 0.92 ppm, 0.99 ppm, 1.35 ppm, 1.74 ppm, and 2.86 ppm arise from the hexyl-protons (Figure 2.5). The signals at 4.97 ppm and 5.34 ppm can clearly be ascribed to the protons of N-CH₂ and CO-CH₂-CO. Both carbonyl groups are shown at 190.7 ppm and 200.4 ppm in the ¹³C NMR spectrum.

The C=C-H group of **7** gives strong bands at 3078 cm⁻¹ and 3044 cm⁻¹ in the infrared spectrum. The stretching vibrations of the C-H group appear at 2956 cm⁻¹ and 2869 cm⁻¹. The band belonging to the vibration of the C=O functional group can be observed at about 1728 cm⁻¹. The measured mass spectra obtained from **7a** (168.30 g/mol) and **7** (639.60 g/mol) are in good agreement with the calculated molecular masses of 168.30 g/mol for **7a** and 639.95 g/mol for **7**, respectively.

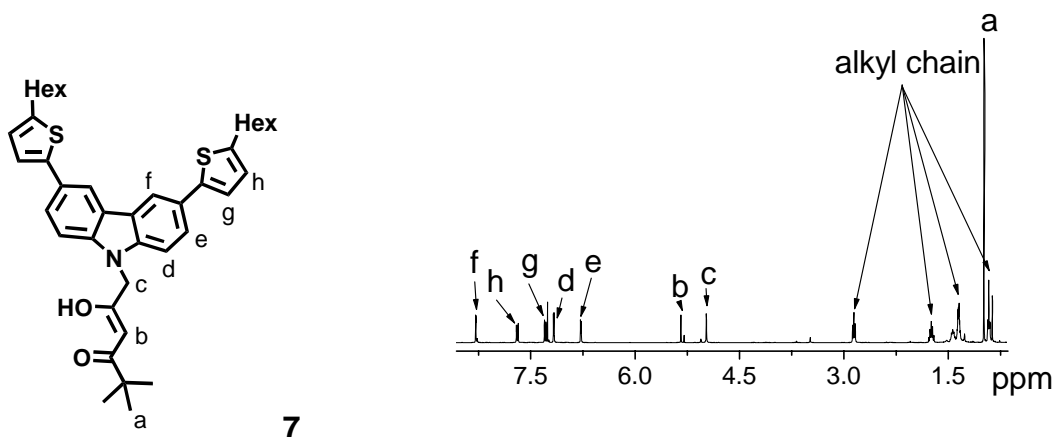


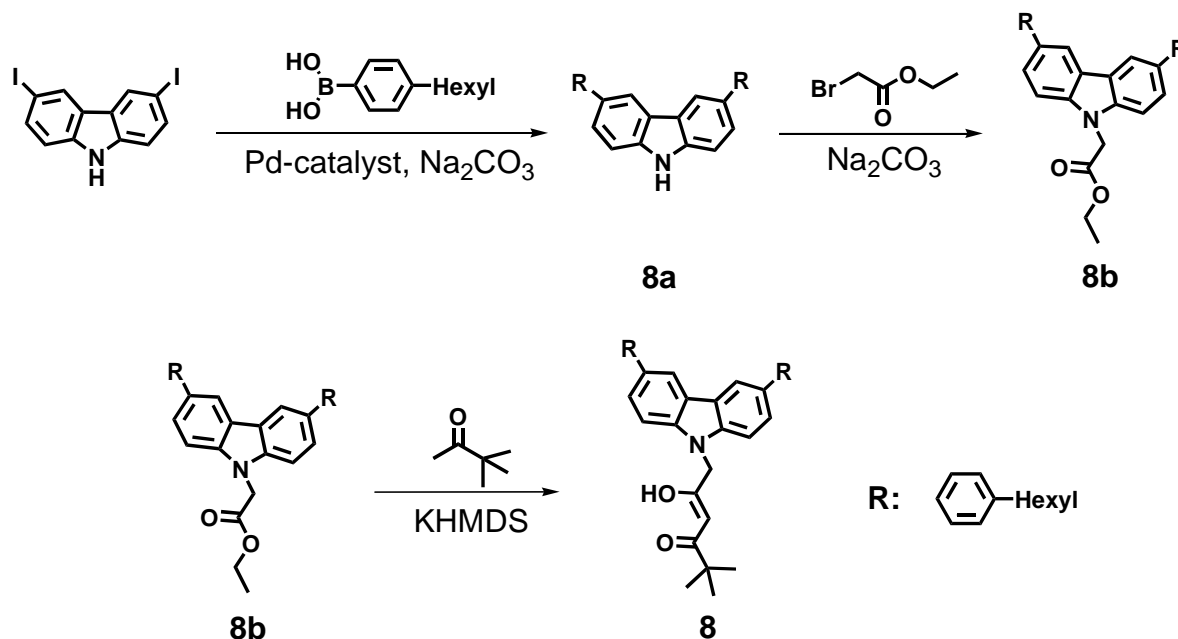
Figure 2.5. ¹H NMR spectrum of acac ligand **7** in CDCl₃.

2.2.2.4 Synthesis of 1-[3,6-bis(4-hexylphenyl)carbazol-9-yl]-5,5-dimethyl-hexane-2,4-dione (**8**)

The synthesis of compound 1-[3,6-bis(4-hexylphenyl)carbazol-9-yl]-5,5-dimethyl-hexane-2,4-dione (**8**, yield: 80%) was carried out in a three-step reaction,

Chapter 2. Ligands

according to the procedures used for compound **5**. First, the compound 3,6-*bis*(4-hexylphenyl)-9*H*-carbazole (**8a**, yield: 81%) was obtained by a Suzuki C-C cross-coupling reaction using a Pd catalyst [35]. The synthesised carbazole derivative **8a** was transformed to ethyl-2-[3,6-*bis*(4-hexylphenyl)carbazol-9-yl]acetate (**8b**, yield: 62%) and, in a further step, compound **8** was obtained (Scheme 2.10).



Scheme 2.10. Efficient synthetic route to compound **8**.

The compounds 3,6-*bis*(4-hexylphenyl)-9*H*-carbazole (**8a**), ethyl-2-[3,6-*bis*(4-hexylphenyl)carbazol-9-yl]acetate (**8b**), and 1-[3,6-*bis*(4-hexylphenyl)carbazol-9-yl]-5,5-dimethylhexane-2,4-dione (**8**) were fully characterised by IR, mass spectrometry, ^1H and ^{13}C NMR spectroscopy, as well as elemental analysis. The singlet signal at 8.38 ppm can be assigned to the proton at position f. Besides this, the resonances of the protons in the aromatic region show doublet splitting. In the ^1H NMR spectrum, compound **8** shows simple quartet and triplet signals for the protons of the CH_2 and CH_3 groups derived from the hexyl chains. The resonance at 5.01 ppm is in the expected range for the protons of $\text{CO}-\text{CH}_2-\text{CO}$ and the resonance at 5.46 ppm is compatible with the protons of $\text{N}-\text{CH}_2$ (Figure 2.6). Both

carbonyl groups of compound **8** are shown at 191.6 ppm and 200.3 ppm in the ^{13}C NMR spectrum.

The C=C-H group from **8** gives a strong band at 3058 cm^{-1} in the infrared spectrum. The stretching vibration of C-H group appears at 2951 cm^{-1} . The band belonging to the vibration of the C=O functional group can be observed at about 1676 cm^{-1} . The observed mass spectra for **8a** (487.32 g/mol), **8b** (537.80 g/mol), and **8** (627.40 g/mol) are in accordance with the theoretical molecular masses of 487.32 g/mol (**8a**), 537.81 g/mol (**8b**), and 627.41 g/mol (**8**), respectively.

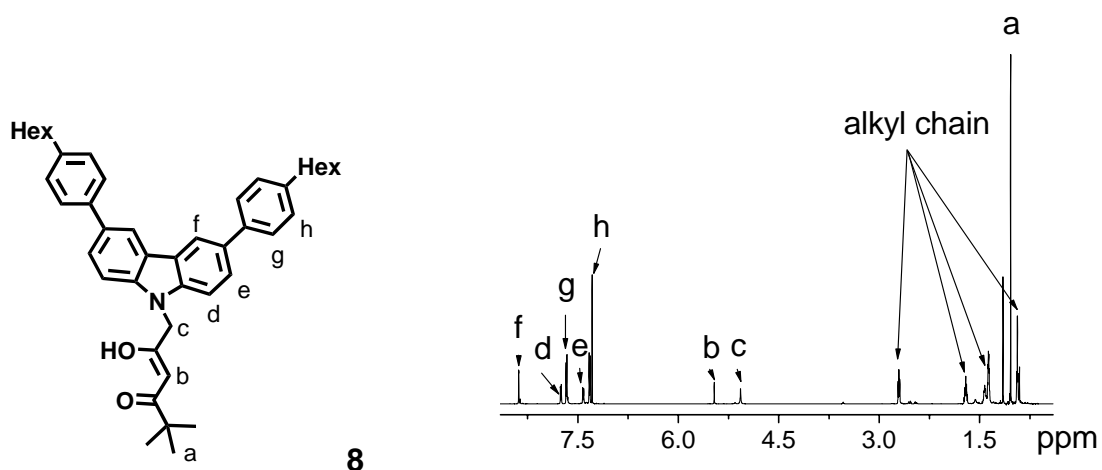


Figure 2.6. ^1H NMR spectrum of acac ligand **8** in CDCl_3 .

2.3 Summary

Both C^N ligands 2-(naphthalen-1-yl)pyridine **2** and 1-phenylisoquinoline **3** were synthesised *via* Suzuki cross-coupling reactions and obtained in good yields. For the different ancillary acac ligands, sodium hydride (NaH) was used as the base for the esterification reaction in the first step. The yields of about 60% motivated us to use a medium base such as Na_2CO_3 or K_2CO_3 in DMF as the solvent, thus giving satisfactory higher yields. Palladium(0)-catalysed cross-coupling reactions

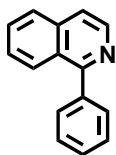
(Suzuki and Stille) were applied to synthesise compounds **7** and **8a**, respectively. The ^{13}C NMR spectra revealed the presence of C=O groups. The synthesised compounds **2**, **3**, and **5-8** were used as cyclometalating C^N ligands (**2** and **3**) and ancillary ligands (**5-8**) to further synthesise phosphorescent heteroleptic iridium(III) complexes.

2.4 Experimental Section

Materials: All manipulations were performed under an atmosphere of dry argon by employing the usual Schlenk techniques. Solvents were carefully dried and distilled from appropriate drying agents prior to use. Commercially available reagents were used without further purification unless otherwise stated. 2-Phenylpyridine, 1-bromo-4-hexylbenzene, potassium hexamethyldisilazane, *n*-butyllithium, tetrahydrofuran, and tetrabutylammonium were purchased from Sigma-Aldrich (www.sigmaaldrich.com). 2-Ethyl-bromoacetate, pinacolone, and *tetrakis*(triphenylphosphine)palladium(0) were delivered by ABCR (www.abcr.de). 9*H*-Carbazole and dimethylformamide were purchased from Acros (www.acros.com).

Instrumentation: ^1H NMR and ^{13}C NMR spectra were acquired on a Bruker Avance 400 or Bruker Avance III 600, respectively (www.bruker.com). Chemical shifts are given relative to the internal standard tetramethylsilane (Me_4Si) in CDCl_3 solution. Chemical shifts in the NMR spectra are given in ppm (s = singlet, d = doublet, t = triplet, q = quartet, and m = multiplet). Fourier transform infrared (FT-IR) spectra were recorded on a Jasco FT/IR-4200 Fourier transform spectrometer (www.jasco.de). Mass spectra were obtained using a Varian MAT 311A instrument with an electro spray ionisation source (ESI). Elemental analyses (EA) were performed on a Perkin Elmer 240 B setup.

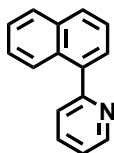
2.4.1 Phenylisoquinoline (1)



A mixture of phenylboronic acid (1.97 g, 15.9 mmol) and *tetrakis*(triphenylphosphine)palladium(0) (462 mg, 0.4 mmol) was stirred in toluene (30 ml) at room temperature under argon. To this mixture, 1-chloroisoquinoline (2.00 g, 12.2 mmol) in ethanol (20 ml) and aqueous saturated Na₂CO₃ solution (20 ml) were added one after the other. The solution was heated to reflux under argon for 4 h, cooled to ambient temperature, and poured into 2N HCl (100 ml). The mixture was subsequently extracted with dichloromethane (3 × 50 ml). The organic layers were combined and washed with saturated Na₂HCO₃ solution (50 ml), then water (50 ml), and dried over MgSO₄. The crude solid was purified by flash chromatography (*n*-hexane/ethyl acetate, 10/3, v/v) to give a white powder. Yield: 2.30 g, 92%.

¹H-NMR (400 MHz, CDCl₃): δ (ppm) 7.34 (t, ³J = 7.6 and 6.6 Hz, 1H), 7.46-7.52 (m, 2H), 7.54-7.62 (m, 3H), 7.83 (t, ³J = 8.6 and 7.6 Hz, 1H), 7.91-7.93 (d, ³J = 7.6 Hz, 2H), 8.08-8.10 (d, ³J = 9.2 Hz, 1H), 8.80-8.81 (d, ³J = 4.6 Hz, 1H). ¹³C-NMR (100 MHz, CDCl₃): δ (ppm) 121.9, 125.0, 125.3, 125.6, 125.8, 126.4, 127.4, 128.3, 128.9, 131.2, 133.9, 136.3, 138.5, 149.5, 159.3. IR: 3048 (C=C-H), 1675, 1586, 1562 (C=N, C=C), 1394, 1118, 863, 835, 807, 783, 649 cm⁻¹. HRMS (ESI): requires m/z C₁₅H₁₁N (M+H)⁺ 205.25, found 205.60. Elem. Anal. Calcd. for C₁₅H₁₁N: C 87.77%, H 5.40%, N 6.82%. Found: C 87.56%, H 5.32%, N 7.12%.

2.4.2 2-(Naphthalen-1-yl)pyridine (2)



A mixture of 4,4,5,5-tetramethyl-2-(naphthalen-1-yl)-1,3,2-dioxaborolane (2 g, 7.87 mmol) and *tetrakis*(triphenylphosphine)palladium(0) (462 mg, 0.4 mmol) was stirred in 1,2-dimethoxyethane (30 ml) at room temperature under argon. To this mixture, 2-bromopyridine (1.244 g, 7.87 mmol) in ethanol (20 ml) and aqueous saturated Na₂CO₃ solution (20 ml) were added one after the other. The solution was heated to reflux under argon for 12 h, cooled to ambient temperature, and poured into 2N HCl (100 ml). The mixture was subsequently extracted with dichloromethane (3 × 50 ml). The organic layers were combined and washed with a saturated Na₂HCO₃ solution (50 ml), then water (10 ml), and dried over MgSO₄. The crude solid was purified by flash chromatography (CH₂Cl₂) to yield a yellow oil. Yield: 1.17 g, 73%.

¹H-NMR (400 MHz, CDCl₃): δ (ppm) 7.34 (t, ³J = 7.6 and 6.6 Hz, 1H), 7.46-7.52 (m, 2H), 7.54-7.62 (m, 3H), 7.83 (t, ³J = 8.6 and 7.6 Hz, 1H), 7.91-7.93 (d, ³J = 7.6 Hz, 2H), 8.08-8.10 (d, ³J = 9.2 Hz, 1H), 8.80-8.81 (d, ³J = 4.6 Hz, 1H). ¹³C-NMR (100 MHz, CDCl₃): δ (ppm) 121.9, 125.0, 125.3, 125.6, 125.8, 126.4, 127.4, 128.3, 128.9, 131.2, 133.9, 136.3, 138.5, 149.5, 159.3. IR: 3048 (C=C-H), 1675, 1586, 1562 (C=N, C=C), 1394, 1118, 863, 835, 807, 783, 649 cm⁻¹. HRMS (ESI): requires m/z C₁₅H₁₁N (M+H)⁺ 205.25, found 205.60. Elem. Anal. Calcd. for C₁₅H₁₁N: C 87.77%, H 5.40%, N 6.82%. Found: C 87.56%, H 5.32%, N 7.12%.

2.4.3 2-Phenylpyridine (3)

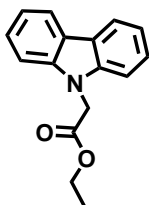
This reagent was purchased from Sigma-Aldrich (www.sigmaaldrich.com).

2.4.4 General procedure for the synthesis of ethyl acetate ligands and ancillary (acac) ligands

Ethyl acetate ligands: Into a 250 ml two-neck flask, NaH (or K_2CO_3) was added and carbazole (or a carbazole derivative) in DMSO (or DMF) was added drop-wise into the flask. The mixture was stirred at 80 °C for 1.5 h. After cooling to room temperature, ethyl-2-bromoacetate was added and stirred for 12 h at 80 °C. The mixture was poured into water and extracted with $CHCl_3$ (3 × 50 ml). The combined organic layers were washed with water and dried with anhydrous sodium sulphate; the solvent was removed under reduced pressure. The crude product was purified by column chromatography (*n*-hexane/ethyl acetate, 10/3, v/v).

Ancillary (acac) ligands: To a solution of 3,3-dimethylbutan-2-one in THF, KHMDS (0.5 M solution in toluene) was added drop-wise at 0 °C. Subsequently, the solution was stirred at room temperature for 1 h. After this time, ethyl-acetate ligands in THF (20 ml) were added drop-wise and the resulting reaction mixture was stirred at room temperature for 12 h. Afterwards, the mixture was poured into water and acidified with diluted hydrochloric acid. The organic layer was extracted with $CHCl_3$ (3 × 50 ml) and washed with water, then dried with anhydrous sodium sulphate. The solvent was removed under reduced pressure. The crude product was purified by column chromatography (*n*-hexane/ethyl acetate, 10/3, v/v).

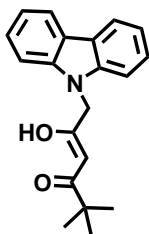
2.4.5 Ethyl-2-carbazol-9-ylacetate (5a)



9*H*-Carbazole (20.0 g, 11.9 mmol), ethyl-2-bromoacetate (44.0 g, 26.3 mmol), and K_2CO_3 (33.1 g, 23.9 mmol) in DMF (100 ml) afforded a colourless powder after purification by silica chromatography using *n*-hexane/ethyl acetate (10/3, v/v) as the eluent. Yield: 27.6 g, 92%.

1H -NMR (400 MHz, $CDCl_3$): δ (ppm) 1.21-1.25 (t, $^3J = 7.1$ and 8.2 Hz, 3H), 4.1-4.2 (m, 2H), 5.00 (s, 2H), 7.25-7.29 (t, $^3J = 7.1$ and 8.6 Hz, 2H), 7.34-7.36 (d, $^3J = 7.6$ Hz, 2H), 7.45-7.49 (t, $^3J = 8.1$ and 9.2 Hz, 2H), 8.10-8.12 (d, $^3J = 8.1$ Hz, 2H). ^{13}C -NMR (100 MHz, $CDCl_3$): δ (ppm) 14.1, 44.8, 61.6, 62.1, 108.3, 119.6, 120.4, 123.2, 125.9, 140.6, 168.5. IR: 3056 (C=C-H), 2996, 2951, 2860 (C-H), 1771 (C=O), 1693, 1562, 1471 (C=C), 1340, 1294, 1252, 1047, 916, 860, 779, 743, 681 cm^{-1} . HRMS (ESI): requires m/z $C_{16}H_{15}NO_2$ (M+H) $^+$ 253.11, found 253.10. Elem. Anal. Calcd. for $C_{16}H_{15}NO_2$: C 75.87%, H 5.97%, N 5.53%. Found: C 75.88%, H 5.92%, N 5.50%.

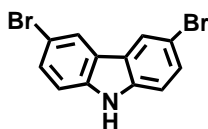
2.4.6 1-Carbazol-9-yl-5,5-dimethyl-hexane-2,4-dione (5)



Ethyl-2-carbazol-9-ylacetate (2.0 g, 7.89 mmol), 3,3-dimethylbutan-2-one (1.17 g, 11.84 mmol) and KHMDS (47.36 ml, 0.5 mol/L) in THF (50 ml) afforded a red powder after purification by column chromatography using *n*-hexane/ethyl acetate (10/3, v/v) as the eluent. Yield: 2.01 g, 83%.

$^1\text{H-NMR}$ (400 MHz, CDCl_3): δ (ppm) 0.97 (s, 9H), 4.99 (s, 2H), 5.33 (s, 1H), 7.25-7.28 (t, $^3J = 6.6$ and 8.1 Hz, 2H), 7.32-7.34 (d, $^3J = 8.1$ Hz, 2H), 7.44-7.48 (t, $^3J = 6.6$ and 8.1 Hz, 2H), 8.10-8.12 (d, $^3J = 8.1$ Hz, 2H). $^{13}\text{C-NMR}$ (100 MHz, CDCl_3): δ (ppm) 26.9, 30.8, 48.6, 92.7, 108.5, 119.6, 119.9, 120.4, 123.2, 126.0, 126.2, 127.2, 140.6, 190.9, 200.2, 206.7. IR: 3071 (C=C-H), 2989, 2973, 2891 (C-H), 1775 (C=O), 1691, 1574, 1489 (C=C), 1356, 1221, 1105, 1049, 942, 871, 769, 742, 688 cm^{-1} . HRMS (ESI): requires m/z $\text{C}_{20}\text{H}_{21}\text{NO}_2$ (M+H) $^+$ 307.39, found 307.40. Elem. Anal. Calcd. for $\text{C}_{20}\text{H}_{21}\text{NO}_2$: C 78.15%, H 6.89%, N 4.56%. Found: C 78.15%, H 6.92%, N 4.53%.

2.4.7 3,6-Dibromo-9H-carbazole (6a)

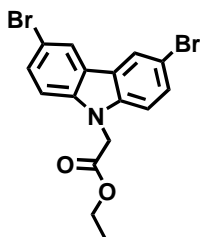


A mixture of 9H-carbazole (30 g, 179.41 mmol) and 1-bromopyrrolidine-2,5-dione

(63.8 g, 358.8 mmol) was stirred in dichloromethane (400 ml) at room temperature for 12 h under argon. After the end of the reaction, the crude product was purified by flash chromatography (dichloromethane) to yield a white solid. Yield: 53 g, 92%.

$^1\text{H-NMR}$ (400 MHz, CDCl_3): δ (ppm) 7.29-7.31 (d, $^3J = 8.6$ Hz, 2H), 7.50-7.53 (d, $^3J = 8.6$ Hz, 2H), 8.12 (s, 2H). $^{13}\text{C-NMR}$ (100 MHz, CDCl_3): δ (ppm) 112.2, 123.2, 124.0, 129.2, 138.4, 177.7. HRMS (ESI): requires m/z $\text{C}_{12}\text{H}_7\text{Br}_2\text{N}$ ($\text{M}+\text{H}$) $^+$ 322.89, found 322.90. Elem. Anal. Calcd. for $\text{C}_{12}\text{H}_7\text{Br}_2\text{N}$: C 44.35%, H 2.17%, N 4.31%. Found: C 44.32%, H 2.18%, N 4.33%.

2.4.8 Ethyl-2-(3,6-dibromocarbazol-9-yl)acetate (6b)

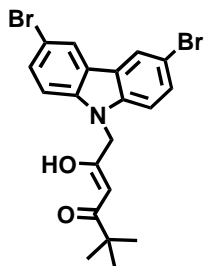


3,6-Dibromo-9*H*-carbazole (2.0 g, 1.65 mmol), ethyl-2-bromoacetate (2.06 g, 12.30 mmol), and NaH (0.37 g, 15.36 mmol) in DMSO (80 ml) afforded a colourless powder after purification by column chromatography using *n*-hexane/ethyl acetate (10/3, v/v) as the eluent. Yield: 1.56 g, 62.5%.

$^1\text{H-NMR}$ (400 MHz, CDCl_3): δ (ppm) 1.20-1.24 (t, $^3J = 6.6$ Hz, 3H), 4.17-4.22 (q, $^3J = 7.1$ Hz, 2H), 4.92 (s, 2H), 7.19-7.21 (d, $^3J = 8.1$ Hz, 2H), 7.55-7.57 (dd, $^3J = 9.2$ and 2.1 Hz, 2H), 8.14 (s, 2H). $^{13}\text{C-NMR}$ (100 MHz, CDCl_3): δ (ppm) 14.3, 44.9, 111.8, 123.2, 123.3, 126.7, 128.9, 139.9, 168.2. IR: 3079 (C=C-H), 2981, 2920, 2869 (C-H), 1733 (C=O), 1624, 1595, 1471 (C=C), 1348, 1289, 1208, 1052, 878, 867, 789, 763, 670 cm^{-1} . HRMS (ESI): requires m/z $\text{C}_{16}\text{H}_{13}\text{Br}_2\text{NO}_2$ ($\text{M}+\text{H}$) $^+$ 411.09, found 412.08. Elem. Anal. Calcd. for $\text{C}_{16}\text{H}_{13}\text{Br}_2\text{NO}_2$: C 46.75%, H 3.19%, N 3.41%.

Found: C 46.67%, H 3.21%, N 3.40%.

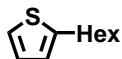
2.4.9 1-(3,6-Dibromocarbazol-9-yl)-5,5-dimethyl-hexane-2,4-dione (6)



Ethyl-2-(3,6-dibromocarbazol-9-yl)acetate (5 g, 12.16 mmol), 3,3-dimethylbutan-2-one (1.83 g, 18.24 mmol) and KHMDS (72.96 ml of a 0.5 M solution in toluene, 36.48 mmol) in THF (80 ml) afforded a red powder after purification by column chromatography using *n*-hexane/ethyl acetate (10/3, v/v) as the eluent. Yield: 3.86 g, 68%.

$^1\text{H-NMR}$ (400 MHz, CDCl_3): δ (ppm) 1.20-1.24 (m, 9H), 4.19 (s, 2H), 4.93 (s, 2H), 7.19-7.21 (d, $^3J = 8.1$ Hz, 2H), 7.55-7.58 (dd, $^3J = 8.6$ and 2.1 Hz, 2H), 8.14-8.14 (d, $^3J = 1.5$ Hz, 2H). $^{13}\text{C-NMR}$ (100 MHz, CDCl_3): δ (ppm) 25.5, 26.7, 44.4, 48.2, 52.4, 93.7, 111.5, 111.6, 111.7, 123.0, 123.3, 126.7, 128.8, 129.0, 129.5, 129.6, 192.0, 196.7, 200.2, 210.6. IR: 3078 (C=C-H), 2964, 2932, 2867 (C-H), 1706, 1596 (C=C), 1392, 1289, 1096, 887, 873, 834, 756, 691 cm^{-1} . HRMS (ESI): requires m/z $\text{C}_{20}\text{H}_{19}\text{Br}_2\text{NO}_2$ ($\text{M}+\text{H}$) $^+$ 465.18, found 465.10. Elem. Anal. Calcd. for $\text{C}_{20}\text{H}_{19}\text{Br}_2\text{NO}_2$: C 51.64%, H 4.12%, N 3.01%. Found: C 51.80%, H 4.14%, N 2.89%.

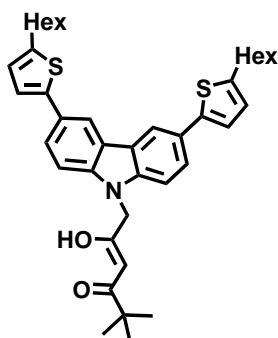
2.4.10 2-Hexylthiophene (7a)



To a cooled (-70 °C) mixture of thiophene (10 g, 118.8 mmol) in anhydrous THF (100 ml), a solution of *n*-BuLi (78 ml, 1.6 M, 124.8 mmol) in *n*-hexane was added drop-wise. After stirring for 1 h at 0 °C, the mixture was cooled to -40 °C, followed by the addition of 1-bromohexane (20.6 g, 124.8 mmol). The mixture was slowly heated to room temperature and subsequently stirred for 2 h. Water (250 ml) was added and the mixture was extracted with diethylether (3 × 150 ml). The combined organic layers were dried over MgSO₄ and concentrated *in vacuo*. The product was purified by means of vacuum distillation. The product was obtained as a colourless liquid. Yield: 18 g, 90%.

¹H-NMR (400 MHz, CDCl₃): δ (ppm) 0.95 (t, 3H), 1.33-1.47 (m, 6H), 1.74 (m, 2H), 2.87 (t, 2H), 6.82 (dd, 1H), 6.96 (dd, 1H), 7.14 (dd, 1H). ¹³C-NMR (100 MHz, CDCl₃): δ (ppm) 14.0, 22.6, 28.8, 29.9, 31.6, 31.8, 122.6, 123.8, 126.6, 145.8. HRMS (ESI): requires *m/z* C₁₀H₁₆S (M+H)⁺ 168.30, found 168.30. Elem. Anal. Calcd. for C₁₀H₁₆S: C 71.37%, H 9.58%. Found: C 71.37%, H 9.57%.

2.4.11 1-[3,6-Bis(5-hexyl-2-thienyl)carbazol-9-yl]-5,5-dimethyl-hexane-2,4-dione (7)

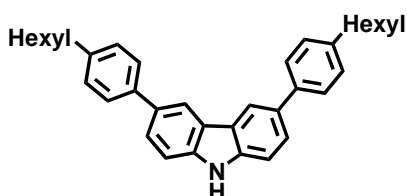


A solution of *n*-BuLi (20.4 ml, 1.6M, 32.7 mmol) in *n*-hexane was added drop-wise to a solution of 2-hexylthiophene (5 g, 29.7 mmol) in anhydrous THF (20 ml) at -25 °C. After 1 h of stirring at -25 °C, Bu₃SnCl (8.5 ml, 31.19 mmol) was slowly added. The reaction mixture was warmed to room temperature and stirred overnight. After dilution with CH₂Cl₂ (40 ml), the organic phase was successively washed with a saturated aqueous NH₄Cl solution and water, dried over Na₂SO₄, and the solvent was removed under reduced pressure. The colourless oil of **7b** (12.9 g, 95%) was directly used in the next step without further purification. Product **7c** (1.13 g, 2.48 mmol) was combined in an oven-dried vacuum flask with compound **7b** (1.18 g, 2.60 mmol), compound **6** (0.48 g, 1.03 mmol), *tetrakis*(triphenylphosphine)palladium(0) (0.12 g, 10.0 mol%) and 20 ml dry toluene (20 ml). The flask was deaerated for 5 minutes with argon, sealed, and brought to 140 °C for 12 h. The solvent was removed under reduced pressure. The crude product was purified by column chromatography (*n*-hexane/ethyl acetate, 10/3, v/v) to give a grey solid. Yield: 0.37 g, 56%.

¹H-NMR (400 MHz, CDCl₃): δ (ppm) 0.92 (s, 6H), 0.99 (s, 9H), 1.35-1.44 (m, 12H), 1.75 (m, 4H), 2.86 (t, ³J = 8.6 and 7.6 Hz, 4H), 4.97 (s, 2H), 5.34 (s, 1H), 6.78 (d, ³J = 3.5 Hz, 2H), 7.17 (d, ³J = 3.6 Hz, 2H), 7.29 (d, ³J = 8.6 Hz, 2H), 7.69 (dd, ³J =

8.6 Hz, 2H), 8.29 (s, 2H). ^{13}C -NMR (100 MHz, CDCl_3): δ (ppm) 14.1, 22.6, 27.1, 28.8, 30.3, 31.6, 31.7, 48.8, 92.7, 108.9, 117.6, 121.8, 123.6, 124.5, 124.9, 127.3, 140.2, 142.5, 144.8, 190.7, 200.4. IR: 3078, 3044 (C=C-H), 2956, 2924, 2869 (C-H), 1728, 1587 (C=C), 1364, 1325, 1252, 1159, 1141, 884, 861, 832, 789, 759, 726, 680 cm^{-1} . HRMS (ESI): requires m/z $\text{C}_{40}\text{H}_{49}\text{NO}_2\text{S}_2$ (M+H) $^+$ 639.95, found 639.60. Elem. Anal. Calcd. for $\text{C}_{40}\text{H}_{49}\text{NO}_2\text{S}_2$: C 75.07%, H 7.72%, N 2.19%. Found: C 75.10%, H 7.69%, N 2.20%.

2.4.12 3,6-Bis(4-hexylphenyl)-9H-carbazole (8a)

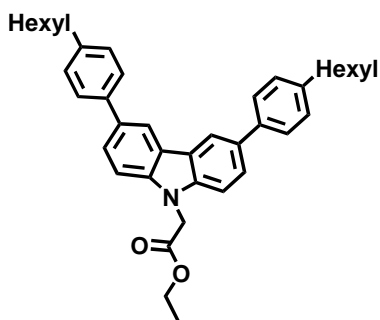


A mixture of 4-hexylphenylboronic acid (6.0 g, 29.1 mmol) and *tetrakis*-(triphenylphosphine)palladium(0) (255 mg, 1.12 mmol) was stirred in anhydrous toluene (50 ml) at room temperature under a nitrogen atmosphere. To this mixture, 3,6-diiodo-9H-carbazole (4.69 g, 11.2 mmol) in ethanol (15 ml) and an aqueous saturated Na_2CO_3 solution (20 ml) were added one after the other. The solution was heated to reflux under argon for 3 h, cooled to ambient temperature, and poured into 2N HCl (100 ml). The mixture was subsequently extracted with chloroform (3 \times 50 ml). The organic layers were combined and washed with a saturated NaHCO_3 solution (50 ml), then with water (10 ml), and dried over MgSO_4 . The crude solid was purified by column chromatography (*n*-hexane/ethyl acetate, 10/3, v/v) to give a white powder. Yield: 3.10 g, 58%.

^1H -NMR (400 MHz, CDCl_3): δ (ppm) 0.93 (m, 6H), 1.37 (s, 12H), 2.67-2.71 (dt, $^3J = 7.33$ and 9.05 Hz, 4H), 7.30-7.32 (d, $^3J = 8.08$ Hz, 4H), 7.47 (s, 2H), 7.64-7.69 (m, 6H), 8.01 (s, 1H). ^{13}C -NMR (100 MHz, CDCl_3): δ (ppm) 14.1, 22.6, 29.1, 31.5, 31.7,

35.6, 110.8, 118.6, 124.0, 125.4, 127.1, 128.8, 139.3 and 141.3. IR: 3080 (N-H), 3062 (C=C-H), 2945 (C-H), 1658, 1633 (C=C), 1478, 1127, 888, 865, 861, 793, 677 cm^{-1} . HRMS (ESI): requires m/z $\text{C}_{36}\text{H}_{41}\text{N}$ ($\text{M}+\text{H}$)⁺ 487.32, found 487.32. Elem. Anal. Calcd. for $\text{C}_{36}\text{H}_{41}\text{N}$: C 88.68%, H 8.46%, N 2.90%. Found: C 88.67%, H 8.47%, N 2.87%.

2.4.13 Ethyl-2-[3,6-bis(4-hexylphenyl)carbazol-9-yl]acetate (**8b**)

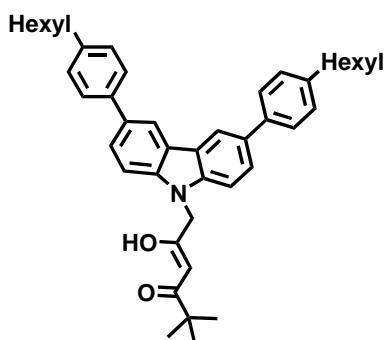


Compound **8a** (1 g, 2.05 mmol), ethyl-2-bromoacetate (0.76 g, 4.51 mmol) and K_2CO_3 (0.85 g, 6.15 mmol) in DMF (100 ml) afforded a colourless powder after purification by column chromatography using *n*-hexane/ethyl acetate (10/3, v/v) as the eluent. Yield: 1.56 g, 62%.

$^1\text{H-NMR}$ (600 MHz, CDCl_3): δ (ppm) 0.93 (s, 6H), 1.25-1.28 (t, $^3J = 7.15$ and 7.91 Hz, 4H), 1.35-1.43 (m, 12H), 1.68-1.73 (m, 4H), 2.68-2.71 (t, $^3J = 7.53$ and 9.03 Hz, 4H), 4.23-4.26 (m, 2H), 5.02 (s, 2H), 7.30-7.32 (d, $^3J = 7.91$ Hz, 4H), 7.38-7.40 (d, $^3J = 8.66$ Hz, 2H), 7.64-7.66 (d, $^3J = 7.91$ Hz, 4H), 7.72-7.74 (d, $^3J = 8.66$ Hz, 2H), 8.35 ppm (s, 2H). $^{13}\text{C-NMR}$ (150 MHz, CDCl_3): δ (ppm) 14.1, 22.6, 29.1, 31.6, 31.8, 35.6, 45.0, 61.7, 108.7, 118.9, 123.9, 125.6, 127.2, 128.8, 133.4, 139.3, 140.4, 141.4, 168.5 ppm. IR: 3058 (C=C-H), 2947 (C-H), 1677, 1658, 1633 (C=O, C=C), 1521, 1345, 891, 863, 852, 793, 668 cm^{-1} . HRMS (ESI): requires m/z $\text{C}_{40}\text{H}_{47}\text{NO}_2$

(M+H)⁺ 573.81, found 573.80. Elem. Anal. Calcd. for C₄₀H₄₇NO₂: C 83.73%, H 8.26%, N 2.44%. Found: C 83.71%, H 8.26%, N 2.43%.

2.4.14 1-[3,6-Bis(4-hexylphenyl)carbazol-9-yl]-5,5-dimethyl-hexane-2,4-dione (8)



Compound **8b** (0.7 g, 1.22 mmol), 3,3-dimethylbutan-2-one (0.18 g, 1.80 mmol) and KHMDS (7.2 ml of a 0.5 M solution in toluene, 3.60 mmol) in THF (30 ml) afforded a red powder after purification by column chromatography using *n*-hexane/ethyl acetate (10/3, v/v) as the eluent. Yield: 0.62 g, 80%.

¹H-NMR (600 MHz, CDCl₃): δ (ppm) 0.94 (m, 6H), 1.04 (m, 6H), 1.35-1.43 (m, 12H), 1.71 (m, 4H), 2.69-2.72 (dt, ³J = 7.53 and 9.03 Hz, 4H), 5.07 (s, 1H), 5.46 (s, 2H), 7.32-7.33 (d, ³J = 8.28 Hz, 4H), 7.41-7.43 (d, ³J = 8.28 Hz, 2H), 7.66-7.68 (d, ³J = 7.91, 4H), 7.75-7.76 (d, ³J = 8.28 Hz, 2H), 8.34 (s, 2H). ¹³C-NMR (150 MHz, CDCl₃): δ (ppm) 14.1, 22.6, 25.8, 26.3, 27.1, 29.1, 31.5, 31.7, 35.6, 38.8, 48.9, 108.9, 118.8, 123.9, 125.6, 127.1, 128.9, 133.4, 139.1, 140.4, 141.4, 191.6, 200.3. IR: 3058 (C=C-H), 2951 (C-H), 1676, 1658, 1641 (C=O, C=C), 1488, 1276, 889, 873, 848, 781, 689 cm⁻¹. HRMS (ESI): requires m/z C₄₄H₅₃NO₂ (M+H)⁺ 627.41, found 627.40. Elem. Anal. Calcd. for C₄₄H₅₃NO₂: C 84.17%, H 8.51%, N 2.23%. Found: C 84.21%, H 8.46%, N 2.27%.

2.5 References

- [1] H. J. Bolink, L. Cappelli, E. Coronado, A. Parham, P. Stössel, *Chem. Mater.* **2006**, *18*, 2778.
- [2] S. Tokito, T. Lijima, T. Tsuzuki, F. Sato, *Appl. Phys. Lett.* **2003**, *83*, 2459.
- [3] M. K. Nazeeruddin, R. Humphry-Baker, D. Berner, S. Rivier, L. Zuppiroli, M. Graetzel, *J. Am. Chem. Soc.* **2003**, *125*, 8790.
- [4] W. Zhu, Y. Mo, M. Yuan, W. Yang, Y. Cao, *Appl. Phys. Lett.* **2002**, *80*, 2045.
- [5] R. Ragni, E. A. Plummer, K. Brunner, J. W. Hofstraat, F. Babudri, G. M. Farinola, F. Naso, L. De Cola, *J. Mater. Chem.* **2006**, *16*, 1161.
- [6] T. Sajoto, P. I. Djurovich, A. Tamayo, M. Yousufuddin, R. Bau, M. E. Thompson, *Inorg. Chem.* **2005**, *44*, 7992.
- [7] Y. M. You, S. Y. Park, *J. Am. Chem. Soc.* **2005**, *127*, 12438.
- [8] C. Adachi, M. A. Baldo, S. R. Forrest, M. E. Thompson, *Appl. Phys. Lett.* **2000**, *77*, 904.
- [9] Y. Kawamura, K. Goushi, J. Brooks, J. J. Brown, H. Sasabe, C. Adachi, *Appl. Phys. Lett.* **2005**, *86*, 071104.
- [10] N. Tian, D. Lenkeit, S. Pelz, D. Kourkoulos, D. Hertel, K. Meerholz, E. Holder, *Dalton Trans.* **2011**, *40*, 11629.
- [11] N. Tian, D. Lenkeit, S. Pelz, L. H. Fischer, D. Escudero, R. Schiewek, D. Klink, O. J. Schmitz, L. Gonzalez, M. Schaeferling, E. Holder, *Eur. J. Inorg. Chem.* **2010**, *30*, 4875.
- [12] N. Tian, Y. V. Aulin, D. Lenkeit, S. Pelz, O. V. Mikhnenko, P. W. M. Blom, M. A. Loi, E. Holder, *Dalton Trans.* **2010**, *39*, 8613.
- [13] N. Tian, A. Thiessen, R. Schiewek, O. J. Schmitz, D. Hertel, K. Meerholz, E. Holder, *J. Org. Chem.* **2009**, *74*, 2718.
- [14] N. Tian, I. Kanelidis, A. Thiessen, D. Hertel, K. Meerholz, E. Holder, *Macromol. Biosci.* **2009**, *9*, F68.
- [15] L. H. Fischer, M. I. J. Stich, O. S. Wolfbeis, N. Tian, E. Holder, M. Schaeferling, *Chem. Eur. J.* **2009**, *15*, 10857.

Chapter 2. Ligands

- [16] E. Holder, B. M. W. Langeveld, U. Schubert, *Adv. Mater.* **2005**, *17*, 1109.
- [17] G. Zhou, W. Y. Wong, W. Y. Yao, Z. Xie, L. Wang, *Angew. Chem. Int. Ed.* **2007**, *46*, 1149.
- [18] M. K. Nazeeruddin, R. Humphry-Baker, D. Berner, S. Rivier, L. Zuppiroli, M. Graetzel, *J. Am. Chem. Soc.* **2003**, *125*, 8790.
- [19] T. D. Anthopoulos, M. J. Frampton, E. B. Namdas, P. L. Burn, I. D. W. Samuel, *Adv. Mater.* **2004**, *16*, 557.
- [20] A. Asuboyama, H. Iwawaki, M. Furugori, T. Mukaide, J. Kamatani, S. Igawa, T. Moriyama, S. Miura, T. Takiguchi, S. Okada, M. Hoshino, K. Ueno, *J. Am. Chem. Soc.* **2003**, *125*, 12971.
- [21] J. Li, P. I. Djurovich, B. D. Alleyne, I. Tsyba, N. N. Ho, R. Bau, M. E. Thompson, *Polyhedron* **2004**, *23*, 419.
- [22] S. J. Yeh, M. F. Wu, C. T. Chen, Y. H. Song, Y. Chi, M. H. Ho, S. F. Hsu, C. H. Chen, *Adv. Mater.* **2005**, *17*, 285.
- [23] C. H. Yang, Y. M. Cheng, Y. Chi, C. J. Hsu, F. C. Fang, K. T. Wong, P. T. Chou, C. H. Chang, M. H. Tsai, C. C. Wu, *Angew. Chem. Int. Ed.* **2007**, *46*, 2418.
- [24] Y. H. Sun, X. H. Zhu, Z. Chen, Y. Zhang, Y. Cao, *J. Org. Chem.* **2006**, *71*, 6281.
- [25] J. P. Wolfe, R. A. Singer, B. H. Yang, S. L. Buchwald, *J. Am. Chem. Soc.* **1999**, *121*, 9550.
- [26] J. J. Yin, M. P. Rainka, X. Zhang, S. L. Buchwald, *J. Am. Chem. Soc.* **2002**, *124*, 1162.
- [27] H. Usta, A. Facchetti, T. J. Marks, *Org. Lett.* **2008**, *10*, 1385.
- [28] D. Eckhardt, M. Groenewolt, E. Krause, H. G. Börner, *Chem. Commun.* **2005**, 2814.
- [29] S. Pelz, Master thesis „*Synthese und Charakterisierung von sternförmigen Donor-Akzeptor-Donor-Strukturen*“, **2011**, University of Wuppertal.
- [30] S. E. Denmark, S. M. Pham, *Org. Lett.* **2001**, *3*, 2201.
- [31] Z. W. Liu, M. Guan, Z. Q. Bian, D. B. Nie, Z. L. Gong, Z. B. Li, C. H. Huang, *Adv. Funct. Mater.* **2006**, *16*, 1441.

Chapter 2. Ligands

- [32] A. J. J. van Breemen, P. T. Herwig, P. C. H. T. Chlon, J. Sweelssen, H. F. M. Schoo, S. Setayesh, W. M. Hardeman, C. A. Martin, D. M. de Leeuw, J. J. Valetton, C. W. M. Bastiaansen, D. J. Broer, A. R. PoPa-Merticaru, S. C. J. Meskers, *J. Am. Chem. Soc.* **2006**, *128*, 2336.
- [33] B. Joussetme, P. Blanchard, E. Levillain, J. Delaunay, M. Allain, P. Richomme, J. Roncali, *Chem. Eur. J.* **2003**, *9*, 5297.
- [34] Y. Nicolas, P. Blanchard, E. Levillain, M. Allain, N. Mercier, J. Roncali, *Org. Lett.* **2004**, *6*, 273.
- [35] A. Suzuki, *Proc. Jpn. Acad. Ser. B* **2004**, *80*, 359.

Chapter 3 Iridium(III) Complexes

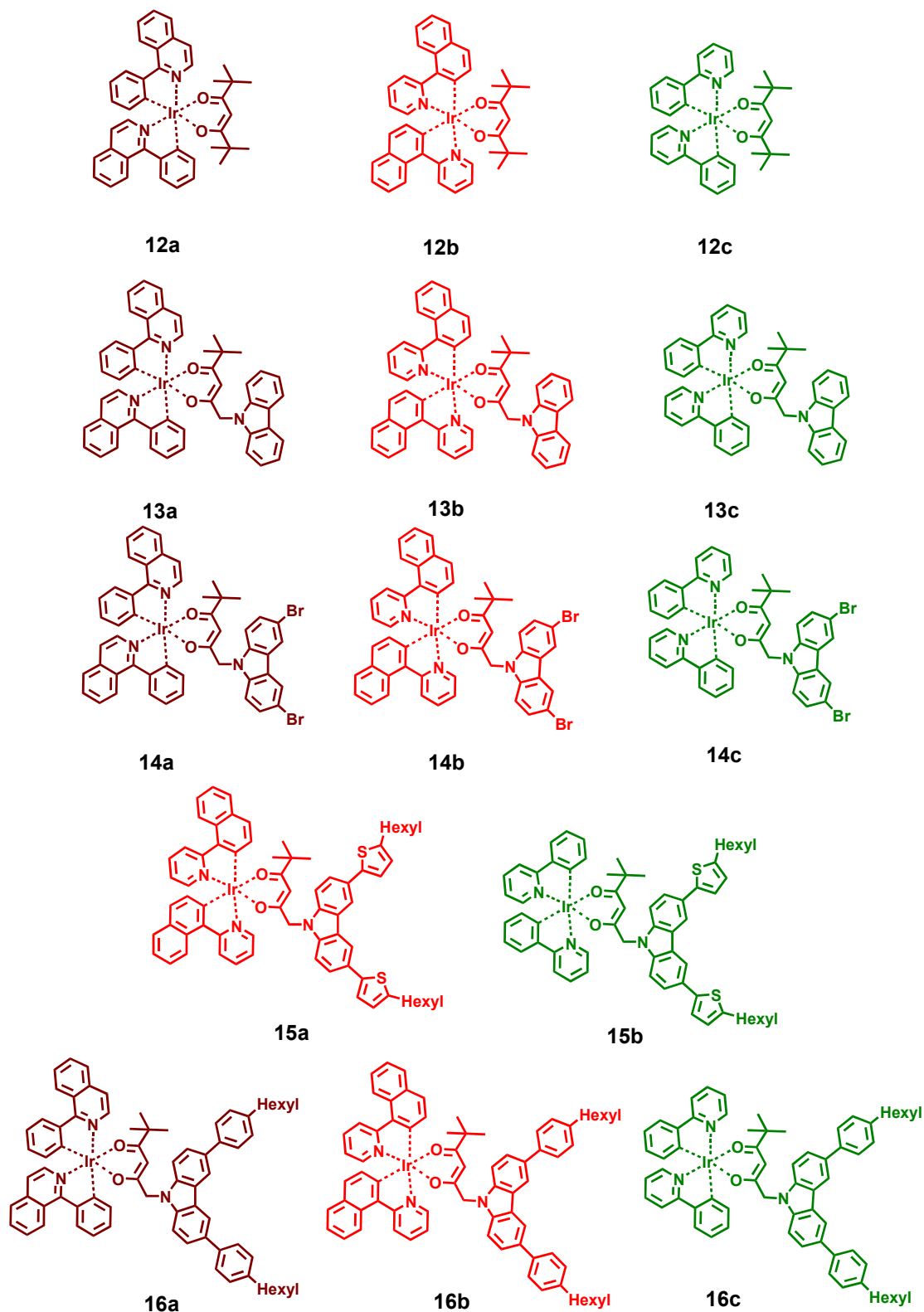
3.1 Introduction

In our chosen iridium(III) systems, solubility, thermal stability, and essential electro/hole transmittability as well as processing probability of emitting layers in OLEDs are closely dependent on the selected ancillary acac ligand, while photo- and electro-optical properties of these heteroleptic Ir(III) complexes, namely emission maximum, lifetime, and essential oxidation potentials, can be determined by the structure of the C^N ligands [1-9]. Adding alkyl chains to ancillary ligands (complexes **12a-c**, **16a-c**) improved the solubility in different organic solvents and in the emitting layer, when the doping with small molecules or using polymers as hosts was facilitated, resulting in an enhanced luminous efficiency of OLEDs. On the other hand, the introduction of carbazole and thiophene moieties in the acac ligands (complexes **13a-c**, **15a-b**) was helpful for the charge recombination process and for miscibility with the polymer matrix [8,10,11]. Brominating the carbazole sides allowed the participation of Ir(III) complexes (**14a-c**) in polymerisation reactions, providing the opportunity to create polymers where segments with a heavy metal like iridium are incorporated.

Our strategy was to design and synthesise a series of heteroleptic Ir(III) complexes **12-16a-c** (Scheme 3.1) possessing C^N cyclometalating ligands like 1-

Chapter 3. Iridium(III) complexes

phenylisoquinoline (1), 2-(naphthalen-1-yl)pyridine (2), or 2-phenylpyridine (3) with different ancillary ligands.



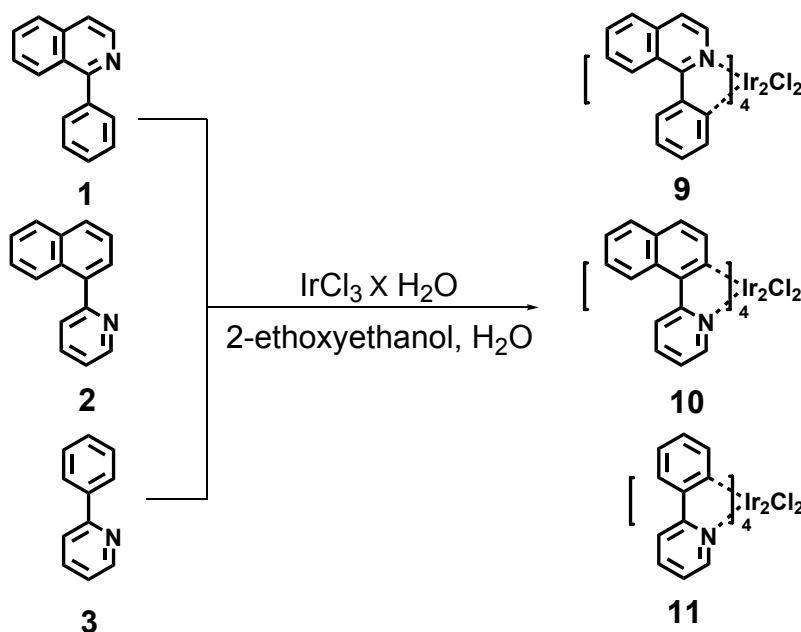
Scheme 3.1. The structures of synthesised heteroleptic Ir(III) complexes **12-16a-c**.

Chapter 3. Iridium(III) complexes

These iridium(III) complexes are air- and thermally- stable. Their emission range varies from green to red and they reveal high quantum yields and short phosphorescence lifetimes. The synthesised complexes with their different characteristics were applied to the fabrication of OLED and sensing devices. Complexes **13a-c** proved to be suitable for OLED devices, while complexes **14b-c** were good as temperature sensors due to their asymmetric structure and their longer lifetimes.

3.2 Synthesis of Ir(III)- μ -chloro-bridged precursor complexes

The method for preparing the Ir(III)- μ -chloro-bridged precursor complexes **9-11** is outlined in Scheme 3.2. $\text{IrCl}_3 \times \text{H}_2\text{O}$ was reacted with synthesised C^N ligands **1-3** under reflux for 24 h in a mixture of 2-ethoxyethanol and water (3:1) as the solvent. The crude product was purified by washing with ethanol and acetone.



Scheme 3.2. Efficient synthetic route to μ -chloro-bridged Ir(III) precursor complexes **9-11**.

Chapter 3. Iridium(III) complexes

The ^1H NMR spectra of Ir(III)- μ -chloro-bridged precursor complexes **9-11** were measured in DMSO-d_6 and the structural confirmation was investigated by applying 2D ^1H - ^1H COSY NMR experiments (Figure 3.1). Theoretically, the formation of Ir(III)- μ -chloro-bridged precursor complexes **9-11** should be symmetrical. Nevertheless, for complexes **9** and **10**, the resonances of the protons belonging to the C[^]N ligand were separated into two peaks, which possess the same integration and multiplicity. This result may show that the Ir(III)- μ -chloro-bridged precursor complexes **9** and **10** have an asymmetrical configuration in comparison with Ir(III)- μ -chloro-bridged complex **11** [2,8]. In particular, the Ir(III) complex **9** has a nitrogen atom neighbouring protons (j,j') in the low-field region (9.75-9.77 ppm); this is also the case for Ir(III) complex **10** (protons a,a' at 9.89-9.91 ppm). The electronegativity of the nitrogen atom creates a deshielding effect by pulling electrons from the neighbouring carbon atoms; this reduced electron density leads to the resonances of the aforementioned protons in the low-field region. The signals of the remaining aromatic hydrogens are obviously shifted to the high-field region with chemical shifts ranging from 8.94 to 5.58 ppm. Assignment of protons j,j' can help us determine the protons of carbons i,i' through their coupling observed in the COSY experiment. The splitting of the signals observed in the case of protons g,f,c,b (g',f',c',b') are also important, where clear triplet peaks arise as expected. Similarly, protons h,e,d,a (h',e',d',a') exhibited a multiplicity of doublets and contributed to the structural characterisation as well. The multiplicity of all signals and the assignment of the coupling relationships between all protons provided evidence for the successful acquisition of Ir(III) complex **9**. The same analytical approach enabled us the full characterisation of

Chapter 3. Iridium(III) complexes

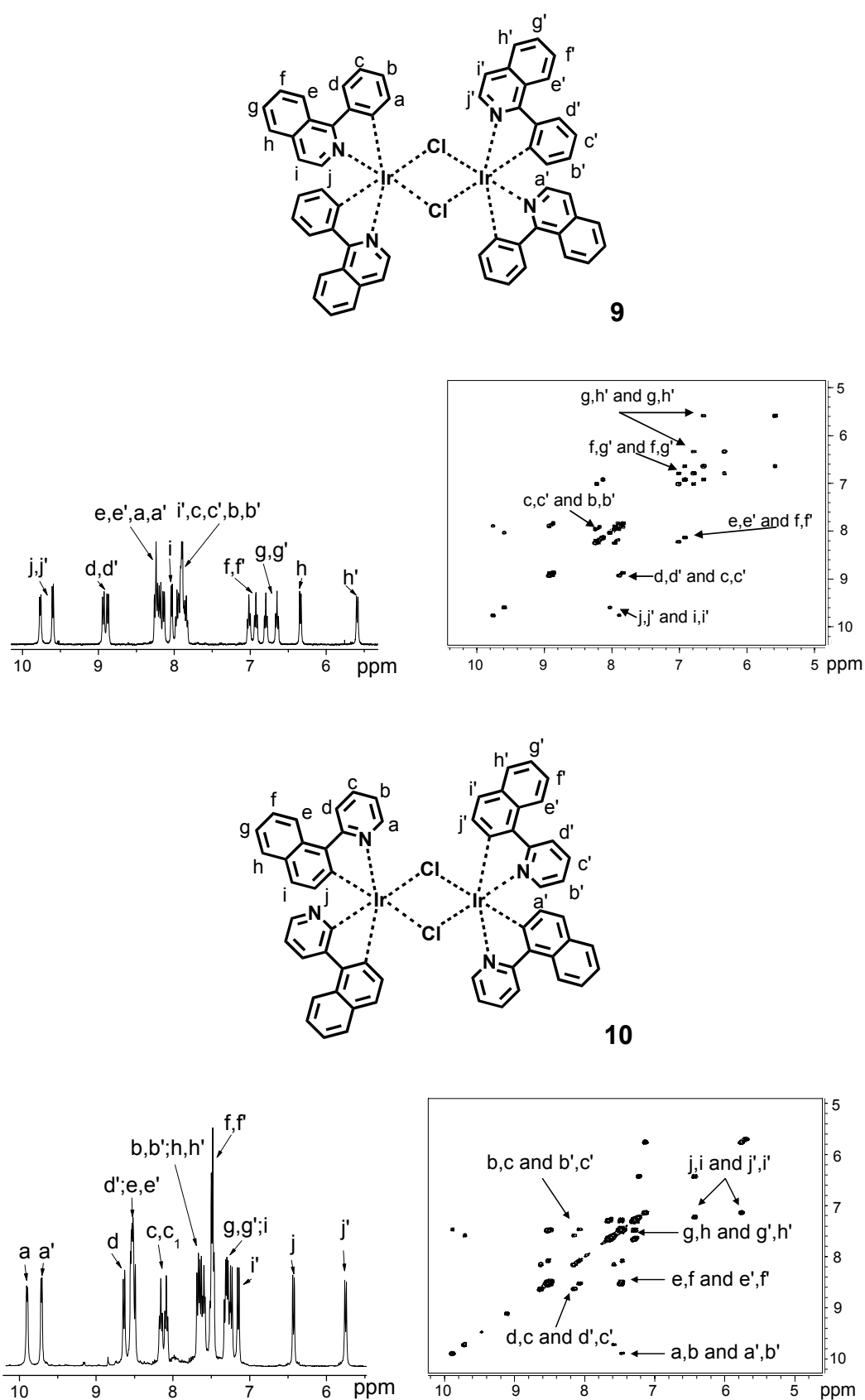


Figure 3.1. ^1H , ^1H - ^1H COSY of Ir(III)- μ -chloro-bridged precursor complexes **10** and **11** recorded in $\text{DMSO}-\text{D}_6$.

Ir(III) complex **10**. The Ir(III) complex **11** is known in the literature and its spectroscopic analysis is explicitly described in the experimental section. The observed IR vibration bands of Ir(III)- μ -chloro-bridged precursor complexes **9-11** were dominated by the respective cyclometalating *piq* (1-phenylisoquinoline), *npy* (2-(naphthalen-1-yl)pyridine), and *ppy* (2-phenylpyridine) ligands. Thus, the Ir(III) complexes **9-11** show almost similar vibrations in the IR spectra due to similar organic functional groups. Strong bands were observed at 3048-3044 cm^{-1} (C=C-H), 1610-1615 cm^{-1} (C=C), and 1468-1476 cm^{-1} (C=N). For the Ir(III) complexes **9-11**, a molecular weight of 1271.90 g/mol for **9** and **10**, and 1073.10 g/mol for **11** could be verified using Matrix-assisted Laser Desorption/Ionization Time of Flight Mass Spectrometry (MALDI-TOF MS). These values are identical with the calculated molecular weights of 1271.90 g/mol (**9**), 1272.19 g/mol (**10**), and 1072.09 g/mol (**11**), respectively.

3.3 Synthesis of heteroleptic iridium(III) complexes

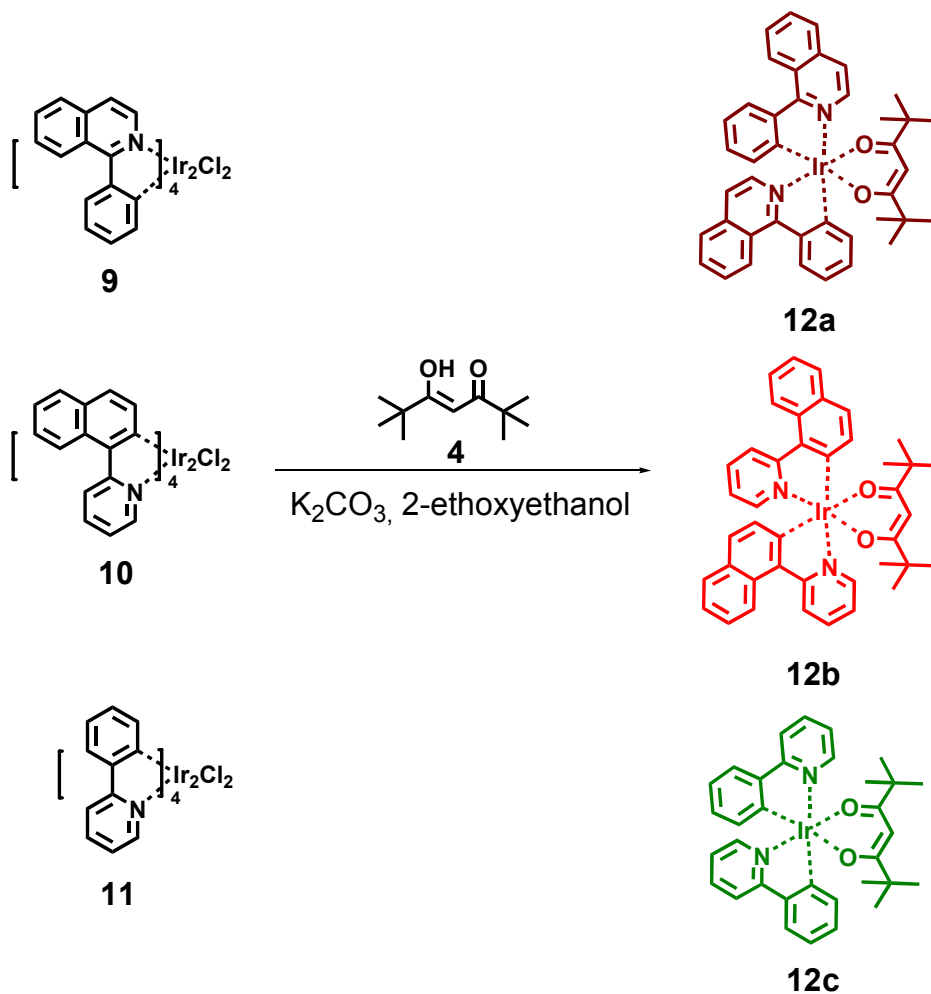
The heteroleptic iridium(III) complexes **12-16a-c** were synthesised by following a two-step procedure [2,12,20]. As mentioned above, the cyclometalation of $[\text{IrCl}_3 \times n\text{H}_2\text{O}]$ with compound 1-phenylisoquinoline (**1**), or 2-(naphthalen-1-yl)pyridine (**2**), or 2-phenylpyridine (**3**) resulted in the Ir(III)- μ -chloro-bridged precursor complexes **9-11**, respectively. Subsequently, the Ir(III)- μ -chloro-bridged precursor complexes **9-11** were treated with the acac ligands **4-8** in 2-ethoxyethanol at 140 °C in the presence of K_2CO_3 in order to yield targeted iridium(III) complexes **12a-c** (Scheme 3.3) [2,3,5,13,14] (Yield: **12a**, 71%; **12b**, 66%; **12c**, 68%), **13a-c** (Scheme 3.4) [2,3,5,15] (Yield: **13a**, 67%; **13b**, 65%; **13c**, 61%), **14a-c** (Scheme 3.5)[8] (Yield: **14a**, 56%; **14b**, 41%; **14c**, 69%), **15a-b** (Scheme 3.6)[8] (Yield: **15a**, 41%; **15b**, 46%), as well as **16a-c** (Scheme 3.7)[2,3] (Yield: **16a**, 72%; **16b**, 65%; **16c**, 68%). The obtained crude products were purified by silica column

Chapter 3. Iridium(III) complexes

chromatography (*n*-hexane/ethyl acetate, 10/3, v/v) and recrystallised from a mixture of *n*-hexane and dichloromethane to yield pure Ir(III) complexes. All obtained iridium(III) complexes were fully characterised by IR, APLI-TOF mass, ¹H- and ¹³C- NMR, UV-*vis*, fluorescence spectroscopy, and elemental analysis. Especially, since the synthesised Ir(III) complexes were of high molar mass and exhibited the properties of low polarity and non-volatility, they could easily be ionised and investigated by using Atmospheric Pressure Laser Ionization Time of Flight Mass Spectrometry (APLI-TOF MS) as the method of detection [16,17].

3.3.1 Synthesis of iridium(III) complexes 12a-c

The efficient synthetic route to heteroleptic iridium(III) complexes **12a-c** is displayed in Scheme 3.3.



Scheme 3.3. Efficient synthetic route to heteroleptic iridium(III) complexes **12a-c**.

The 1H NMR spectra of heteroleptic iridium(III) complexes **12a-c** were recorded in $CDCl_3$ and are shown in Figure 3.2. Due to symmetrical configuration of complexes **12a-c**, the 1H NMR spectra show simple and distinct resonances in the aromatic region compared to the other complex series (Figure 3.2). In addition, their 1H NMR spectra are similar to the respective C^N ligands.

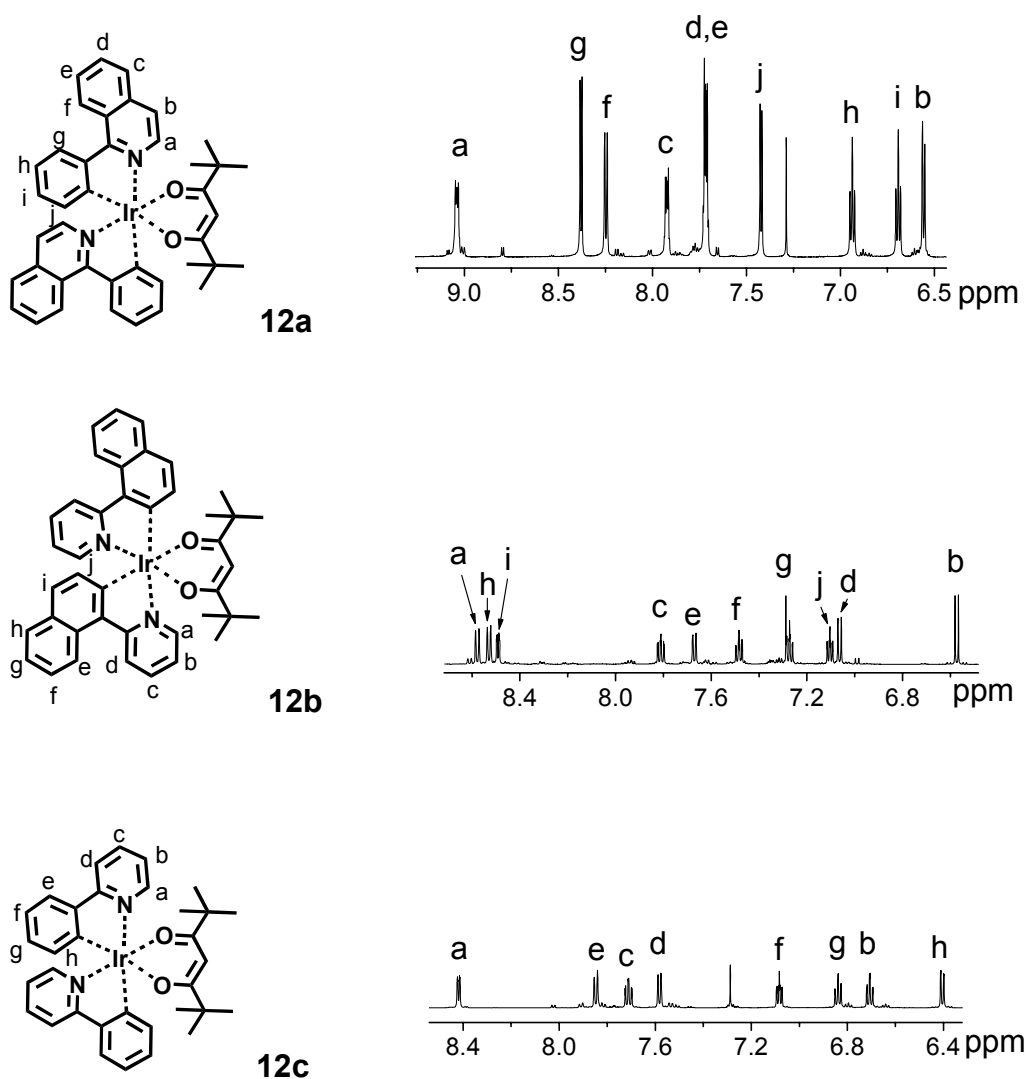


Figure 3.2. ^1H NMR spectra of heteroleptic iridium(III) complexes **12a-c** in CDCl_3 .

In the IR spectra of **12a-c**, the vibration bands of C=CH stretching vibrations are located at 3055 cm^{-1} for **12a**, at 3045 cm^{-1} for **12b** and at 3049 cm^{-1} for **12c**. The stretching vibrations at $2961\text{-}2880\text{ cm}^{-1}$ can be assigned to C- CH_3 bonds. The IR spectra show weak absorptions for C=O stretching vibrations in the range of $1678\text{-}1688\text{ cm}^{-1}$ and C=N stretching vibrations in the range of $1562\text{-}1557\text{ cm}^{-1}$. The APLI mass spectra of **12a-c** exhibited the expected results. The measured molecular weight of **12a-c** was identical with the calculated molecular weight (see Table 3.1, Figure 3.3).

Chapter 3. Iridium(III) complexes

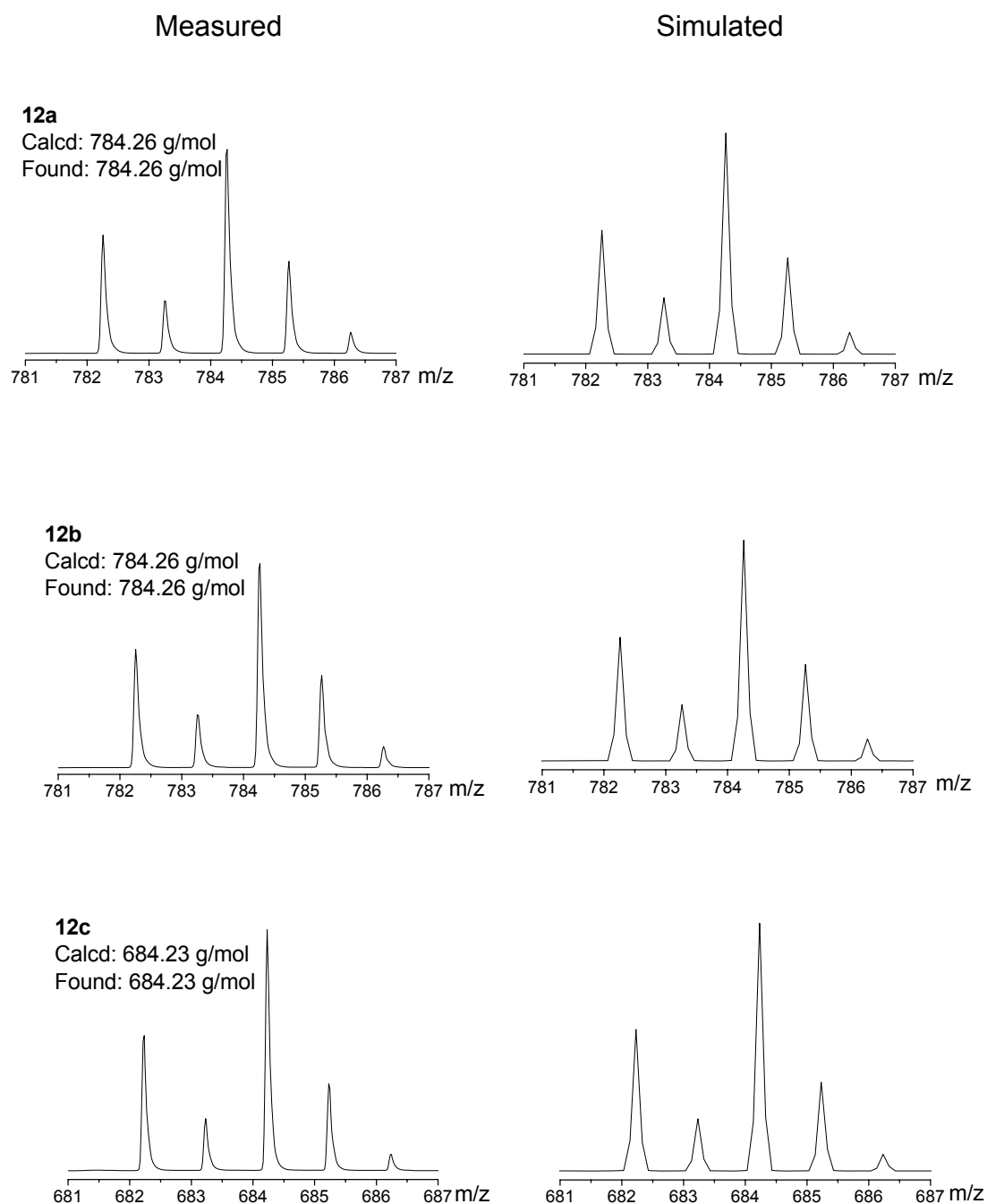


Figure 3.3. The measured and simulated mass spectra of iridium(III) complexes **12a-c**.

The thermal stability of the iridium(III) complexes was evaluated by thermogravimetric analysis (TGA) under a nitrogen atmosphere. TGA revealed that the complexes **12a-c** are thermally stable up to 302 °C with 5% weight loss. The green emitting complex **12c** revealed the highest quantum yield of 58% in solution

compared to **12a** at 35% and **12b** at 37%. The decomposition temperature (T_d at 5% weigh loss) of iridium(III) complexes **12a-c** are summarised in Table 3.2.

The UV-vis spectra of iridium(III) complexes **12a-c** are shown in Figure 3.4.

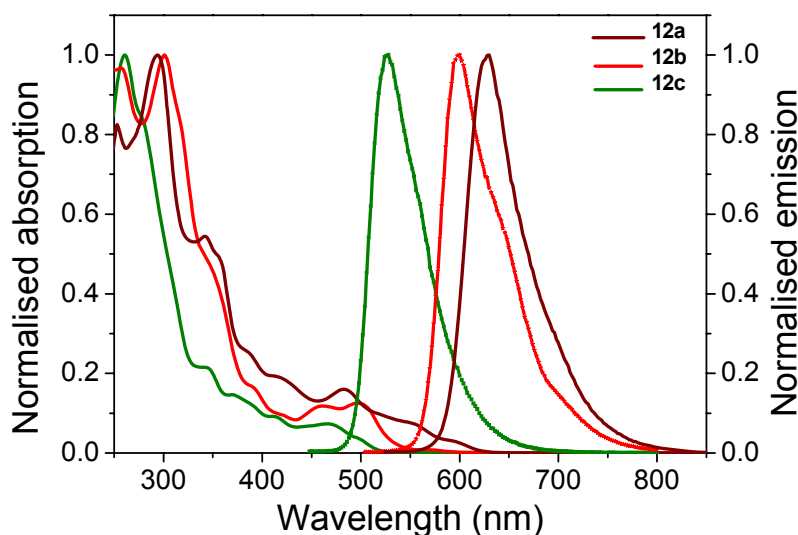
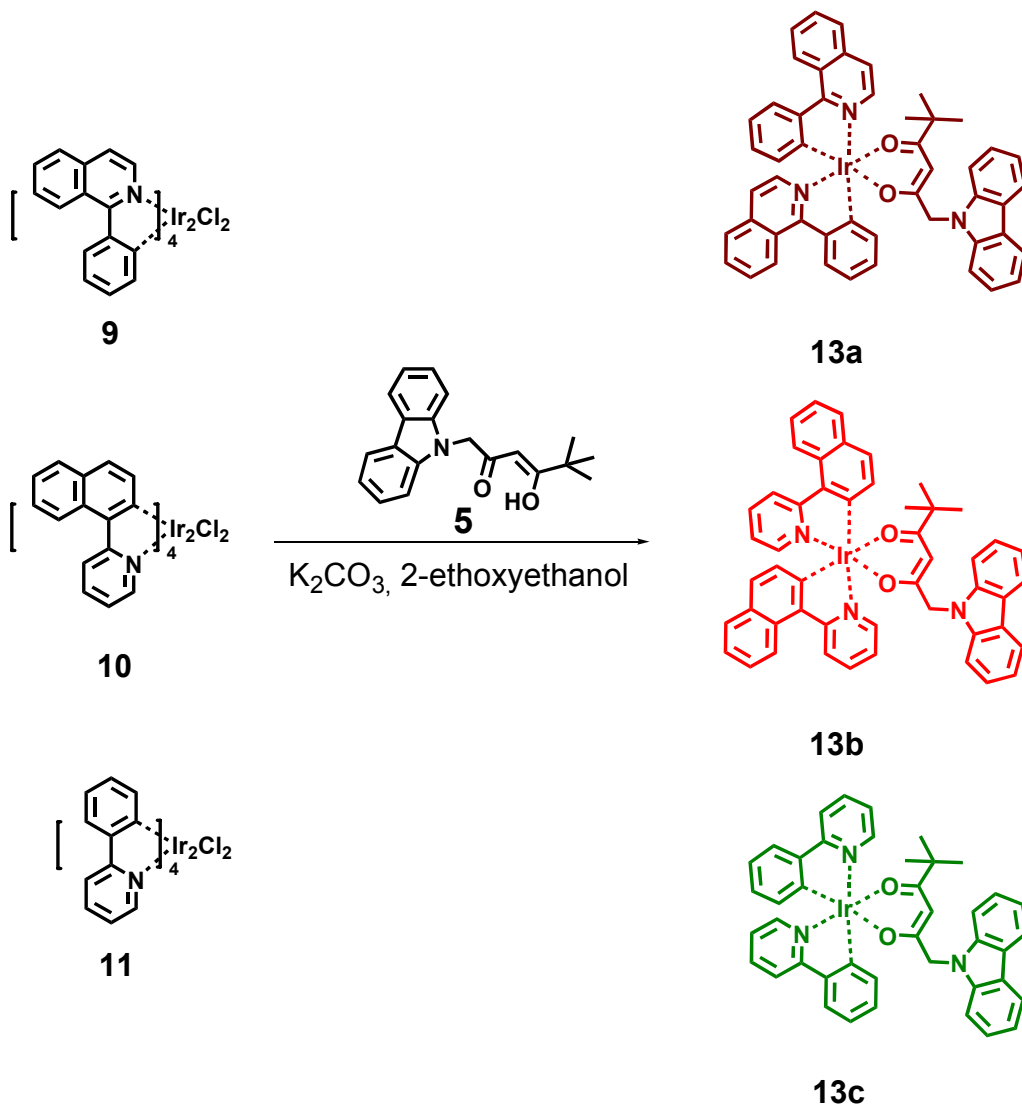


Figure 3.4. UV-vis absorption spectra of iridium(III) complexes **12a-c** (10^{-5} M in CHCl_3 solutions).

For complexes **12a** and **12b**, the strong absorption bands at about 253 nm, 254 nm, 241 nm, and 300 nm were assigned to spin-allowed $\pi \rightarrow \pi^*$ transitions of the cyclometalating *piq* and *npv* ligands. For complex **12c**, the intense absorption band at about 261 nm was attributed to spin-allowed $\pi \rightarrow \pi^*$ transitions of the cyclometalating *ppy* ligand. For complexes **12a-c**, the spin-allowed singlet $^1\text{MLCT}$ transition is located at about 400 nm, visible as a shoulder overlapping with the ligand $\pi \rightarrow \pi^*$ transitions. The absorptions at 482 nm for **12a**, 496 nm for **12b**, and 466 nm for **12c**, followed by a poorly resolved vibronic progression, are due to the transition from the ground state to spin-forbidden triplet $^3\text{MLCT}$ excited state. Excitation at 360 nm revealed a strong red and orange-red emission maximum of **12a** at 595 nm and **12b** at 596 nm. The emission band of **12c** was blue-shifted and displayed a deep green emission with a maximum at 525 nm.

3.3.2 Synthesis of iridium(III) complexes 13a-c

The efficient synthetic route to heteroleptic iridium(III) complexes **13a-c** is displayed in Scheme 3.4.



Scheme 3.4. Efficient synthetic route to heteroleptic iridium(III) complexes **13a-c**.

The heteroleptic iridium(III) complexes $[Ir^{III}(piq)_2\{1\text{-carbazol-9-yl-5,5-dimethyl-hexane-2,4-dione}\}]$ **13a**, $[Ir^{III}(npq)_2\{1\text{-carbazol-9-yl-5,5-dimethyl-hexane-2,4-dione}\}]$ **13b**, and $[Ir^{III}(ppq)_2\{1\text{-carbazol-9-yl-5,5-dimethyl-hexane-2,4-dione}\}]$ **13c** were fully characterised by IR, mass, 1H and ^{13}C NMR, UV-vis, emission spectra, and elemental analysis. The 1H NMR spectra of heteroleptic iridium(III) complexes **13a-**

Chapter 3. Iridium(III) complexes

c were measured in CDCl₃. Due to the inserted carbazole unit functioning as asymmetrical ancillary ligand, complexes **13a-c** are more complicated in the aromatic region of the ¹H NMR spectra compared to the respective precursor complexes **13a-c**. The ¹H NMR spectra of complexes **13a-c** are exhibited in Figure 3.5.

For the heteroleptic iridium(III) complex **13a-c**, the IR vibration properties were dominated by the vibrations of the acac ligand. The vibration bands at 3052 cm⁻¹ for **13a**, 3047 cm⁻¹ for **13b**, and 3037 cm⁻¹ for **13c** can be assigned to C=CH stretching vibrations. The characteristic bands for the C-CH₃, stretching vibrations (2961-2880 cm⁻¹) were observed in the expected region. The IR spectra show also weak IR-absorptions in the range of 1677-1559 cm⁻¹ (**13a**), 1681-1556 cm⁻¹ (**13b**), and 1678-1556 cm⁻¹ (**13c**), which can be attributed to the stretching vibrations of C=O and C=N groups.

The APLI mass spectra of **13a-c** are shown in Figure 3.6 along with the measured and simulated molecular weights. The agreement in the measured and calculated molecular weights powerfully verifies the existence of iridium(III) complexes **13a-c**.

Chapter 3. Iridium(III) complexes

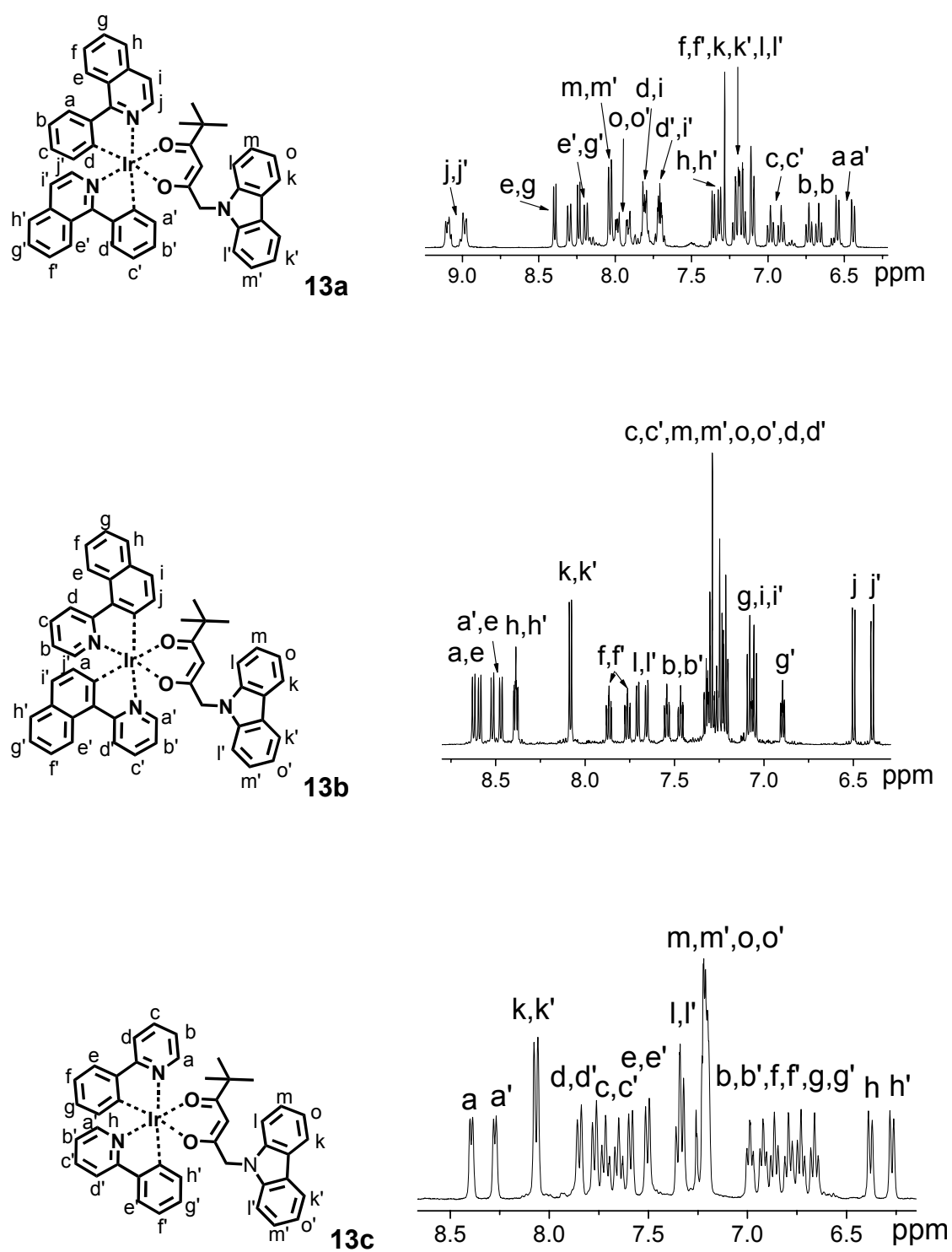


Figure 3.5. ^1H NMR spectra of heteroleptic iridium(III) complexes **13a-c** in CDCl_3 .

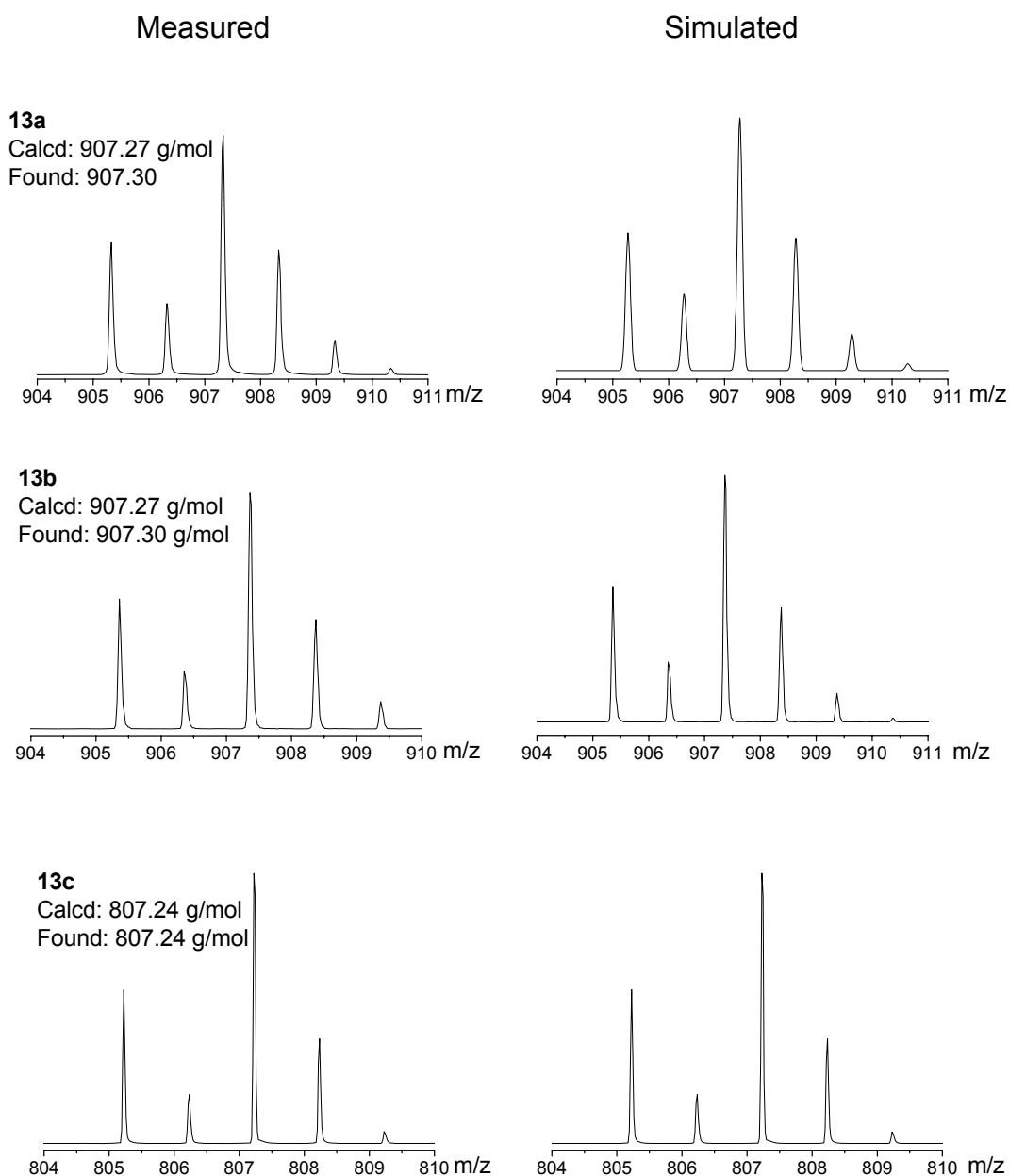


Figure 3.6. The measured and simulated APLI mass spectra of iridium(III) complexes **13a-c**.

The TGA measurements revealed the decomposition temperature (T_d at 5% weight loss) at 356 °C for **13a**, 336 °C for **13b**, and 337 °C for **13c**, respectively; these results are summarised in Table 3.2. The analysis of the quantum yields in solution showed very similar results compared to each other (31% **13a**, 34% **13b**, and 37% **13c**).

The UV-Vis absorption spectra of complexes **13a-c** in chloroform (CHCl_3) solution are shown in Figure 3.7 and the data are listed in Table 3.2.

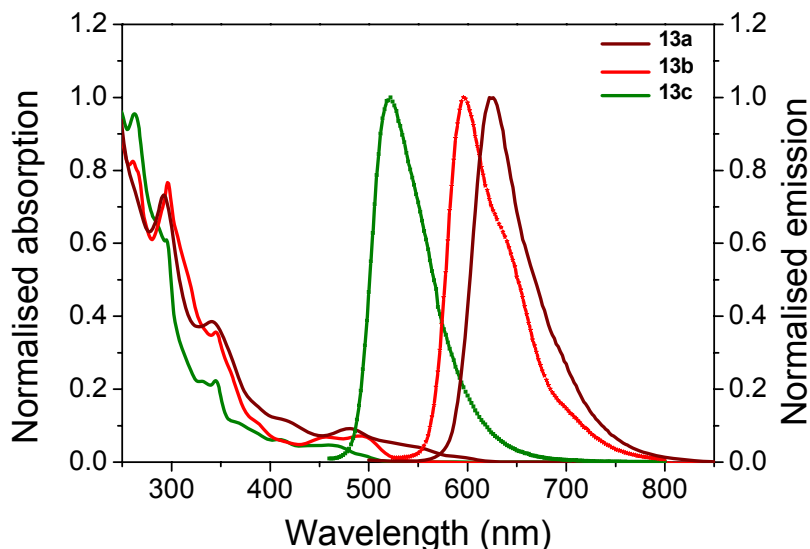
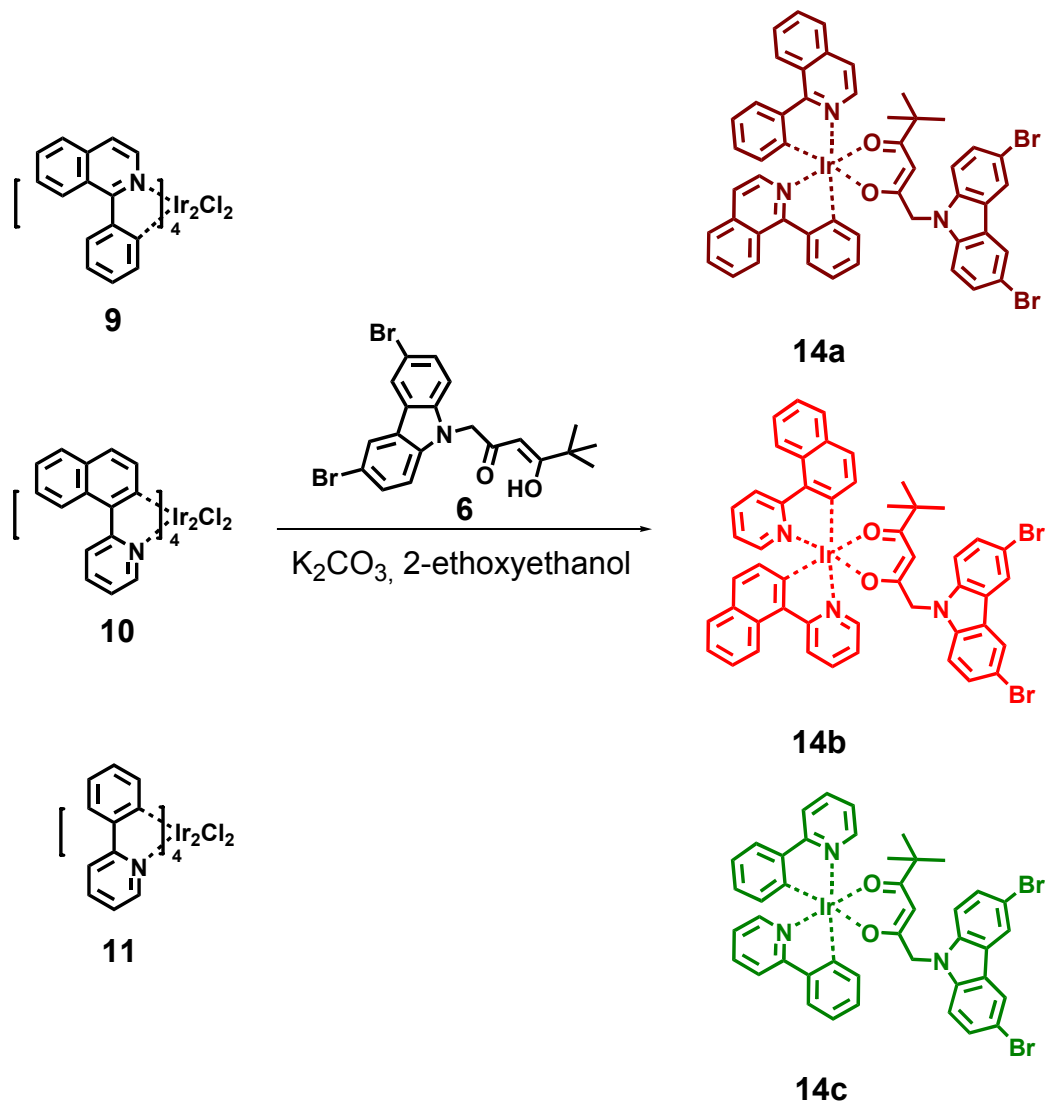


Figure 3.7. UV-vis absorption spectra of iridium(III) complexes **13a-b** (10^{-5} M in CHCl_3 solutions).

For these Ir(III) complexes, the absorption spectra show broad bands from 240 nm to 500 nm, whereby the most intense bands are at $\lambda < 300$ nm while moderately intense bands are at longer wavelengths, which extend in the visible region. The bands between 250 nm and 300 nm can be assigned to spin-allowed singlet ligand-centred (^1LC) transitions. The absorption bands around 350–450 nm are attributed to the spin-allowed singlet charge-transfer ($^1\text{MLCT}$) transitions. The absorption features at lowest energy ($\lambda > 470$ nm) are likely to be assigned to spin-forbidden triplet charge-transfer ($^3\text{MLCT}$) transitions. The strong emission spectra of **13a-c** excited at 360 nm were observed in the green region (521 nm for **13c**) and in the red region (597 nm for **13b** and 624 nm for **13a**).

3.3.3 Synthesis of iridium(III) complexes 14a-c

The efficient synthetic route to heteroleptic iridium(III) complexes **14a-c** is displayed in Scheme 3.5.



Scheme 3.5. Efficient synthetic route to heteroleptic iridium(III) complexes **14a-c**.

The 1H NMR spectra of the heteroleptic iridium(III) complexes $[Ir^{III}(piq)_2\{1-(3,6\text{-dibromocarbazol-9-yl})\text{-5,5-dimethyl-hexane-2,4-dione}\}]$ (**14a**, yield: 56%), $[Ir^{III}(npq)_2\{1-(3,6\text{-dibromocarbazol-9-yl})\text{-5,5-dimethyl-hexane-2,4-dione}\}]$ (**14b**, yield: 41%), and $[1-(3,6\text{-dibromocarbazol-9-yl})\text{-5,5-dimethyl-hexane-2,4-dione}\}]$ (**14c**, yield: 69%) are exhibited in Figure 3.8. The complicated and diversified 1H

Chapter 3. Iridium(III) complexes

NMR spectra of these complexes can directly portray the asymmetrical configuration of these complexes.

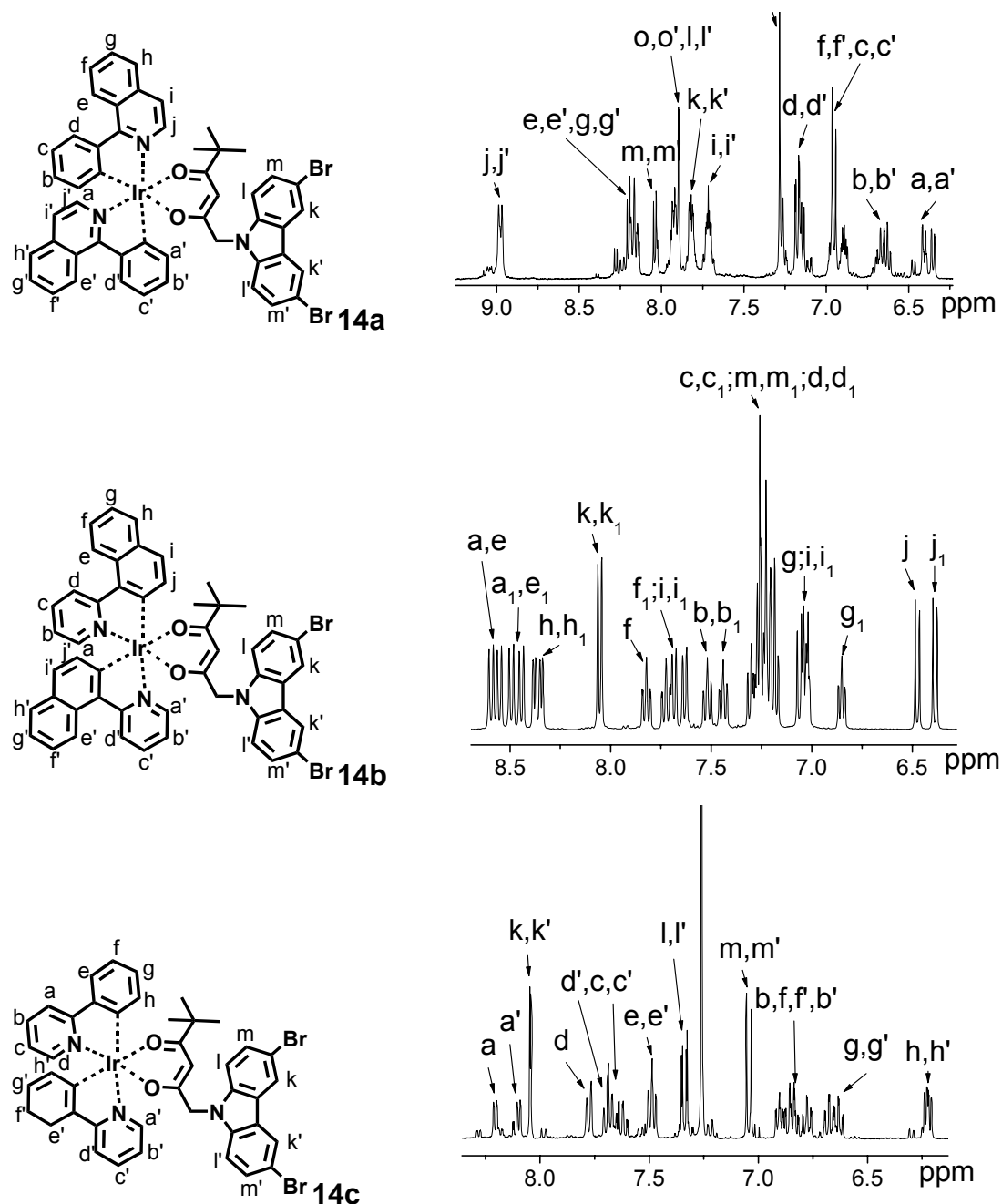


Figure 3.8. ^1H NMR spectra of heteroleptic iridium(III) complexes **14a-c** in CDCl_3 .

The bands in the range of $3037\text{--}3056\text{ cm}^{-1}$ represent the $\text{C}=\text{CH}$ stretching vibrations of **14a-c**, while the peaks in the region $2961\text{--}2880\text{ cm}^{-1}$ stand for the $\text{C}-$

Chapter 3. Iridium(III) complexes

CH₃, stretching vibrations. The vibrations at 1677-1705 cm⁻¹ prove the existence of C=O functional groups, whereas the vibration at 1500-1578 cm⁻¹ confirms the presence of C=N functional groups. The molecular masses of **14a-c** were investigated by the use of APLI mass and molecular weights of 1063.10 g/mol (**14a**), 1063.10 g/mol (**14b**), and 963.10 g/mol (**14c**) (Table 3.1, Figure 3.9) were detected.

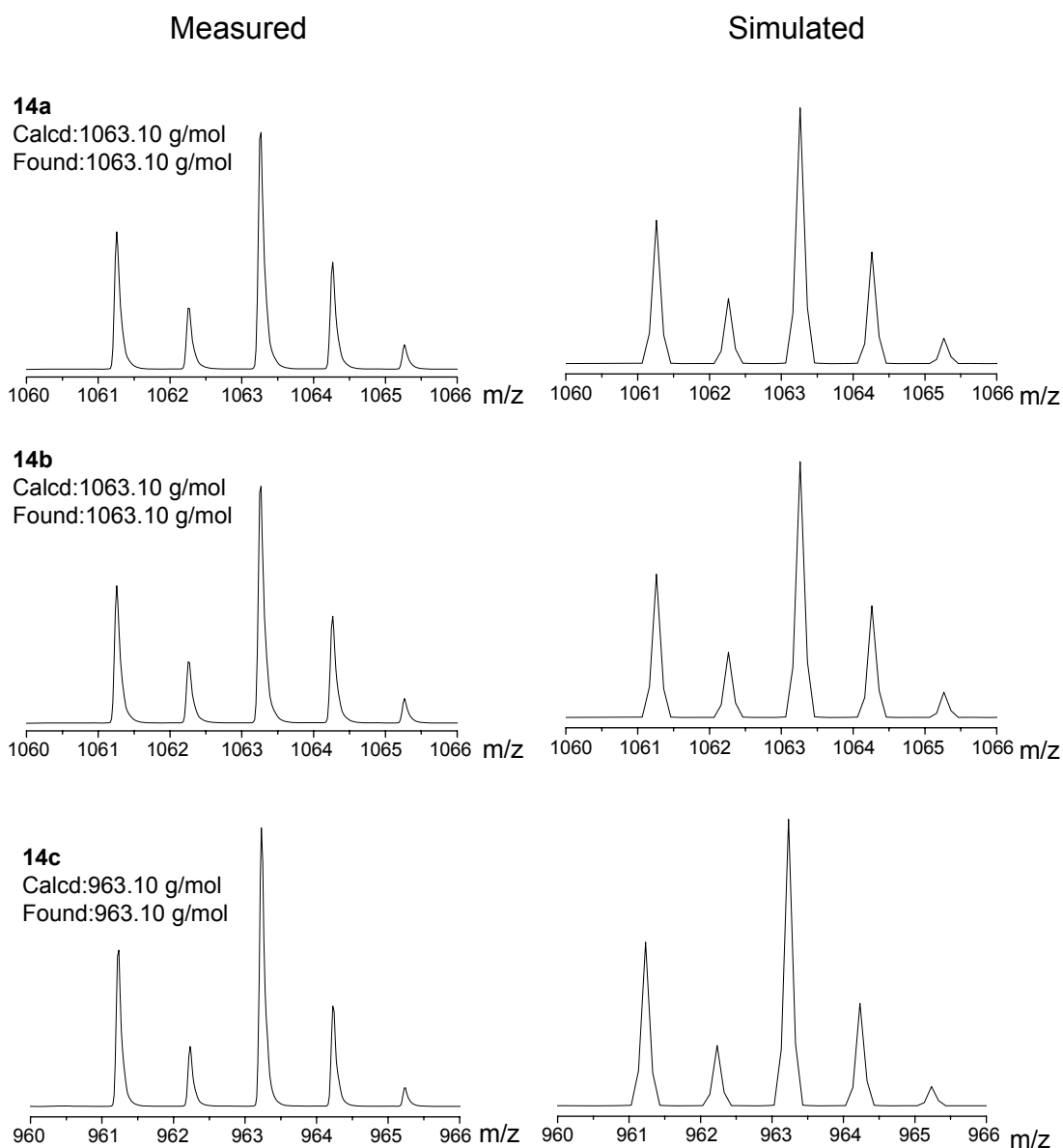


Figure 3.9. The measured and simulated mass spectra of iridium(III) complexes **14a-c**.

The measured quantum yields of **14a-c** were in the range of 26-35% (Table 3.2). The decomposition temperatures (T_d) of **14a-c**, which correspond to a 5% weight loss upon heating during TGA, were in the range of 223–353 °C.

The absorption spectra of complexes **14a-c** in chloroform are depicted in Figure 3.10.

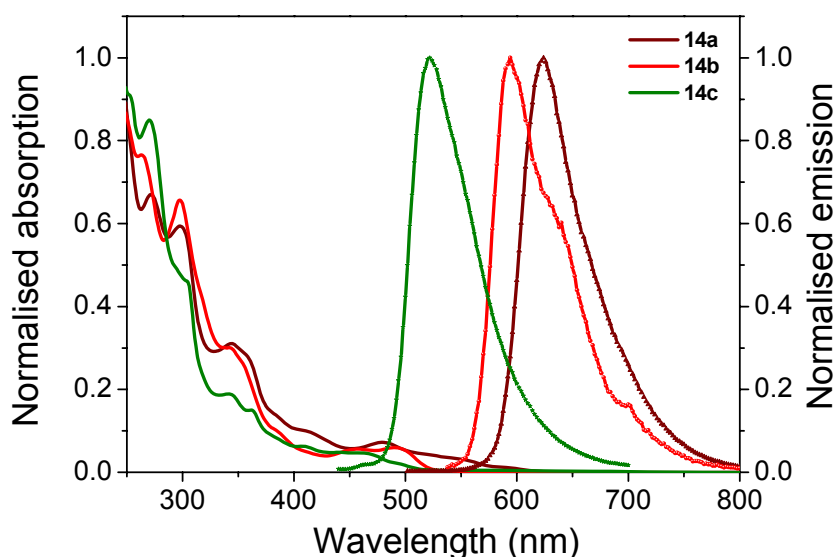
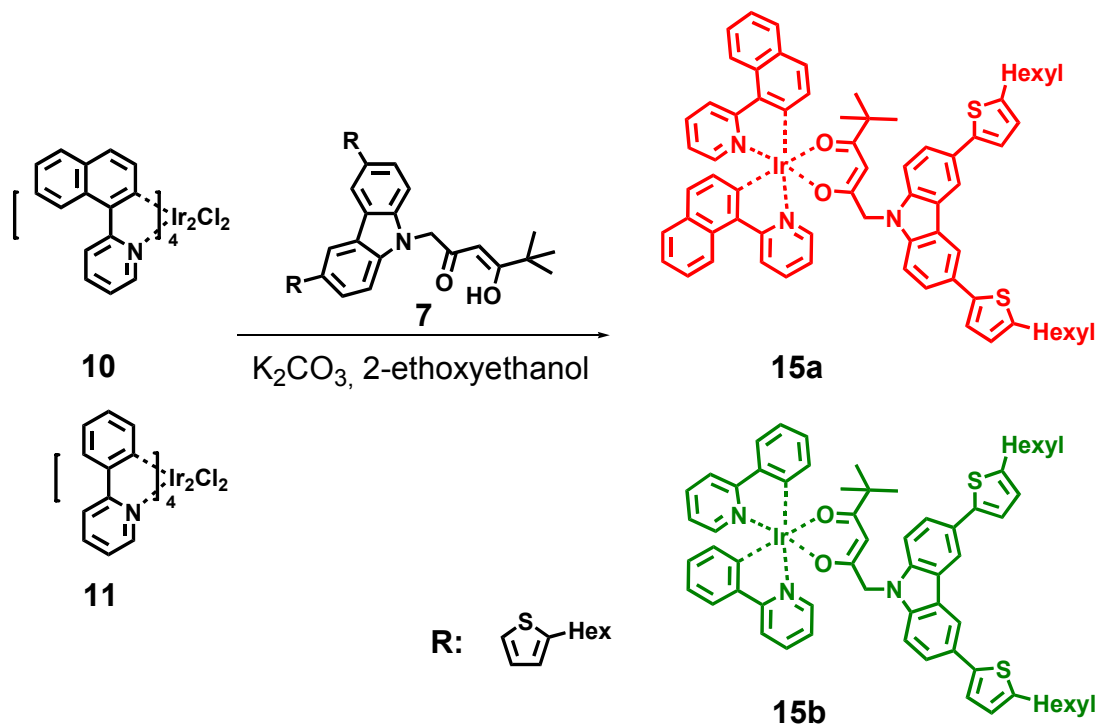


Figure 3.10. UV-vis absorption spectra of iridium(III) complexes **14a-c** (10^{-5} M in CHCl_3 solutions).

The strong absorption bands <300 nm in the UV region with distinct vibronic features are assigned to the spin-allowed singlet ligand-centred (^1LC) transition of the cyclometalated *piq*, *npq*, and *ppy* ligands and β -diketonate-based transitions that resemble the absorptions of the free β -diketone. The next lower energy absorption with peak wavelengths in the region of 350-450 nm can be ascribed to a typical spin-allowed metal to ligand charge-transfer ($^1\text{MLCT}$) transition, while the weak shoulder (450-500 nm) extending into the visible region is believed to be associated with both spin-orbit coupling enhanced $^3\text{MLCT}$ transitions. For **14a-c**, the maximal emissions in CHCl_3 were at 624 nm, 595 nm, and 522 nm, respectively.

3.3.4 Synthesis of iridium(III) complexes 15a-b

The efficient synthetic route to heteroleptic iridium(III) complexes **15a-b** is displayed in Scheme 3.6.



Scheme 3.6. Efficient synthetic route to heteroleptic iridium(III) complexes **15a** and **15b**.

The 1H NMR spectra of the heteroleptic iridium(III) complexes $[Ir^{III}(npy)_2\{1-[3,6-bis(5-hexyl-2-thienyl)carbazol-9-yl]-5,5-dimethyl-hexane-2,4-dione\}]$ (**15a**, yield: 41%) and $[Ir^{III}(ppy)_2\{1-[3,6-bis(5-hexyl-2-thienyl)carbazol-9-yl]-5,5-dimethyl-hexane-2,4-dione\}]$ (**15b**, yield: 46%) are shown in Figure 3.11.

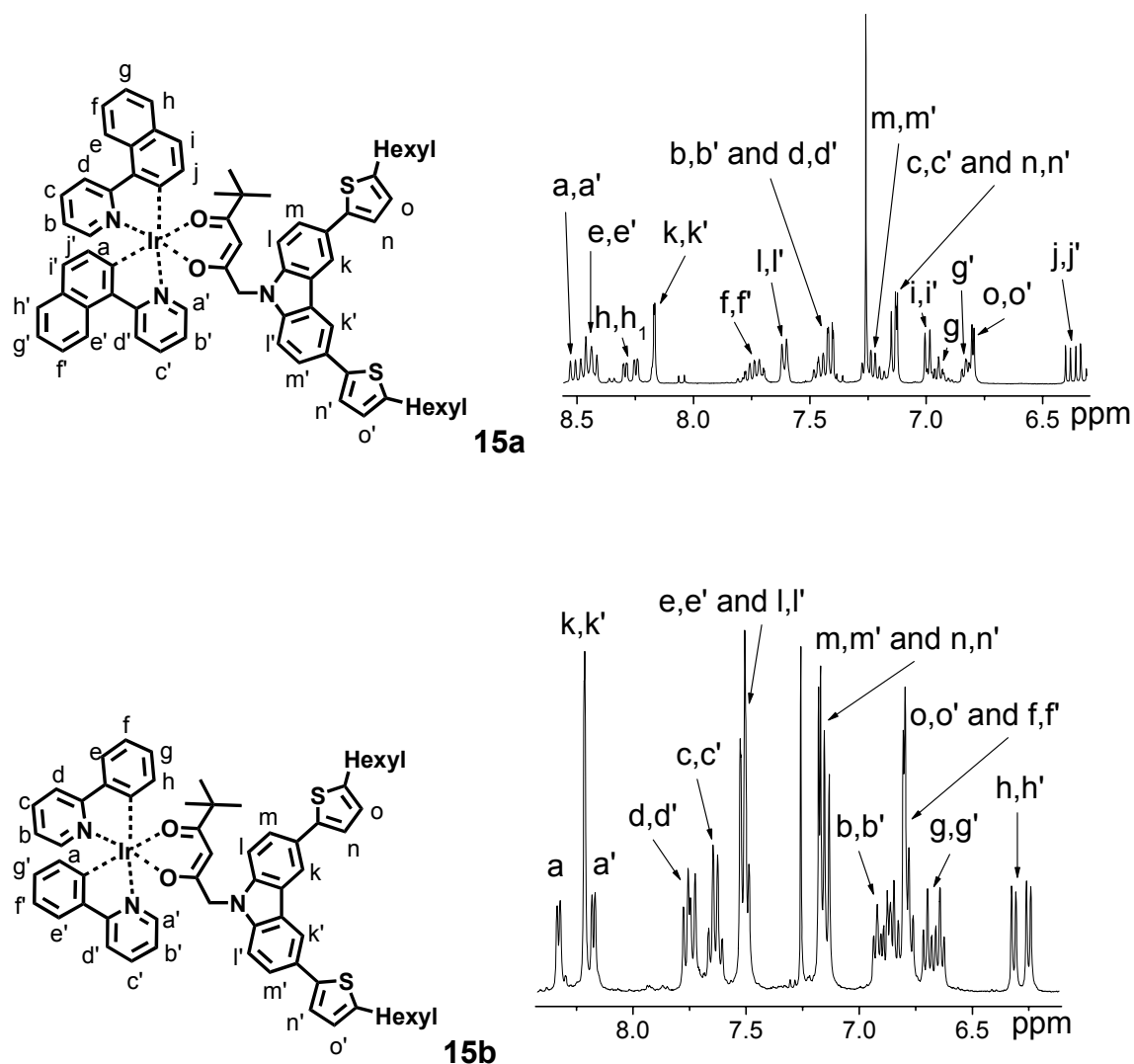


Figure 3.11. ^1H NMR spectra of heteroleptic iridium(III) complexes **15a-b** in CDCl_3 .

The vibration bands at 3043 cm^{-1} for **15a** and 3058 cm^{-1} for **15b** can be assigned to C=CH stretching vibrations in the IR spectra. The characteristic bands for C-CH₃ stretching vibrations ($2961\text{-}2880\text{ cm}^{-1}$) are observed in the expected region. The stretching vibration of the C=O groups is found at 1625 cm^{-1} for **15a** and at 1698 cm^{-1} for **15b**, while the C=N stretching vibrations are located in the range of $1498\text{-}1575\text{ cm}^{-1}$ for **15a-b**. The results of the APLI mass spectrometric analysis of **15a-b** show agreement between the measured and calculated molecular weights (Figure 3.12).

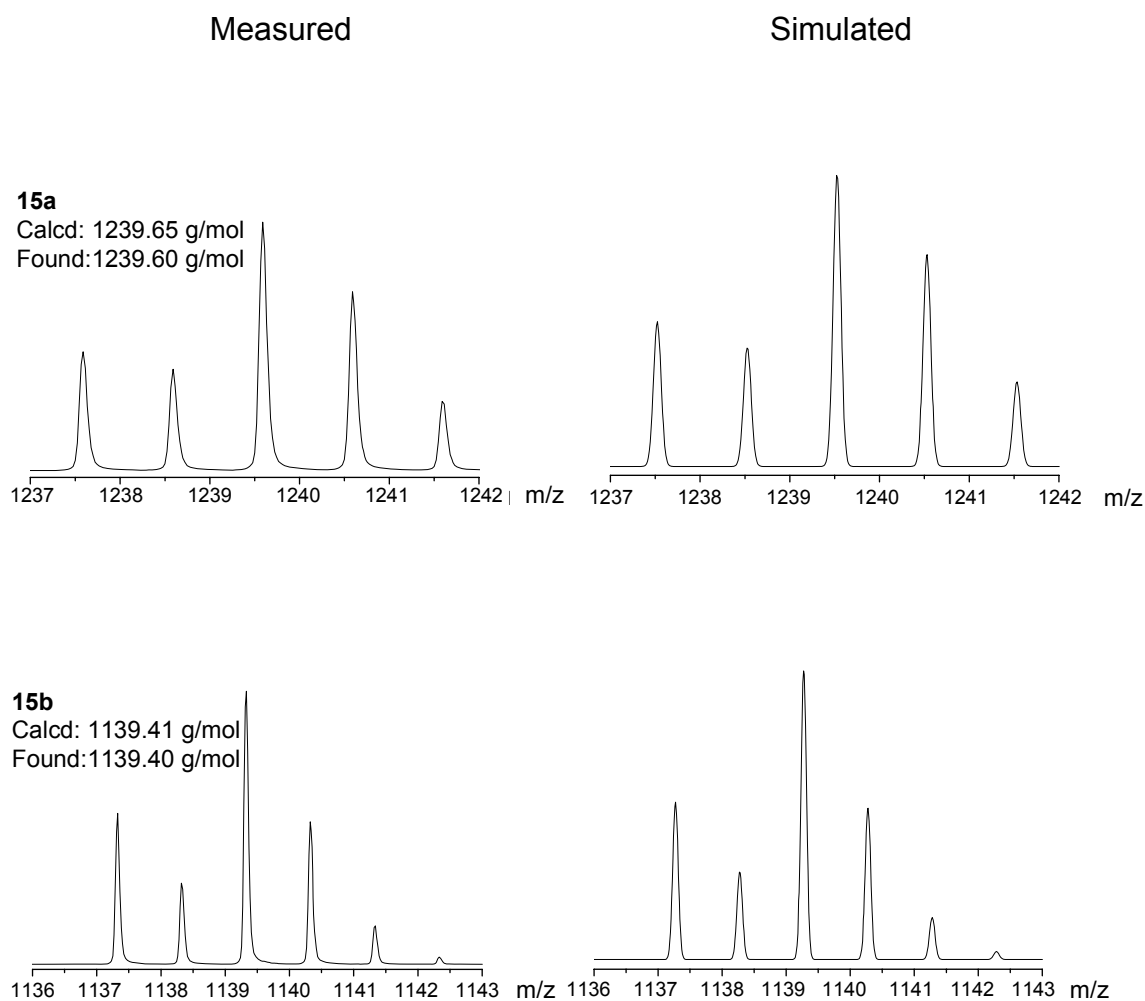


Figure 3.12. The measured and simulated mass spectra of iridium(III) complexes **15a-b**.

The thermal properties of Ir(III) complexes **15a-b** were evaluated by TGA. Excellent thermal stability was manifested in their TGA profiles with onset of decomposition temperatures (T_d at 5% weigh loss) of 302 °C for **15a** and 353 °C for **15b** (Table 3.2). The quantum yields were 36% (**15a**) and 28% (**15b**). Compared to the TGA measurements of the other complexes, both complexes revealed a relatively higher T_d , which can be attributed to the replacement of the H-atom by a Br-atom at the 3,6-positions of carbazole, which most likely increased their thermal stability.

The photophysical properties of **15a-b** in CHCl_3 solution were investigated, and the data are given in Table 3.2. The UV-vis absorption spectra of both complexes are shown in Figure 3.13.

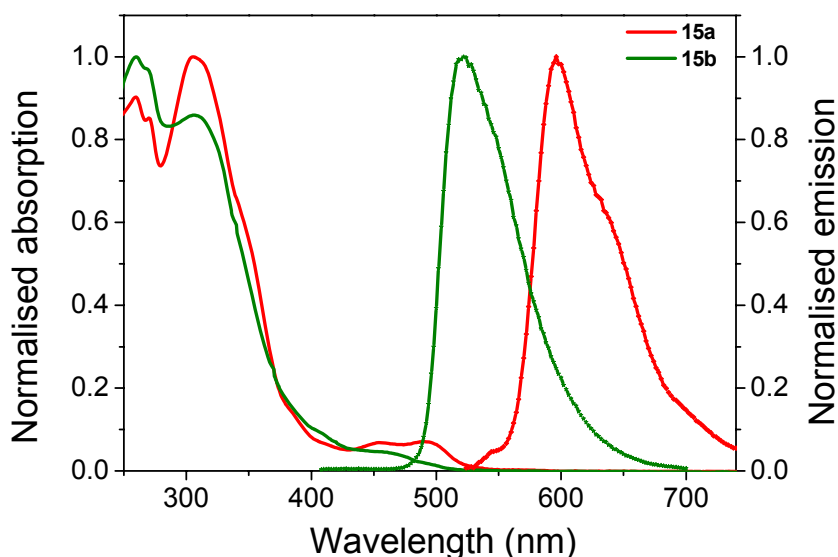
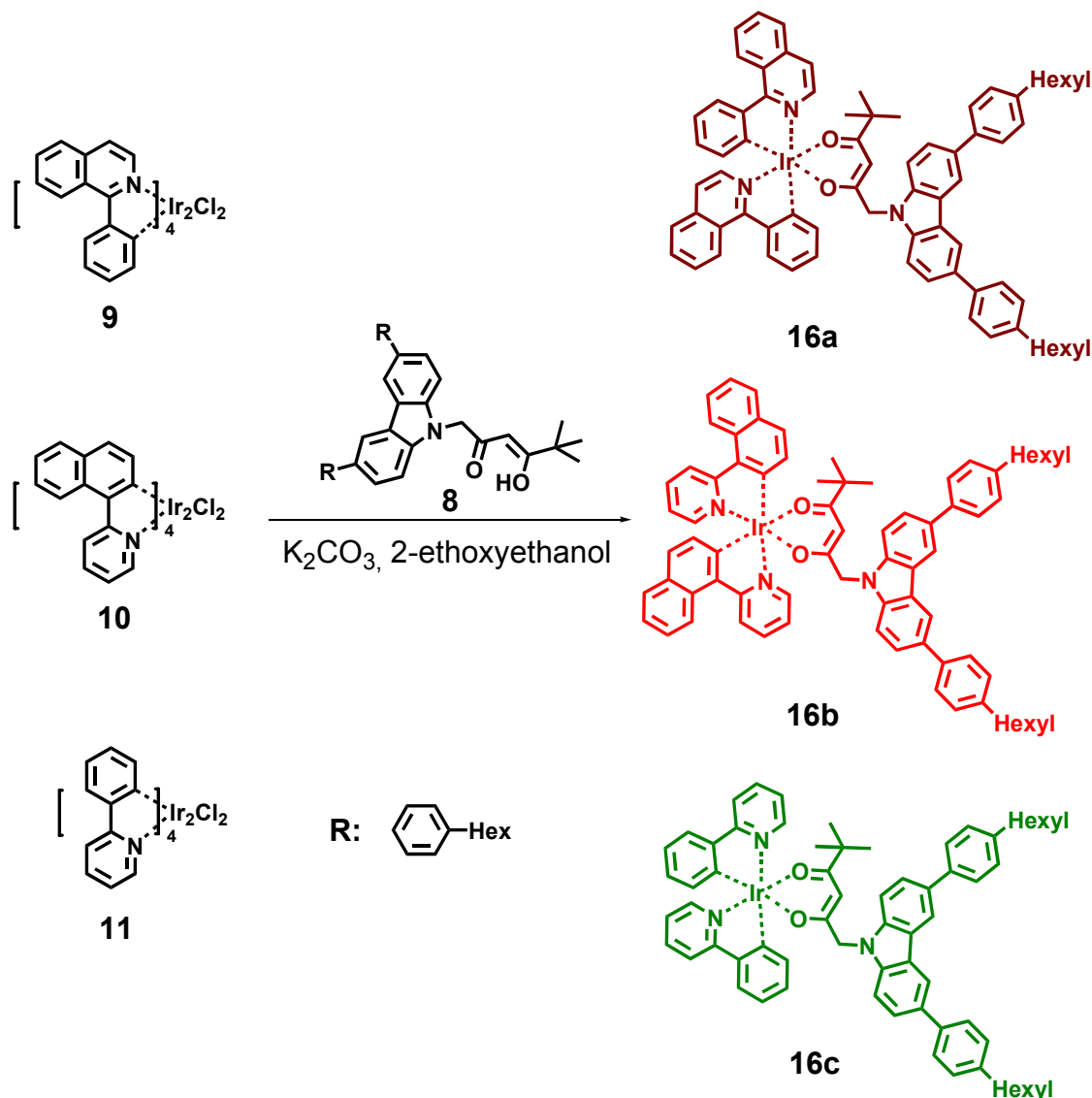


Figure 3.13. UV-vis absorption spectra of iridium(III) complexes **15a-b** (10^{-5} M in CHCl_3 solutions).

Complexes **15a-b** displayed intense absorption bands in the ultraviolet region of 260-320 nm, which are assigned to the spin-allowed $\pi \rightarrow \pi^*$ transitions of the cyclometalating *piq*, *npq*, and *ppy* ligands. The weak bands at 400-450 nm are assigned to spin-allowed $^1\text{MLCT}$ transitions. In addition, all complexes show weaker absorption tails above 450 nm, which are attributed to spin-forbidden $^3\text{MLCT}$ and ^3LC transitions. The emission spectra of **15a-b** exhibit intensive peaks at 595 nm for **15a** and 522 nm for **15b**, which are almost at the same position as the major emission peaks of complexes **12-14b** containing the *npq* ligand and **12-14c** containing the *ppy* ligand in solution.

3.3.5 Synthesis of iridium(III) complexes 16a-c

The straight-forward synthetic route to heteroleptic iridium(III) complexes **16a-c** is displayed in Scheme 3.7.



Scheme 3.7. Efficient synthetic route to heteroleptic iridium(III) complexes **16a-c**.

The ^1H NMR spectra of the heteroleptic iridium(III) complexes $[\text{Ir}^{\text{III}}(\text{piq})_2\{1\text{-}[3,6\text{-bis}(4\text{-hexylphenyl})\text{carbazol-9-yl}]\text{-5,5-dimethyl-hexane-2,4-dione}\}]$ (**16a**, yield: 72%), $[\text{Ir}^{\text{III}}(\text{npq})_2\{1\text{-}[3,6\text{-bis}(4\text{-hexylphenyl})\text{carbazol-9-yl}]\text{-5,5-dimethyl-hexane-2,4-dione}\}]$ (**16b**, yield: 65%), and $[\text{Ir}^{\text{III}}(\text{ppq})_2\{1\text{-}[3,6\text{-bis}(4\text{-hexylphenyl})\text{carbazol-9-yl}]\text{-5,5-dimethyl-hexane-2,4-dione}\}]$ (**16c**, yield: 68%) are shown in Figure 3.14.

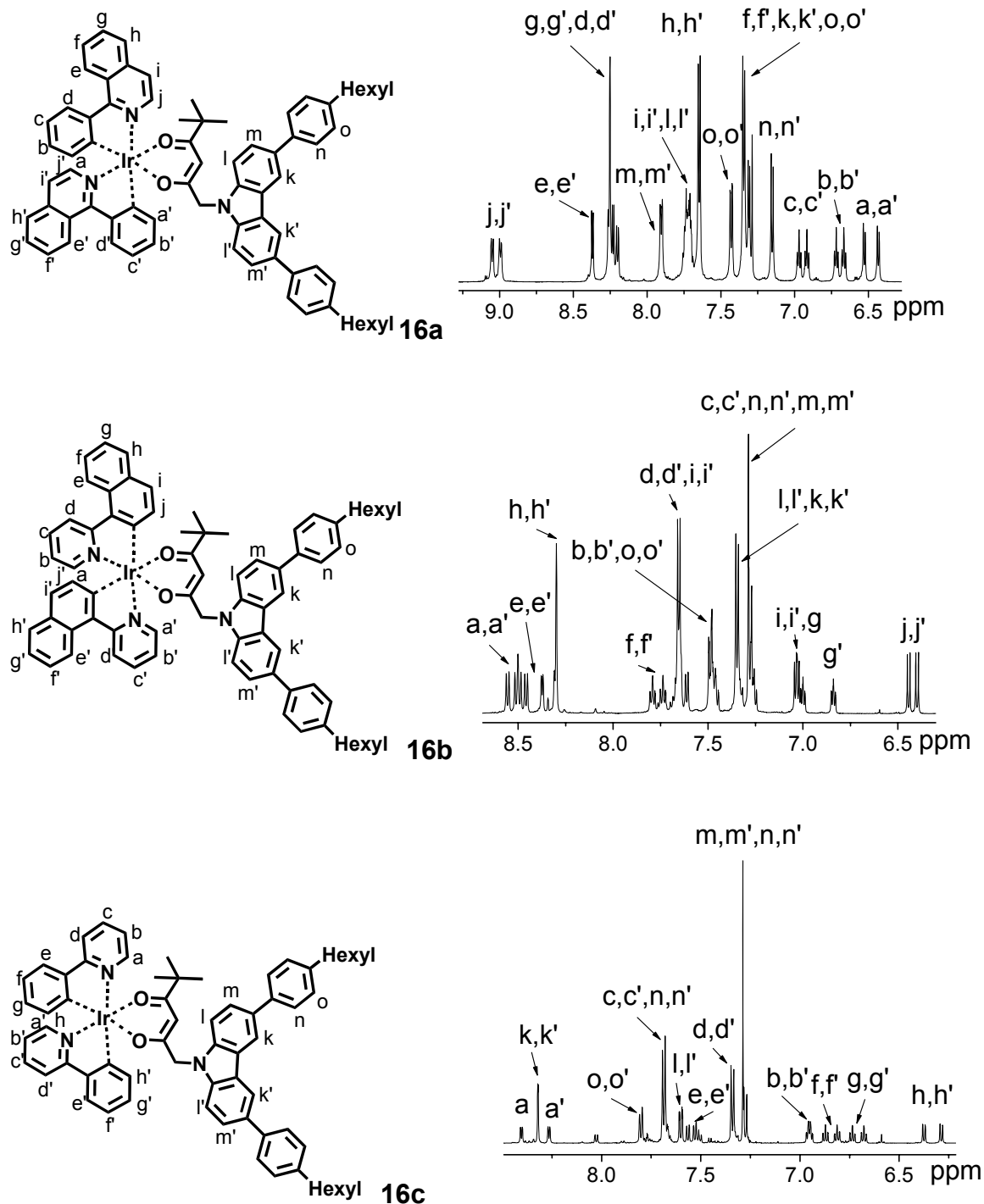


Figure 3.14. ^1H NMR spectra of heteroleptic iridium(III) complexes **16a-c** in CDCl_3 .

By means of infrared spectroscopy, the $\text{C}=\text{CH}$ functional groups of **16a-c** can be confirmed by the vibration bands between $3049\text{-}3047\text{ cm}^{-1}$. The characteristic

Chapter 3. Iridium(III) complexes

bands for the C-CH₃ stretching vibrations (2961-2880 cm⁻¹) are found in the expected region. The stretching vibration of the C=O groups is dominant in the region of 1657-1688 cm⁻¹, while the stretching vibration of C=N groups is revealed at about 1556 cm⁻¹. The APLI mass spectra of **16a-c** exhibited the expected results (Figure 3.15). The measured molecular weights of **16a-c** were identical with the calculated molecular weights (see Table 3.1).

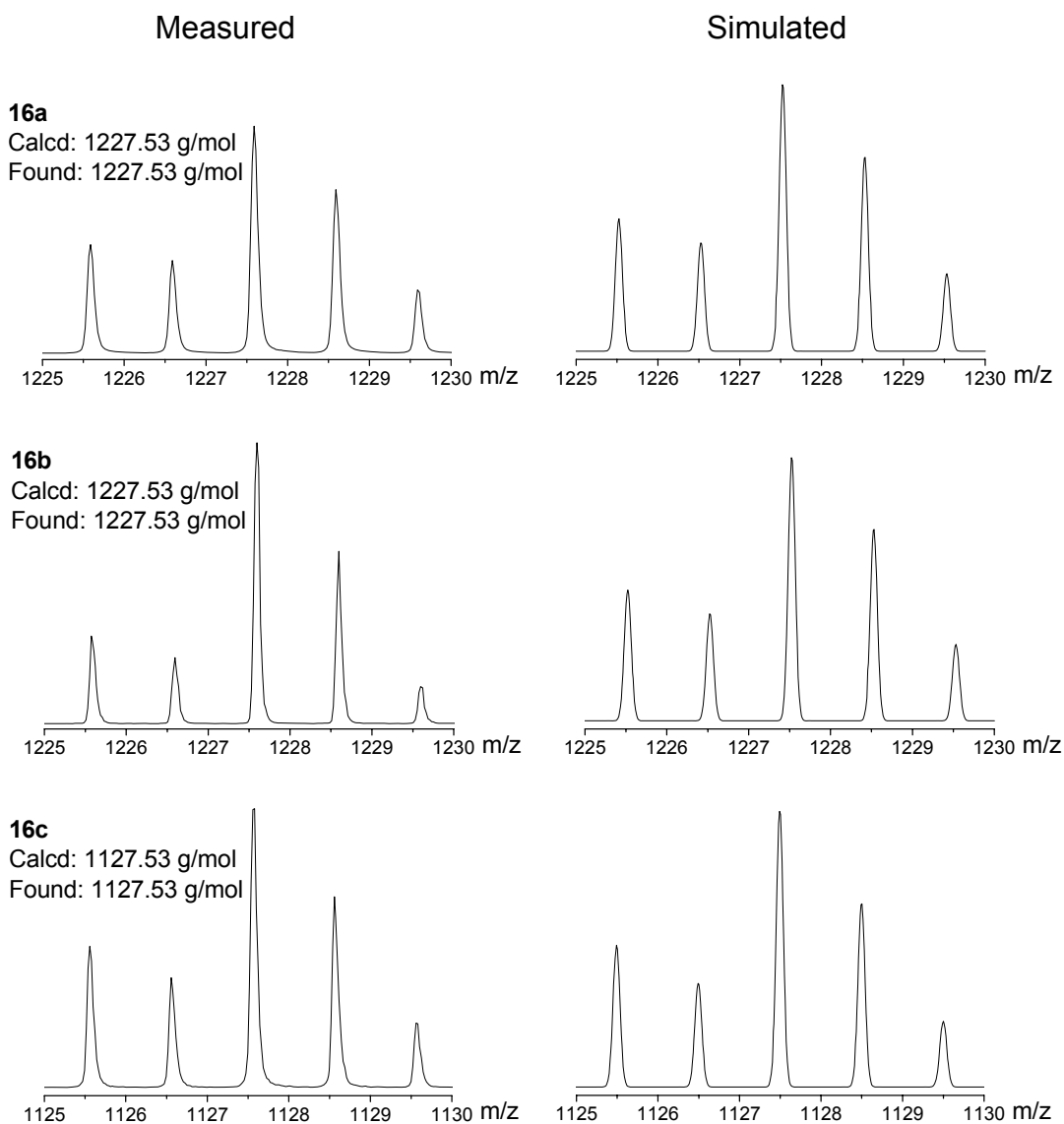


Figure 3.15. The measured and simulated mass spectra of Ir(III) complex **16a-c**.

The thermal stability of iridium(III) complexes **16a-c** was evaluated by TGA under a nitrogen atmosphere. TGA revealed that complexes **16a-c** were thermally stable

up to 315 °C. The quantum yields were 30% (**16a**), 32% (**16b**), and 44% (**16c**). The decomposition temperatures of iridium(III) complexes **16a-c** are summarised in Table 3.2.

The UV-vis spectra of iridium(III) complexes **16a-c** in CHCl_3 are shown in Figure 3.16.

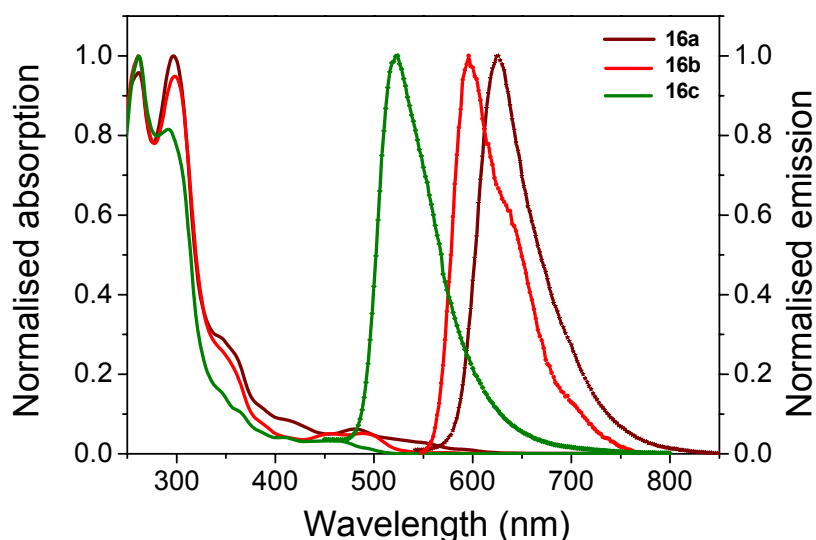


Figure 3.16. UV-vis absorption spectra of iridium(III) complexes **16a-c** (10^{-5} M in CHCl_3 solution).

The intense absorption bands at about 259 nm and 297 nm for **16a**, 260 nm and 296 nm for **16b**, and 259 nm and 292 nm for **16c** are attributed to spin-allowed $\pi \rightarrow \pi^*$ transitions of the cyclometalating *piq*, *npq*, and *ppy* ligands. The slight absorption peaks at 482 nm for **16a**, 492 nm for **16b**, and 454 nm for **16c** arise as spin-forbidden triplet $^3\text{MLCT}$ excited states. However, the absorptions for Ir(III) complexes **16a-c** in the UV region below 240 nm are most likely due to β -diketonate-based transitions that resemble the absorptions of the free β -diketone. The emission maximum excited at 360 nm for **16a** in CHCl_3 solution is located at

Chapter 3. Iridium(III) complexes

625 nm, whereas those for iridium(III) complexes **16b** and **16c** have λ_{\max} at 595 nm and 522 nm, respectively.

Table 3.1. Identified and calculated molecular weights of iridium(III) complexes **12-16a-c**.

Ir(III) compound	Identified molecular weight (g/mol)	Calculated molecular weight (g/mol)
12a	784.26	784.26
12b	784.26	784.26
12c	684.23	684.23
13a	907.27	907.27
13b	907.27	907.27
13c	807.24	807.24
14a	1063.10	1063.10
14b	1063.10	1063.10
14c	963.10	963.10
15a	1239.65	1239.60
15b	1139.41	1139.40
16a	1227.53	1227.53
16b	1227.53	1227.53
16c	1127.52	1127.50

The experimental UV-vis absorption and emission spectra of iridium(III) complexes **12-16a-c** recorded in CHCl_3 are depicted in Figure 3.2, 3.5, 3.8, 3.11, and 3.14. The detailed data on their photophysical characteristics and T_d are shown in Table 3.2.

Chapter 3. Iridium(III) complexes

Table 3.2. The data of absorption and emission maxima, of quantum yields and decomposition temperature of iridium(III) complexes **12-16a-c**.

Ir(III) compound	Absorbance [nm] (log ϵ [L \times mol ⁻¹ \times cm ⁻¹])	Maximum of Emission [nm]	Quantum yield ^[a] [%]	T _d [°C] ^[b]
12a	293 (4.98), 344 (3.73) 419 (3.28), 484 (3.20)	630	35	284.3
12b	240 (4.03), 300 (4.04) 458 (3.11), 497 (3.14)	600	37	281.2
12c	260 (5.29), 341 (3.62) 412 (3.25), 468 (3.14)	522	58	302.3
13a	247 (5.33), 291 (5.20) 341 (3.93), 478 (3.29)	624	31	356.0
13b	242 (3.99), 296 (3.87) 346 (3.54), 490 (2.83)	597	34	336.0
13c	240 (4.02), 262 (3.99) 345 (3.37), 462 (2.70)	521	37	337.3
14a	242 (4.91), 270 (3.89) 342 (3.26), 453 (2.68)	624	26	223.0
14b	260 (4.67), 297 (4.61) 342 (4.27), 488 (3.57)	595	27	207.0
14c	270 (4.71), 342 (4.06) 408 (3.58), 459, (3.45)	522	35	353.0
15a	260 (4.95), 308 (4.81) 400 (3.67), 488 (3.57)	595	36	302.0
15b	270 (4.93), 313 (4.91) 408 (3.67), 459, (3.44)	522	28	353.0
16a	264 (3.97), 299 (3.98) 359 (3.40), 481 (2.79)	625	30	340.0
16b	262 (5.06), 296 (5.02) 356 (3.66), 490 (3.18)	595	32	315.6
16c	235 (3.86), 262 (5.08) 291 (3.98), 466 (2.49)	522	44	324.6

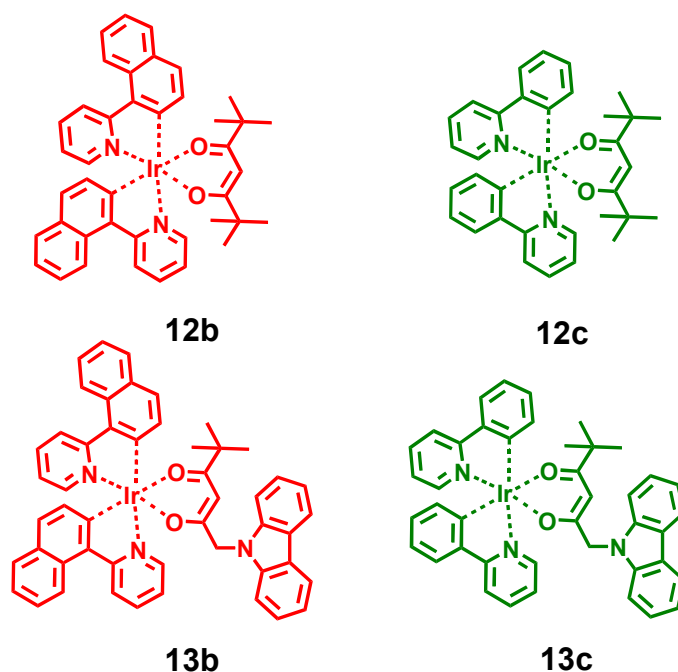
[a] determined according to the method of Demas and Crosby [18].

[b] at 5% weight loss.

3.4 Electrophosphorescence

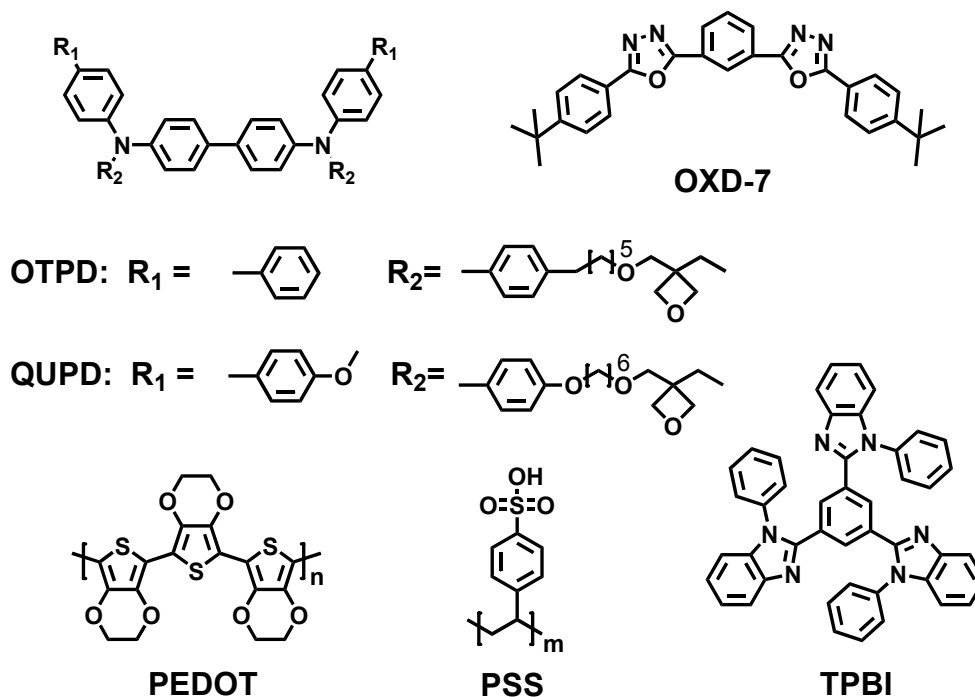
In order to investigate the electrophosphorescence properties of the neutral Ir(III) complexes in polymer or organic LED devices, some of them were chosen as emitters and implemented in devices prepared by Yaroslav V. Aulin and Oleksandr Mikhnenko in the Physics of Organic Semiconductors group of Prof. Maria Antonietta Loi and Prof. Paul. W. M. Blom at the Zernike Institute for Advanced Materials at the University of Groningen and by Alexander Thiessen, Dimitrios Kourkoulos and Dirk Hertel at the Physical Chemistry group of Prof. Klaus Meerholz at the Institute of Physical Chemistry at the University of Cologne. The measurements were compared to well-known homoleptic and heteroleptic Ir(III) complexes.

In order to investigate electroluminescence properties of OLED devices consisting of different layers, three different layer-structured assemblies (Scheme 3.10) based on iridium(III) complexes **12b-c** and **13b-c** (Scheme 3.8) as emitter materials were fabricated [5]. These measurements were performed by Dimitrios Kourkoulos and Dirk Hertel at the Physical Chemistry group of Prof. Klaus Meerholz at the Institute of Physical Chemistry at the University of Cologne.

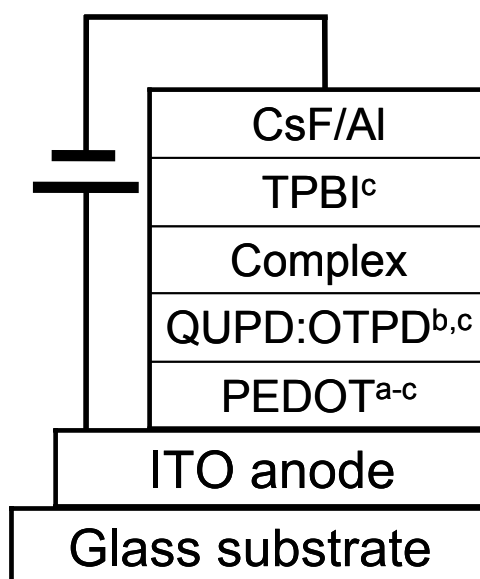


Scheme 3.8. Schematic representation of selected iridium(III) complexes **12b-c** and **13b-c**.

The investigation of the electroluminescent properties was conducted by fabricating different devices of ITO/PEDOT:PSS/COMPLEX/metal, ITO/PEDOT:PSS/HTL/COMPLEX/metal, and ITO/PEDOT:PSS/HTL/COMPLEX/ETL/metal, in which PEDOT:PSS worked as the anode and COMPLEX as the phosphorescent dopant emitter (PEDOT: [poly(3,4-ethylenedioxy-thiophene)], PSS: poly(styrenesulphonate), QUPD: (*N,N'*-bis(4-(6-((3-ethyloxetane-3-y)methoxy)-hexyloxy)phenyl)-*N,N'*-bis(4-methoxy-phenyl)biphenyl-4,4'-diamine), OTPD: *N,N'*-bis(4-[6-[(3-ethyloxetane-3-yl)-methoxy]-hexylphenyl]-*N,N'*-diphenyl-4,4'-diamine), TPBI: 1,3,5-*tris*(1-phenyl-1*H*-benzo[d]imidazol-2-yl)benzene) (Scheme 3.9). QUPD:OTPD were used as hole transporting materials and TPBI as the electron-transporting material (Scheme 3.10).



Scheme 3.9. The structures of OTPD, QUPD, PEDOT, PSS, and TPBI.



Scheme 3.10. The three different OLED devices based on complexes **12b-c** and **13b-c** (a: device 1, b: device 2, c: device 3).

The first device structure was fabricated with ITO/PEDOT(28 nm)/COMPLEX(**12b**: 44 nm, **12c**: 67 nm, **13b**: 44 nm, **13c**: 73 nm, respectively)/CsF(3 nm)/Al(120 nm).

The second device was based on the structure of ITO/PEDOT(28 nm)/QUPD(18

Chapter 3. Iridium(III) complexes

nm):OTPD(20 nm)/COMPLEX(**12c**: 67 nm, **13c**: 73 nm, respectively)/CsF(3 nm)/Al(120 nm). For the third device containing QUPD:OTPD as the hole-transporting layer and TPBI as the electron-transporting layer, the device structure had the following layout: ITO/PEDOT(28 nm)/QUPD(18 nm):OTPD(18 nm)/COMPLEX(**13b**: 21 nm, **13c**: 21 nm, respectively)/TPBI(30 nm)/CsF(3 nm)/Al(120 nm). The performance data of the investigated OLED devices with iridium(III) complexes **12a-b** and **13a-b** are summarised in Table 3.3. The remarkably higher performance of complexes **12c** and **13b** in device 3 may be due to the configuration with hole- and electron-transporting layers and showed that the composition of the device is very important in order to obtain higher luminous efficiency.

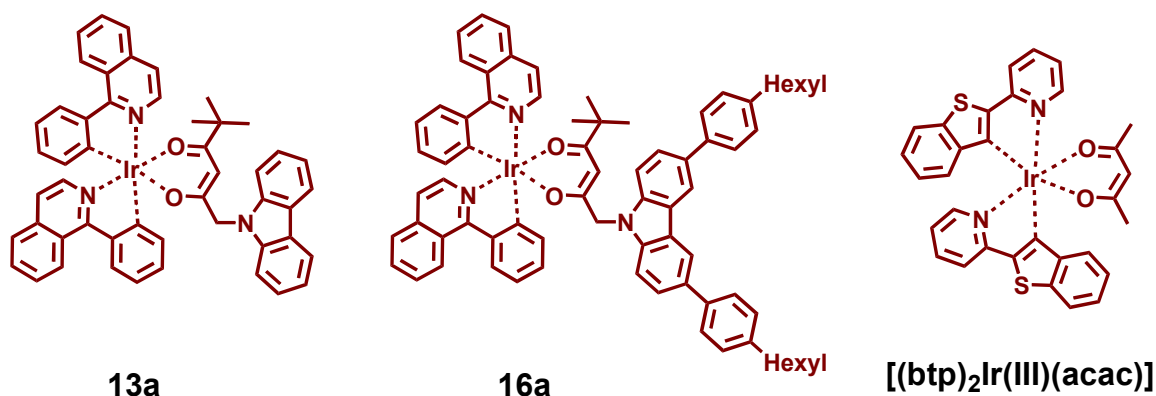
Table 3.3. Performance data of the investigated OLED devices with iridium(III) complexes **12b-c** and **13b-c**. Devices were prepared and measured by Dimitrios Kourkoulos and Dirk Hertel at the Physical Chemistry group of Prof. Klaus Meerholz at the Institute of Physical Chemistry at the University of Cologne.

Ir(III) complexes	Max luminous Efficiency [Cd/A]	Max power Efficiency [lm/W]	Performance at 100 Cd/m ² [Cd/A] at [V]	Performance at 500 Cd/m ² [Cd/A] at [V]	Performance at 100 Cd/m ² [Cd/A] at [V]
12b (PEDOT)	1.6	0.8	1.4 (5.7)	1.4 (6.9)	1.3 (7.7)
12c (PEDOT)	12.6	5.4	9.5 (6.2)	10.9 (7.5)	11.4 (8.2)
12c (PEDOT/HTL)	35.0	29.0	32.0 (5.2)	32.0 (6.7)	31.0 (7.4)
12c (PEDOT/HTL/ETL)	36.8	34.7	36.3 (3.9)	34.6 (4.7)	33.1 (5.1)
13b (PEDOT)	4.3	2.3	4.0 (7.7)	4.1 (9.4)	---
13b (PEDOT/HTL)	9.4	6.3	9.2 (7.1)	8.5 (9.1)	---
13b (PEDOT/HTL/ETL)	10.8	9.9	10.3 (5.4)	9.2 (6.7)	8.3 (7.4)
13c (PEDOT)	4.1	2.0	2.4 (4.8)	3.2 (5.6)	3.6 (6.1)

Chapter 3. Iridium(III) complexes

Moreover, in a further attempt, a series of polymer LED devices were fabricated with Ir(III) complexes **13a** and **16a** and their photophysical properties were compared to the commonly used complex **[(btp)₂Ir(III)(acac)]** [19]. The configuration of the devices was designed by Yaroslav V. Aulin and Oleksandr Mikhnenko in the Physics of Organic Semiconductors group of Prof. Maria Antonietta Loi and Prof. Paul. W. M. Blom at the Zernike Institute for Advanced Materials at the University of Groningen, and consisted of PVK and the electron conducting oligomer 2-(biphenyl-4-yl)-5-(4-*tert*-butylphenyl)-1,3,4-oxadiazole (PBD) at a ratio of 70:30 (PVK: PBD) as the matrix; further details regarding the device construction can be found in reference [20]. The dopant ratios were varied from 4 to 16 molecules of **13a**, **16a**, and **[(btp)₂Ir(III)(acac)]** per 1000 monomer units of PVK, which correspond to a 1 to 4% weight percentage differentiation (Table 3.3). When the molar ratios were 4:1000 and 8:1000, the Ir(III) complex **13a** revealed its best luminous efficiency of 3.41 and 4.15 Cd/A, respectively. On the other hand, complex **16a**, when mixed at molar ratios of 12:1000 and 16:1000, exhibited the best efficiency (4.18 and 3.77 Cd/A, respectively) compared to **13a** and **[(btp)₂Ir(III)(acac)]** (Table 3.4). In general, the devices built with complexes **13a** and **16a** exhibited, independently of the degree of blending with the PVK:PBD polymer, a clear advantage and even an increase in luminous efficiency of nearly 30% compared to the universally employed red emitting material **[(btp)₂Ir(III)(acac)]** (Scheme 3.11). This improvement in the electroluminescence properties in PLEDs can be attributed to the introduction of hole-accepting moieties at the ancillary ligands of these complexes. In particular, carbazolyl functional units enhance charge recombination at the emitter sites and simultaneously increase miscibility with the PVK:PBD polymer matrix.

Chapter 3. Iridium(III) complexes



Scheme 3.11. Schematic representation of selected iridium(III) complexes **13a** and **16a** as well as the reference iridium(III) complex **[(btp)₂Ir(III)(acac)]**.

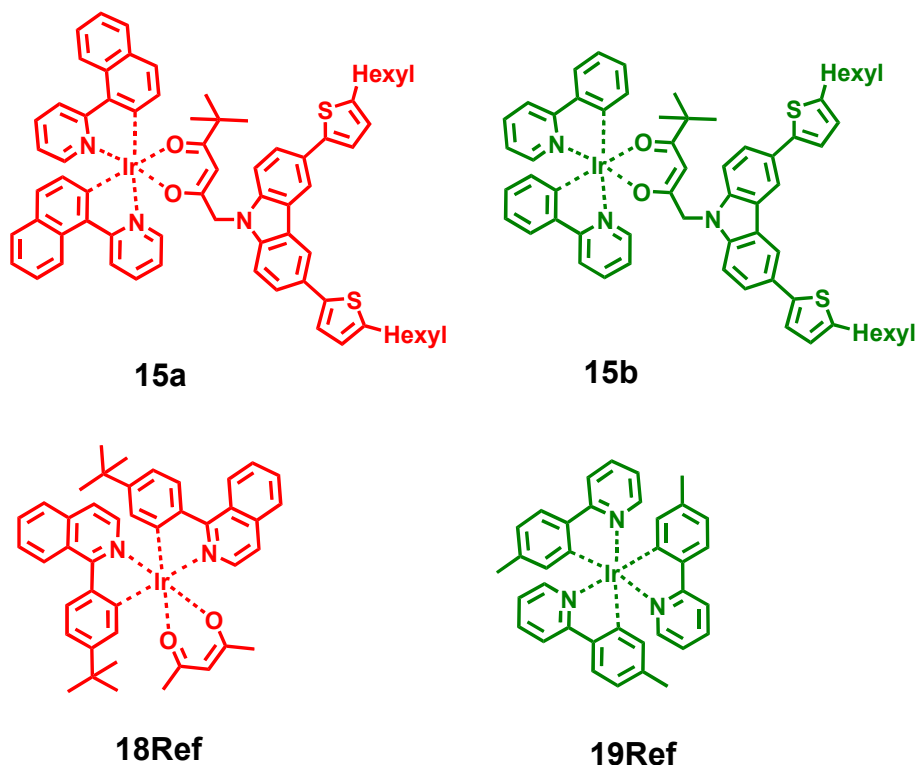
Table 3.4. Luminous efficiency of complexes **13a**, **16a**, and **[(btp)₂Ir(III)(acac)]**. Devices were prepared and measured by Yaroslav V. Aulin and Oleksandr Mikhnenko in the Physics of Organic Semiconductors group of Prof. Maria Antonietta Loi and Prof. Paul. W. M. Blom at the Zernike Institute for Advanced Materials at the University of Groningen.

Ir(III) complex	Luminous efficiency [Cd/A]			
	Molar ratio [Complex:PVC/PBD]			
	4:1000	8:1000	12:1000	16:1000
13a	3.41	4.15	3.95	3.28
16a	2.77	4.04	4.18	3.77
[(btp)₂Ir(III)(acac)]	2.62	2.94	3.33	2.78

Apart from this property, the measurement of the phosphorescence decay times resulted in decay times of 1.2 μ s for both complexes **13a** and **16a**, while the decay time of the commercial available complex **[(btp)₂Ir(III)(acac)]** (**17Ref**) under the same analytical conditions was 5.1 μ s. The shorter decay time can reduce the T-T annihilation rate of excited complexes and can result in increased luminous efficiency [20,21].

Chapter 3. Iridium(III) complexes

In an ongoing study, OLED device fabrication (Scheme 3.13) was continued with complexes **15a** and **15b** as the material in the emitting layer, which were blended in a mixture of 1,3-bis(5-(4-*tert*-butylphenyl)-1,3,4-oxadiazol-2-yl)benzene (OXD-7) and a PVK matrix and were compared to commonly used red emitters like [bis(1-(4-*tert*-butylphenyl)isoquinoline)Ir(III)acetylacetonate] **18Ref** [22,23] and [tris(2-*p*-tolylpyridine)Ir(III)] **19Ref** [22,24], confirming their suitability as triplet emitting sources in these devices (Scheme 3.12 and 3.13). The fabrication of these particular OLED devices and measurements were performed by Alexander Thiessen and Dirk Hertel at the Physical Chemistry group of Prof. Klaus Meerholz at the Institute of Physical Chemistry at the University of Cologne.



Scheme 3.12. Schematic representation of selected iridium(III) complexes **15a-b** and reference iridium(III) complexes **18-19Ref**.

Similarity in terms of the luminous efficiency was observed between complexes **15a** and **18Ref** (7.7 Cd/A and 8.1 Cd/A at 100 Cd/m², respectively), while the

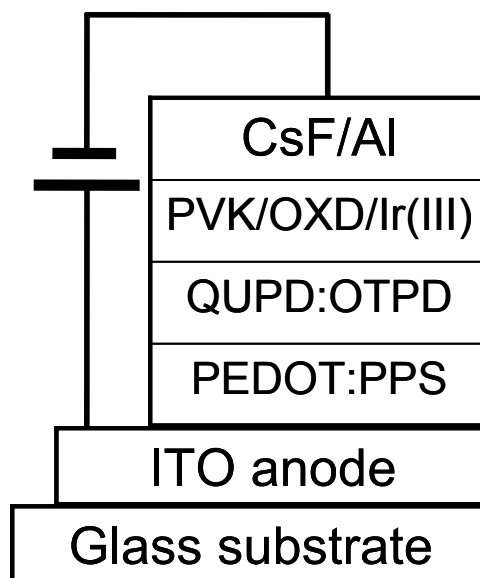
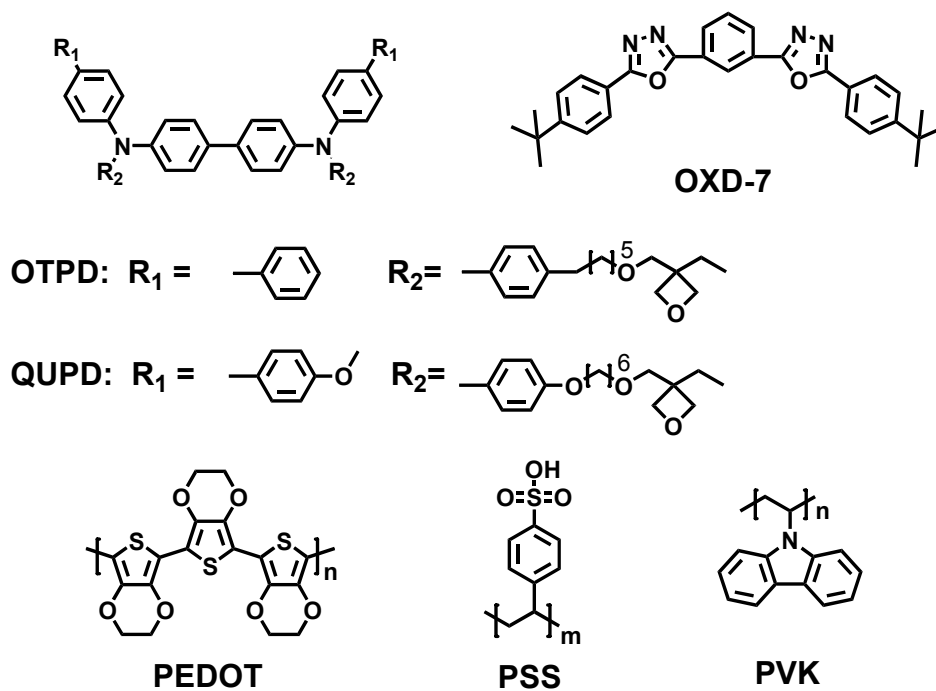
Chapter 3. Iridium(III) complexes

green emitting complexes **15b** and **19Ref** differentiated themselves significantly (17.3 Cd/A and 56.7 Cd/A at 100 Cd/m², respectively), a phenomenon attributed to the homoleptic configuration of **19Ref**, which is absent in the other complexes (**15a-b** and **18Ref** are heteroleptic-structured) (Table 3.5). Due to the herein introduced dual donor species design concept, based on the interconnection of carbazolyl and thienyl moieties, a potential improvement in charge recombination at the emitter site takes place and contributes to the good electrophosphorescence performance of **15a**. This design concept is used to tune the emission colours, when combined with the respective cyclometalating co-ligands, and might even be useful for the enhancement of diode performance as well [8].

Table 3.5. Performance data of the investigated OLED devices with iridium(III) complexes **15a-b** and **18-19Ref**. Devices were prepared and measured by Alexander Thiessen and Dirk Hertel at the Physical Chemistry group of Prof. Klaus Meerholz at the Institute of Physical Chemistry at the University of Cologne.

Compound	15a	15b	18Ref	19Ref
Max. luminous efficiency [Cd/A]	7.8	8.7	17.6	57.9
Max. power efficiency [lm/W]	5.4	7.5	14.2	53.3
Performance at 100 Cd/m ² [Cd/A] at [V]	7.7 (7.4)	8.1 (6.5)	17.3 (6.9)	56.7 (4.8)
Performance at 1000 Cd/m ² [Cd/A] at [V]	6.0 (10.8)	6.2 (9.8)	14.9 (8.5)	48.2 (7.2)
CIE X, Y	0.60, 0.38	0.68, 0.31	0.33, 0.60	0.32, 0.61

Chapter 3. Iridium(III) complexes

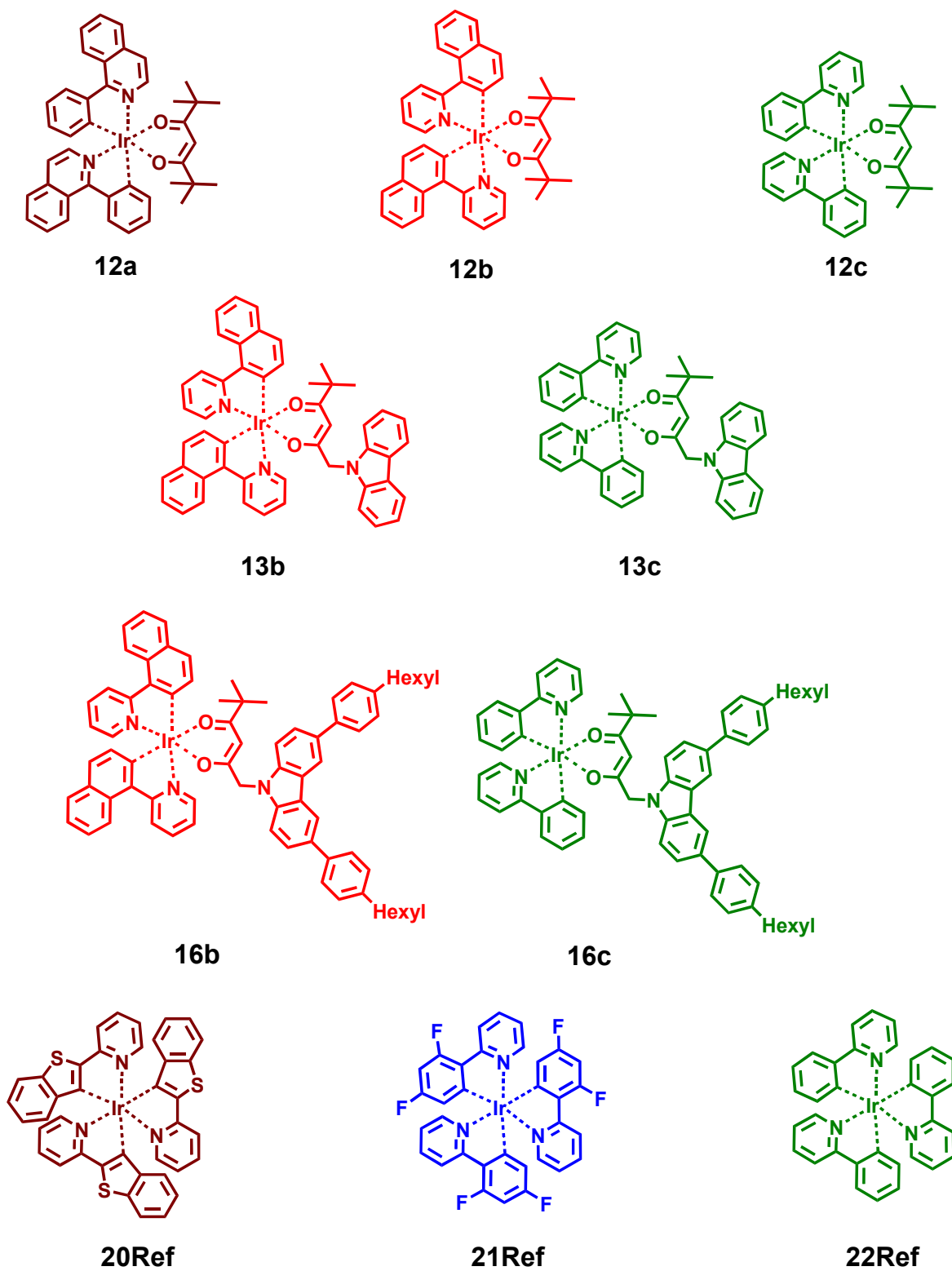


Scheme 3.13. OLED devices based on complexes **15a-b** and **18-19Ref.**

3.5 Pressure and temperature sensitivity

The sensitivity of the phosphorescence lifetimes of compounds **12a-c**, **13b-c**, and **16b-c** upon pressure and temperature manipulations was investigated by Lorenz H. Fischer and PD. Dr. Michael Schäferling in the group of Prof. Otto. S. Wolfbeis at the Institute of Analytical Chemistry, Chemo- and Biosensors at the University of Regensburg and compared to three commercially available homoleptic iridium(III) complexes: $[\text{tris}[2\text{-(benzo}[b]\text{thiophen-2-yl)pyridinato-C}^3\text{,N}]\text{iridium(III)}]$ (**Ir(btpy)₃**, **20Ref**), $[\text{tris}[2\text{-(4,6-difluorophenyl)pyridinato-C}^2\text{,N}]\text{iridium(III)}]$ (**Ir(Fppy)₃**, **21Ref**), and $[\text{tris}[2\text{-phenylpyridinato-C}^2\text{,N}]\text{iridium(III)}]$ (**Ir(ppy)₃**, **22Ref**) [2,3]. The structures of the above-mentioned complexes are illustrated in Scheme 3.14.

The luminescence lifetimes were obtained according to the rapid lifetime determination (RLD) method [25,26] by means of a pulsed 405 nm LED with an internal frequency of 125 kHz (measurement at the University of Regensburg). Details of the experimental procedure and the imaging process applied can be found in the literature [3]. Except for the lifetime determination and the corresponding pressure and temperature sensitivities, the electrochemical properties of the complexes were determined *via* cyclic voltametry vs. ferrocene in dry THF. All calculated the parameters are listed for compounds **12a-c**, **13b-c**, **16b-c**, and **Ref20-22** in Table 3.6.



Scheme 3.14. Schematic representations of the investigated iridium(III) complexes **12a-c**, **13b,c**, **16b,c**, and reference iridium(III) complexes **20-22Ref**.

Chapter 3. Iridium(III) complexes

Table 3.6. The lifetimes of the selected and reference iridium(III) complexes and their pressure and temperature sensitivities were measured by Lorenz H. Fischer and PD. Dr. Michael Schäferling in the group of Prof. Otto. S. Wolfbeis at the Institute of Analytical Chemistry, Chemo- and Biosensors at the University of Regensburg.

Ir(III) complex	τ [μs]^[a]	T-coeff. [% (t)/°C]^[a]	K_{sv} [10^{-4} mbar⁻¹]^[b]
12a	1.1	0.21	0.61
12b	3.6	0.4	1.33
12c	1.2	0.37	0.73
13b	3.4	0.43	1.49
13c	1.3	0.48	0.65
16b	3.3	0.40	1.26
16c	1.1	0.43	0.63
20Ref	6.6	0.35	2.17
21Ref	1.0	0.31	0.40
22Ref	1.2	0.19	0.47

[a] at 50 mbar air pressure and 30 °C.

[b] in 6 μ m PS film.

The criteria for an ideal air pressure and temperature sensor include high emission quantum yields, long emission lifetimes, and high sensitivity. Additionally, their variation in emission intensity and long excited-state lifetime should show some changing trends with varying air pressure and temperature. In theory, the quenching ratio is in direct proportion to increased air pressure and temperature. In other words, more excited states are quenched under higher air pressures or at higher temperatures, which leads to a reduced luminescence lifetime. For an air-pressure sensor, this relationship can be investigated through the Stern-Volmer (SV) equation, where τ_0 is the lifetime in the absence of a quencher (oxygen in air)

Chapter 3. Iridium(III) complexes

under standard conditions, τ is the luminescence lifetime in the presence of air pressure and $K_{sv}(Q)$ is the Stern-Volmer constant, assumed to contain all constants related to air pressure (Q), inducing changes in the lifetime. In addition, $K_{sv}(Q)$ depends on the luminescence lifetime of Ir(III) complexes and the enhanced sensitivity is normally associated with complexes with long luminescence lifetimes. In the case of Ir(III) complexes, a single uniform quenching environment and linear Stern-Volmer behaviour is expected with varying air pressure (Q). Moreover, the oxygen permeability of the matrix polymer evidently influences the testing sensitivity, as these complexes were incorporated into a polymer film prior to the measurements. In our study, all complexes were incorporated into a standardised polystyrene film, which possesses an oxygen permeability of $1.9 \times 10^{-13} \text{cm}^3 \text{ (STP) cm (cm}^2\text{sPa)}^{-1}$ (STP = standard temperature and pressure) [27]. As the polystyrene matrix provides moderate oxygen permeability, the oxygen sensitivity and K_{SV} values shall be increased and the differences between the single complexes will be more pronounced as well [2,3].

$$\frac{\tau_0}{\tau} = 1 + K_{sv}(Q) \quad (3.1)$$

The lifetime variations of the synthesised complexes **12a-c**, **13b-c**, **16b-c** and the referenced complexes **20-22Ref** in the presence of different air pressure values are shown in Figure 3.17. As expected consequence, τ_0/τ of all complexes showed a linear Stern-Volmer relationship with increased pressure. Besides this, we found that every SV-line had a different slope and the magnitudes of these slopes were different for each complex. This result can be attributed to the fact that every complex possesses a different excited-state lifetime. Generally, complexes with longer lifetimes are more suitable as sensors. In other words, the sensitivity of complexes with a long lifetime is higher compared to those with a short lifetime.

Thus, these sensitive complexes exhibit sharp slopes compared to the other probes. As a consequence, **20Ref** ($\tau = 6.6 \mu\text{s}$) and **13b** ($\tau = 3.4 \mu\text{s}$) revealed good pressure sensitivity. Apart from this, the complex configuration is also an important factor for the choice of a sensor, as asymmetrical structures possess higher environmental sensitivity. Hence, although complex **12b** has a lifetime of $\tau = 3.6 \mu\text{s}$, compared to the lifetime of complex **13b**, its relatively symmetrical structure decreases its sensitivity as an air pressure sensor.

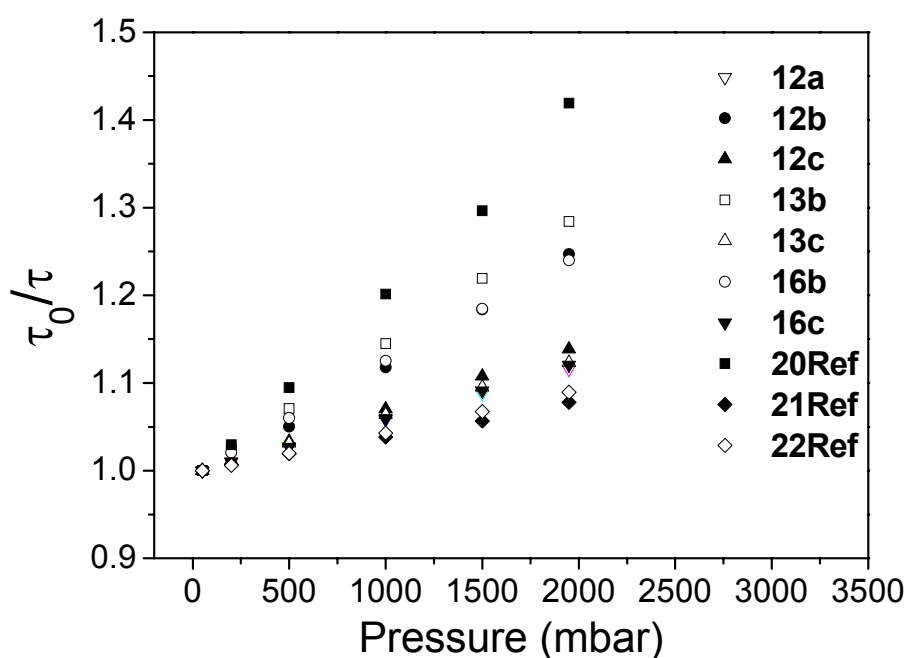


Figure 3.17. The variation in τ_0/τ values with varying air pressure for selected iridium(III) complexes in 6 μm PS films at $T = 30 \text{ }^\circ\text{C}$. Investigations were carried out by Lorenz H. Fischer and PD. Dr. Michael Schäferling in the group of Prof. Otto. S. Wolfbeis at the Institute of Analytical Chemistry, Chemo- and Biosensors at the University of Regensburg [2].

The dependence of the normalised luminescence lifetimes of iridium(III) complexes **12a-c**, **13b-c**, **16b-c**, and **Ref20-22** on the temperature are shown in Figure 3.18. Based on the obtained data, the variations in the luminescence lifetimes of these complexes with varying temperature revealed a non-linear curve.

Especially for complex **13c**, its luminescence lifetime with rising temperature was quickly reduced compared to the other complexes, which can be presumably attributed to rapid quenching when increasing the temperature and applying stable pressure.

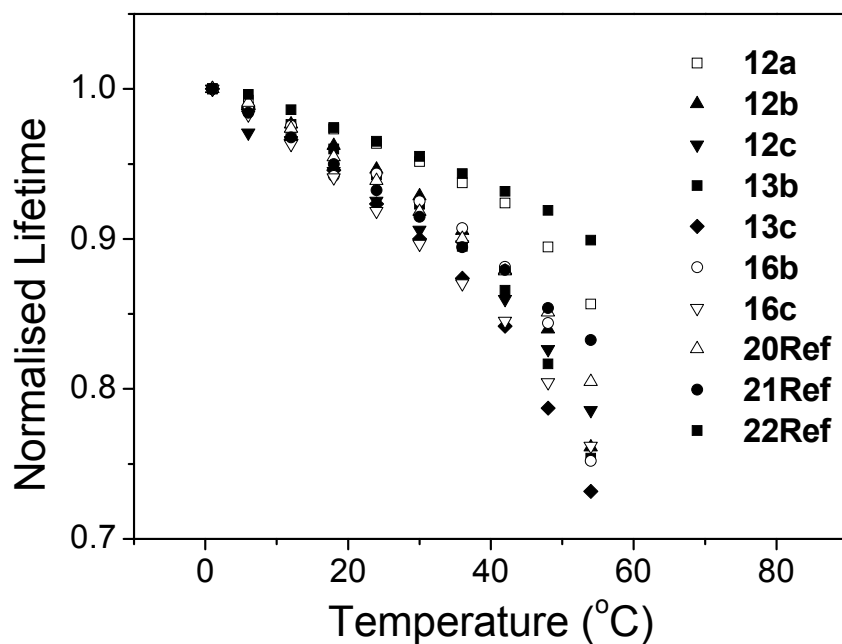


Figure 3.18. The variation in τ values with varying temperature for selected iridium(III) complexes in 6 μm PS films under constant pressure. Investigations were carried out by Lorenz H. Fischer and PD. Dr. Michael Schäferling in the group of Prof. Otto. S. Wolfbeis at the Institute of Analytical Chemistry, Chemo- and Biosensors at the University of Regensburg [2].

The relationship between the luminescence lifetime and temperature can be classified as the Arrhenius type by means of mathematical computation (Equation 3.2), in which τ is the luminescence lifetime, k_0 is the temperature-independent decay rate for the deactivation of the excited state, k_1 is the pre-exponential factor, ΔE is the energy gap between the emitting level and an upper deactivating excited state, R is the gas constant, and T is the temperature in Kelvin.

$$\frac{1}{\tau} = k_0 + k_1 \cdot \exp\left(-\frac{\Delta E}{RT}\right) \quad (3.2)$$

In general, compared to referenced iridium(III) complex **20**, these synthesised iridium(III) complexes (**12b**, **13b**, **16b** or **12c**, **13c**, **16c**) as air-pressure sensors do not reveal an obvious advantage. However, the iridium (III) complex **13** is quite suitable for applications as a temperature sensor compared to the other iridium(III) complexes because of its green emission colour and obvious Arrhenius-type variation in luminescence lifetime with changes in temperature, which is rare in this spectral region.

3.6 Summary

A series of neutral heteroleptic iridium(III) complexes equipped with 2-phenylpyridine, 2-(naphthalen-1-yl)pyridine, and 1-phenylisoquinoline as cyclometalating ligands and different diketonates as ancillary ligands was presented. All introduced Ir(III) complexes were obtained in yields over 60%, and their structural properties were fully characterised. They showed high thermal stability to at least 207 °C, but no phase transitions. The Ir(III) complexes demonstrated favourable short phosphorescence lifetimes and high photoluminescence quantum yields of up to 58%. Their incorporation into OLED devices revealed favourable colour stability and the green Ir(III) complex **12c** exhibited a luminous efficiency as high as 36.3 Cd/A at 3.9 V. Moreover, the properties of the heteroleptic iridium(III) complexes **12a-c** were compared to structures of homoleptic Ir(III) complexes revealing symmetrical architectures. In addition, the applications of the iridium(III) complexes as air pressure and temperature sensors are associated with their luminescence lifetimes. The red emitting iridium(III) complexes **12b**, **13b**, and **16b**, which possess longer luminescence lifetimes than the other synthesised iridium(III) complexes (**12a**, **12c**, **13c**, and **16c**) (Table 3.6), were more sensitive to varying air

pressure, although the iridium(III) complex **20Ref** for applications as an air pressure sensor is the best candidate of these complexes. However, in the case of applying these complexes as temperature sensors, the synthesised iridium(III) complex **13** demonstrated more obvious variations in luminescence lifetime with varying temperature compared to the reference iridium(III) complexes (**20-22Ref**).

3.7 Experimental Section

Materials: All manipulations were performed under an atmosphere of dry argon by employing the usual Schlenk techniques. Solvents were carefully dried and distilled from appropriate drying agents prior to use. Commercially available reagents were used without further purification unless otherwise stated. 2-Phenylpyridine, 1-bromo-4-hexylbenzene, potassium hexamethyldisilazane, *n*-butyllithium, tetrahydrofuran, ferrocene, tetrabutylammonium [*tris*[2-(benzo[*b*]thiophen-2-yl)pyridinato-C³,N]iridium(III)], titanium dioxide, hexafluorophosphate, [*tris*[2-(4,6-difluorophenyl)pyridinato-C²,N]iridium(III)], and [*tris*[2-phenylpyridinato-C²,N]iridium(III)] were purchased from Sigma-Aldrich (www.sigmaaldrich.com). IrCl₃ × *n*H₂O, 2-ethyl-bromoacetate, *tetrakis*(triphenylphosphine)palladium(0), and pinacolone were delivered by ABCR (www.abcr.de). 2-Ethoxyethanol, 9*H*-carbazole, and 2-ethoxyethanol were purchased from Acros (www.acros.com).

Instrumentation: ¹H NMR and ¹³C NMR spectra were acquired on a Bruker Avance 400 or Bruker Avance III 600, (www.bruker.com) chemical shifts are given relative to the internal standard tetramethylsilane (Me₄Si) in CDCl₃ solution. Chemical shifts in NMR spectra are given in ppm (s = singlet, d = doublet, t = triplet, q = quartet, and m = multiplet). Fourier transform infrared (FT-IR) spectra were recorded on a Jasco FT/IR-4200 Fourier transform spectrometer

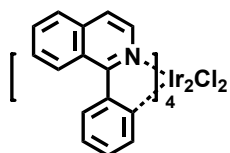
(www.jasco.de). The UV-vis spectra were measured with a JASCO V-550 UV-vis spectrophotometer (www.jasco.de; 1 cm cuvettes, CHCl₃) at concentrations of about 1×10^{-5} mol/L. The emission spectra were obtained using a CARY Eclipse fluorescence spectrophotometer (www.varianinc.com) at concentrations of about 1×10^{-5} mol/L. Thermogravimetric analysis (TGA) was performed on a Mettler Toledo TGA/DSC STAR System (www.mettler-toledo.de; heating rate: 10 K/min; argon; T_d @ 5% weight loss). Mass spectra were obtained using a Varian MAT 311 instrument (www.varianinc.com) with an electrospray source (ESI-MS), a Varian MAT 311 instrument with an electrospray source (ESI-MS), and a micrOTOF instrument from Bruker Daltonik (Bremen, Germany) equipped with a multi-purpose ion source (MPIS) [28] made by the machine shop at the University of Wuppertal. In this case, the atmospheric-pressure laser ionisation (APLI) method was used as the ionisation technique [29]. Elemental analyses (EA) were performed on a Perkin Elmer 240 B setup.

3.7.1 General procedure of Ir(III)- μ -chloro-bridged

precursor complexes [(C^N)₄Ir^{III}₂Cl₂]

Iridium(III) trichloride hydrate was combined with the respective C^N ligand ppy or npy, and dissolved in a mixture of 2-ethoxyethanol (30 ml) and water (10 ml). The mixture was stirred for 24 h under reflux. The solution was cooled to room temperature, and the precipitate was collected on a glass filter. The precipitate was washed with ethanol (30 ml) and dichloromethane (20 ml).

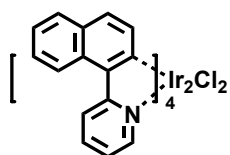
3.7.2 Ir(III)- μ -chloro-bridged precursor complex



Iridium(III) trichloride hydrate (233 mg, 0.78 mmol) and 1-phenylisoquinoline (**1**) (400 mg, 1.95 mmol) afforded a deep-green powder. Yield: 336 mg, 78%.

$^1\text{H-NMR}$ (600 MHz, dimethylsulfoxide- d_6): δ (ppm) 5.58-5.60 (d, $3J = 7.33$ Hz, 2H), 6.33-6.35 (d, $3J = 7.32$ Hz, 2H), 6.63-6.67 (t, $3J = 7.07$ and 8.58 Hz, 2H), 6.78-6.81 (t, $3J = 7.58$ and 9.09 Hz, 2H), 6.91-6.94 (t, $3J = 7.33$ and 8.84 Hz, 2H), 7.00-7.04 (t, $3J = 7.07$ and 8.84 Hz, 2H), 7.82-8.04 (m, 12H), 8.13-8.26 (m, 8H), 8.86-8.88 (d, $3J = 8.59$ Hz, 2H), 8.92-8.94 (d, $3J = 8.58$ Hz, 2H), 9.59-9.61 (d, $3J = 6.31$ Hz, 2H), 9.75-9.77 ppm (d, $3J = 6.31$ Hz, 2H). IR: 3049 (C=C-H), 1676, 1658, 1641, 1587 (C=N, C=C), 1392, 1179, 910, 867, 838, 792, 688 cm^{-1} . APLI-MS: requires m/z $\text{C}_{60}\text{H}_{40}\text{Cl}_2\text{Ir}_2\text{N}_4$ ($\text{M}+\text{H}$) $^+$ 1271.20, found 1271.20. Elem. Anal. Calcd. for $\text{C}_{60}\text{H}_{40}\text{Cl}_2\text{Ir}_2\text{N}_4$: C 56.64%, H 3.17%, N 4.40%. Found: C 56.22%, H 3.21%, N 4.42%.

3.7.3 Ir(III)- μ -chloro-bridged precursor complex



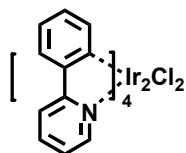
Iridium(III) trichloride hydrate (233 mg, 0.78 mmol) and 2-(naphthalen-1-yl)pyridine

(2) (400 mg, 1.95 mmol) afforded a deep-green powder. Yield: 327 mg, 76%.

$^1\text{H-NMR}$ (400 MHz, CDCl_3): δ (ppm) 5.74-5.76 (d, $^3J = 8.6$ Hz, 2H), 6.42-6.44 (d, $^3J = 8.5$ Hz, 2H), 7.14-7.16 (d, $^3J = 8.5$ Hz, 2H), 8.23-8.25 (d, $^3J = 8.5$ Hz, 2H), 7.26-7.33 (m, 6H), 7.46-7.52 (m, 4H), 7.58-7.69 (m, 8H), 8.06-8.11 (t, $^3J = 9.2$ and 7.6 Hz, 2H), 8.14-8.18 (t, $^3J = 9.2$ and 7.6 Hz, 2H), 8.49-8.55 (m, 6H), 8.63-8.65 (d, $^3J = 8.5$ Hz, 2H), 9.70-9.72 (d, $^3J = 5.6$ Hz, 2H), 9.89-9.91 (d, $^3J = 5.1$ Hz, 2H). IR: 3048 (C=C-H), 1637, 1610, 1468, 1419 (C=C, C=N), 1312, 1263, 1241, 1074, 762, 740, 720, 667 cm^{-1} . APLI-MS: requires m/z $\text{C}_{60}\text{H}_{40}\text{C}_{12}\text{Ir}_2\text{N}_4$ ($\text{M}+\text{H}$) $^+$ 1272.19, found 1271.90. Elem. Anal. Calcd. for $\text{C}_{60}\text{H}_{40}\text{C}_{12}\text{Ir}_2\text{N}_4$: C 56.64%, H 3.17%, N 4.40%. Found: C 56.22%, H 3.21%, N 4.42%.

3.7.4 Ir(III)- μ -chloro-bridged precursor complex

$[(\text{ppy})_4\text{Ir}^{\text{III}}_2\text{Cl}_2]$ (11)



Iridium(III) trichloride hydrate (770 mg, 2.58 mmol) and 2-phenylpyridine (3) (1 g, 6.44 mmol) afforded a yellow powder after washing. Yield: 964 mg, 70%.

$^1\text{H-NMR}$ (400 MHz, CDCl_3): δ (ppm) 5.86 (d, $^3J = 7.91$ Hz, 2H), 6.59 (t, $^3J = 7.03$ Hz, 2H), 6.74-6.97 (m, 4H), 7.54 (d, $^3J = 7.03$ Hz, 2H), 7.72-7.86 (m, 2H), 7.92 (d, $^3J = 7.91$ Hz, 2H), 9.24 (d, $^3J = 6.15$ Hz, 2H). IR: 3058 (C=C-H), 1605, 1581, 1476, 1414, (C=C and C=N), 1305, 1267, 1224, 1159, 1061, 1029, 753, 734, 727, 669 cm^{-1} . APLI-MS: requires m/z $\text{C}_{44}\text{H}_{32}\text{C}_{12}\text{Ir}_2\text{N}_4$ 1072.09, found 1073.10. Elem. Anal. Calcd. for $\text{C}_{44}\text{H}_{32}\text{C}_{12}\text{Ir}_2\text{N}_4$: C 42.29%, H 3.01%, N 5.23%. Found: C 42.58%, H 3.16%, N 5.09%.

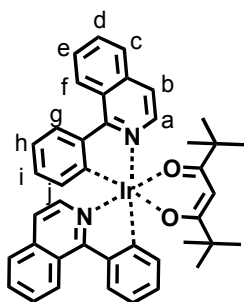
3.7.5 General procedure of heteroleptic iridium(III)

complexes $[\text{Ir}^{\text{III}}(\text{C}^{\wedge}\text{N})_2\{\text{acac}\}]$

In a 50 ml flask, the Ir(III)- μ -chloro-bridged precursor complex, the acac ligand and K_2CO_3 were mixed with 2-ethoxyethanol (30 ml) and the mixture was stirred under reflux for 3 h. After cooling to room temperature, 2-ethoxyethanol was removed under reduced pressure. The crude product was dissolved in dichloromethane (20 ml) and the obtained solid was filtered off. The dichloromethane solution (20 ml) was concentrated under reduced pressure. Subsequently, *n*-hexane was utilised in order to precipitate the complexes and the obtained solid was filtered off. The residue was purified by silica column chromatography (*n*-hexane/ethyl acetate, 10/3, v/v); if needed, purification on a BioBeads SX-1 column (dichloromethane) followed.

3.7.6 $[\text{Ir}^{\text{III}}(\text{piq})_2\{2,2,6,6\text{-tetramethylheptane-3,5-dione}\}]$

(12a)

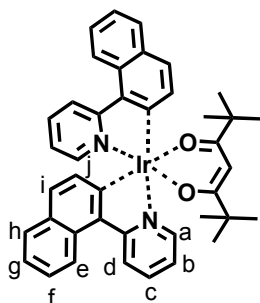


$[\text{Ir}^{\text{III}}(\text{piq})_2\text{-}\mu\text{-Cl}]_2$ (200 mg, 0.157 mmol), 2,2,6,6-tetramethylheptane-3,5-dione (87 mg, 0.472 mmol) and K_2CO_3 (152 mg, 1.100 mmol) afforded a deep-red powder after purification. Yield: 175 mg, 71%.

$^1\text{H-NMR}$ (400 MHz, CDCl_3 , ppm): δ 0.85 (s, 18H), 5.46 (s, 1H), 6.55-6.56^b (d, $^3J = 7.15$ Hz, 2H), 6.68-6.70ⁱ (t, d, $^3J = 7.15$ and 8.66 Hz, 2H), 6.92-6.95^h (t, $^3J = 7.15$ and 8.28 Hz, 2H), 7.42-7.43^j (d, $^3J = 6.02$ Hz, 2H), 7.71-7.72^{d,e} (m, 4H), 7.92-7.93^c (m, 2H), 8.24-8.25^f (d, $^3J = 8.28$ Hz, 2H), 8.37-8.38^g (d, $^3J = 6.40$ Hz, 2H), 9.00-9.05^a (m, 2H). $^{13}\text{C-NMR}$ (100 MHz, CDCl_3 , ppm): δ 28.1, 41.1, 119.2, 119.8, 126.2, 126.8, 127.1, 127.4, 128.4, 129.4, 130.3, 134.3, 137.0, 140.7, 146.5, 153.9, 169.3, 194.5. IR: 3055 (C=C-H), 1688, 1569, 1572 (C=N, C=C), 1388, 1116, 863, 834, 817, 783, 648 cm^{-1} . APLI-MS: requires m/z $\text{C}_{41}\text{H}_{39}\text{IrN}_2\text{O}_2$ (M+H)⁺ 784.26, found 784.26. Elem. Anal. Calcd. for $\text{C}_{44}\text{H}_{32}\text{C}_{12}\text{Ir}_2\text{N}_4$: C 42.29%, H 3.01%, N 5.23%. Found: C 42.58%, H 3.16%, N 5.09%.

3.7.7 $[\text{Ir}^{\text{III}}(\text{npy})_2\{2,2,6,6\text{-tetramethylheptane-3,5-dione}\}]$

(12b)



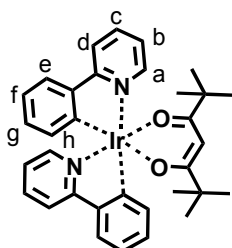
$[\text{Ir}^{\text{III}}(\text{npy})_2\text{-}\mu\text{-Cl}]_2$ (200 mg, 0.157 mmol), 2,2,6,6-tetramethylheptane-3,5-dione (87 mg, 0.472 mmol) and K_2CO_3 (152 mg, 1.100 mmol) afforded a red powder after purification. Yield: 175 mg, 66%.

$^1\text{H-NMR}$ (400 MHz, CDCl_3 , ppm): δ 0.91 (s, 18H), 5.54 (s, 1H), 6.57-6.58^b (d, $^3J = 8.28$ Hz, 2H), 7.06-7.07^d (d, $^3J = 8.66$ Hz, 2H), 7.09-7.11^j (t, $^3J = 6.02$ and 7.90 Hz, 2H), 7.26-7.29^g (m, 2H), 7.47-7.50^f (t, $^3J = 8.28$ and 8.66 Hz, 2H), 7.66-7.67^e (d, $^3J = 8.28$ Hz, 2H), 7.80-7.82^c (t, $^3J = 9.03$ and 8.28 Hz, 2H), 8.49-8.50ⁱ (d, $^3J = 4.52$ Hz, 2H), 8.52-8.53^h (d, $^3J = 8.66$ Hz, 2H), 8.57-8.58^a (d, $^3J = 8.28$ Hz, 2H). $^{13}\text{C-}$

NMR (100 MHz, CDCl₃, ppm): δ 28.1, 41.2, 89.4, 119.8, 120.9, 121.8, 121.9, 126.1, 128.0, 129.7, 130.9, 131.7, 133.0, 136.5, 137.7, 148.7, 157.5, 169.3, 194.5. IR: 3045 (C=C-H), 1678, 1578, 1562 (C=N, C=C), 1398, 1117, 863, 855, 817, 783, 690 cm⁻¹. APLI-MS: requires m/z C₄₁H₃₉IrN₂O₂ (M+H)⁺ 784.26, found 784.26. Elem. anal. Calcd. for C₄₁H₃₉IrN₂O₂: C 62.81%, H 5.01%, N 3.57%. Found: C 62.53%, H 5.05%, N 3.32%.

3.7.8 [Ir^{III}(ppy)₂{2,2,6,6-tetramethylheptane-3,5-dione}]

(12c)

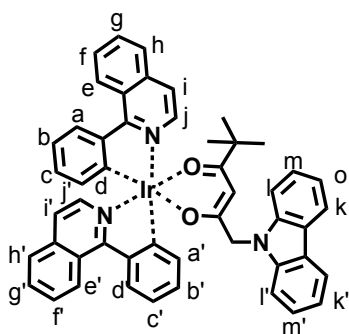


[Ir^{III}(ppy)₂- μ -Cl]₂ (200 mg, 0.187 mmol), 2,2,6,6-tetramethylheptane-3,5-dione (68 mg, 0.373 mmol) and K₂CO₃ (152 mg, 1.100 mmol) afforded a red powder after purification. Yield: 182 mg, 68%.

¹H-NMR (600 MHz, CDCl₃, ppm): δ 0.92 (s, 18H), 5.50 (s, 1H), 6.40-6.41^h (d, ³J = 6.78 Hz, 2H), 6.69-6.72^b (t, ³J = 7.53 and 8.66 Hz, 2H), 6.82-6.85^g (t, ³J = 8.28 and 8.66 Hz, 2H), 7.07-7.09^f (t, ³J = 6.02 and 7.53 Hz, 2H), 7.57-7.58^d (d, ³J = 6.40 Hz, 2H), 7.70-7.72^c (t, ³J = 8.66 and 9.03 Hz, 2H), 7.84-7.85^e (d, ³J = 7.90 Hz, 2H), 8.41-8.42^a (d, ³J = 5.00 Hz, 2H). ¹³C-NMR (150 MHz, CDCl₃, ppm): δ 28.1, 41.1, 89.4, 117.8, 120.1, 120.9, 123.4, 128.6, 133.6, 136.5, 144.8, 148.1, 149.7, 168.7, 194.3. IR: 3049 (C=C-H), 1668, 1579, 1557 (C=N, C=C), 1388, 1116, 883, 864, 854, 783, 647 cm⁻¹. APLI-MS: requires m/z C₃₃H₃₅IrN₂O₂ (M+H)⁺ 684.23, found

684.23. Elem. anal. Calcd. For $C_{33}H_{35}IrN_2O_2$: C 57.96%, H 5.16%, N 4.10%.
 Found: C 57.61%, H 5.15%, N 4.65%.

3.7.9 $[Ir^{III}(\text{piq})_2\{1\text{-carbazol-9-yl-5,5-dimethyl-hexane-2,4-dione}\}]$ (13a)

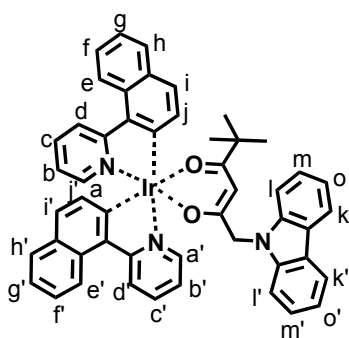


$[Ir^{III}(\text{piq})_2-\mu\text{-Cl}]_2$ (200 mg, 0.157 mmol), compound **5** (97 mg, 0.314 mmol), and K_2CO_3 (152 mg, 1.100 mmol) afforded a red powder after purification. Yield: 200 mg, 67%.

$^1\text{H-NMR}$ (600 MHz, $CDCl_3$, ppm): δ 0.52 (9s, 9H), 4.12-4.18 (m, 1H), 4.49-4.75 (m, 1H), 5.03 (s, 1H), 6.43-6.45^{a'} (d, $^3J = 7.83$ Hz, 1H), 6.53-6.55^a (d, $^3J = 7.58$ Hz, 1H), 6.65-6.68^{b'} (t, $^3J = 7.83$ and 8.28 Hz, 1H), 6.71-6.75^b (t, $^3J = 7.58$ and 7.83 Hz, 1H), 6.89-6.93^{c'} (t, $^3J = 8.08$ and 9.09 Hz, 1H), 6.96-7.00^c (t, $^3J = 8.08$ and 9.09 Hz, 1H), 7.09-7.11^{n',n} (d, $^3J = 8.08$ Hz, 2H), 7.15-7.23^{f',f,k',k,o',o} (m, 6H), 7.31-7.32^{h'} (d, $^3J = 6.32$ Hz, 1H), 7.35-7.36^h (d, $^3J = 6.57$ Hz, 1H), 7.70-7.72^{i',d'} (m, 2H), 7.79-7.82^{i,d} (m, 2H), 7.90-7.92^{l'} (m, 1H), 7.97-7.99^l (m, 1H), 8.02-8.04^{m',m} (d, $^3J = 7.07$ Hz, 2H), 8.18-8.20^{g'} (d, $^3J = 7.83$ Hz, 1H), 8.23-8.25^{e'} (d, $^3J = 6.57$ Hz, 1H), 8.29-8.31^g (d, $^3J = 7.83$ Hz, 1H), 8.39-8.40^e (d, $^3J = 6.57$ Hz, 1H), 8.97-8.99^{i'} (d, $^3J = 9.10$ Hz, 1H), 9.08-9.10^j (d, $^3J = 8.84$ Hz, 1H). $^{13}\text{C-NMR}$ (150 MHz, $CDCl_3$, ppm): δ 14.2, 21.0, 27.4, 40.9, 51.4, 60.4, 92.2, 109.0, 118.9, 119.3, 119.6, 120.1, 120.2, 120.4, 122.8, 125.4, 126.1, 126.3, 126.7, 126.8, 127.2, 127.3, 127.5, 127.6, 128.5,

129.0, 129.4, 129.7, 130.5, 130.6, 133.8, 134.3, 137.0, 137.2, 140.5, 140.6, 146.4, 146.5, 151.9, 152.0, 169.0, 169.1, 181.1, 196.6 ppm. IR: 3052 (C=C-H), 1677, 1565, 1559 (C=N, C=C), 1388, 1134, 893, 876, 867, 798, 699 cm^{-1} . APLI-MS: requires m/z $\text{C}_{50}\text{H}_{40}\text{IrN}_3\text{O}_2$ ($\text{M}+\text{H}$)⁺ 907.27, found 907.27. Elem. anal. Calcd. for $\text{C}_{50}\text{H}_{40}\text{IrN}_3\text{O}_2$: C 66.20%, H 4.44%, N 4.63%. Found: C 66.20%, H 4.57%, N 4.55%.

3.7.10 $[\text{Ir}^{\text{III}}(\text{npy})_2\{\text{1-carbazol-9-yl-5,5-dimethyl-hexane-2,4-dione}\}]$ (13b)

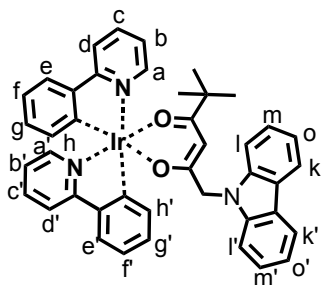


$[\text{Ir}^{\text{III}}(\text{npy})_2-\mu\text{-Cl}]_2$ (200 mg, 0.157 mmol), compound **5** (97 mg, 0.314 mmol), and K_2CO_3 (152 mg, 1.100 mmol) afforded a red powder after purification. Yield: 193 mg, 65%.

$^1\text{H-NMR}$ (600 MHz, CDCl_3 , ppm): δ 0.60 (s, 9H), 4.60-4.74 (m, 2H), 5.13 (s, 1H), 6.39-6.40ⁱ (d, $^3J = 8.28$ Hz, 1H), 6.49-6.50^j (d, $^3J = 8.66$ Hz, 1H), 6.89-6.90^{g'} (t, $^3J = 7.15$ and 7.53 Hz, 1H), 7.04-7.09^{g,i,i'} (m, 3H), 7.20-7.33^{c',c,m',m,o',o,d,d'} (m, 8H), 7.45-7.47^{b'} (t, $^3J = 6.77$ and 8.66 Hz, 1H), 7.53-7.55^b (t, $^3J = 8.28$ and 9.03 Hz, 1H), 7.65-7.66^{i'} (d, $^3J = 7.15$ Hz, 1H), 7.70-7.71^l (d, $^3J = 6.77$ Hz, 1H), 7.75-7.77^f (t, $^3J = 8.66$ and 9.21 Hz, 1H), 7.85-7.88^f (t, $^3J = 9.03$ and 9.03 Hz, 1H), 8.07-8.08^{k',k} (d, $^3J = 7.53$ Hz, 2H), 8.37-8.39^{h',h} (t, $^3J = 6.40$ and 8.28 Hz, 2H), 8.46-8.47^{e'} (d, $^3J = 8.28$ Hz, 1H), 8.51-8.52^{a'} (d, $^3J = 8.28$ Hz, 1H), 8.58-8.59^e (d, $^3J = 8.28$ Hz, 1H), 8.61-

8.63^a (d, ³J = 8.66 Hz, 1H). ¹³C-NMR (150 MHz, CDCl₃, ppm): δ 27.5, 41.0, 51.3, 92.3, 109.1, 119.0, 119.9, 120.1, 120.3, 121.0, 121.2, 122.0, 122.1, 122.2, 122.3, 122.9, 125.5, 126.2, 126.3, 128.1, 128.5, 129.6, 129.8, 130.1, 131.2, 131.6, 131.7, 132.5, 132.7, 136.8, 136.9, 137.9, 140.6, 148.6, 148.7, 155.5, 155.7, 169.0, 169.4, 181.1, 196.8. IR: 3047 (C=C-H), 1681, 1567, 1556 (C=N, C=C), 1378, 1126, 883, 873, 855, 782, 659 cm⁻¹. APLI-MS: requires m/z C₅₀H₄₀IrN₃O₂ (M+H)⁺ 907.27, found 907.27. Elem. anal. Calcd. for C₅₀H₄₀IrN₃O₂: C 66.20%, H 4.44%, N 4.63%; Found: C 66.08%, H 4.44%, N 4.29%.

3.7.11 [Ir^{III}(ppy)₂{1-carbazol-9-yl-5,5-dimethyl-hexane-2,4-dione}] (13c)

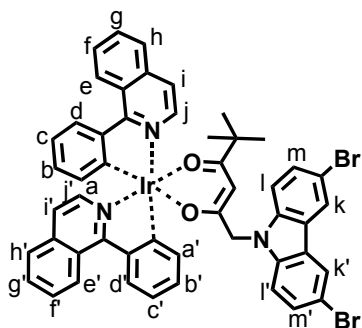


[Ir^{III}(ppy)₂-μ-Cl]₂ (200 mg, 0.187 mmol), K₂CO₃ (180 mg, 1.3 mmol), and compound **5** (115 mg, 0.373 mmol) afforded a red powder after purification. Yield: 192 mg, 61%.

¹H-NMR (600 MHz, CDCl₃, ppm): δ 0.57 (s, 9H), 4.54-4.73 (m, 2H), 5.01 (s, 1H), 6.26-6.28^{h'} (d, ³J = 7.62 Hz, 1H), 6.37-6.39^h (d, ³J = 7.63 Hz, 1H), 6.64-6.68^{g'} (t, ³J = 7.62 and 7.63 Hz, 1H), 6.71-6.75^g (t, ³J = 7.62 and 8.14 Hz, 1H), 6.77-6.81^{f'} (t, ³J = 7.12 and 8.12 Hz, 1H), 6.85-6.88^f (t, ³J = 7.12 and 8.65 Hz, 1H), 6.90-6.94^{b'} (t, ³J = 6.10 and 7.63 Hz, 1H), 6.97-7.00^b (t, ³J = 6.10 and 7.63 Hz, 1H), 7.22^{m',m,o',o} (m, 4H), 7.32-7.36^{l',l} (t, ³J = 8.14 and 8.65 Hz, 2H), 7.50-7.51^{e'} (d, ³J = 7.63 Hz, 1H), 7.58-7.60^e (d, ³J = 7.63 Hz, 1H), 7.63-7.67^{c'} (t, ³J = 7.13 and 8.14 Hz, 2H), 7.70-

7.73^c (t, ³J = 7.63 and 8.66 Hz, 2H), 7.76-7.78^{d'} (d, ³J = 8.14 Hz, 1H), 7.84-7.86^d (d, ³J = 8.14 Hz, 1H), 8.01-8.07^{k',k} (d, ³J = 7.63 Hz, 1H), 8.26-8.28^{a'} (d, ³J = 5.06 Hz, 1H), 8.38-8.40^a (d, ³J = 5.60 Hz, 1H). ¹³C-NMR (150 MHz, CDCl₃, ppm): δ 27.5, 40.9, 92.2, 109.1, 117.9, 118.2, 119.0, 120.1, 120.4, 120.7, 120.9, 121.2, 122.9, 123.4, 123.8, 125.6, 128.6, 129.1, 133.2, 133.6, 136.7, 140.6, 144.7, 144.8, 147.5, 147.7, 148.1, 148.2, 168.5, 168.7, 180.9, 196.5. IR: 3037 (C=C-H), 1678, 1568, 1556 (C=N, C=C), 1389, 1126, 893, 865, 854, 783, 649 cm⁻¹. APLI-MS: requires m/z C₄₂H₃₆IrN₃O₂ (M+H)⁺ 807.24, found 807.24. Elem. anal. Calcd. for C₄₂H₃₆IrN₃O₂: C 62.51%, H 4.50%, N 5.21%. Found: C 62.53%, H 4.46%, N 5.31%.

3.7.12 [Ir^{III}(piq)₂{1-(3,6-dibromocarbazol-9-yl)-5,5-dimethylhexane-2,4-dione}] (14a)

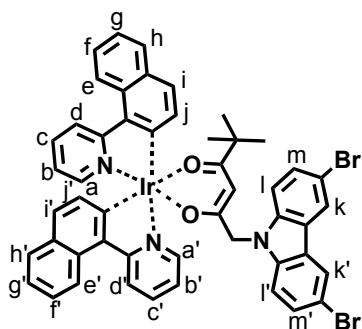


[Ir^{III}(piq)₂-μ-Cl]₂ (200 mg, 0.157 mmol), K₂CO₃ (152 mg, 1.100 mmol), and compound **6** (183 mg, 0.393 mmol) afforded a deep-red powder after purification. Yield: 192 mg, 56%.

¹H-NMR (400 MHz, CDCl₃, ppm): δ 0.66 (s, 9H), 4.51-4.61 (m, 2H), 5.20 (s, 1H), 6.34-6.36^{a'} (d, ³J = 6.8 Hz, 1H), 6.40-6.41^a (d, ³J = 7.6 Hz, 1H), 6.60-6.69^{b,b'} (m, 2H), 6.87-6.90^{c,c'} (m, 2H), 6.94-6.96^{f,f'} (d, ³J = 8.8 Hz, 2H), 7.13-7.18^{d,d'} (m, 2H), 2.26-7.28^{h,h'} (m, 2H), 7.70-7.73^{i,i'} (m, 2H), 7.81-7.83^{k,k'} (m, 2H), 7.89-7.90^{l,l'} (d, ³J =

2.0 Hz, 2H), 7.92-7.93^m (d, ³J = 6.3 Hz, 1H), 8.03-8.05^m (d, ³J = 6.3 Hz, 1H), 8.13-8.21^{e,e'.g,g'} (m, 4H), 8.97-8.99^{j,j'} (d, ³J = 8.1 Hz, 2H). ¹³C-NMR (100 MHz, CDCl₃, ppm): δ 27.5, 41.1, 51.4, 92.9, 110.8, 112.0, 119.3, 119.4, 120.2, 120.4, 122.8, 123.3, 126.1, 127.1, 127.2, 127.6, 128.6, 128.9, 129.4, 130.5, 130.6, 133.9, 134.0, 137.1, 139.4, 140.1, 140.3, 146.4, 151.6, 179.4, 197.0. IR: 3061 (C=C-H), 2959, 2927, 2885 (C-H), 1712, 1601, 1534 (C=C, C=N, C=O), 1367, 1249, 1101, 1043, 883, 817, 783, 690, 671 cm⁻¹. APLI-MS: requires m/z C₅₀H₃₉Br₂IrN₃O₂ (M+H)⁺ 1063.10, found 1063.10. Elem. anal. Calcd. for C₅₀H₃₉Br₂IrN₃O₂: C 56.34%, H 3.69%, N 3.94%. Found: C 56.41%, H 3.71%, N 3.90%.

3.7.13 [Ir^{III}(npy)₂{1-(3,6-dibromocarbazol-9-yl)-5,5-dimethyl-hexane-2,4-dione}] (14b)

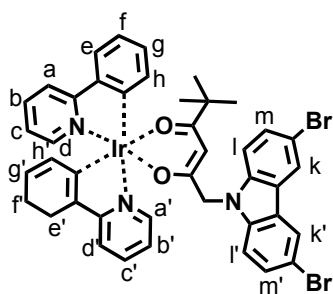


[Ir^{III}(npy)₂-μ-Cl]₂ (200 mg, 0.157 mmol), K₂CO₃ (152 mg, 1.100 mmol), and compound **6** (183 mg, 0.393 mmol) afforded a deep-red powder after purification. Yield: 137 mg, 41%.

¹H-NMR (400 MHz, CDCl₃, ppm): δ 0.59 (s, 9H), 4.61(s, 1H), 5.13 (s, 2H), 6.35-6.38 (d, ³J = 8.3 Hz, 2H), 6.44-6.46 (d, ³J = 8.3 Hz, 2H), 6.85 (t, ³J = 7.6 and 7.1 Hz, 2H), 7.00-7.05 (m, 6H), 7.15-7.30 (m, 16H), 7.41-7.44 (t, ³J = 8.6 and 7.1 Hz, 2H), 7.48-7.53 (t, ³J = 8.1 and 8.6 Hz, 2H), 7.61-7.63 (d, ³J = 8.1 Hz, 2H), 7.66-7.68 (t, ³J = 7.6 Hz, 2H), 7.71-7.75 (t, ³J = 8.6 and 6.7 Hz, 2H), 7.81-7.85 (t, ³J =

8.6 and 6.7 Hz, 2H), 8.03-8.05 (d, $^3J = 8.1$ Hz, 4H), 8.32-8.33 (d, $^3J = 5.6$ Hz, 2H), 8.35-8.37 (d, $^3J = 5.6$ Hz, 2H), 8.42-8.45 (d, $^3J = 8.5$ Hz, 2H), 8.47-8.49 (d, $^3J = 8.6$ Hz, 2H), 8.54-8.56 (d, $^3J = 8.5$ Hz, 2H), 8.57-8.59 (d, $^3J = 8.6$ Hz, 2H). ^{13}C -NMR (100 MHz, CDCl_3 , ppm): δ 27.5, 41.0, 51.3, 92.4, 109.1, 119.0, 119.8, 120.1, 120.2, 120.9, 121.2, 121.9, 122.0, 122.1, 122.3, 123.0, 125.5, 126.2, 126.3, 128.1, 128.5, 129.6, 129.8, 131.0, 131.2, 131.6, 131.8, 132.5, 132.8, 136.8, 136.9, 137.8, 137.9, 140.7, 148.6, 148.7. 155.5, 155.7, 169.0, 169.4, 181.1, 196.8. IR: 3043 (C=C-H), 2948, 2922, 2863 (C-H), 1705, 1569, 1500 (C=C, C=N, C=O), 1354, 1272, 1153, 1118, 897, 862, 813, 744, 669, 659 cm^{-1} . APLI-MS: requires m/z $\text{C}_{50}\text{H}_{39}\text{Br}_2\text{IrN}_3\text{O}_2$ (M+H) $^+$ 1063.10, found 1063.10. Elem. anal. Calcd. for $\text{C}_{50}\text{H}_{39}\text{Br}_2\text{IrN}_3\text{O}_2$: C 56.34%, H 3.69%, N 3.94%. Found: C 56.47%, H 3.67%, N 3.93%.

3.7.14 $[\text{Ir}^{\text{III}}(\text{ppy})_2\{\mu\text{-}1\text{-}(3,6\text{-dibromocarbazol-9-yl})\text{-}5,5\text{-dimethyl-hexane-}2,4\text{-dione}\}]$ (14c)

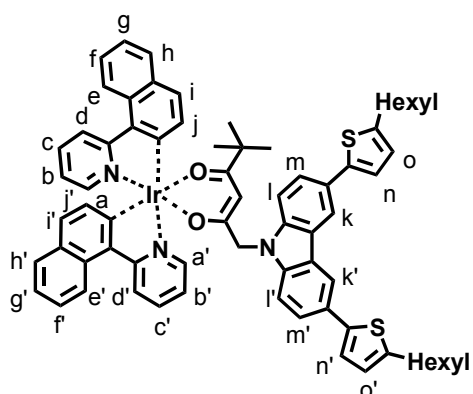


$[\text{Ir}^{\text{III}}(\text{ppy})_2\text{-}\mu\text{-Cl}]_2$ (200 mg, 0.187 mmol), K_2CO_3 (181 mg, 1.309 mmol), and compound **6** (217 mg, 0.468 mmol) afforded a green powder after purification. Yield: 250 mg, 69%.

^1H -NMR (400 MHz, CDCl_3 , ppm): δ 0.69 (s, 9H), 4.54 (s, 1H), 5.16 (s, 2H), 6.21-6.24 $^{\text{h,h'}}$ (m, 2H), 6.61-6.70 $^{\text{g,g'}}$ (m, 2H), 6.76-6.80 $^{\text{b'}}$ (t, $^3J = 8.6$ and 7.1 Hz, 1H), 6.82-6.92 $^{\text{b,f,f'}}$ (m, 3H), 7.03-7.05 $^{\text{m,m'}}$ (d, $^3J = 8.6$ Hz, 2H), 7.33-7.35 $^{\text{l,l'}}$ (d, $^3J = 8.6$ Hz, 2H),

7.47-7.50^{e,e'} (t, ³J = 8.1 and 6.1 Hz, 2H), 7.60-7.71^{e,e',d'} (m, 3H), 7.76-7.79^d (d, ³J = 8.5 Hz, 1H), 8.04^{k,k'} (s, 2H), 8.09-8.11^{a'} (d, ³J = 5.6 Hz, 1H), 8.20-8.21^a (d, ³J = 5.6 Hz, 1H). ¹³C-NMR (100 MHz, CDCl₃, ppm): δ 27.7, 41.2, 51.5, 92.7, 111.0, 112.2, 117.9, 120.5, 120.7, 120.9, 122.9, 123.5, 123.6, 123.7, 128.7, 128.9, 133.3, 133.4, 136.6, 136.8, 139.7, 147.6, 147.7, 147.9, 168.4, 168.6, 179.1, 196.9. IR: 3037 (C=C-H), 2952 (C-H), 1698, 1578 (C=C, C=N, C=O), 1469, 1414, 856, 834, 783, 749, 727, 674 cm⁻¹. APLI-MS: requires m/z C₄₂H₃₅Br₂IrN₃O₂ (M+H)⁺ 963.10, found 963.10. Elem. anal. Calcd. for C₄₂H₃₅Br₂IrN₃O₂: C 52.23%, H 3.65%, N 4.35%. Found: C 52.04%, H 3.83%, N 3.57%.

3.7.15 [Ir^{III}(npy)₂{1-[3,6-bis(5-hexyl-2-thienyl)carbazol-9-yl]-5,5-dimethyl-hexane-2,4-dione}] (15a)

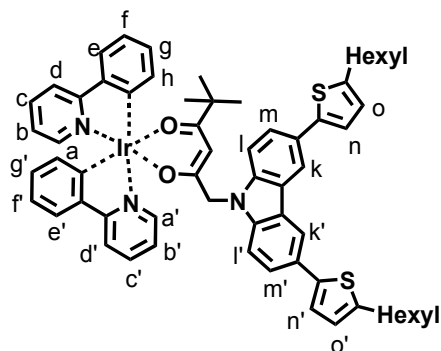


[Ir^{III}(npy)₂-μ-Cl]₂ (119 mg, 0.094 mmol), K₂CO₃ (91mg, 0.819 mmol), and compound **7** (120 mg, 0.188 mmol) afforded a red powder after purification. Yield: 95 mg, 41%.

¹H-NMR (400 MHz, CDCl₃, ppm): δ 0.66 (s, 9H), 0.93 (s, 6H), 1.37 (m, 8H), 1.46 (m, 4H), 1.77 (m, 4H), 2.88 (m, 4H), 4.62 (m, 2H), 5.26 (s, 1H), 6.34-6.36^j (d, ³J = 8.6 Hz, 1H), 6.38-6.40^j (d, ³J = 8.1 Hz, 1H), 6.80-6.81^{o,o'} (d, ³J = 3.6 Hz, 2H), 6.82-6.85^{g'} (t, ³J = 7.6 and 6.6 Hz, 1H), 6.93-6.96^g (t, ³J = 7.6 and 6.1 Hz, 1H), 6.98-7.00^{i,i'} (d, ³J = 8.6 Hz, 2H), 7.12-7.15^{c,c',n,n'} (m, 4H), 7.20-7.24^{m,m'} (m, 2H), 7.44-

7.46^{b,b',d,d'} (m, 4H), 7.60-7.62^{l,l'} (d, $^3J = 8.1$ Hz, 2H), 7.70-7.77^{f,f'} (m, 2H), 8.17^{k,k'} (s, 2H), 8.24-8.25^{h'} (d, $^3J = 4.6$ Hz, 1H), 8.29-8.30^h (d, $^3J = 4.6$ Hz, 1H), 8.42-8.53^{a,a',e,e'} (m, 4H). ^{13}C -NMR (100 MHz, CDCl_3 , ppm): δ 14.1, 22.6, 27.6, 28.9, 29.7, 30.4, 31.7, 41.1, 51.5, 92.8, 109.6, 117.1, 119.8, 120.1, 120.9, 121.1, 121.5, 121.9, 122.0, 122.1, 122.2, 123.3, 124.0, 124.9, 126.3, 126.4, 127.3, 128.1, 128.5, 129.6, 129.8, 131.0, 131.6, 131.7, 132.5, 132.7, 136.8, 140.4, 142.9, 144.5, 148.4, 169.3, 180.4, 202.1. IR: 3043 (C=C-H), 2953, 2920, 2852 (C-H), 1725, 1573, 1498 (C=C, C=N, C=O), 1357, 1289, 1156, 862, 808, 790, 740, 657, 640 cm^{-1} . APLI-MS: requires m/z $\text{C}_{70}\text{H}_{68}\text{IrN}_3\text{O}_2\text{S}_2$ ($\text{M}+\text{H}$)⁺ 1239.65, found 1239.60. Elem. anal. Calcd. for $\text{C}_{70}\text{H}_{68}\text{IrN}_3\text{O}_2\text{S}_2$: C 67.82%, H 5.53%, N 3.39%. Found: C 68.39%, H 5.51%, N 3.40%.

3.7.16 $[\text{Ir}^{\text{III}}(\text{ppy})_2\{1\text{-}[3,6\text{-bis}(5\text{-hexyl-2-thienyl)carbazol-9-yl]}\text{-5,5-dimethyl-hexane-2,4-dione}\}]$ (15b)

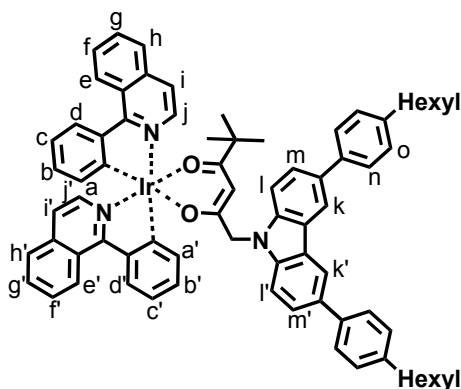


$[\text{Ir}^{\text{III}}(\text{ppy})_2\text{-}\mu\text{-Cl}]_2$ (93 mg, 0.086 mmol), K_2CO_3 (84 mg, 2.500 mmol), and 1-[3,6-bis(5-hexyl-2-thienyl)carbazol-9-yl]-5,5-dimethyl-hexane-2,4-dione (110 mg, 0.172 mmol) afforded a green powder after purification. Yield: (90 mg, 46%).

^1H -NMR (400 MHz, CDCl_3 , ppm): δ 0.66 (s, 9H), 0.92 (s, 6H), 1.36 (m, 8H), 1.47 (m, 4H), 1.77 (m, 4H), 2.87 (m, 4H), 4.63 (m, 2H), 5.19 (s, 1H), 6.23-6.25^{h'} (d, $^3J = 7.6$ Hz, 1H), 6.30-6.32^h (d, $^3J = 7.1$ Hz, 1H), 6.62-6.66^{g'} (t, $^3J = 8.6$ and 7.1 Hz, 1H),

6.67-6.71^g (t, ³J = 8.6 and 7.6 Hz, 1H), 6.79-6.92^{o,o',f,f',b,b'} (m, 6H), 7.13-7.17^{m,m',n,n'} (m, 4H), 7.49-7.52^{e,e',l,l'} (m, 4H), 7.63-7.65^{c,c'} (m, 2H), 7.72-7.74^{d'} (d, ³J = 8.6 Hz, 1H), 7.76-7.78^d (d, ³J = 8.6 Hz, 1H), 8.16-8.17^{a'} (d, ³J = 5.1 Hz, 1H), 8.21^{k,k'} (s, 2H), 8.32-8.33^a (d, ³J = 5.1 Hz, 1H). ¹³C-NMR (100 MHz, CDCl₃, ppm): δ 14.0, 22.6, 27.0, 27.6, 28.8, 30.3, 30.8, 31.7, 41.1, 51.5, 92.7, 108.9, 109.6, 117.1, 117.6, 117.9, 118.2, 120.4, 120.6, 120.9, 121.0, 121.4, 121.8, 123.3, 123.4, 123.7, 124.0, 124.5, 124.9, 126.4, 127.2, 128.6, 128.9, 133.3, 133.5, 136.6, 136.7, 140.3, 142.5, 142.9, 144.5, 144.7, 147.7, 147.8, 148.1, 168.4, 168.5, 180.1, 196.7. IR: 3058 (C=C-H), 2952, 2922, 2822 (C-H), 1698, 1620, 1575 (C=C, C=N, C=O), 1472, 1422, 1314, 874, 849, 791, 753, 727, 680 cm⁻¹. APLI-MS: requires m/z C₆₂H₆₄IrN₃O₂S₂ (M+H)⁺ 1139.41, found 1139.40. Elem. anal. Calcd. for C₆₂H₆₄IrN₃O₂S₂: C 65.35%, H 5.66%, N 3.69%. Found: C 65.21%, H 5.65%, N 3.70%.

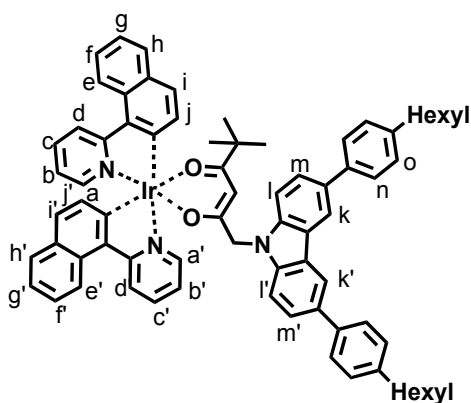
3.7.17 [Ir^{III}(piq)₂{1-[3,6-bis(4-hexylphenyl)carbazol-9-yl]-5,5-dimethyl-hexane-2,4-dione}] (16a)



[Ir^{III}(piq)₂-μ-Cl]₂ (200 mg, 0.157 mmol), K₂CO₃ (152 mg, 1.100 mmol), and compound **8** (197 mg, 0.314 mmol) afforded a red powder after purification. Yield: (286 mg, 72%).

$^1\text{H-NMR}$ (600 MHz, CDCl_3 , ppm): δ (s, 6H), 0.96 (s, 4H), 1.38-1.45 (m, 8H), 1.74 (s, 4H), 2.73 (s, 4H), 4.55-4.77 (m, 2H), 5.22 (s, 1H), 6.42-6.43^{a'} (d, $^3J = 7.53$ Hz, 1H), 6.52-6.53^a (d, $^3J = 7.53$ Hz, 1H), 6.65-6.67^{b'} (t, $^3J = 7.15$ and 8.66 Hz, 1H), 6.70-6.73^b (t, $^3J = 7.15$ and 8.66 Hz, 1H), 6.91-6.93^{c'} (t, $^3J = 7.15$ and 8.28 Hz, 1H), 6.96-6.98^c (t, $^3J = 7.53$ and 8.28 Hz, 1H), 7.16-7.19^{n',n} (d, $^3J = 8.28$ Hz, 2H), 7.30-7.35 (m, 6H), 7.42-7.44^{o',o} (d, $^3J = 8.66$ Hz, 2H), 7.64-7.65^{h',h} (d, $^3J = 7.91$ Hz, 2H), 7.71-7.74^{i',i,l',l} (m, 4H), 7.90-7.91^{k',k} (d, $^3J = 8.28$ Hz, 2H), 8.19-8.26^{g',g, d',d} (m, 4H), 8.36-8.37^{e',e} (d, $^3J = 6.40$ Hz, 2H), 8.99-9.00^{j'} (d, $^3J = 7.53$ Hz, 1H), 9.04-9.06^j (d, $^3J = 7.91$ Hz, 1H). $^{13}\text{C-NMR}$ (150 MHz, CDCl_3 , ppm): δ 14.1, 22.6, 27.5, 29.1, 31.5, 31.8, 35.6, 41.0, 51.7, 92.6, 109.3, 118.3, 119.3, 119.6, 120.2, 120.4, 123.5, 124.9, 126.1, 126.3, 126.7, 126.8, 127.0, 127.1, 127.2, 127.3, 127.5, 127.6, 128.5, 128.8, 128.9, 129.0, 129.4, 129.6, 130.5, 130.6, 132.3, 133.9, 134.3, 137.1, 137.2, 139.4, 140.4, 140.5, 140.6, 141.1, 146.5, 151.9, 169.1, 180.8, 196.7. IR: 3049 (C=C-H), 1668, 1579, 1557 (C=N, C=C), 1388, 1116, 883, 864, 854, 783, 647 cm^{-1} . APLI-MS: requires m/z $\text{C}_{74}\text{H}_{72}\text{IrN}_3\text{O}_2$ (M+H)⁺ 1227.60, found 1227.60. Elem. anal. Calcd. for $\text{C}_{74}\text{H}_{72}\text{IrN}_3\text{O}_2$: C 72.40%, H 5.91%, N 3.42%, Found: C 72.42%, H 5.27%, N 3.15%.

3.7.18 [Ir^{III} (npy) $_2$ {1-[3,6-bis(4-hexylphenyl)carbazol-9-yl]-5,5-dimethyl-hexane-2,4-dione}] (16b)



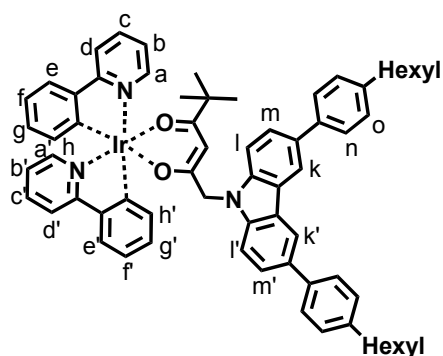
Chapter 3. Iridium(III) complexes

$[\text{Ir}^{\text{III}}(\text{npy})_2-\mu\text{-Cl}]_2$ (200 mg, 0.157 mmol), K_2CO_3 (152 mg, 1.100 mmol), and compound **8** (197 mg, 0.314 mmol) afforded a red powder after purification. Yield: (258 mg, 65%).

$^1\text{H-NMR}$ (600 MHz, CDCl_3 , ppm): δ 0.69 (s, 6H), 0.96 (s, 4H), 1.39-1.45 (m, 8H), 1.73 (s, 4H), 2.73 (s, 4H), 4.64-4.76 (m, 2H), 5.32 (s, 1H), 6.39-6.40^j (d, $^3J = 8.66$ Hz, 1H), 6.44-6.45^j (d, $^3J = 8.66$ Hz, 1H), 6.83-6.85^g (t, $^3J = 6.77$ and 7.91 Hz, 1H), 6.99-7.04^{i,i,g} (m, 3H), 7.24-7.28^{c',c,n',n,m',m} (m, 6H), 7.34-7.35^{l,i,k,k} (m, 4H), 7.48-7.50^{b',b,o',o} (m, 4H), 7.61-7.62ⁱ (d, $^3J = 8.28$ Hz, 1H), 7.64-7.66^{d',d,i} (d, $^3J = 7.91$ Hz, 3H), 7.72-7.75^f (t, $^3J = 8.66$ and 9.03 Hz, 1H), 7.78-7.80^f (t, $^3J = 8.66$ and 10.16 Hz, 1H), 8.30^{h,h} (s, 2H), 8.37-8.38^{e'} (d, $^3J = 5.27$ Hz, 1H), 8.45-8.51^{a',e} (m, 2H), 8.55-8.56^a (d, $^3J = 8.66$ Hz, 1H). $^{13}\text{C-NMR}$ (150 MHz, CDCl_3 , ppm): δ 14.1, 22.6, 26.3, 27.6, 29.1, 31.6, 31.8, 35.6, 41.1, 51.6, 92.8, 109.6, 118.3, 119.8, 120.1, 120.9, 121.1, 121.9, 122.0, 122.2, 123.6, 125.0, 126.1, 126.3, 127.0, 127.1, 128.1, 128.5, 128.8, 129.6, 129.7, 131.0, 131.1, 131.6, 131.7, 132.4, 132.5, 132.7, 136.8, 137.8, 139.4, 140.5, 141.2, 148.5, 148.7, 155.8, 169.0, 169.3, 180.7, 196.9. IR: 3051 (C=C-H), 1657, 1610, 1558 (C=N, C=C), 1279, 1117, 885, 871, 859, 791, 652 cm^{-1} . APLI-MS: requires m/z $\text{C}_{74}\text{H}_{72}\text{IrN}_3\text{O}_2$ (M+H)⁺ 1227.60, found 1227.60. Elem. anal. Calcd. for $\text{C}_{74}\text{H}_{72}\text{IrN}_3\text{O}_2$: C 72.40%, H 5.91%, N 3.42%, Found: C 72.56%, H 5.45%, N 3.34%.

3.7.19 $[\text{Ir}^{\text{III}}(\text{ppy})_2\{1\text{-}[3,6\text{-bis}(4\text{-hexylphenyl})\text{carbazol-9-yl}]\text{-5,5-dimethyl-hexane-2,4-dione}\}]$ (**16c**)

Chapter 3. Iridium(III) complexes



$[\text{Ir}^{\text{III}}(\text{ppy})_2-\mu\text{-Cl}]_2$ (200 mg, 0.19 mmol), compound **8** (234 mg, 0.37 mmol), and K_2CO_3 (152 mg, 1.100 mmol) afforded a green powder after purification. Yield: (295 mg, 68%).

$^1\text{H-NMR}$ (600 MHz, CDCl_3 , ppm): δ 0.66 (s, 6H), 0.94 (s, 4H), 1.37-1.44 (m, 8H), 1.72 (s, 4H), 2.71 (s, 4H), 4.61-4.76 (m, 2H), 5.22 (m, 1H), 6.28-6.29^{h'} (d, $^3J = 7.53$ Hz, 1H), 6.37-6.38^h (d, $^3J = 7.53$ Hz, 1H), 6.66-6.69^{g'} (t, $^3J = 7.91$ and 7.90 Hz, 1H), 6.72-6.75^g (t, $^3J = 7.91$ and 7.53 Hz, 1H), 6.80-6.82^f (t, $^3J = 6.77$ and 8.66 Hz, 1H), 6.86-6.88^f (t, $^3J = 6.40$ and 8.28 Hz, 1H), 6.94-6.96^{b',b} (m, 2H), 7.29^{m',m,n',n} (s, 4H), 7.33-7.34^{d',d} (d, $^3J = 7.91$ Hz, 2H), 7.51-7.57^{e',e} (m, 2H), 7.59-7.61^{l',l} (d, $^3J = 8.66$ Hz, 2H), 7.68-7.69^{c',c,n',n} (d, $^3J = 7.91$ Hz, 4H), 7.79-7.81^{o',o} (d, $^3J = 7.91$ Hz, 2H), 8.26-8.27^{a'} (d, $^3J = 5.65$ Hz, 1H), 8.32^{k',k} (s, 2H), 8.40-8.41^a ppm (d, $^3J = 5.27$ Hz, 1H). $^{13}\text{C-NMR}$ (150 MHz, CDCl_3 , ppm): δ 14.1, 22.6, 27.6, 29.1, 31.5, 35.6, 41.1, 92.6, 109.5, 118.2, 118.4, 120.4, 120.9, 121.1, 123.4, 123.6, 123.7, 125.1, 126.9, 127.0, 128.6, 128.8, 129.0, 132.5, 133.3, 133.5, 136.7, 136.8, 139.4, 140.4, 141.2, 144.7, 144.8, 147.2, 147.9, 148.2, 168.5, 180.5, 196.6. IR: 3047 (C=C-H), 1668, 1571, 1556 (C=N, C=C), 1378, 1231, 885, 874, 864, 783, 657 cm^{-1} . APLI-MS: requires m/z $\text{C}_{66}\text{H}_{68}\text{IrN}_3\text{O}_2$ ($\text{M}+\text{H}$)⁺ 1127.50, found 1127.50. Elem. anal. Calcd. for $\text{C}_{66}\text{H}_{68}\text{IrN}_3\text{O}_2$: C 70.31%, H 6.08%, N 3.73%, Found: C 70.87%, H 5.98%, N 3.49%.

3.8 References

- [1] K.-C. Tang, K. L. Liu, I.-C. Chen, *Chem. Phys. Lett.* **2004**, 386, 437.
- [2] N. Tian, D. Lenkeit, S. Pelz, L. H. Fischer, D. Escudero, R. Schiewek, D. Klink, O. J. Schmitz, L. González, M. Schäferling, E. Holder, *Eur. J. Inorg. Chem.* **2010**, 30, 4875.
- [3] L. H. Fischer, M. I. J. Stich, O. S. Wolfbeis, N. Tian, E. Holder, M. Schäferling, *Chem. Eur. J.* **2009**, 15, 10857.
- [4] S. Lamansky, P. Djurovich, D. Murphy, F. A. Razzaq, R. Kwong, I. Tsyba, M. Bortz, B. Mmui, R. Bau, M. E. Thompson, *Inorg. Chem.* **2001**, 40, 1704.
- [5] N. Tian, D. Lenkeit, S. Pelz, D. Kourkoulos, D. Hertel, K. Meerholz, E. Holder, *Dalton Trans.* **2011**, 40, 11629.
- [6] N. Rehmman, C. Ulbricht, A. Koehnen, P. Zacharias, M. C. Gather, D. Hertel, E. Holder, K. Meerholz, U. S. Schubert, *Adv. Mater.* **2008**, 20, 129.
- [7] E. Holder, B. M. W. Langeveld, U. S. Schubert, *Adv. Mater.* **2005**, 17, 1109.
- [8] N. Tian, A. Thiessen, R. Schiewek, O. J. Schmitz, D. Hertel, K. Meerholz, E. Holder, *J. Org. Chem.* **2009**, 74, 2718.
- [9] Z. W. Liu, M. Guan, Z. Q. Bian, D. B. Nie, Z. L. Gong, Z. B. Li, C. H. Huang, *Adv. Funct. Mater.* **2006**, 16, 1441.
- [10] H. E. Katz, J. G. Laquindanum, A. J. Lovinger, *Chem. Mater.* **1998**, 10, 633.
- [11] J. Teetsov, M. A. Fox, *J. Mater. Chem.* **1999**, 9, 2117.
- [12] J. I. Kim, I. S. Shin, H. Kim, J. K. Lee, *J. Am. Chem. Soc.* **2005**, 127, 1614.
- [13] C. Adachi, M. A. Baldo, M. E. Thompson, S. R. Forrest, *J. Appl. Phys.* **2001**, 90, 5048.
- [14] Md. K. Nazeeruddin, R. Humphry-Baker, D. Berner, S. Rivier, L. Zuppiroli, M. Graetzel, *J. Am. Chem. Soc.* **2003**, 125, 8790.
- [15] Z. W. Liu, M. Guan, Z. Q. Bian, D. B. Nie, Z. L. Gong, Z. B. Li, C. H. Huang, *Adv. Funct. Mater.* **2006**, 16, 1441.
- [16] M. Constapel, M. Schellenträger, O. J. Schmitz, S. Gäb, K. J. Brockmann, R. Giese, T. Benter, *Rapid Commun Mass Spectrom.* **2005**, 19, 326.

Chapter 3. Iridium(III) complexes

- [17] S. Schmidt, M. F. Appel, R. M. Garnica, R. N. Schindler, T. Benter, *Anal. Chem.* **1999**, *71*, 3721.
- [18] J. N. Demas, G. A. Crosby, *J. Phys. Chem.* **1971**, *75*, 991.
- [19] C. Adachi, M. A. Baldo, S. R. Forrest, *Appl. Phys. Lett.* **2001**, *78*, 1622.
- [20] N. Tian, Y. V. Aulin, D. Lenkeit, S. Pelz, O. Mikhnenko, P. W. M. Blom, M. A. Loi, E. Holder, *Dalton Trans.* **2010**, *39*, 8613.
- [21] Y. H. Song, S. J. Yeh, C. T. Chen, *Adv. Func. Mater.* **2004**, *14*, 1221.
- [22] S. Lamansky, P. Djurovich, M. E. Thompson, *J. Am. Chem. Soc.* **2001**, *123*, 4304.
- [23] R. C. Kwong, D. B. Knowles, M. E. Thompson, U.S. Patent Application. 20030072964, **2003**.
- [24] H. Konno, Y. Sasaki, *Chem. Lett.* **2003**, *32*, 252.
- [25] M. I. Stich, O. S. Wolfbeis, *Fluorescence Sensing and Imaging Using Pressure-Sensitive Paints and Temperature-Sensitive Paints*, Springer, **2008**.
- [26] C. Moore, S. P. Chan, J. N. Demas, B. A. DeGraff, *Appl. Spectrosc.* **2004**, *58*, 603.
- [27] J. Brandrup, E. H. Immergut, E. A. Grulke, *Polymer Handbook*, Wiley-VCH, **1999**.
- [28] R. Schiewek, M. Lorenz, R. Giese, K. J. Brockmann, T. Benter, S. Gäb, O. J. Schmitz, *Anal. Bioanal. Chem.* **2008**, *392*, 87.
- [29] M. Constapel, M. Schellenträger, O. J. Schmitz, S. Gäb, K. J. Brockmann, R. Giese, T. Benter, *Rapid Commun. Mass Spectrom.* **2005**, *19*, 326.

Chapter 4

Copolymers containing iridium(III) complexes

4.1 Introduction

Conjugated phosphorescent copolymers containing iridium(III) complexes are of interest for use as emitting dyes in PLED devices. Due to the fact that an internal host (copolymer main chain)-guest (doped complexes) system is present in these metallo-copolymers, high photoluminescence (PL) efficiency and good charge-transport can be expected *via intrachain* energy-transfer, in comparison to blended polymer/iridium(III) complexes systems, in which possible energy loss, aggregation of the dopant and phase separation with increasing current density can limit the efficiency of devices [1,2]. Since the small complexes are located in the polymer chain, the possibility of self- and triplet-triplet annihilation is greatly decreased and the quantum efficiency can be intrinsically enhanced [3,4]. Additionally, the fabrication of PLED devices by a spin-coating or printing techniques promises to be easier and less expensive than that of OLEDs, where the emitting layers require high-vacuum deposition [5-7]. The use of conjugated polyfluorenes, in which red emitting iridium(III) complexes or/and fluorenone units are incorporated as emitting dyes, has attracted attention because of the high photoluminescence (PL) efficiency, good charge-transport and thermal stability provided by these systems [8,9].

In our study, for the design and synthesis of conjugated copolymers, comprising

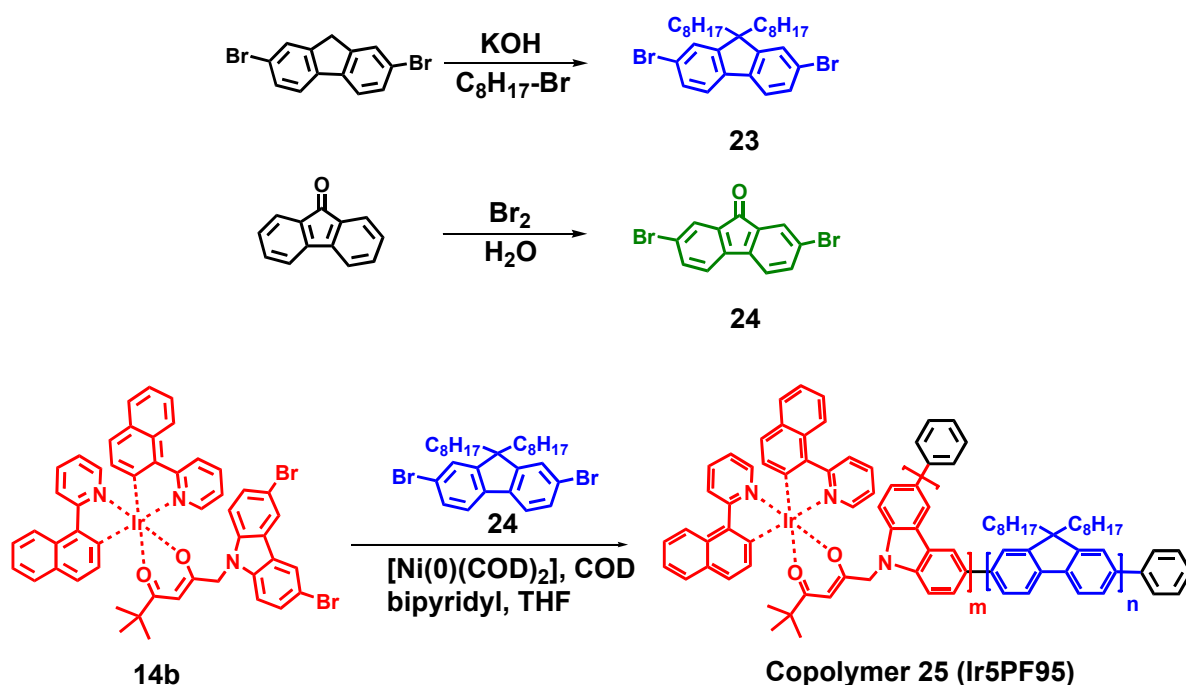
Chapter 4. Copolymers containing iridium(III) complexes

fluorene-based comonomers and phosphorescent iridium(III) emitters, a variety of synthetic approaches is available. Prominent ones are the Suzuki [10-13] and Yamamoto [14,15] polymerisations leading to alternating or random on-chain complexes, correspondingly. Yamamoto is advantageous due to its less demanding, synthetic procedures towards the comonomers used, whereas Suzuki represents copolymers of well-defined comonomer alternating sequences. Additionally, Yamamoto deals with monomers of the AA constitution namely dihalogenide functionalised derivatives while in Suzuki reactions comonomers including halogenide and boronic acid or ester derivatives (AB, AA and BB constitutions) are required. In order to exploit the advantages of the Yamamoto protocol, three iridium(III)-based copolymers namely **25-27** (Scheme 4.1) were synthesised, whereby the first copolymer **25** is embracing the orange-red emitting iridium(III) complex **14b** (feed ratio: 5 mol%) in the polyfluorene backbone. The in-here introduced heteroleptic Ir(III) emitter [16] **14b** does not only promote orange-red emission due to the 2-(naphthalene-1-yl)pyridine cyclometalating ligands but supports hole trapping at the on-chain complexes as well, due to the carbazolyl functionalised ancillary ligand [16,17]. The carbazolyl-based iridium(III) complexes with their function as hole acceptors [18-20], were combined with fluorene- and fluorenone-based counterparts giving the afore-mentioned copolymers **26** (feed ratios of **14b**, **23** and **24**: 5%, 90% and 5%) and **27** (feed ratios of **14b**, **23** and **24**: 10%, 89% and 1%). The concurrently appearance of iridium(III) complexes (**14b**) and fluorenone units (**24**) in the copolymer backbone served the target of synthesising copolymers with the property of white-light emission and balanced charge transport, respectively.

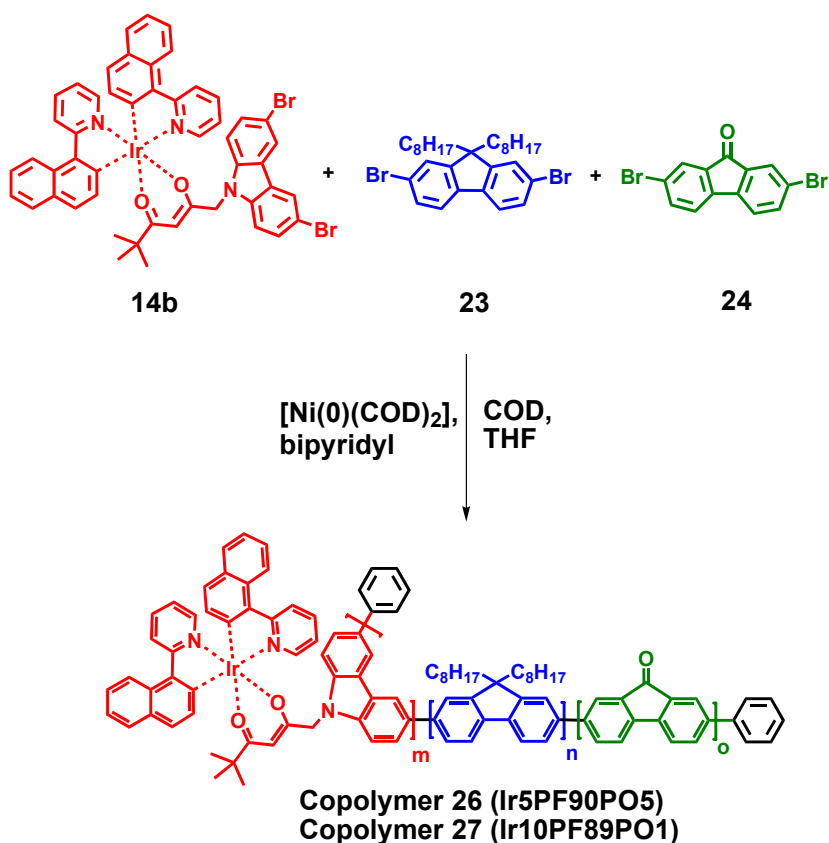
4.2 Results and discussions

4.2.1 Synthesis of iridium(III)-based copolymers 25-27

The series of novel iridium(III)-based copolymers **25-27** (Scheme 4.1 and 4.2) were designed and synthesised by a Yamamoto coupling procedure [21] in the presence of excess 1,5-cyclooctadiene (COD), $[\text{Ni}(0)(\text{COD})_2]$, and 2,2'-bipyridyl in THF, while stirring the reaction mixture at 80 °C for 3 days. After endcapping with bromobenzene and treating with HCl (2 mol/L), Na-EDTA, NaHCO_3 and H_2O , the crude copolymers were precipitated from methanol and Soxhlet-extracted with ethanol for 24 h. The synthetic route of monomer **14b** is given in chapter 3. The starting materials, 2,7-dibromo-9,9-di-*n*-octyl-9*H*-fluorene [22] (**23**, yield: 89%) and 2,7-dibromo-9*H*-fluoren-9-one [23] (**24**, yield: 68%) were synthesised by introducing two octyl groups in the 9-position of 2,7-dibromo-9*H*-fluorene under basic conditions (Scheme 4.1) and brominating 9*H*-fluoren-9-one (Scheme 4.1), respectively.



Scheme 4.1. Schematic representation of the synthetic routes of monomers **23**, **24** as well as of the random copolymer **25**.



Scheme 4.2. Schematic representation of the synthetic route of the random copolymers **26** and **27**.

The random copolymers **25-27** were investigated by ¹H NMR (Figure 4.1) and elemental analysis. All polymers exhibited NMR spectra of same pattern where fluorene signals predominate. Moreover, Table 4.1 summarizes the molecular weights, PDIs and thermal stabilities of all copolymers.

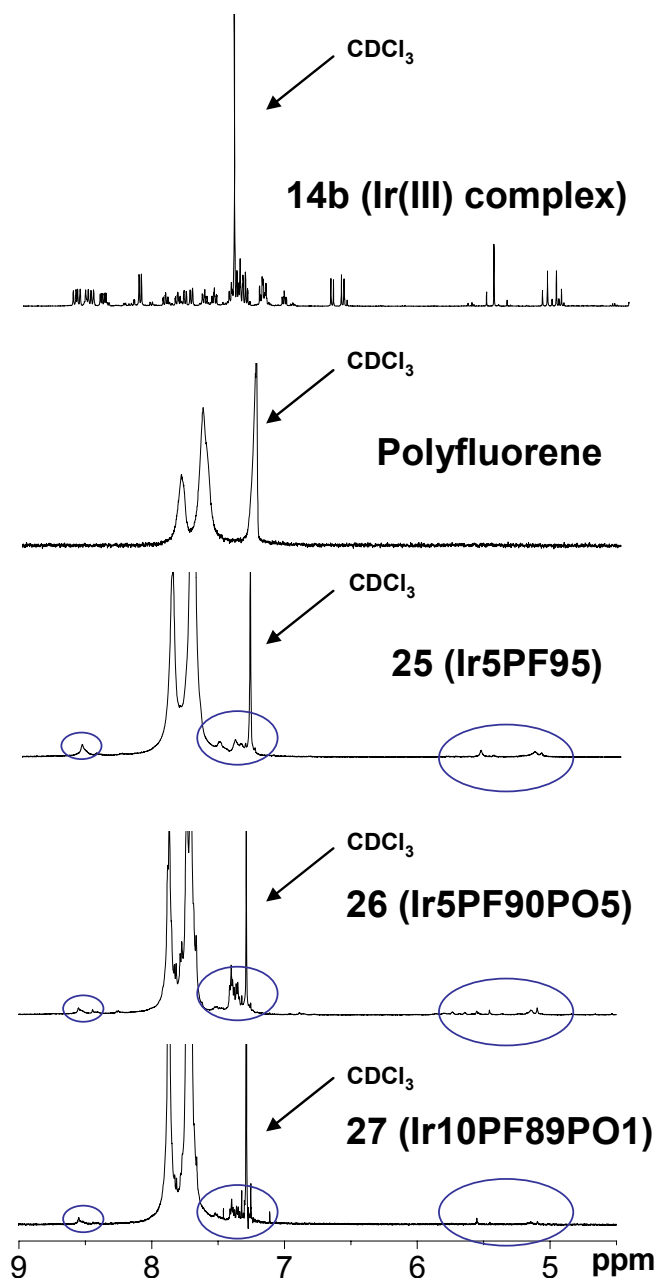


Figure 4.1. ^1H NMR spectra of Ir(III) complex **14b**, polyfluorene, and copolymers **25-27**.

Figure 4.1 show ^1H NMR spectra of Ir(III) complex **14b**, polyfluorene and synthesised copolymers **25-27**. Comparing the spectra of copolymer **25-27** to those of monomer **14b** and polyfluorene, allowed us to believe that Ir(III) complex **14b** as starting monomer was successfully embedded in the copolymer respective main chain by using Yamamoto polymerisation. Here, the intense peaks are attributed to

Chapter 4. Copolymers containing iridium(III) complexes

in-chain fluorene repeating units and most of the additional small peaks can be assigned to the Ir(III) complex moieties.

Gel permeation chromatography (GPC) measurements were firstly conducted at a concentration of 1mg/ml indicating aggregation phenomena in these copolymers. Therefore, measurements were repeated at a concentration of 0.5 mg/ml in chloroform whereby all three copolymers exhibited reduced polydispersity indices (PDI)s and weight-average molecular weights (M_w) of 299000 g/mol for **25**, 87400 g/mol for **26** and 207000 g/mol for **27**. The achieved PDIs (M_w/M_n) revealed values of 3.19 for **25**, 2.56 for **26** and 3.20 for **27**, respectively (Table 4.1). The higher PDI values [24] of **25** and **27** are believed to be due to *interchain* interactions like physical entanglements or π -stacks. The impact of these interactions is most likely dependent on the fluorene-content and the chain length. The longer the polymer chains, the higher the molecular weight of the respective polymers are and thus the greater their ability to form physical entanglements or π -stacks. A further measurement with even lower concentration of the GPC samples in order to avoid *interchain* interactions could not be performed due the sensitivity of the available GPC instrument.

Table 4.1. Molecular weights and thermal properties of copolymers **25-27**.

Copolymer	M_n^a	M_w^a	PDI	T_g / T_c (°C)	T_d (°C) ^b
25	93500	299000	3.19	80 / 168	403
26	34100	87400	2.56	110 / 164	408
27	64600	207000	3.20	120 / 162	405

^aMolecular weight determined by GPC (eluent: CHCl₃, concentration: 0.5 mg/ml, calibration: polystyrene).

^bTemperature at which 5% weight-loss of the initial weight occurred.

The thermal stability of the copolymers was moreover investigated by DSC and TGA under inert atmosphere (see Table 4.1). According to literature, the glass

transition temperature (T_g) of polyfluorene based on dioctyl side chains is about 75-120 °C [25]. An addition of fluorenone is known to only slightly increase the T_g [26]. These copolymer shows a T_g (80 °C) consistent to the literature values. The DSC measurements, performed in the temperature range from 30 to 250 °C, exhibited T_g and T_{ic} at around 80 °C and 168 °C for **25**, 110 °C and 164 °C for **26** and 120 °C and 162 °C for **27**. These results can be attributed to liquid-crystalline phase transitions. The decomposition temperatures (T_d), which correspond to a 5% weight-loss upon heating, range from 403 to 408°C.

4.2.2 Optical properties

The UV-vis absorption and photoluminescence (PL) emission spectra of the copolymers **25-27** were analysed in chloroform solution at concentration of 10^{-5} mol/L. Thin films were prepared from a chloroform solution (concentration: 2 mg/ml) followed by spin-coating onto quartz plates and annealing at 60 °C for 12h at room temperature.

Figure 4.2 shows the UV-vis and emission spectra of **25**.

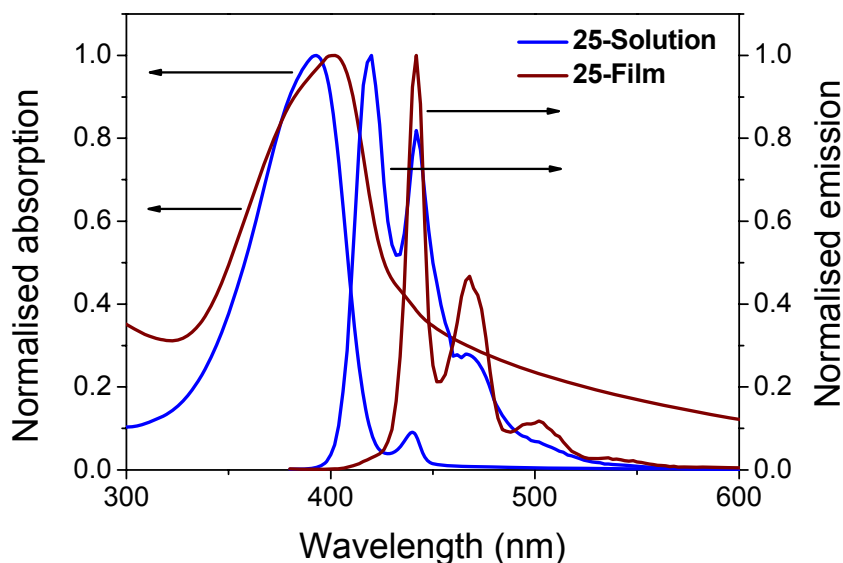


Figure 4.2. UV-vis absorption and emission spectra of copolymer **25** recorded in a CHCl_3 solution (10^{-5} M) and as film (1 mg/ml in CHCl_3).

The absorption maximum in solution was found at 391 nm while the solid state maximum was found at 399 nm (Figure 4.2, Table 4.2). The observed red-shifted values in the film varied only about 10 nm in contrast to the absorption maxima in solution. The stronger absorption peak at around 390 nm confirmed the existence of π - π^* transitions in the main chain of the conjugated systems [27,28]. The weaker absorption peak at about 440 nm was assigned to a typical β -phase formation known to occur in copolymer backbones comprised of dioctylfluorene. In solution, the maxima in the emission spectra appeared with typical vibronic progressions with the 0-0 PL emission band situated at 419-420 nm and the 0-1 transition at 441-442 nm. Unfortunately, for copolymer **25**, energy-transfer between polyfluorene and iridium complex moieties could not to be monitored either in solution or in solid state.

Figure. 4.3 shows the UV-vis and emission spectra of **25** and **26**.

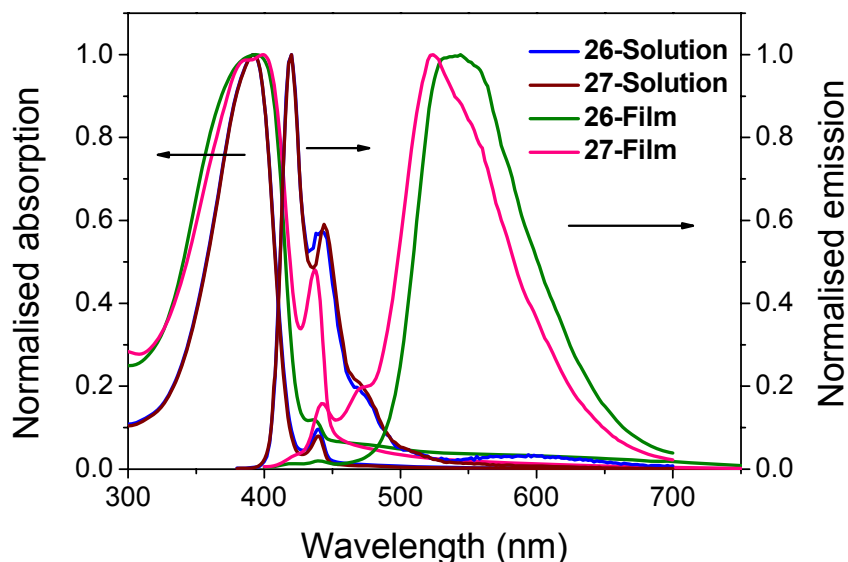


Figure 4.3. UV-vis absorption and emission spectra of copolymers **26** and **27** recorded in CHCl_3 solution (10^{-5} M) and in films (1 mg/ml in CHCl_3).

The absorption peaks originating from the conjugated backbone of copolymers **26** and **27** appeared at around 393 nm in chloroform solutions and exhibited absorption maxima at around 398 nm in solid state (Figure 4.3, Table 4.2). Additionally, the intensity of the peak at about 440 nm caused by the β -phase is enhanced and thus more obvious when compared to copolymer **25** (Figure 4.2). The increase can be assigned to enhanced intermolecular aggregation by adding fluorenone moieties, which can cause a more flat polymer backbone. The photoluminescence emission spectra of copolymers **26** and **27** in chloroform solution show maxima at 419 nm. In thin films, the peaks of the copolymers appeared at 543 nm (**26**), 522 nm (**27**), about 110 nm red-shift compared to the solution maxima. The large red-shift is attributed to energy-transfer to the fluorenone segments. In other words, the emission maxima of this series in the solid state are dominated by the fluorenone moieties, even at a feed ratio of

Chapter 4. Copolymers containing iridium(III) complexes

fluorenone segments in copolymer backbone as low as 1 mol%. Very slight emission peaks at around 600 nm are observed in solution, as well. Because of the intensive fluorenone emission in the solid state measurements, which covers the emission area from 500 nm to 700 nm, the emission of the orange-red iridium(III) complexes is rather difficult to be verified.

Table 4.2. UV-vis absorption and emission maxima of copolymers **25-27**.

Complexes	Solution		Film	
	Absorbance [nm] (log ϵ , [L \times mol ⁻¹ \times cm ⁻¹])	Maximum of Emission [nm]	Absorbance [nm] (log ϵ [L \times mol ⁻¹ \times cm ⁻¹])	Maximum of Emission [nm]
25	391 (5.07)	419	399 (4.86)	442
26	393 (5.11)	420	398 (4.92)	540
27	394 (5.08)	421	398 (4.89)	524

To conclude, comparing the emission spectra of copolymer **25** containing red emitting Ir(III) complexes units to copolymers **26** and **27** comprising red Ir(III) complexes and fluorenone segments, a large red-shift is monitored for the latter in the film measurements. The normalised emission spectra of the random copolymers **26** and **27** reveal slight shoulders of orange red Ir(III) complex **14b** in the emission range of 580-620 nm and intensive emission at around 524-540 nm, which are attributed to the fluorenone moieties in the polyfluorene backbone. In copolymer **25**, which is only functionalised with fluorene moieties, discrete emission bands of the polyfluorene backbone and the orange red Ir(III) complex **14b** appeared, only. Non-significant energy-transfer from fluorene segments to the iridium(III) complexes in solution can be observed. In solid state, the emission spectra of copolymers **26-27** were dominated by fluorene- and fluorenone segments.

4.2.3 Electroluminescence properties

Statement: Because of the missing reference copolymers, the results described in the following section can be only treated as a preliminary conclusion.

The copolymers **25-27** were implemented as emitting materials in polymer light-emitting diodes (PLEDs). The device architecture was fabricated by Dimitrios Kourkoulos and Alexander Thiessen (group of Prof. Klaus Meerholz at the Institute of Physical Chemistry at the University of Cologne) und consisted of: (ITO/PEDOT [28 nm] /QUPD [18 nm]/OTPD [10 nm]/**25** or **26** or **27**/TPBI [30 nm]/CsF [3 nm]:Al [120 nm]). The emitting layer thickness was 56 nm, 27 nm and 55 nm for **25**, **26** and **27**, respectively. The electroluminescence properties of the copolymer **25** were recorded at driving voltages between 12 and 22 V and are exemplary depicted in Figure 4.4.

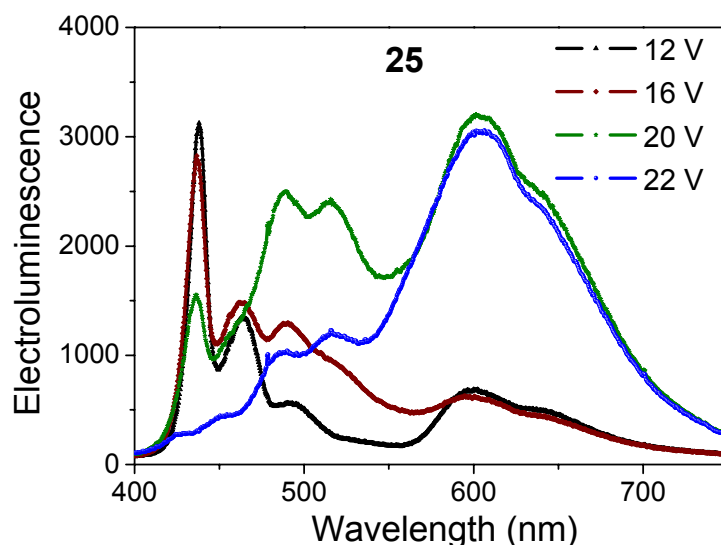


Figure 4.4. Electroluminescence spectra of copolymer **25** recorded in multi-layer PLEDs @ driving voltages ranging from 12 V to 22 V (measurements: group of Prof. Klaus Meerholz at the University of Cologne).

Chapter 4. Copolymers containing iridium(III) complexes

Figure 4.4 clearly reveals substantial red Ir(III) complex emission when traversing from low to higher voltage values. By increasing the voltage on the device a suppression of the polyfluorene emission is observed and a simultaneous enhancement of the emission deriving from the Ir(III) units on the copolymer backbone can be monitored. By a driving voltage of 12 V, the fluorene band at 437 nm dominates the spectrum and a weak signal of the iridium units at 598 nm arises. Until the threshold value of 16 V, the same weak signal for the iridium moieties is present and only by a driving voltage of 20 V, a significant suppression of the blue emission is possible. Thus, a pronounced red band at 604 nm comes into sight assigned to the iridium counterparts. By applying the highest voltage of 22 V, a complete suppression of the fluorene emission takes place and the spectrum is now predominated by the red Ir(III) units emission, which exhibits a 4.5 times larger intensity compared to the intensity achieved at the lowest driving voltage. As the iridium(III) complex consists an important part of the copolymer being embedded into the its main chain at higher operating voltages charge trapping at the complex sites and synchronously the decrease of the potential triplet energy back transfer from the iridium(III) complex to the copolymer backbone comes into light. Hence, the energy-transfer from fluorene backbone to iridium(III) complexes and charge trapping on iridium(III) complexes can be achieved under high voltage but is not present in the photoluminescence spectra *via* application of ultraviolet excitation. Moreover, the bands at the green emission region lose intensity when higher driving voltage is applied, which allows us to conclude that emission is more likely a result of emissive states like β -phase and is not deriving from fluorenone moieties. PLED devices of the same configuration as previously described were also built using copolymers **26** and **27**, as well and were investigated, respectively (Figure 4.5). The measurements were now conducted by applying just 9 V of driving voltage and as can be seen in Figure 4.4 a strongly red-shifted emission can be monitored for both copolymers **26** and **27** at about 610 nm to 650 nm, respectively. This means that the presence of fluorenone units

or a higher content of iridium can facilitate the operating device conditions by lowering the required voltage value. The fluorene emission in the spectra is again almost eliminated due to efficient energy-transfer to the fluorenone and probably to the Ir(III) complex segments.

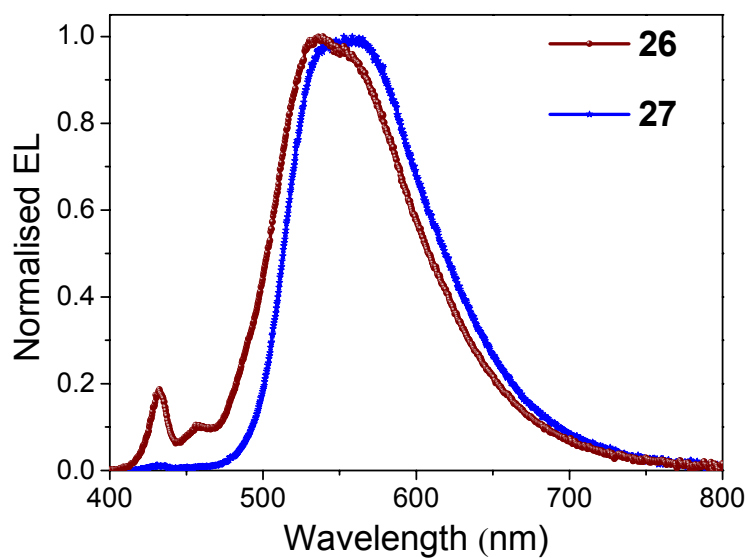


Figure 4.5. Electroluminescence spectra of copolymers **26** (red) and **27** (blue) recorded in multi-layer PLEDs at 9 V (measurements by the group of Prof. Klaus Meerholz at the University of Cologne).

The maximum electroluminescence efficiencies of the devices with copolymers **25-27** are given in Table 4.3, whereby the device based on copolymer **27** exhibits the best electroluminescence performance (9.65 Cd/A) and power efficiency (6.68 lm/W) while the device based on copolymer **25** showed an electroluminescence efficiency of just 0.88 Cd/A and marginal power performance of 0.60 lm/W. The difference in the devices behaviour can be assigned to the presence of fluorenone segments and/or higher iridium(III) content complex, which is the case for copolymers **26** and **27**. The fluorenone units through their n-type character create a bipolar polymer structure leading to superior interface charge-recombination at the emitter sites [29].

Table 4.3. Electro- and photoluminescence efficiencies of copolymers **25-27**.

Copolymers	Eff (max) [Cd/A]	Eff (av) [Cd/A]	Peff (max) [lm/W]	Peff (av) [lm/W]
25	0.88	(0.85 ± 0.02)	0.60	(0.53 ± 0.04)
26	8.45	(8.39 ± 0.1)	5.01	(4.9 ± 0.1)
27	9.65	(9.1 ± 0.1)	6.68	(6.4 ± 0.4)

Table 4.4 represents the phosphorescence quantum yields of copolymers **25-27** measured in chloroform solutions and in thin films solely or by addition of polystyrene as blends. In solution, **25** revealed the highest quantum yield of the investigated materials but the lowest in solid state measurements. As a blend with polystyrene, **25** had once more the highest quantum yield. These measurements allowed us to suggest that quantum yields are not an absolute measure of materials performance in opto-electronic devices even when they bear values in the range of poly(9,9-di-*n*-octylfluorene).

Table 4.4. The PL quantum efficiencies and CIE data of OLED devices measured at 9 V.

Copolymers	$\Phi_{\text{sol}}^{\text{a}}$	$\Phi_{\text{polystyrene}}^{\text{b}}$	$\Phi_{\text{film}}^{\text{c}}$	CIE X-coordinate	CIE Y-coordinate
25	0.86	0.54	0.14	0.19	0.12
26	0.16	0.43	0.27	0.43	0.55
27	0.47	0.49	0.35	0.38	0.52

^a Phosphorescence quantum yields (Φ) in CHCl_3 solution (10^{-4} g/L).

^b Phosphorescence quantum yields (Φ) in a polystyrene matrix (0.1 mol%).

^c neat films spin coated from toluene solution; experimental error ± 0.03 .

4.3 Summary

A set of fluorene-based copolymers containing orange-red iridium(III) complexes (**25**) and iridium(III) complexes as well as fluorenone units (**26** and **27**) were synthesised and characterised. The polymers revealed number average molecular weights up to 93500 g/mol and high thermal stabilities of around 400 °C at 5% weight-loss. The designed copolymers comprised Ir(III) emitters because they can serve as hole transporters and are thus expected to efficiently trap holes. Using also PF-PFO backbone leads to bipolar charge traps and this is an important prerequisite for the implementation of such materials in efficient light-emitting diodes. The electroluminescence spectra of these devices showed that indeed iridium(III) complexes were incorporated to the backbone of the copolymers, implied by the band appearing at around 604 nm. The observation of the concurrent blue emission suppression and the red emission increase is most likely evidence for energy-transfer from the fluorene backbone to the iridium-containing carbazole segments or for charge trapping.

4.4 Experimental Section

Materials: All manipulations were performed under an atmosphere of dry argon by employing usual Schlenk techniques. Solvents were carefully dried and distilled from appropriate drying agents prior to use. Commercially available reagents were used without further purification unless otherwise stated. *Bis*(1,5-cyclooctadiene)nickel(0) [Ni(0)(COD)₂] and 2,2'-bipyridine were purchased from Sigma-Aldrich. 2,7-Dibromo-9*H*-fluorene, 9*H*-fluoren-9-one, were delivered by ABCR. Potassium hydroxide, and 1-bromooctane were purchased from Acros.

The detailed synthesis of the the heteroleptic iridium(III) complexes **14b** was introduced on chapter 3. 2,7-Dibromo-9,9-di-*n*-octyl-9*H*-fluorene **23** [22] and 2,7-dibromo-9*H*-fluoren-9-one **24** [23] were synthesised according to modified procedures known from literature.

Instrumentation: ¹H NMR and ¹³C NMR spectra were performed on a Bruker avance 400 or Bruker avance III 600; chemical shifts were quoted relative to the internal standard tetramethylsilane (Me₄Si) in CDCl₃ solutions. For ¹H (s = singlet, d = doublet, t = triplet, q = quartet, and m = multiplet) and ¹³C NMR data; J values are given in Hertz (Hz). Fourier transform infrared (FT-IR) spectra were recorded on a JASCO FT/IR-4200 Fourier transform spectrometer. Elemental analysis (EA) was performed on a Perkin Elmer 240 B setup. Differential scanning calorimetry (DSC) measurements have been carried out on a Perkin Elmer DSC 7 under N₂ at a heating rate of 10 °C/min. Thermogravimetric analysis (TGA) was performed on a Mettler Toledo TG50. UV-vis spectra were measured with a JASCO V-550 UV-vis spectrophotometer (1 cm cuvettes, CHCl₃) at concentrations of 1 × 10⁻⁵ mol/L. The emission spectra were performed using a CARY Eclipse fluorescence spectrophotometer at concentrations of 1 × 10⁻⁵ mol/L. Gel permeation

Chapter 4. Copolymers containing iridium(III) complexes

chromatography (GPC) analysis was carried out on a Jasco AS950 apparatus using Jasco UV-2070, Jasco RI-930 and Viscotek T60 as detectors (column MZSD of particle size 5 μm , eluent chloroform). For the determination of the molecular weights, a calibration based on polystyrene standards was applied.

Electro-optical Methods: Measurements of quantum yields were made on drop-casted films of the selected metallo-copolymers in polystyrene, solutions in chloroform or in neat spin-coated films (from toluene). The compounds and polystyrene were dissolved in toluene at a ratio of 0.1% (molar). The quantum yields of the films of selected metallo-copolymers were obtained using a Hamamatsu quantum yield measurement system (integrating sphere, excitation source, monochromator, detector). The photoluminescence was excited at 340 nm. A detailed description of the experimental setup for the time-resolved photoluminescence measurements can be found elsewhere [30]. The PL has been collected and focused onto the entrance slit of the monochromator and detected by an intensified gateable CCD camera. The spectral resolution was set to 2 nm. The instrument response function is about 1.7 ns. Time resolved measurements have been done at 295 K under continuous flow of nitrogen.

Electrophosphorescence: The PLEDs of the selected metallo-copolymers were prepared on pre-cleaned, UV-ozon-treated ITO-coated glass substrates. A layer of PEDOT:PSS was spin-coated onto the substrates under clean-room conditions and baked at 120 °C for 2 minutes to remove residual water. The hole-transporting layers *N,N'*-bis(4-[6-[(3-ethyloxetane-3-yl)methoxy]-hexyloxy)phenyl]-*N,N'*-bis(4-methoxyphenyl)biphenyl-4,4'-diamine) QUPD and *N,N'*-bis(4-[6-[(3-ethyloxetane-3-yl)methoxy]-hexylphenyl]-*N,N'*-diphenyl-4,4'-diamine) OTPD were prepared as described in literature [31]. The selected metallo-copolymers were dissolved in *ortho*-dichlorobenzene and subsequently spin-coated. The cathode consisting of CsF and Al was deposited by thermal evaporation at a base pressure of 10^{-6} mbar.

The current-voltage-luminescence characteristics were measured with a source-measure unit and a calibrated photodiode under argon atmosphere. The EL spectra were measured with a calibrated Ocean Optics CCD spectrometer.

4.4.1 2,7-Dibromo-9,9-di-*n*-octyl-9*H*-fluorene (23)

The synthesis and analysis of compound **23** were synthesised according to modified procedures known from literature [22].

4.4.2 2,7-Dibromo-9*H*-fluoren-9-one (24)

The synthesis and analysis of compound **24** were synthesised according to modified procedures known from literature [23].

4.4.3 Copolymer Ir5PF95 (25)

2,7-Dibromo-9,9-di-*n*-octyl-9*H*-fluorene **23** (300 mg, 0.572 mmol), orange-red Ir(III) complex **14b** (32 mg, 0.031 mmol), [Ni(0)(COD)₂] (379 mg, 1.445 mmol), 2,2'-bipyridine (207 mg, 1.325 mmol) and COD (143 mg, 1.325 mmol) were added together in a Schlenk tube. Subsequently, THF (20 ml) was added to the reaction system and was allowed to stir for 3 days at 80 °C. Then, 3 hours before stopping the reaction, 0.05 ml of bromobenzene were added and after cooling down to room temperature the reaction solution was extracted with chloroform and washed with 2 N HCl (2 × 100 ml), saturated NaHCO₃ solution (1 × 100 ml) and water (2 × 100 ml). The organic phase was dried over Na₂SO₄ and the solvent removed under reduced pressure. The residue was dissolved in chloroform (1-3 ml), precipitated in methanol (300 ml) and the yellow solid was further extracted with ethanol.

Copolymer **25** was obtained yielding a pale yellow solid (205 mg, 62%).

$^1\text{H-NMR}$ (400 MHz, CDCl_3 , ppm): δ 0.83, 1.17, 2.16, 7.73, 7.88. IR: 3056 (C=C-H), 2947, 2934, 2867 (C-H), 1734, 1577, 1539 (C=C, C=N, C=O), 1401, 1376, 1262, 1133, 890, 863, 824, 787, 690, 671 cm^{-1} . UV-Vis [CHCl_3 , λ_{max} , nm, $\log \epsilon$, $\text{L} \times \text{mol}^{-1} \times \text{cm}^{-1}$]: 391 (5.07). Emission (CHCl_3 , λ_{max} , nm): 419. T_g/T_{ic} : 80/168 °C. T_d (5% decomposition): 403 °C. M_n (g/mol): 93500. M_w (g/mol): 299000. PDI: 3.19. Elem. Anal. Calcd.: C 86.88%, H 9.70%. Found: C 86.39%, H 11.87%.

4.4.4 General procedure of copolymers **26** and **27**

A mixture of orange-red Ir(III) complex **14b**, 2,7-dibromo-9,9-di-*n*-octyl-9*H*-fluorene **23**, 2,7-dibromo-9*H*-fluoren-9-one **24**, $[\text{Ni}(0)(\text{COD})_2]$, 2,2'-bipyridyl and COD in 25 ml of toluene in a Schlenk tube was stirred at 80 °C for 60 h under an argon atmosphere. Then, 3 hours before stopping the reaction, 0.05 ml of bromobenzene were added and after cooling down to room temperature the reaction solution was extracted with chloroform and washed with 2 N HCl (2 \times 100 ml), saturated NaHCO_3 solution (1 \times 100 ml) and water (2 \times 100 ml). The solvent was removed by vacuum. The residue was dissolved in chloroform and precipitated into methanol, Soxhlet extracted with ethanol for one day and dried in vacuum at room temperature.

4.4.5 Copolymer Ir5PF90PO5 (**26**)

Orange-red Ir(III) complex **14b** (33.8 mg, 0.032 mmol), 2,7-dibromo-9,9-di-*n*-octyl-9*H*-fluorene **23** (300 mg, 0.572 mmol), 2,7-dibromo-9*H*-fluoren-9-one **24** (10.8 mg, 0.012 mmol), $[\text{Ni}(0)(\text{COD})_2]$ (379 mg, 1.445 mmol), 2,2'-bipyridine (207 mg, 1.325 mmol) and 1,5-cyclooctadiene (143 mg, 1.325 mmol). Copolymer **26** was obtained

yielding a pale yellow solid (217 mg, 63%).

$^1\text{H-NMR}$ (400 MHz, CDCl_3 , ppm): δ 0.81, 1.14, 2.12, 7.67, 7.82. IR: 3091 (C=C-H), 2965, 2959, 2885 (C-H), 1777, 1613, 1564 (C=C, C=N, C=O), 1488, 1357, 1221, 1179, 1091, 943, 876, 796, 721, 694 cm^{-1} . UV-Vis [CHCl_3 , λ_{max} , nm, $\log\epsilon$, $\text{L} \times \text{mol}^{-1} \times \text{cm}^{-1}$]: 393 (5.11). Emission (CHCl_3 , λ_{max} , nm): 420. T_g/T_{IC} : 110/164 $^{\circ}\text{C}$. T_d (5% decomposition): 408 $^{\circ}\text{C}$. M_n (g/mol): 39400. M_w (g/mol): 94600. PDI: 2.40. Elem. Anal. Calcd.: C 86.77%, H 9.53%. Found: C 88.27%, H 11.48%.

4.4.6 Copolymer Ir10PF89PO1 (27)

Orange-red Ir(III) complex **14b** (68.4 mg, 0.064 mmol), 2,7-dibromo-9,9-di-*n*-octyl-9*H*-fluorene **23** (300 mg, 0.572 mmol), 2,7-dibromo-9*H*-fluorene-9-one **24** (2.2 mg, 0.006 mmol), $[\text{Ni}(0)(\text{COD})_2]$ (379 mg, 1.445 mmol), 2,2'-bipyridine (207 mg, 1.325 mmol) and 1,5-cyclooctadiene (143 mg, 1.325 mmol). Copolymer **27** was obtained yielding a pale yellow solid (252 mg, 68%).

$^1\text{H-NMR}$ (400 MHz, CDCl_3 , ppm): δ 0.81, 1.16, 2.12, 7.65, 7.83. IR: 3089 (C=C-H), 2987, 2954, 2884 (C-H), 1765, 1638, 1543 (C=C, C=N, C=O), 1469, 1356, 1249, 1180, 1075, 937, 891, 832, 751, 694 cm^{-1} . UV-Vis [CHCl_3 , λ_{max} , nm, $\log\epsilon$, $\text{L} \times \text{mol}^{-1} \times \text{cm}^{-1}$]: 394 (5.08). Emission (CHCl_3 , λ_{max} , nm): 421. T_g/T_{IC} : 120/162 $^{\circ}\text{C}$. T_d (5% decomposition): 405 $^{\circ}\text{C}$. M_n (g/mol): 50600. M_w (g/mol): 150000. PDI: 2.96. Elem. Anal. Calcd.: C 84.63%, H 9.08%. Found: C 88.51%, H 12.05%.

4.5 References

- [1] R. J. Holmes, S. R. Forrest, Y. J. Tung, R. C. Kwong, J. J. Brown, S. Garon, M. E. Thompson, *Appl. Phys. Lett.* **2003**, *82*, 2422.
- [2] C. Adachi, M. A. Baldo, S. R. Forrest, M. E. Thompson, *Appl. Phys. Lett.* **2000**, *77*, 904.
- [3] S. Lamansky, R. C. Kwong, M. Nugent, P. I. Djurovich, M. E. Thompson, *Org. Electron.* **2001**, *2*, 53.
- [4] K. Zhang, Z. Chen, Y. Zou, S. Gong, C. Yang, J. Qin, Y. Cao, *Chem. Mater.* **2009**, *21*, 3306.
- [5] A. B. Padmaperuma, L. S. Sapochak, P. E. Burrows, *Chem. Mater.* **2006**, *18*, 2389.
- [6] M. H. Tsai, H. W. Lin, H. C. Su, T. H. Ke, C. C. Wu, F. C. Fang, Y. L. Liao, K. T. Wong, C. I. Wu, *Adv. Mater.* **2006**, *18*, 1216.
- [7] S. Lamansky, R. C. Kwong, M. Nugent, P. I. Djurovich, M. E. Thompson, *Org. Electron.* **2001**, *2*, 53.
- [8] X. Gong, D. Moses, A. J. Heeger, *J. Phys. Chem. B* **2004**, *108*, 8601.
- [9] K. Zhang, Z. Chen, C. Yang, Y. Tao, Y. Zou, J. Qin, Y. Cao, *J. Mater. Chem.* **2008**, *18*, 291.
- [10] K. Zhang, Z. Chen, C. Yang, S. Gong, J. Qin, Y. Cao, *Macromol. Rapid Commun.* **2006**, *27*, 1926.
- [11] K. Zhang, Z. Chen, Y. Zou, C. Yang, J. Qin, Y. Cao, *Organometallics*. **2007**, *26*, 3699.
- [12] K. Zhang, Z. Chen, C. Yang, Y. Zou, S. Gong, Y. Tao, J. Qin, Y. Cao, *J. Mater. Chem.* **2008**, *18*, 3366.
- [13] K. Zhang, Z. Chen, C. Yang, Y. Zou, S. Gong, J. Qin, Y. Cao, *J. Phys. Chem. C* **2008**, *112*, 3907.
- [14] P. I. Lee, S. L. C. Hsu, J. F. Lee, *J. Polym. Sci., Part A: Polym. Chem.* **2007**, *46*, 464.
- [15] J. Langecker, M. Rehahn, *Macromol. Chem. Phys.* **2008**, *209*, 258.
- [16] N. Tian, A. Thiessen, R. Schiewek, O. J. Schmitz, D. Hertel, K. Meerholz, E. Holder, *J. Org. Chem.* **2009**, *74*, 2718.

Chapter 4. Copolymers containing iridium(III) complexes

- [17] N. Tian, Y. V. Aulin, D. Lenkeit, S. Pelz, O. V. Mikhnenko, P. M. W. Blom, M. A. Loi, E. Holder, *Dalton Trans.* **2010**, 39, 8613.
- [18] F. Uckert, S. Setayesh, K. Müllen, *Macromolecules* **1999**, 32, 4519.
- [19] L. L. Chua, J. Zaumseil, J. F. Chang, E. C. W. Ou, P. K. H. Ho, H. Sirringhaus, R. H. Friend, *Nature*, **2005**, 434, 194.
- [20] F. Uckert, Y.-H. Tak, K. Müllen, H. Bässler, *Adv. Mater.* **2000**, 12, 905.
- [21] T. Yamamoto, S. Wakabayashi, K. Osakada, *J. Organomet. Chem.* **1992**, 428, 223.
- [22] B. Liu, B. S. Gaylord, G. C. Bazan, *J. Am. Chem. Soc.* **2003**, 125, 6705.
- [23] X. Zhang, J. B. Han, P. F. Li, X. Z. Zhao, *Synth. Commun.* **2009**, 39, 3804.
- [24] J. Schelter, G. F. Mielke, A. Köhnen, J. Wies, S. Köber, O. Nuyken, K. Meerholz, *Macromol. Rapid Commun.* **2010**, 31, 1560.
- [25] W. L. Yu, J. Pei, W. Huang, A. J. Heeger, *Adv. Mater.* **2000**, 12, 828.
- [26] A. P. Kulkarni, X. Kong, S. A. Jenekhe, *J. Phys. Chem. B* **2004**, 108, 8689.
- [27] J. H. Kim, H. Lee, *Chem. Mater.* **2002**, 14, 2270.
- [28] B. J. Jung, C. B. Yoon, H. K. Shim, L. M. Do, T. Zyung, *Adv. Funct. Mater.* **2001**, 11, 430.
- [29] W. Zhao, T. Cao, J. M. White, *Adv. Funct. Mater.* **2004**, 14, 783.
- [30] D. Hertel, K. Meerholz, *J. Phys. Chem. B* **2007**, 111, 12075.
- [31] P. Zacharias, M. C. Gather, M. Rojahn, O. Nuyken, K. Meerholz, *Angew. Chem. Int. Ed.* **2007**, 46, 4388.

List of Symbols and Abbreviations

APLI-TOF MS	Atmospheric Pressure Laser Ionization Time of Flight Mass Spectrometry
bipy	2,2'-Bipyridyl
bm	Broad multiplet
COSY	Correlated spectroscopy
CzSi	9-(4- <i>Tert</i> butylphenyl)-3,6- <i>bis</i> (triphenylsilyl)-9 <i>H</i> -carbazole
d	Doublet
DFT	Density functional theory
DMF	<i>N,N</i> -dimethylformamide
DMSO	Dimethyl sulfoxide
DSC	Differential Scanning Calorimetry
eq.	Equivalent
h	Hours
HOMO	Highest occupied molecular orbital
Ir(III)	Iridium(III)
IR	Infrared
KHDMS	Potassium hexamethyldisilazane
LUMO	lowest unoccupied molecular orbital
MALDI-TOF MS	Matrix-assisted Laser Desorption/Ionization Time of Flight Mass Spectrometry
MLCT	Metal to ligand charge transfer
M_n	Number average molecular weight
M_w	Weight average molecular weight
LC ¹	Singlet ligand-centered
LC ³	Triplet ligand-centered
NMR	Nuclear magnetic resonance
[Ni(0)(COD) ₂]	<i>Bis</i> (1,5-cyclooctadiene)nickel(0)
OLED	Organic Light-Emitting Diode

PBD	2-(Biphenyl-4-yl)-5-(4- <i>tert</i> -butylphenyl)-1,3,4-oxadiazole
PD	Polydispersity
PEGMA	Polyethylene glycol methacrylate
PF	Polyfluorene
PL	Photoluminescence
PO6	2,7- <i>Bis</i> (diphenylphosphine oxide)-9,9-dimethylfluorene
PODBF	2,8- <i>Bis</i> (diphenylphosphine oxide)dibenzofuran
PPV	Poly(phenylvinylene)
PT	Polythiophenes
PtOEP	Pt(II) Octaethylporphine
PVK	Polyvinylcarbazole
q	Quartet
T_d	Decomposition temperature
T_g	Glass transition temperature
THF	Tetrahydrofuran
η_{ex}	External quantum efficiencies

List of Publications out of this work

“Screening structure-property-correlations and device performance of Ir(III) complexes in multi-layer PhOLEDs” **Tian, Nan**; Lenkeit, Daniel; Pelz, Simon; Kourkoulos, Dimitrios; Hertel, Dirk; Meerholz, Klaus; Holder, Elisabeth *Dalton Transactions* (2011), 40, 11629-11635.

“Synthesis of red and green emitting iridium(III) complexes and characterization of their temperature and oxygen sensitivity” **Tian, Nan**; Lenkeit, Daniel; Pelz, Simon; Fischer, Lorenz H.; Escudero, Daniel; Schiewek, Ralf ; Klink, Dennis; Schmitz, Oliver J.; González, Leticia; Schäferling, Michael; Holder, Elisabeth *European Journal of Inorganic Chemistry* (2010), 30, 4875-4885

“Cyclometalated red iridium(III) complexes containing carbazolyl-acetylacetonate ligands: efficiency enhancement in polymer LED devices” **Tian, Nan**; Aulin, Yaroslav V.; Lenkeit, Daniel; Pelz, Simon; Mikhnenko, Oleksandr V.; Blom, Paul W. M.; Loi, Maria Antonietta and Holder, Elisabeth *Dalton Transactions* (2010), 39, 8613-8615

“Efficient synthesis of carbazolyl- and thienyl-substituted beta-diketonates and properties of their red and green light-emitting Ir(III) complexes” **Tian, Nan**; Thiessen, Alexander; Schiewek, Ralf; Schmitz, Oliver J.; Hertel, Dirk; Meerholz, Klaus; Holder, Elisabeth *Journal of Organic Chemistry* (2009), 74, 2718-2725.

“Phosphorescent, light-emitting copolymers: Synthesis and characterization” **Tian, Nan**; Kanelidis, Ioannis; Thiessen, Alexander; Hertel, Dirk; Meerholz, Klaus; Holder, Elisabeth *Macromolecular Bioscience* (2009), 9, F68-F69.

“Red and green emitting iridium(III) complexes for a dual barometric and temperature sensitive paint” Fischer, Lorenz H.; Stich, Matthias I. J.; Wolfbeis, Otto S.; **Tian, Nan**; Holder, Elisabeth; Schäferling, Michael *Chemistry - A European Journal* (2009), 15, 10857-10863.

“Decoupling 2D inter- and intra-chain energy transfer in conjugated polymers”. Shekhar, Shashank; Aharon, Eyal; **Tian, Nan**; Galbrecht, Frank; Scherf, Ullrich; Holder, Elisabeth; Frey, Gitti L. *ChemPhysChem: A European Journal of Chemical Physics and Physical Chemistry* (2009), 10, 576-581.

“High-Quality White Light Generation using Dually Hybridized Nanocrystals and Conjugated Polymers” Nizamoglu, Sedat; Ozel, Tuncay; Mutlugun, Evren; Huyal, Ilkem O.; Sari, Emre; **Tian, Nan**; Holder, Elisabeth; Demir, Hilmi V. *Proceedings of IEEE Lasers and Electro-Optics Society* (2007), Paper MO5.

“White light generation tuned by dual hybridization of nanocrystals and conjugated polymers” Demir, Hilmi V.; Nizamoglu, Sedat; Ozel, Tuncay; Mutlugun, Evren; Huyal,

Ilkem O.; Sari, Emre; Holder, Elisabeth; ***Tian, Nan*** *New Journal of Physics* (2007), 9, 362 (1-13).

Posters

“Cyclometalated red iridium(III) complexes containing carbazoyl-acetylacetonate ligands: Efficiency Enhancement in Polymer LED Devices” ***Tian, Nan***; V. Aulin, Yaroslav; V. Mikhnenko, Oleksandr; W. M. Blom, Paul; Loi Antonietta, Maria, Holder, Elisabeth 3rd EuCheMS Chemistry Congress, Chemistry - the Creative Force. Nürnberg, Germany. August 29-September 02, 2010

“Oxygen and temperature sensitivities of cyclometalated Ir(III) triplet emitters” Fischer, Lorenz H.; ***Tian, Nan***; Holder, Elisabeth; Schäferling, Michael EUROPT(R)ODE X, Prague, Czech Republic. March 28-31, 2010.

“Red and green emitting Ir(III) complexes for dual barometric and temperature sensors” ***Tian, Nan***; Fischer, Lorenz H.; Stich, Matthias I. J.; Wolfbeis, Otto S.; Schäferling, Michael; Holder, Elisabeth GDCh-Frühjahrskolloquium, Wuppertal, Germany. April 23, 2009.

“Phosphorescent, light-emitting copolymers: Synthesis and characterization” ***Tian, Nan***; Kanelidis, Ioannis; Thiessen, Alexander; Hertel, Dirk; Meerholz, Klaus; Holder, Elisabeth Makromolekulares Kolloquium, Freiburg i. Br., Germany. February 26-28, 2009.

“Mannich-reaction for novel phenyl-tetrahydroquinolines and their light-emitting iridium(III) picolinates” ***Tian, Nan***; Heuser, Eike; Hummel, Johanna; Risch, Nikolaus; Holder, Elisabeth EuCHEMS Chemistry Congress, Chemistry the Global Science. Torino, Italy. September 16-20, 2008.

“Novel bipolar light-emitting iridium(III) acetylacetonates” ***Tian, Nan***; Holder, Elisabeth; Altintas, Ozcan; 2nd EuCHEMS Chemistry Congress, Chemistry the Global Science. Torino, Italy. September 16-20, 2008.

“Synthesis of donor-functionalized, phosphorescent iridium(III) complexes containing carbazole-functionalized β -diketonates” ***Tian, Nan***; Holder, Elisabeth F π 8, the 8th International Symposium on Functional π -Electron Systems, Graz, Austria. July 21-25, 2008.

“New hybrid white light-emitting diodes by hybridizing inorganic InGaN/GaN diodes with nanocrystals and conjugated polymers” ***Tian, Nan***; Holder, Elisabeth; Nizamoglu, Sedat; Ozel, Tuncay; Mutlugun, Evren; Hoyal, Ilkem O.; Sari, Emre; Demir, Hilmi V. MRS International Materials Research Conference, Chongqing, China. June 9-12, 2008.

“Synthesis and characterization of polymerizable carbazole-based iridium(III) acetylacetonate complexes for multi-layer polymer light-emitting diodes” **Tian, Nan**; Holder, Elisabeth; Thiessen, Alexander; Hertel, Dirk; Meerholz, Klaus MRS International Materials Research Conference, Chongqing, China. June 9-12, 2008.

“Characterization of building blocks of organic LEDs with atmospheric pressure laser ionization-(TOF)MS” Schiewek, Ralf; Mangas Suárez, Ana Lydia; **Tian, Nan**; Holder, Elisabeth; Bilge, Askin; Scherf, Ullrich; Brockmann, Klaus J.; Benter, Thorsten; Schmitz, Oliver J.; Gäb, Siegmur 56th ASMS Conference on Mass Spectrometry and Allied Topics, Colorado Convention Center, Denver, Colorado, USA. May 31-June 1, 2008.

“Synthesis of phosphorescent iridium(III) complexes containing carbazole-functionalized β -diketonates” **Tian, Nan**; Holder, Elisabeth GDCh-Frühjahrskolloquium, Wuppertal, Germany, 15. April 2008.

“Polymer lighting with new triplet emitters and multi-layer structural design” **Tian, Nan**; Holder, Elisabeth; Thiessen, Alexander; Hertel Dirk Second DPI Mini-Symposium Functional Polymer Systems, Maastricht, the Netherlands, October 11-12, 2007.

“Nanocrystal hybridized light emitting diodes to generate and tune white light” Nizamoglu, Sedat; Mutlugun, Evren; Ozel, Tuncay; Huyal, Ilkem Ozge; Sari, Emre; Perkgoz, Nihan Kosku; Demir, Hilmi Volkan; Sapra, Sameer; Gaponik, Nikolai; Liebscher, Lydia; Eychmüller, Alexander; **Tian Nan**; Holder, Elisabeth PhOREMOST Nanophotonics Workshop, Istanbul, Turkey. September 13-15, 2007.

“Iridium(III) complexes with donor motifs: Synthesis and electro-optical properties” **Tian, Nan**; Holder, Elisabeth; Thiessen, Alexander; Hertel, Dirk ICP2007 - XXIII. International Conference on Photochemistry 2007 Cologne, Germany, July 29-August 03 2007.

“White light generation by dual hybridization of conjugated polymers and nanocrystals on *n*-UV LEDs” Nizamoglu, Sedat; Ozel, Tuncay; Mutlugun, Evren; Huyal, Ilkem Ozge; Sari, Emre; Demir, Hilmi Volkan, **Tian, Nan**; Holder, Elisabeth GDCh-Frühjahrskolloquium, Wuppertal, Germany, April 14, 2007.

“White light generation by dual hybridization of conjugated polymers and nanocrystals on *n*-UV LEDs” Nizamoglu, Sedat; Ozel, Tuncay; Mutlugun, Evren; Huyal, Ilkem Ozge; Sari, Emre; Demir, Hilmi Volkan, **Tian, Nan**; Holder, Elisabeth PhOREMOST General Assembly Meeting, ROMA, Italy, March 20-21, 2007.

Acknowledgement

First of all I would like to express my appreciation to my supervisor Prof. Elisabeth Holder for the financial and professional support during the past four years. The good working environment and her permanent motivation and dedication contributed in the delivery of a successful work.

Many thanks go to Prof. Ullrich Scherf for his support in all kinds of directions and being my second referee.

Prof. Hans-Josef Altenbach and Prof. Fabian Mohr are acknowledged for reviewing my thesis and participating in my defense.

I am grateful to Prof. Oliver Schmitz for performing APLI experiments.

Prof. Klaus Meerholz is acknowledged for the smooth cooperation and device preparation.

Dr. Dirk Hertel, Alexander Thiessen and Dimitrios Kourkoulos are acknowledged for their competent support and cooperation at the University of Cologne.

My sincere thanks go to Lorenz. H. Fischer, PD. Dr. Michael Schäferling and Prof. Otto. S. Wolfbeis for their competent support and cooperation at the University of Regensburg.

Yaroslav V. Aulin, Oleksandr Mikhnenko, Prof. Maria Antonietta Loi and Prof. Paul. W. M. Blom are thanked for their smooth and competent cooperation supporting this work at the University of Groningen.

I am grateful to Anke Helfer for GPC-, DSC- and TGA measurements, Melanie Dausend for LC-MS spectrometry measurements and Jürgen Dönecke for performing GC-MS spectrometry.

Andreas Siebert is acknowledged for countless NMR measurements.

Dennis Klink and Ralf Schiewek are thanked for their APLI mass spectrometry contribution while Ralf Radon is thanked for his elemental analysis measurements.

I would like to express my thanks to Sylwia Adamczyk for performing AFM measurements and Dr. Michael Forster for his support.

I thank my former laboratory mates Jinming Zhang, Ioannis Kanelidis, Cüneyt Karakus, Eike Heuser, Daniel Lenkeit, Simon Pelz, Jiajie Shen, and Yi Ren for helpful discussions and lots of funny moments.

The Dutch Polymer Institute is gratefully acknowledged for financial support, which enabled the performance of this interesting project.